M(055)
QC
801
.U55
no.36
v.1

TN-60-427

GRD RESEARCH NOTES

No. 36

CONTRIBUTIONS TO SATELLITE METEOROLOGY

Edited by
William K. Widger, Jr.

June 1960

GEOPHYSICS RESEARCH DIRECTORATE
AIR FORCE CAMBRIDGE RESEARCH CENTER
AIR RESEARCH AND DEVELOPMENT COMMAND
UNITED STATES AIR FORCE
BEDFORD, MASSACHUSETTS

search Notes are published
m for disseminating, in a
rapid and informal way,
research results obtained
e of a broader investigation,
information pending comple-
or research effort."

110 876

R
D
g

A
A
A

D
fo
fie
or

Al

U.
OF
WA

AFCRC-TN-60-427

GRD Research Notes

No. 36

CONTRIBUTIONS TO SATELLITE METEOROLOGY

LIBRARY
SEP 6 - 1960
U.S. WEATHER BUREAU

John J. Aiken, John H. Conover, Robert C. Curtis
Major James C. Sadler, William K. Widger, Jr.
Geophysics Research Directorate

Roland J. Boucher, Gerald Cooper, Arnold H. Glaser
A. Leon Goldshlak, S. N. Milford, Raymond Wexler
Allied Research Associates, Inc.

Julius London, New York University
K. L. Coulson, Stanford Research Institute

QC
801
.U53
no.36
v.1

Edited by

William K. Widger, Jr.

LIBRARY
N.O.A.A.
U.S. Dept. of Commerce

June 1960

Projects 4982 and 6698

Atmospheric Circulations Laboratory
GEOPHYSICS RESEARCH DIRECTORATE
AIR FORCE CAMBRIDGE RESEARCH CENTER
AIR RESEARCH AND DEVELOPMENT COMMAND
UNITED STATES AIR FORCE
Bedford, Mass.

110 876

National Oceanic and Atmospheric Administration
TIROS Satellites and Satellite Meteorology

ERRATA NOTICE

One or more conditions of the original document may affect the quality of the image, such as:

Discolored pages
Faded or light ink
Binding intrudes into the text

This has been a co-operative project between the NOAA Central Library and the Climate Database Modernization Program, National Climate Data Center (NCDC). To view the original document contact the NOAA Central Library in Silver Spring, MD at (301) 713-2607 x124 or Library.Reference@noaa.gov.

HOV Services
Imaging Contractor
12200 Kiln Court
Beltsville, MD 20704-1387
January 26, 2009

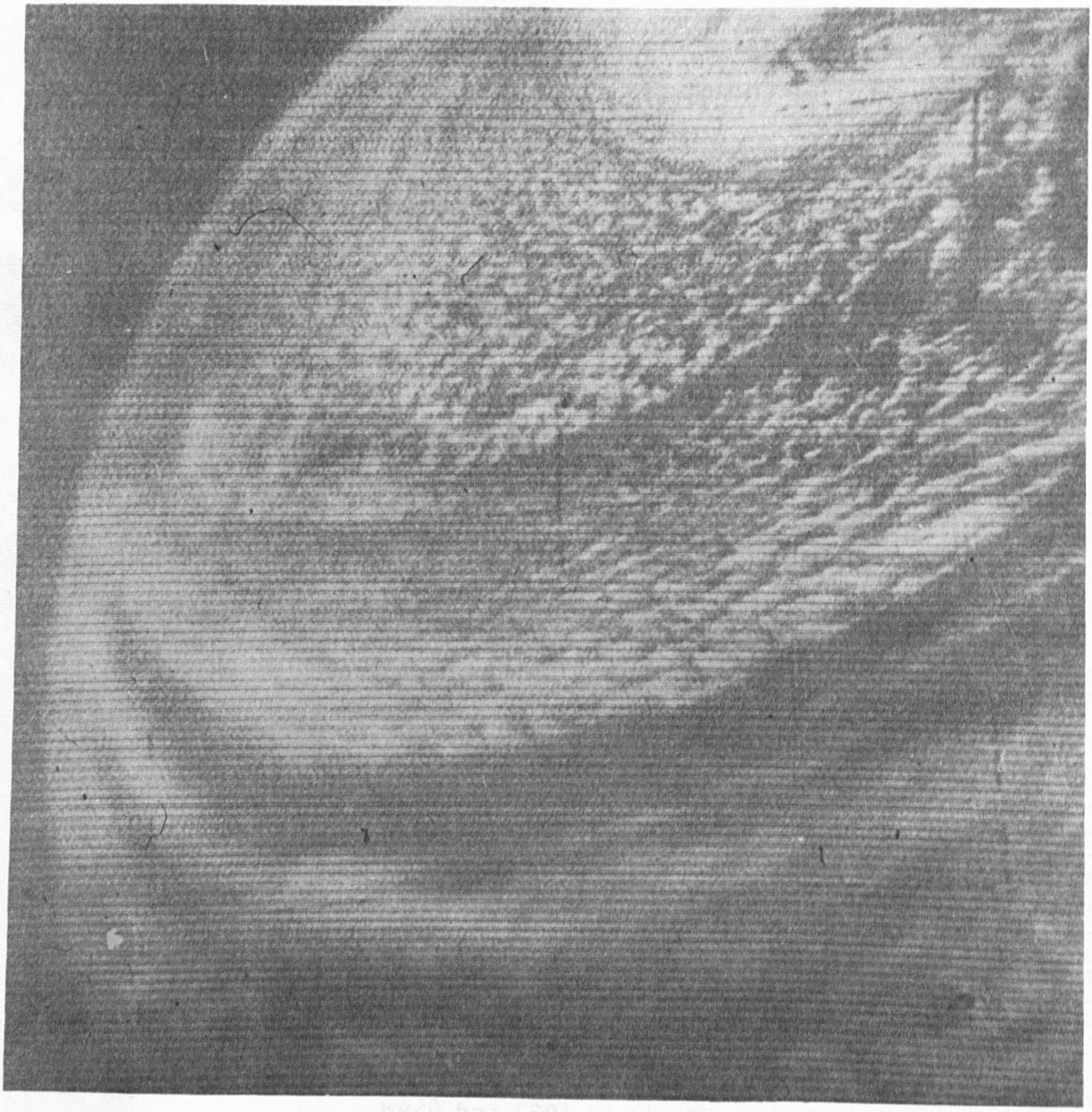

A great vortex storm in the North Pacific Ocean

as observed by TIROS on 4 April 1960

FOREWORD

Some five years ago W. K. Widger set out to demonstrate the answer to a question that was being debated in Air Force R & D circles: How valuable would a meteorological satellite be, and how would one go about using its observations? Since then this activity has grown from the part-time occupation of a single man into a major program that is the sole responsibility of one of GRD's branches.

This Research Note is a collection of some of the results to date. When it was conceived earlier this year, one hopeful purpose was to encourage more widespread professional interest and participation in satellite meteorology. (As usual, the pioneer is keenly disappointed by the seeming indifference of his colleagues-at-large to the marvelous vistas that he sees unfolding.) I dare say that the subsequent, magnificently successful performance of NASA's TIROS I has relieved this publication of any burden of promotion. There still remains the normal goal of a scientific communication, perhaps more so here, for but few papers on this subject have appeared in truly public print.

Dr. Widger's original question remains substantially unanswered. Military interest was initially spurred by the obvious applicability of the meteorological satellite to the silent-area problem which, harrassing enough to the forecaster in peacetime, becomes a particular plague in wartime. So now we know what clouds look like when viewed from far above. But how much of the initial information required in modern forecasting technology can be extracted from such observations?

Suomi's experiment aboard Explorer VII has demonstrated the feasibility of heat balance measurements. But what is the total

information content, the ultimate implication of such measurements?

How about the potential of the more sophisticated probing techniques--infrared, ultraviolet, radar--yet to be flown?

Does the unique world-view of the satellite promise information in more than bit-size pieces? This is a truly provocative question. Even the early samples--for example, the exciting by-product of the Atlas test-firing in August 1959--suggest a gestalt message. Is this illusory or are we on the brink of new concepts as to how the atmosphere is organized?

For my final comment I turn from technical factors to economic. For some years I have held the moderate opinion that, as a forecaster, I should always prefer a radiosonde network to a satellite and should be interested in the latter only when the former is denied me. Recently, from some projections of the declining cost of rocketry, I have been startled to learn that before long even my own paycheck will suffice to buy a pound in orbit. That same paycheck will operate a weather ship for no time at all. So now I am wondering--as a forecaster and a taxpayer should I always clearly prefer the radiosonde?

C. N. Touart

ABSTRACT

To define some of the information requirements of the meteorological consumer, a literature survey of possible meteorological Satellite applications is provided. An examination of some photographs of the earth, taken from an Atlas nose cone, illustrates the problems involved in transmitting such information to the designated consumer. Preliminary results of studies of large-scale cloudiness and cloud patterns and their relationship to cloud-producing processes and standard synoptic features are discussed. Time lapse films of the earth from high-flying ballistic missiles are analyzed to show the first cloud patterns over an area corresponding to one-twentieth of the earth's total surface. Comparisons of the rectified cloud positions with the high and low-level synoptic charts show large-scale cloud patterns directly associated with high-level vertices and trough as well as patterns associated with a quasi-stationary front and the intertropical convergence zone. Details suggesting low-level vortices, frontal waves, and a squall line appear which cannot be verified due to sparse surface observations. Other details, such as the effects of large and small islands, coastlines, and rivers upon the pattern of vertical motion are indicated by the clouds.

An attempt to devise methods of measuring cloud velocity from a satellite, including the mathematics involved in the application to obtain the cloud velocity to a known degree of accuracy, is discussed. It is shown that the accuracy of measurement required in using these methods is much too stringent for practical application. Since this is true, other methods which have been considered are mentioned.

A system is then described that will facilitate the meteorological utilization of television-type pictures to be telemetered from a satellite vehicle. Geographical location of features seen in the pictures

is facilitated by the use of a library of perspective grids. The pictures are superposed on the appropriate perspective grid, while a corresponding transfer grid is superposed on a map in the proper position and orientation. There is then a one-to-one correspondence between points on the two grids, permitting ready transfer of significant meteorological information from the picture to its map position. The grids serve the further purpose of aiding the eye in the appreciation of perspective and the establishment of the relative sizes of features in the pictures. To facilitate mapping, it is found desirable to prepare a special transverse Mercator map, generated on a tangent cylinder inclined at the orbital inclination to the equator. A special code is used to describe significant features abstracted from the pictures in a form which will permit ready reconstruction by the user. The techniques described depend on the knowledge of the position and attitude of the satellite camera at the time of picture taking. If attitude information is lacking, it can be reconstructed by the use of information contained in the picture and telemetered information on the relative position of the sun.

A technique is developed for establishing the camera axis azimuth and time of photograph from landmarks when the other data cannot supply this information.

Two brief surveys of synoptic scale radiation processes are presented. The first treats the relative importance of the radiation budgets of the very high atmosphere, the ozonosphere, the lower stratosphere, and the troposphere. The ozonosphere and troposphere are found to be by far the more significant layers and are discussed in some detail. The effects of cloud distributions and surface temperature are considered. The second survey discusses the problem of the variation of the effective emission level

with change of nadir angle of observation and specifically considers the variations for measurements in the eleven-micron window. The view of the earth's atmosphere in an infrared water-absorption band is examined and found to correspond to a picture of the temperature of a constant dew-point surface. Some of these constant dew-point surfaces are analyzed in connection with the corresponding conventional surface and upper-air weather maps and indicate the existence of interesting meteorological relationships which should be studied further.

The infrared spectrum is then divided into convenient intervals according to the location of the principal absorbing bands for atmospheric gases. From available experimental data, transmissions from a given pressure level to the top of the atmosphere are derived for different angles of view of the satellite.

For 0000Z, 6 March 1959, maps of equivalent temperature in the 6.3-micron water-vapor band (using somewhat more sophisticated techniques than those in the preceding study), the carbon dioxide bands, and the infrared ozone band are derived and compared with a "window" map. Interpretations are made of the patterns of infrared radiation associated with the deep cyclonic system located over Illinois.

A method for determining atmospheric ozone amounts by measuring the scattered radiation at two different wave lengths in the ultraviolet is investigated to determine the theoretical ratios of radiation intensities to be expected.

The problem of the reduction and processing of the mass of photographic and radiation data to be expected from meteorological satellites is considered. A generalized, schematic, flow chart, illustrating the nature of the steps and processes that must be undertaken, is presented, described, and discussed.

Blank page retained for pagination

CONTENTS

	Page
Foreword	iii
Abstract	v
Table of Contents	ix
List of Illustrations	xv
Chapter I. Introduction	
1. Background and Objectives	1
2. A Concept of a Meteorological Satellite System	2
3. A Preview	3
Chapter II. Applications of Meteorological Satellites	
1. A Survey of Applications of Meteorological Satellites	7
1.1 Introduction	7
1.2 Planetary Parameters	8
1.3 Nephanalysis	14
1.4 Some Specific Meteorological Parameters	16
1.5 Useful Meteorological Orbits	20
Chapter III	
Section 1. Studies of Large-Scale Cloudiness in the Northern Hemisphere	
1.1 Introduction	23
1.2 Studies being conducted	23
1.3 Results	28
1.4 Interrelationships Between Studies of Large and Small-scale Cloudiness	30
Section 2. Cloud Patterns as Seen from Altitudes of 250-850 miles	
2.1 Introduction	31
2.2 Photography	31
2.3 Analysis	33

Page

2.3.1 Low-level 33

2.3.2 High-level 36

2.3.3 Photographic 36

2.4 Acknowledgments 45

Section 3. On the Possibility of Measuring Cloud Velocities from a Satellite

3.1 Introduction 47

3.2 Case I, Two Dimensional Case 48

3.2.1 Deriving a formula for "v" using ground distance 49

3.2.2 Error Analysis Computations 50

3.2.3 Conclusion 53

3.3 Case II, Two Dimensional Case 53

3.3.1 Deriving "v" by the Use of Angle Measurement 53

3.3.2 Error Analysis Computations 54

3.3.3 Conclusions 56

3.4 Case III, The General Case in Three Dimensions 56

3.4.1 Data Given 56

3.4.2 Deriving "v" from the Given Data 56

3.4.3 Error Analysis Computations 58

3.5 Concluding Remarks 61

Chapter IV

Section 1. A System for the Meteorological Use of Satellite Television Observations

1.1 Introduction 63

1.1.1 General 63

1.1.2 Objectives of the Program 66

1.1.3 Scope of the Program 66

Page

1.1.4 General View of Procedures 67

1.2 Perspective Rectification 68

1.2.1 The Problem 68

1.2.2 Facilities for Picture Location 69

1.2.3 Perspective Grids 70

1.2.4 Procedures for Perspective Rectification 75

1.3 Mapping 77

1.3.1 Map Selection 77

1.3.2 Mapping Procedures 79

1.4 Equipment 81

1.4.1 Projectors 81

1.4.2 Light Box 83

1.5 Data Abstraction and Interpretation 83

1.5.1 Recognition 83

1.5.2 Abstraction 84

1.5.3 Early Trials 86

1.6 Codification and Data Transmission 86

1.6.1 Codification 86

1.7 Emergency Procedures 87

1.7.1 Establishment of Location with Certain Data Missing 87

1.8 Recommendations for Future Activities 88

1.8.1 Suggestions as to Improved Techniques 88

Section 2. A Photogrammetric Method of Obtaining the Camera Axis and Its Application in Determining the Time of Photographs Taken from a Space Vehicle 93

2.1 Introduction 93

2.2 Description of the Techniques 94

2.3 Conclusion 98

Page

Chapter V

Section 1. Synoptic-Scale Radiation Processes 101

1.1 Introduction 101

1.2 Radiation Budget of the Ozonosphere 103

1.3 Radiation Budget of the Troposphere 105

1.4 Vertical Profile of the Infrared Radiation Balance 106

1.5 Cloud Distribution and its Effects on Atmospheric Radiation 106

1.6 Effect of Surface Temperature on the Atmospheric Radiation Balance 107

1.7 Use of Radiation Data Obtained by Satellites 108

Section 2. Studies of Atmospheric Radiation as Observed from Satellites 109

2.1 General 109

2.2 The Fundamental Radiation Transfer Equation 111

2.3 Case I 113

Section 3. A Preliminary Investigation of the Nature of the Infrared View of the Earth's Atmosphere from a Satellite 115

3.1 Introduction 115

3.2 Radiation Source in the Atmosphere 116

3.3 A Heuristic Approach 121

3.4 Synoptic Behavior of Water-Vapor Infrared Emission 130

Section 4. Satellite Observations of Infrared Radiation 153

4.1 Introduction 153

4.2 Atmospheric Transmission in the Infrared 155

4.2.1 Division of the spectrum 155

4.2.2 Radiation theory 156

Page

4.2.3 6.3μ H_2O band 158

4.2.4 Rotational water 160

4.2.5 mP for H_2O 161

4.2.6 15μ CO_2 162

4.2.7 4.3 and 4.8μ CO_2 164

4.2.8 Ozone band 164

4.3 Infrared Maps for 0000Z, 6 March 1959 167

4.3.1 Weather Map 167

4.3.2 The Window Map 169

4.3.3 Temperatures in the Stratospheres 172

4.3.4 The 6.3μ H_2O band 173

4.3.5 The 15μ CO_2 band 173

4.3.6 The 4.3μ CO_2 band 176

4.3.7 The ozone band 176

4.4 Conclusion 179

Section 5. Detection of Ozone Amounts from Satellite Measurements 181

5.1 Introduction 181

5.2 Theory 182

5.3 Calculations 185

5.4 Discussion 186

Chapter VI 191

Section 1. A Generalized, Schematic Flow Chart for the Reduction and Processing of Satellite Meteorological Data 191

1.1 Introduction 191

1.2 Types of Data and Initial Recording 192

Page

1.2.1 Types of Data 192

1.2.2 Orbit tracking and attitude data 194

1.2.3 TV data 194

1.2.4 Radiation data 195

1.3 Transmission to Processing Centrals 195

1.4 Analysis and Use of Tracking and Attitude Data 196

1.5 Reduction and Processing of Visual Data 196

1.5.1 Photographically Recorded Data 196

1.5.2 Semi-quantitative photographic data 198

1.5.3 Quantitative TV Data 198

1.5.4 IR TV Data 199

1.6 Reduction and Processing of Radiation Data 199

1.6.1 Pictorial presentations 199

1.6.2 Semi-quantitative presentations 200

1.6.3 Quantitative, digital presentations 200

1.7 Distribution of Use of the Processed and Presented Satellite Meteorological Data 201

1.7.1 Research Use 201

1.7.2 Weather Analysis and Forecasting Use 202

1.7.3 Climatological Use 202

1.8 On-Board Analysis 202

1.9 Conclusion 203

Appendix A. Perspective Grids 205

Appendix B. Accuracy Requirements for Perspective Grid Library 209

Appendix C. Mapping 223

Appendix D. Interpretive Abbreviated Plain Language Code 231

Appendix E. A Manual of Emergency Computational Procedures 239

References 259

LIST OF ILLUSTRATIONS

Figure No.			Page
Chapter II	- 1	Cloud cover as viewed from an Atlas Missile at a height of approximately 450 statute miles	11
	- 2	Cloud cover as viewed from an Atlas Missile at a height of approximately 750 statute miles	12
	- 3	Cloud cover as viewed from an Atlas Missile at a height of approximately 750 statute miles	13
Chapter III	- 1	Nephanalysis, 1800Z, 24 August 1959	25
	- 2	Examples of Frequency Distributions of Total Sky Cover	27
	- 3	Surface streamline chart, 1200Z, 24 August 1959	34
	- 4	250mb (35,000 feet) streamline chart, 1200Z, 24 August 1959.	35
	- 5	Cloud distribution, 1600Z, 24 August 1959	37
	- 6	Photo toward 325° from an altitude of 484 miles	40
	- 7	Photo toward 151° from an altitude of 690 miles	41
	- 8	Measuring cloud velocity "v" by using ground distance	48
	- 9	Similar triangles used in deriving "v" for Case I	49
	- 10	Similar triangles used in deriving "v" for Case I	50
	- 11	Measuring cloud velocity by using angle measurement	54
	- 12	Top view of cloud and satellite in Case III	57
	- 13	Side view of cloud and satellite in Case III	57
Chapter IV	- 1	Perspective Grid	71
	- 2	Transfer Grid	72
	- 3	Transverse Mercator Chart	80

Figure No.			Page
Chapter IV	- 4	Use of Projector for Superimposition of the Image on the Perspective Grid	82
	- 5	Sketch showing method of locating principal line on space vehicle photograph	96
	- 6	Frame number vs time for Atlas 11c photographs	99
	- 7	Frame number vs azimuth for Atlas 11c photographs	99
Chapter V	- 1	The calculated height of the effective emission layer	111
	- 2	Calculated distribution of intensity of radiation from water vapor in the atmosphere over Southern England, 19 January 1954	120
	- 3	Total equivalent water path length vs altitude in the atmosphere over Southern England, 19 January 1954	123
	- 4	Total equivalent water path length and dewpoint temperature vs. altitude in the atmosphere over Southern England, 19 January 1954	125
	- 5	Observed rate of increase of equivalent water path length with depth vs dewpoint temperature	127
	- 6	Observed rate of increase of equivalent water path length with depth vs temperature corresponding to data of Figure 5	128
	- 7	Distribution of Temperatures associated with the -30°C dewpoint	129
	- 8	Distribution of Radiation associated with the -30°C dewpoint	129

Figure No.		Page
Chapter V - 9	0300Z, 26 April 1955, temperature at 0° dewpoint surface	132
- 10	Surface map, 0630Z, 26 April 1955	133
- 11	0300Z, 26 April 1955, temperature at -20° dewpoint surface	134
- 12	500 mb chart, 26 April 1955, 0300Z	136
- 13	0300Z, 27 April 1955, temperature at 0° dewpoint surface	137
- 14	Surface map, 0630Z, 27 April 1955	138
- 15	0300Z, 27 April 1955, temperature at -20° dew-point surface	139
- 16	500 mb chart, 27 April 1955, 0300Z	141
- 17	0300Z, 28 April 1955, temperature at 0° dewpoint surface	142
- 18	Surface map, 0630Z, 28 April 1955	143
- 19	0300Z, 28 April 1955, temperature at -20° dewpoint surface	144
- 20	500 mb chart, 28 April 1955, 0300Z	145
- 21	0300Z, 29 April 1955, temperature at 0° dew-point surface	147
- 22	Surface map, 0630Z, 29 April 1955	148
- 23	0300Z, 29 April 1955, temperature at 20° dewpoint surface	149
- 24	500 mb chart, 29 April 1955 0300Z	150
- 25	Transmission for 6.3μ H_2O from Howard's data	159
- 26	Distribution of q and mP for standard atmos-phere above 400 mb. (Murgatroyd's observations are indicated by x).	163

Figure No.		Page
Chapter V - 27	Transmission for 6.3μ H_2O above 45°mb for standard (S) and tropical (T) atmosphere of air mass 1.	163
- 28	Transmissions for 15μ CO_2 for air masses 1, 2 and 3.	165
- 29	Transmissions for 4.3μ CO_2 for air masses 1, 2 and 3.	165
- 30	Transmissions for 4.8μ CO_2 for air masses 1, and 2 and 3.	166
- 31	Transmissions for O_3 (1100-1200 cm^{-1})	166
- 32	Surface Map for 0000Z, 6 March 1959.	168
- 33	"Window" Map for 0000Z, 6 March 1959, showing Temperatures at Cloud Top or at the Surface (for clear skies).	170
- 34	Equivalent Isotherms for 6.3μ H_2O Band, Air Mass 1, 0000Z, 6 March 1959. Equivalent Temperatures for Air Mass 1, 2 and 3 are plotted according to the model:	174
- 35	Equivalent Isotherms 15μ CO_2 Band, Air Mass 1, 0000Z, 6 March 1959.	175
- 36	Equivalent Isotherms 4.3μ CO_2 Band, Air Mass 1, 0000Z, 6 March 1959.	177
- 37	Equivalent Isotherms 9.6μ O_3 Band, Air Mass 1, 0000Z, 6 March 1959.	178
- 38	Variation of ratio of scattered radiation at .311μ to that at .329μ vs total mass of ozone in the atmosphere.	187

Figure No.			Page
Chapter V - 39		Slant path length correction factor (X)	188
Chapter VI- 1		Block Diagram - Schematic Data Reduction and Processing System	193
Appendix B.	- 1	Schematic of Nomenclature	210
	- 2	Location Errors for Lens Angle of $+25^{\circ}$	213
	- 3	Location Errors for Lens Angle of $+45^{\circ}$	213
	- 4	Location Errors for Lens Angle of -25°	214
	- 5	Location Errors for Lens Angle of -45°	215
	- 6	Location Errors for Lens Angle of -52.5°	216
	- 7	Location Errors for Lens Angle of $+30^{\circ}$	218
	- 8	Location Errors for Lens Angle of $+45^{\circ}$	219
	- 9	Location Errors for Lens Angle of $+52.5^{\circ}$	219
	- 10	Location Errors for Lens Angle of -30°	220
	- 11	Location Errors for Lens Angle of -45°	221
	- 12	Location Errors for Lens Angle of -52.5°	222
Appendix C.	- 1	Arc-to-Chord Correction	224
	- 2	Relative Scales of Selected Maps	227
Appendix E	- 1	Emergency Manual Worksheet Headings	243
	- 2	Emergency Manual Worksheet Headings	244
	- 3	Correction for Lens Distortion	246

CONTRIBUTIONS TO SATELLITE METEOROLOGY

CHAPTER I*

INTRODUCTION

1 BACKGROUND AND OBJECTIVES

For several years the Satellite Meteorology Branch of the Atmospheric Circulations Laboratory, Geophysics Research Directorate has been conducting an increasingly active program in the use of satellite observations for meteorological research and for the improvement of weather analysis and forecasting. The results of the earlier portions of this program, both in-house and contractual, have been published in scientific journals or in contractor's technical reports [1-6].

Early in 1959, support provided by the Advanced Research Projects Agency through ARPA Order No. 26-59 permitted a very significant expansion and acceleration of this program. At the same time, data from primitive meteorological satellites, and especially from high-altitude vehicles (particularly the cloud photographs from ballistic missile nose-cone tests) which provided data closely simulating that to be expected from satellities, made it possible to focus the program. Incentive was provided by definitive plans for relatively sophisticated meteorological satellites scheduled to be flown in the near future. (The first such vehicle is expected to be in orbit prior to the publication of this report.)

---

* This Chapter was written by William K. Widger, Jr., of the Geophysics Research Directorate, and A. H. Glaser and G. Cooper of Allied Research Associates, Inc.

(Authors' manuscripts approved for publication 2 May 1960.)

The first technical results of this accelerated program are now available and are being published here to acquaint the meteorological community with a relatively recent view of the opportunities satellite data will provide and the problems it will present. Also included are certain papers that were written in the earlier stages of the work but, for various reasons, were not published at that time. Few, if any, of the papers presented here should be considered as final results; nevertheless it is felt that, as a collection representing some measure of the present state-of-the-art, their combined value is such as to merit wider distribution that the work has gotten to date. If they in some degree interest and challenge those who are not now closely connected with the field, a major objective will have been served.

2 A CONCEPT OF A METEOROLOGICAL SATELLITE SYSTEM

A meteorological satellite system may be viewed as a connecting link between the real atmosphere and an operational or research user of meteorological information. It is primarily distinguished from otherweather-observing systems by the use of the satellite as a vehicle for carrying the meteorological sensors and by having the sensing elements remote from the atmosphere. Other distinctions between a meteorological satellite system and conventional weather-observing systems are natural consequences of the vehicle properties.

Recognizing that a meteorological satellite system is a weather-observing system, its only purpose then is to abstract and transfer information from the atmosphere to the consumer. The information presented to the consumer is only useful insofar as it serves a purpose. Ideally the meteorologist should always

have available the appropriate information to permit a definitive answer to each decision that may be required. Any information provided beyond this requirement is superfluous.

The function of the satellite meteorological system is thus to abstract from the atmosphere those events which are of importance to the activities of the consumer and to transmit to the consumer information on those events in unambiguous fashion. The most efficient and effective system will be the one that provides this service and no more. Appropriate system design will thus depend on detailed knowledge of the needs of the meteorological consumer and knowledge of the observational material available from the atmosphere to satisfy these needs. Actual design of the system then becomes a matter of arranging the transfer of this information in the most expeditious fashion.

Accordingly an analysis of meteorological satellite systems should be devoted to an examination of the various aspects of the information transfer process. Starting at the consumer and working back towards the information source in the atmosphere, the information transfer process may be divided into the following broad categories for study purposes:

a. Applications of Meteorological Satellites
b. Data Processing and Interpretation
c. Data Storage and Transmission
d. Orbital Sampling Characteristics
e. Sensors and Sensor Techniques

3. A PREVIEW

It is not our intention to imply that this report adequately covers each of the above broad categories, nor even that it specifically treats each of them. To date, there just has

not been enough time or information to prepare the "full-course banquet" for which the list in Section 2, above, could be considered an outline menu. Rather, this report provides a sample of and, hopefully, a look towards things to come.

Chapter II presents a survey of the applications that seem possible, using data expected from meteorological satellites, and suggestions as to possible means of using satellite observations to derive more common meteorological parameters. While it is essentially solely a survey of material already in the literature and, as such, contains nothing really new, it is of value as a general consolidation of widely separated material and provides a handy index to the original references.

Chapter III considers the visual observations of greatest probable value, cloud systems and cloud patterns. Section 1 of Chapter III treats large-scale cloudiness while Section 2 considers more detailed cloud patterns using photographic data provided from a recent nose-cone test. Section 3 analyzes the problem of observing cloud motions as indicators of the wind velocity, unfortunately with rather negative results.

Chapter IV presents, in Section 1, a method for geographically locating the pictures of the earth and clouds; this is a routine but necessary preliminary to any useful analysis. The procedures are described in the chapter, itself, while their derivations are included in the five appendices to this report. Section 2 discusses a technique for locating the geographical position in those cases where recognizable features are seen and the physical position of the satellite, but not the orientation, is known.

In Chapter V we turn from visual observations to those in the infrared and ultraviolet spectra, which are expected in due course

of time to be equally valuable. Sections 1 and 2 give two somewhat different general views of synoptic-scale radiative processes. Presented in Section 3 is a preliminary investigation of how the atmosphere would be expected to appear when viewed in the 6.3-micron water-vapor band; the approach is simplifed and heuristic. Section 4 also considers the appearance at 6.3 microns but on a more exact basis; it further investigates the patterns to be expected in the 8 to 12-micron water-vapor window, the 15 and 4.3- micron carbon dioxide bands, and the 9.6-micron ozone band. Section 5 suggests a possible method for determining ozone amount from a satellite, using measurements in the vicinity of 0.3 microns.

Chapter VI discusses the various steps and processes that must be considered in designing a system for the over-all reduction and processing of satellite meteorological data.

Blank page retained for pagination

CHAPTER II

APPLICATIONS OF METEOROLOGICAL SATELLITES*

To establish the requirements of the consumer of meteorological satellite data, it is necessary to investigate the possible applications of such data. Since there is an abundant literature in this field, a survey provides a picture of at least some of the consumer information requirements. This literature also provides some suggestions relating to the design of the satellite meteorology system.

1. A SURVEY OF APPLICATIONS OF METEOROLOGICAL SATELLITES

1.1 Introduction

The following section is concerned with some phases of the use of a meteorological satellite. Selected material from a litereature search has been integrated with the applicable findings and experience obtained from closely associated fields of study. An attempt has been made to avoid extremely generalized and all-inclusive statements about the utilization of a satellite for meteorological investigations.

The discussion of meteorological parameters in Section 1.4 contains references to literature which makes some specific suggestions as to methodology and/or instrumentation.

Supplementary and/or complementary information concerning applications for meteorological satellites will be available in the future. It is anticipated that scheduled experiments will provide

---

* This work was sponsored under Contract No. AF19(604)-5582, under ARPA Order No. 26-59. The Chapter was written by A. L. Goldshlak, Allied Research Associates, Inc.

additional information concerning various aspects of satellite meteorology.

1.2 Planetary Parameters

1.2.1 The Solar Constant

"The ultimate source of thermal energy for the earth's atmosphere is the incident solar radiation, and we must know its precise form outside the limits of the atmosphere."[7] The presently accepted value of the solar constant is approximately 2 ly min^{-1}. The measurement error is of the order of 2 percent and is largely attributable to uncertainties in the assumptions used to correct the measurements for atmospheric effects.

An earth satellite orbiting above the atmosphere and equipped with a bolometer pointing towards the sun could measure the solar constant directly. Daily measurements over a long period of time could provide the research worker with answers to the following questions: Is the solar constant a true constant? If not, how much does it vary? Observers at the Smithsonian Institute claim that the value of the solar constant actually varies by 1 or 2 percent. This claimed value is of the same order as the present measurement error; therefore, it cannot be verified through current measurement techniques.

1.2.2 The Planetary Albedo

The planetary albedo of the earth "...plays a critical role in the radiation budget of our planet and thus in specifying the manner in which the general circulation of the atmosphere must operate to balance this budget."[8]

Various indirect methods have been used [9] in an attempt to determine the planetary albedo. The best determination of

the planetary albedo would be accomplished by measuring it directly through extraterrestrial means. Appropriate photocell sensors mounted on a satellite can provide a direct total albedo value. Godson [8] suggests the utilization of a television sensor to determine the visual albedo of the earth. He also suggests an orbit of 4000 miles (period of about 4 hours) with a high resolution system.

1.2.3 General Circulation of the Earth

The general circulation of the earth is fundamentally driven by the radiation balance between the earth and outer space. Godson [8] suggests that this balance be measured continuously as a function of space and time.

Differentiation between radiation in the various frequencies is necessary for proper interpretation of the radiation balance. A pair of parallel-plate radiometers with surface absorptions which vary with wavelength is the satellite instrumentation suggested by Godson.

The energy balance of the earth and atmosphere can be formulated separately if synoptic cloud images are available and the individual energy components of the radiation budget are known.

1.2.4 Global Cloud Climatology — Cloud Albedo

The cloud albedo provides the greatest contribution to the planetary albedo. Different types of clouds and cloud combinations contribute in varying amounts to the total cloud albedo, depending on the optical properties of the clouds, cloud thickness, and the zenith angle of the sun.

As a result of the importance of cloud albedo, it is strongly urged that a global cloud climatology be assembled. [2, 10] To facilitate associated avenues of future research, the cloud climatology should be divided into continental and oceanic areas. Further sub-

division into diurnal and seasonal variations are also desirable.

A reconnaissance satellite equipped with relatively simple instrumentation such as a television camera would be adequate for initial studies. Inspection of the photographs taken from the Atlas 11C (24 August 1959) nose cone reveals the feasibility of determining cloud cover over large areas from high-altitude pictures. Figure 1 is a photograph of the earth taken at an altitude of about 450 miles; Figs. 2 and 3 were taken from an altitude of about 750 miles over a different sector of the earth. The cloud cover is readily visible on these photographs. *

Reliable determination of cloud types would require a high-resolution (at least 1000 lines per frame) television camera. The desired cloud scale and cloud detail would dictate the resolution required as a function of satellite altitude. Minimum orbital heights would be appropriate for observations of cloud types. Cloud cover information may also be obtained from higher orbits.

A report by Glaser [2] deals with the recognition of cloud forms from a satellite. Of particular interest in that report is the section on the significance of large-scale reflectivity patterns. In addition, Glaser has tabulated typical reflectivity values for various cloud cover combinations.

One of the great advantages of utilizing a system of satellites for cloud reconnaissance (as well as for other meteorological parameters) will be the ability to obtain nearly simultaneous measurements over large areas of the earth [11]. Since the life period

---

* For a more detailed discussion of this case, see also Chapter III, Section 2, of this report.

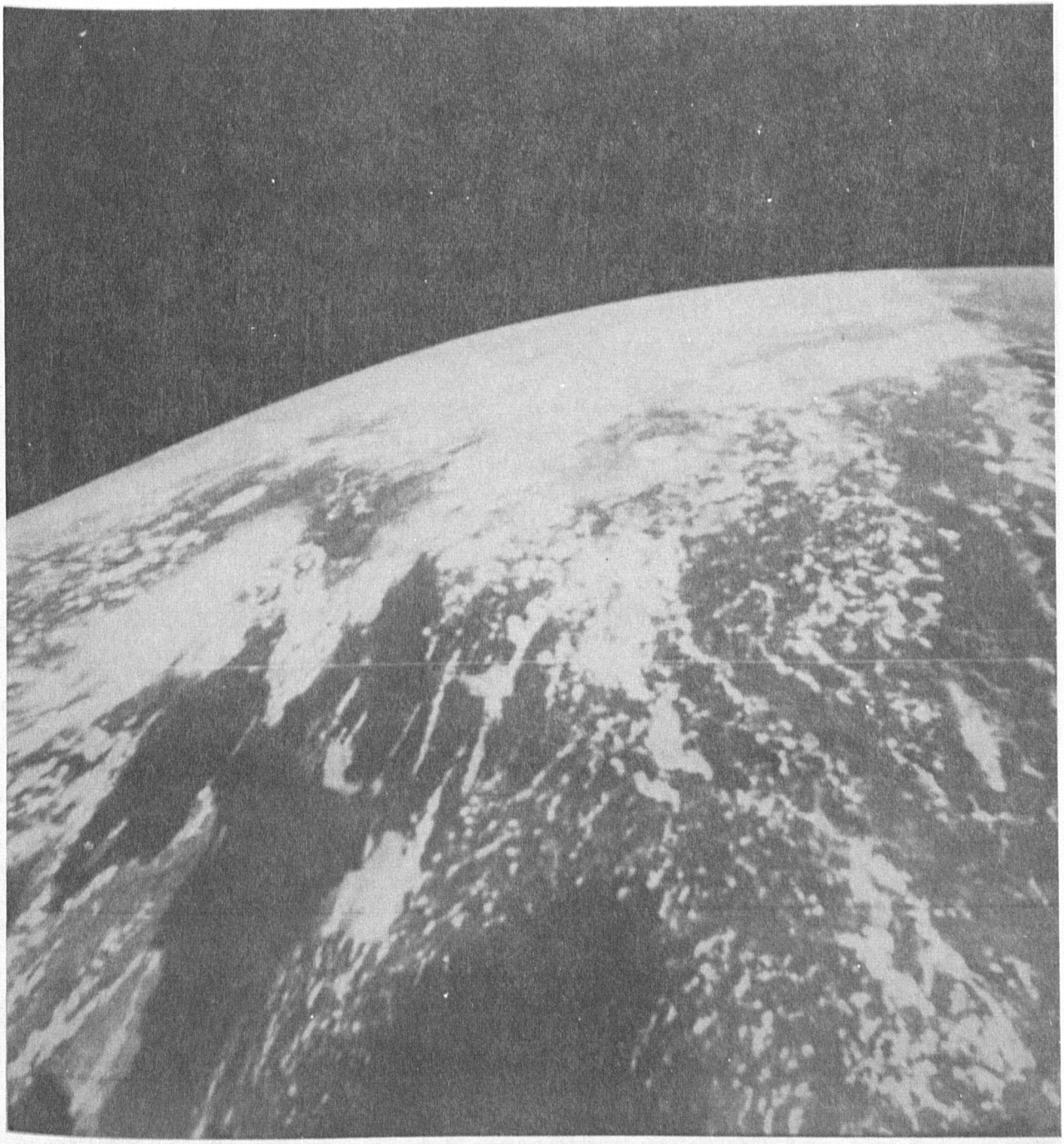

Fig. 1 Cloud cover as viewed from an Atlas Missile at a height of approximately 450 statute miles

Fig. 2 Cloud cover as viewed from an Atlas Missile at a height of approximately 750 statute miles

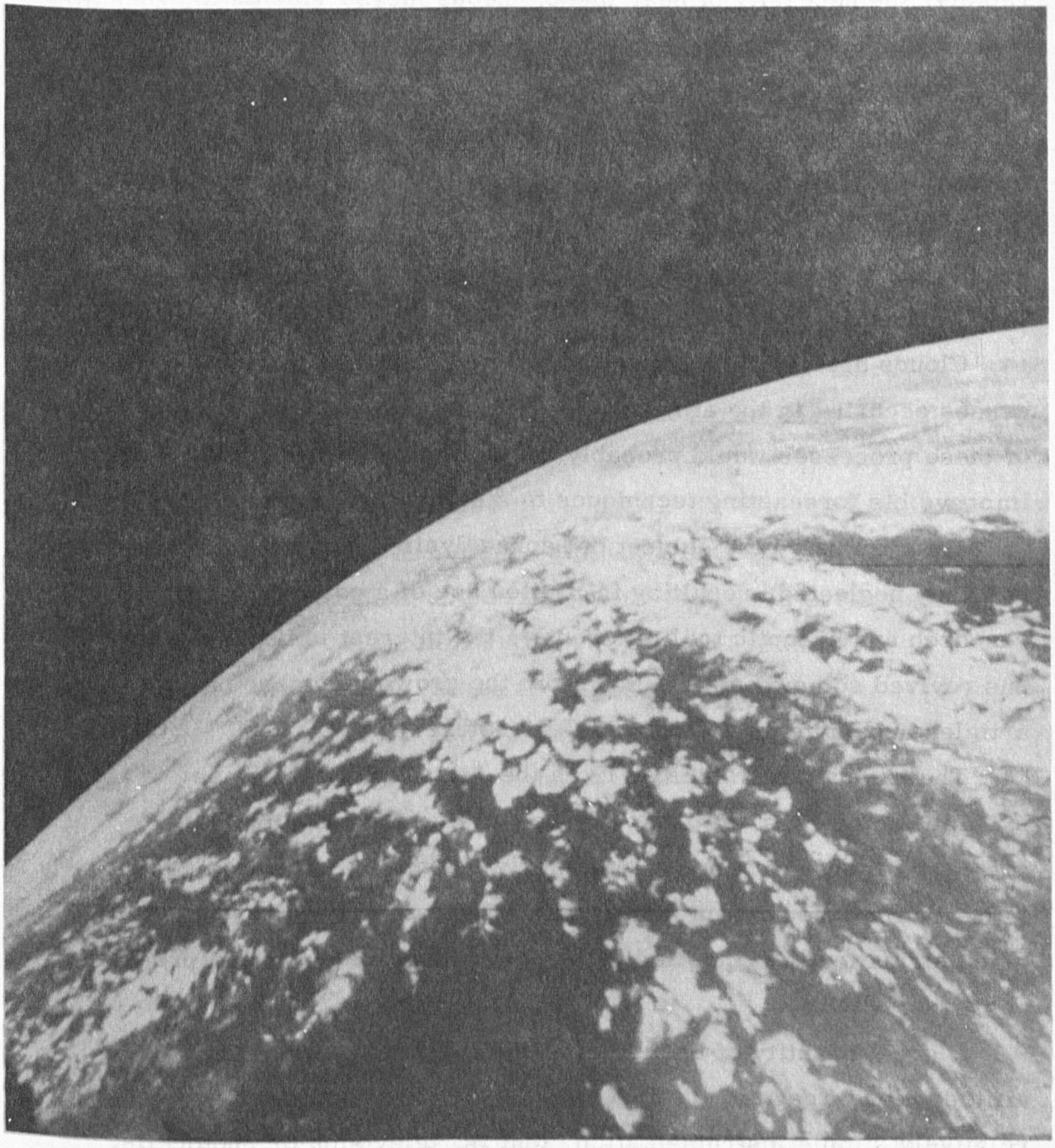

Fig. 3 Cloud cover as viewed from an Atlas Missile at a height of approximately 750 statute miles

of clouds is relatively short and cloud transformations can occur rapidly, the necessity of near instantaneous measurements is desirable. Furthermore, it is extremely difficult, if not impossible, for a surface-stationed observer to obtain a valid image of an entire cloud system, with the exception of very small-scale or local phenomena.

The photographs shown in Figs. 1, 2, and 3 present an entirely novel and most useful image to the meteorologist.

1.3 Nephanalysis

Clouds are visible evidence of physical and dynamical processes occuring in the atmosphere. A complete understanding of these processes would probably enable the meteorologist to improve his forecasting techniques to a significant degree.

Unfortunately, the subject of nephanalysis (cloud analysis) has been neglected, resulting in limited use of a potentially fertile research and synoptic tool. Recently, the interest in nephanalysis has revived somewhat, as noted from the growing number of articles appearing in the technical literature.

The photographs obtained from the Atlas 11C missile, as exemplified by Figs. 1, 2, and 3, reveal that the cloud patterns are certainly not random. The orderly orientation of cloud patterns in bands and streaks (on many scales) indicate that large-scale cloud formation is controlled by some physical or dynamical processes.

A great quantity of useful data can be extracted from high-altitude cloud images [2, 4, 5, 10, 12, 13] through the use of relatively simple instrumentation, that is, television or photocells. Admittedly, the initial data reduction will most probably be of the

semi-quantitative form. Improved data "quality" may be anticipated with advanced technology. The utilization of cloud data obtained from a satellite will be valued by both the synoptician and the researcher.

A report by Goldshlak, Boucher, and Glaser [10] was prepared to organize the miscellaneous aspects of cloud-weather relationships. The form of the report is such that it may be used as a manual for extracting meteorological information from a cloud field. The report also contains a case study comparing the nephanalysis with conventional synoptic analysis.

Another report by Glaser [2] illustrates some of the more quantitative aspects of cloud analysis techniques from high-altitude reconnaissance.

No attempt will be made here to repeat all the material available in References 2, 10 and 12; instead, a tabular listing of the information capable of being extracted from cloud images is presented.

A Identification of Synoptic Systems

1. Extra tropical cyclones
2. Anticyclones
3. Hurricanes
4. Fronts
5. Easterly waves
6. The westerly trough
7. Intertropical convergence zone
8. Squall lines
9. Shear line
10. Thunderstorms

B Climatologies -- Annual, Seasonal, Diurnal

1. Global cloud atlas
2. Cloud types

3. Cloud cover
4. Source regions of storms
5. Storm tracks
6. Snow cover
7. Atmospheric pollutants

C. Dynamics
1. Waves
2. Convergent areas
3. Divergent areas
4. Wind fields -- wind shear -- jet stream

D Thermodynamics
1. Convective areas
2. Turbulence
3. Stability
4. Humidity
5. Advection

E Research Requirements
1. Cloud formation and dissipation
2. Cloud dynamics
3. Improved cloud-weather inferences

1.4 Some Specific Meteorological Parameters

1.4.1 Cloud Velocities

Aiken and Widger report in Chapter III, Section 3, on the possibility of measuring cloud velocities from cloud images obtained from satellites. The authors show that the measurement accuracy required to determine cloud speeds to within $\pm$ 10 mph cannot be obtained in practice. The meteorological value of cloud velocities in error by more than 10 mph is minimal.

Other suggested methods for determining cloud velocities are by the use of parallax or multiple sightings over small time intervals. These require phenomenal accuracy of satellite orientation.

1.4.2 Ozone

An interpretation of the vertical distribution of ozone can be made from observations of scattered UV radiation at various wavelengths since the ozone absorption coefficient (Hartley Band) varies more rapidly with wavelength than does the coefficient of molecular scattering.

Singer and Wentworth [14] discuss a method for determining the vertical ozone distribution from a satellite, utilizing the optical absorption properties of ozone near 2900 A^{o}. A method of measuring total ozone mass by a comparison of scattered UV radiation at two wavelengths (3110 and 3290 A^{o}) is discussed in Chapter V, Section 5, of this report.

Below 30 km, ozone has a relatively long lifetime; therefore, ozone concentrations may be used as an indication of air-mass motion.

1.4.3 Stability

Cloud street spacing may be used as an indication of the depth of the overturning layer [15]. In temperate latitudes the presence of streets indicates a lapse rate which is near dry adiabatic from the surface to the cloud level.

1.4.4 Temperature

Kaplan [16] outlines a method of determining a three-dimensional distribution of atmospheric temperature by obtaining spectral measurements of radiation in the 15μ carbon dioxide band. The carbon dioxide band is preferred to the water-vapor bands

because the carbon dioxide in the atmosphere is uniformly distributed, whereas the distribution of water vapor is variable.

The radiation in the far wings of the carbon dioxide spectrum emanates largely from cloud tops or from the ground. Observations of this portion of the spectrum might be obtained with a sensor mounted on a balloon or aircraft at 100 mb or above. However, measurement at the dense center of the band would be pointless at these altitudes since considerable atmosphere still exists at greater heights. A satellite orbits at sufficient altitude so that it can receive the emission from the "effective" top of the atmosphere. Then, the center of the 15μ band could be clearly interpreted as emission from the highest emitting layers of the atmosphere.

After establishing the emission from the top and bottom (ground) of the atmosphere, additional layers within the atmosphere may be determined, since "...different fractions of the black-body radiation are received from the various intervening air layers."[16].

The suggested sensing instrument is a multiple-slit or multiple-detector grating spectrometer capable of resolving 10 cm^{-1} at 15μ. Rather complicated calculations are required to reduce these observations to actual temperature distributions.

1.4.5 Moisture Distribution

Moisture measurements [16] could be made simultaneously and through the same optics as the temperature measurements (see Section 1.4.4). The water-vapor emission may be interpreted in terms of the moisture distribution once the temperature distribution is known.

Surface and cloud-top measurements measurements may be obtained at 11μ; stratospheric humidity from the 24μ peak (with

additional detail if measurements can reach 40μ). Humidity at the lower heights can be measured at shorter wavelengths.

Some quantitative aspects of humidity measurements are discussed in Chapter V, Sections 3 and 4, of this report.

1.4.6 Visibility

Balloon techniques for determining visual range have been extended for possible use on a satellite vehicle. Stakutis and Brennan [17] discuss some methods for visual range measurements and required satellite instrumentation. The Weston photronic barrier-layer cell is proposed as the essential portion of the instrumentation. Provisions for increased sensitivity of the sensor elements can be made for adaptation to the higher altitude conditions necessitated by satellite carriers.

Visibility is an air-mass characteristic and may therefore be used for air-mass identification purposes. Visibility may also be used as an index of air pollution. A knowledge of visibility conditions has further application in military decisions and transportation.

1.4.7 Winds

The report by Goldshlak, Boucher, and Glaser [10] presents a case study in which both low- and high-level winds were inferred as a part of the synoptic analysis determined from a mosaic of cloud images. Although no isolated cloud can, at present, provide conclusive wind information, the meteorologist can make good wind-direction inferences from a knowledge of the cloud field associated with synoptic systems .

As an example of wind inferences from cloud patterns, the presence of cumulus cloud streets are indicative of the wind direction (parallel to the streets) at the cloud street levels. However, the wind direction may be ambiguous by 180 degrees. The correct

wind direction can usually be established from other significant features.

Widger and Touart [1] suggest that some estimates of low-level wind speed and direction may be deduced from visible atmospheric pollutants. Over large water bodies the state of the sea surface may also provide surface wind information.

Although some general methods appear to be available for determining wind directions, the problem of determining wind speeds with sufficient accuracy for meteorological application still exists.

1.4.8 Jet Stream

Certain cloud patterns, that is, banded cirrus or cirrus sheets with sharp edges, may be used as aids in locating the jet stream. "Wide belts of cirrus with a clear space or zone of cirrocumulus between indicate a jet to the north of the northermost cirrus belt and another just south of the break in the cloud. Pronounced bands of cirrus oriented from the southwest indicate jets which are rapidly moving eastward; 'streaky' cirrus suggests double jets which are not migrating appreciably sidewise."[15]

The above statements, extracted from a report by Conover [15], may apply only to the section of southern New England where the observational sites for the investigation were located. Further investigations of a similar nature (throughout the atmosphere) could be most efficiently accomplished by satellite reconnaissance.

1.5 Useful Meteorological Orbits

Singer [11] considera a polar orbit as one of the most useful for a meteorological satellite. Such an orbit would permit the scanning of the entire earth's surface, thus obtaining global data.

H. Wexler [18] suggests that an orbit 4000 miles above the earth's surface would be satisfactory for a television satellite. Full advantage of a high-resolution television camera may then be obtained. It should be pointed out that orbits closer to the earth will probably be necessary, depending on the required observational detail.

Other useful satellite orbits and area-of-coverage problems are discussed by Dryden [3]. He states that the apparent longitudinal displacements (on the earth) of an orbit fixed in space may be used advantageously for tracking mid-latitude systems. The variable orbital " . . . displacements for intervals of time shorter than a period do not seem to be important on a synoptic scale." Of greater importance is the ". . . varying range of visual observations and the changes in resolution resulting from the varying elevation. . ."

Blank page retained for pagination

CHAPTER III

SECTION 1

STUDIES OF LARGE-SCALE CLOUDINESS IN THE NORTHERN HEMISPHERE

Robert C. Curtis
Geophysics Research Directorate

1.1 Introduction

The work conducted during the recent past has consisted of studies of the large-scale cloudiness in the Northern Hemisphere and of small-scale cloud patterns as observed in photographs made from aircraft and missile nose cones. These later studies will be reported in the following section.

The nature and causes of the large-scale distribution of cloudiness that will be observed by the satellite are being investigated to establish the knowledge needed for interpreting and determining the utility of the satellite observations.

In addition, investigations have been started on the relationships of the large-scale cloud patterns to the synoptic features of the standard meteorological charts including the vertical velocities computed by the JNWP Unit, Suitland, Maryland and on the use of these cloud patterns in forecasting cloudiness.

1.2 Studies being Conducted

The following work has been completed:

The analyses of cloud cover and the occurrence of precipitation on the six-hourly Northern Hemisphere and the three-hourly North American weather charts have been completed for August through October 1959.

These analyses, besides providing background information on the large-scale cloudiness for use with studies of aircraft, rocket, and satellite pictures, are being used for studies of the relationships between large-scale cloudiness and such synoptic features of the atmosphere as cyclones, anticyclones, and upper troughs and ridges. The cloud analyses are also being used to determine the extent to which the large-scale features of the cloud distribution, namely, the large areas of essentially clear skies and the large areas of essentially overcast skies, can be used to make 24-hour forecasts of total sky cover (N) by simple extrapolation methods. These studies will be continued until an evaluation is completed for both a winter and a summer period.

Figure 1 exemplifies the simple analysis or large-scale cloudiness that is being used. This chart shows the North American area during the mid-day in summer when the large clear areas are at a minimum due to the cloud forming action of eddy-convection and diffusion of water-vapor from the surface. The analysis in the arctic regions is sketchy because of insufficient data. In the middle latitudes, however, the analyses is representative of all seasons and shows the large areas of essentially overcast skies which represent areas of large-scale convergence that will be visible in greater detail in satellite photographs.

Frequency distributions of the total sky cover (N) are being used as a basic tool for investigating the nature and causes of the large-scale distribution of cloudiness because their shapes can be interpreted in terms of the interaction of large-scale vertical motion and of eddy-convection and diffusion of water-vapor from the surface. Frequency distributions of total sky cover at 1200Z for 12 regions comprising the entire Northern Hemisphere have been

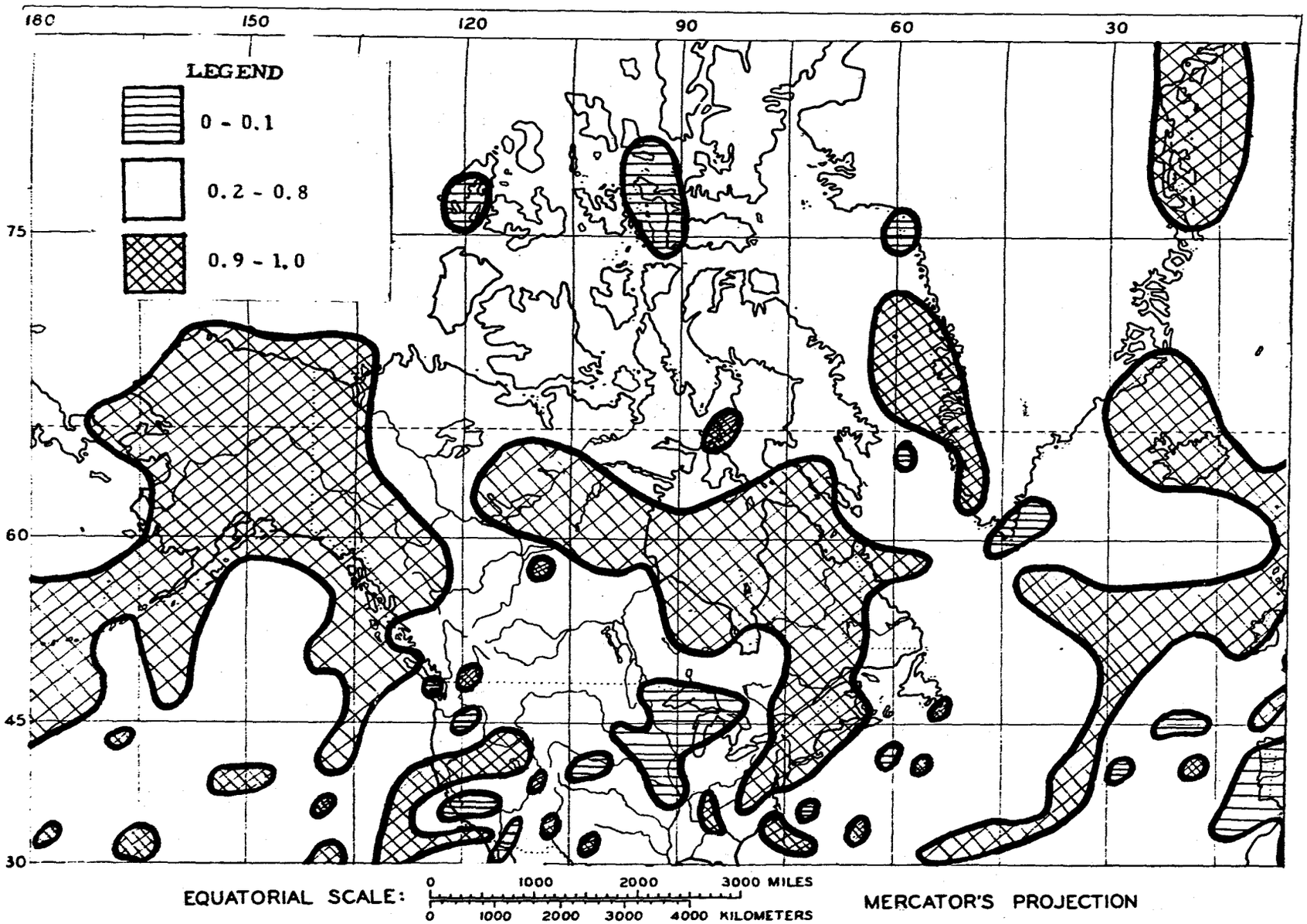

Fig. 1 Nephanalysis, 1800Z, 24 August 1959

tabulated and graphed for January, April, July, and October 1957. Studies of diurnal variation of the frequency distributions in various regions of the Northern Hemisphere have been started. Frequency distributions of total sky cover are also being used to investigate the extent to which the large-scale vertical velocities computed by the JNWP Unite, Suitland, Maryland indicate regions where cloudiness is reduced by downward motion and increased by upward motion. This has been done for the initial condition and 24-hour forecast vertical velocities during a 12-day period in September 1959; and it will be done for a winter and another summer period before an evaluation is made.

Figure 2 shows some examples of frequency distributions of (N) that are being used. The U-shaped frequency distributions are considered to be the result of large-scale vertical motion predominating over eddy-convection and diffusion of water-vapor from the surface. The frequency distributions which lack the left-hand mode show the production of partial cloudiness by eddy-convection and diffusion of water-vapor from the surface despite the cloud inhibiting action of large-scale downward motion.

Graphical records of the daily values of total sky cover at 1200Z for the year 1956 have been completed for 29 stations at various locations throughout the Northern Hemisphere. These are being used to study the characteristics of the daily changes of total cloud cover in various localities. Frequency distributions of (N) have been tabulated and graphed for each of these stations for the entire year and for the Winter, Spring, Summer, and Fall seasons. These data are being used with other tabulations of frequency distributions of (N) obtained from the National Weather Records Center, Asheville, N. C. to study the characteristics of local, short-term

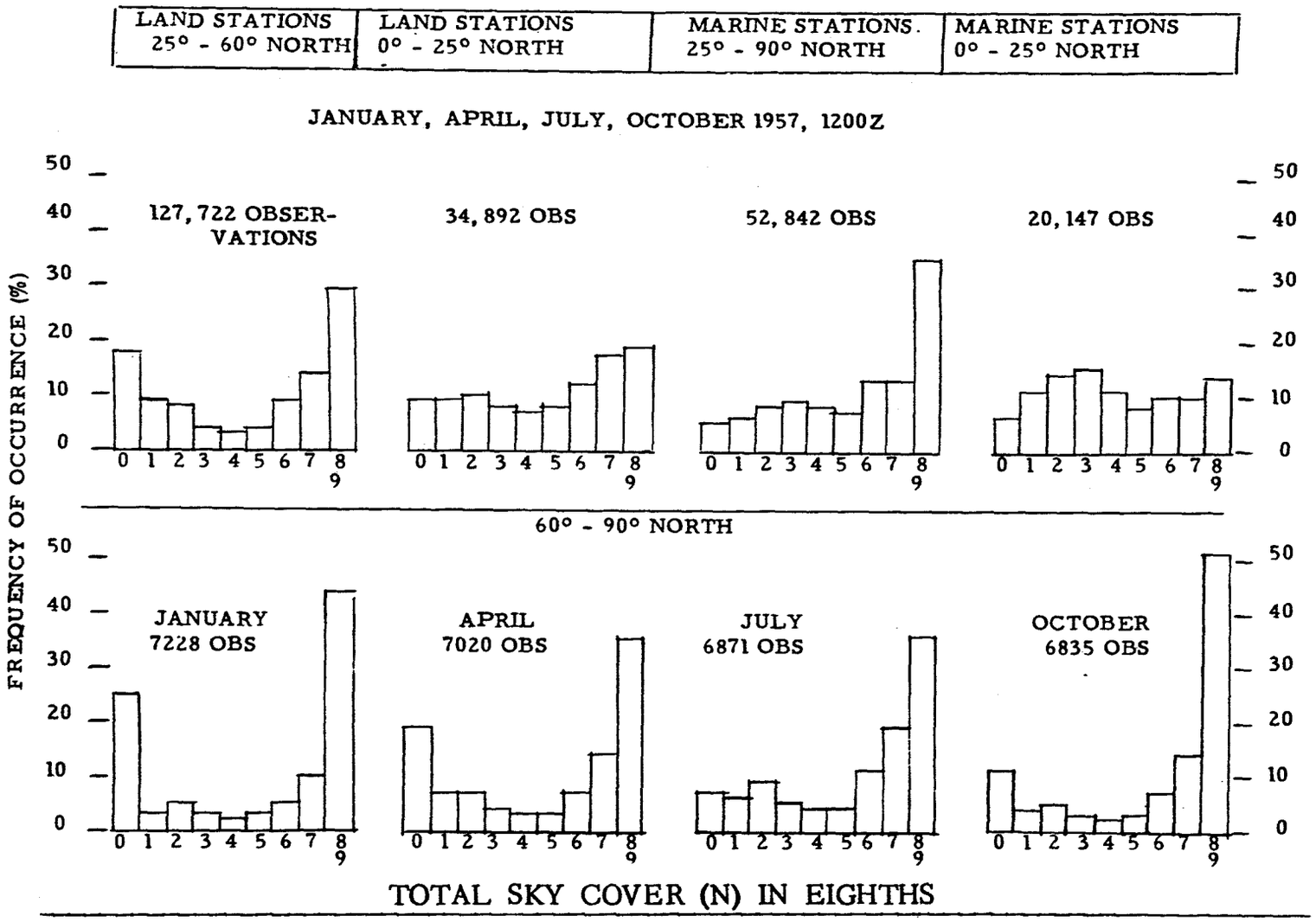

Fig. 2 Examples of Frequency Distributions of Total Sky Cover

(one year or less) and local, long-term (3 years or more) frequency distributions of total sky cover.

1.3 Results

The results to date indicate that the observed large-scale distribution of extensive and deep overcasts is primarily the result of large-scale vertical motion. The cloud-producing actions of eddy-convection and eddy-diffusion of water vapor from the surface appear to be dominated by the large-scale vertical motion, with upward motion producing regions of thick and essentially continuous cloudiness and downward motion producing regions of partial and generally thin cloudiness.

The principal conclusion of practical interest is that the large-scale cloudiness as observed from a satellite will show the patterns of large-scale convergence which will appear as patterns of marked brightness produced by reflection of sunlight from the deep and continuous cloudiness occurring in these areas. These areas contain all of the restricting weather conditions that are of operational importance and they appear to have sufficient continuity so that forecasts of cloudiness, precipitation, and generally restricting weather conditions can be made for periods of 24 hours or less simply by following the motions and changes in these areas. These forecasts will not be as accurate or as specific as those that can be made with conventional meteorological charts and forecasting methods in regions where large amounts of data are available. These forecasts, however, will be very useful in regions were conventional meteorological data are sparse or unobtainable.

Besides showing the patterns of convergence, the cloudiness will also indicate regions of large-scale divergence (subsidence). These regions will appear as the least bright areas which either

contain no clouds or only the partial and generally thin cloudiness which is produced by eddy-convection, turbulence, gravity waves, and other small-scale vertical motions. The regions of large-scale divergence contain the least restricting weather conditions. These regions also have sufficient continuity so that forecasts of generally favorable operational conditions can be made by extrapolation methods.

The ability to observe the large-scale patterns of convergence and divergence in terms of the distribution of cloudiness will provide meteorologists with a research tool that can be used to study the vertical circulations of the atmosphere, especially in the tropics which contain a large part of the atmosphere and where our knowledge of the vertical circulations is most limited.

The photographs taken from the nose cone of the Atlas missile on 24 August 1959 have provided some evidence for the validity of these ideas*. The regions of continuous deep cloudiness, and therefore of large average brightness, are considered to show essentially the patterns of large-scale convergence. These patterns are easily observed because they are in contrast with the areas of lesser average brightness that contain the partial and generally thin cloudiness produced by small-scale vertical motions in the absence of large-scale upward motion or in the presence of large-scale downward motion.

Figure 1 shows the large-scale cloudiness in extratropical regions at the time of the Atlas nose-cone photographs. The large-scale pattern of overcast skies shown on this chart over the Atlantic Ocean and East Coast region of the U.S. is essentially the same as that

---

* For a more detailed discussion of this case, see Section 2 of this Chapter.

seen in the photographs. The photographs, of course, present a much more complete and detailed view of these regions of extensive and deep overcast produced by convergence.

1.4 Interrelationships Between Studies of Large and Small Scale Cloudiness

To utilize small-scale cloud data received from satellites as an aid in weather analysis and forecasting, one must not only be familiar with known relationships between clouds and the associated dynamic state of the atmosphere but must acquire additional knowledge of this relationship and apply it to the interpretation of very high altitude photography.

The proper identification of clouds and interpretation of cloud patterns observed in high-altitude photographs were first attempted on cloud data which had been obtained from high-flying aircraft over the U.S. Later, photographs from high-flying aircraft over Europe became available for analysis. However excellent time-lapse films have been obtained recently from missile nose cones at 200 - 800 miles above the earth and emphasis has shifted to the analysis of these films.

CHAPTER III (Continued)

SECTION 2

CLOUD PATTERNS AS SEEN FROM ALTITUDES OF 250-850 MILES-PRELIMINARY RESULTS

John H. Conover and Major James C. Sadler
Geophysics Research Directorate

2.1 Introduction

In the late Spring and Summer of 1959 the Missile and Space Department of the General Electric Company succeeded in obtaining black-and-white 16mm time-lapse films of the earth from ballistic missiles flying down the Atlantic Missile Range. These films were made to record the attitude of the nose cones as various stabilization mechanisms operated during the flights. To meteorologists, especially those concerned with the interpretation of cloud patterns which will be transmitted from satellites, the clouds shown on the films were of great interest. In fact this by-product of another experiment may be regarded as the first step in a new direction of data collection and in the portrayal of "weather" in the science of meteorology. Therefore it is appropriate to show the results of the first work derived from the photographs even though much remains to be done.

2.2 Photography

The most striking of the four films which were obtained was that of 24 August 1959. During this flight, which was launched at about 1600Z, the nose cone containing the camera-bearing data capsule was separated from an Atlas rocket at 234 miles (all miles are statute) altitude and the photography began. The film

continued at a variable rate of about 3 frames per second for 10.1 minutes before ending as the nose cone approached apogee at 856 miles altitude and over a point about 2200 miles ESE of Cape Canaveral, Florida. During most of this portion of the flight the camera axis was aimed downward at angles between 16° and 26° from the horizontal as it rotated clockwise 5 1/2 times. Since the lens was of 5.7mm focal length the field of view was wide, amounting to about 90° across the diagonal in the specially-built camera. This combination of motion and wide field permitted complete coverage of the earth's surface out to the horizons in all directions as the camera traveled downrange. The photography is considered excellent*, but, unfortunately for those who wanted to analyze the pictures, precise calibrations of the focal length and distortion of the lens, principal points of each frame, and the exact timing of frame exposures are non-existent.

---

* Recordak fine grain panchromatic film having an ASA rating of 6 was used. Also used was a Kinoptik lens with K3 filter which cuts out at about 470 millimicrons. Exposure was 1/300 sec, at f5.6. This exposes for an average of 3100 ft-candles. Details of the photographic instrumentation during flights before 24 August are contained in a paper presented at the National Technical Symposium of the Society of Photographic Instrumentation Engineers, Los Angeles, 4 August 1959, titled "Photographic Instrumentation from Cuter Space," Lathrop, P.A. and Rush, D. H. Copies are available from Mr. Lathrop, Missile and Space Vehicle Department, G. E. Co., 3198 Chestnut Street, Philadelphia, Pennsylvania.

2.3 Analysis

Preliminary analysis consists of the preparation of extensive streamline charts and nephcharts from the synoptic reports and a map showing the rectified positions of the clouds.

The principal effort in the large-scale synoptic analysis has been concentrated on the 1200Z maps approximately four hours before the time of the photographs. These analyses included a surface pressure analysis and streamline analyses of 2,000, 10,000, and 35,000 foot levels. The 2000 foot analysis, including surface-ship winds, was chosen to represent the low-level circulation pattern, Fig. 3 and the 35,000 foot (250 mb) analysis to represent the upper troposphere pattern, Fig. 4. As background and continuity for these analyses, streamline analyses were performed on the U.S. Weather Bureau Northern Hemisphere 700, 500, and 250-mb series for 48 hours previous and 12 hours subsequent to the above map time for an area considerably larger than the area of the photographs. The notations of Figs. 3 and 4 are common except for the cells marked "B" near the Equator on Fig. 3. These are "buffer cells" between two independently-driven currents, in this case, between the Southern Hemisphere easterly trades and the westerly current of the continental monsoon and equatorial trough. These maps were prepared prior to the cloud rectification and therefore show no bias toward the cloud patterns, especially over sparse data areas.

2.3.1 Low-level

The pattern of Fig. 3 is rather typical for the season. The Northern Hemisphere subtropical ridge extends from Georgia eastward thence north-eastward into Europe. North of this ridge in

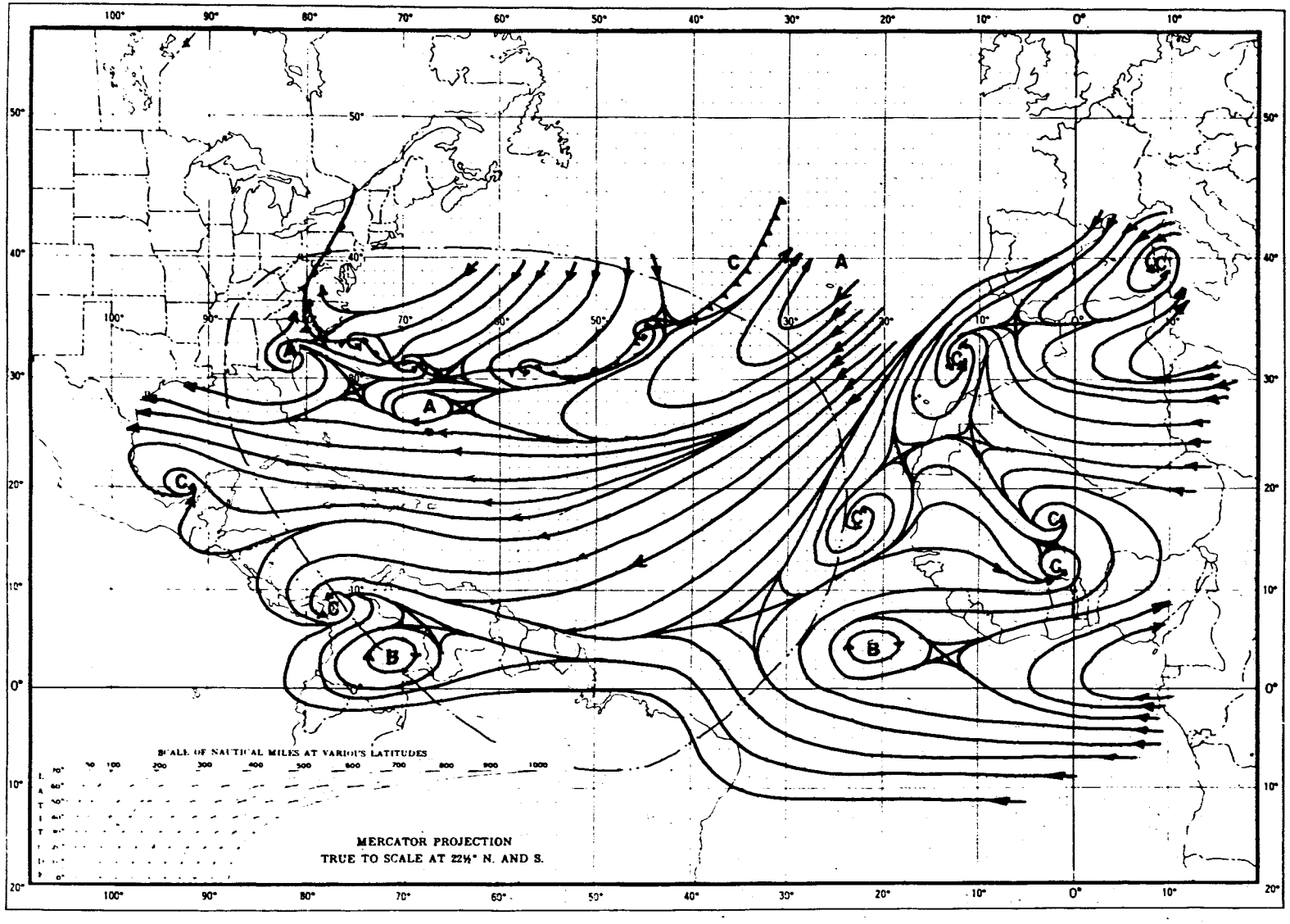

Fig. 3 Surface streamline chart, 1200Z, 24 August 1959

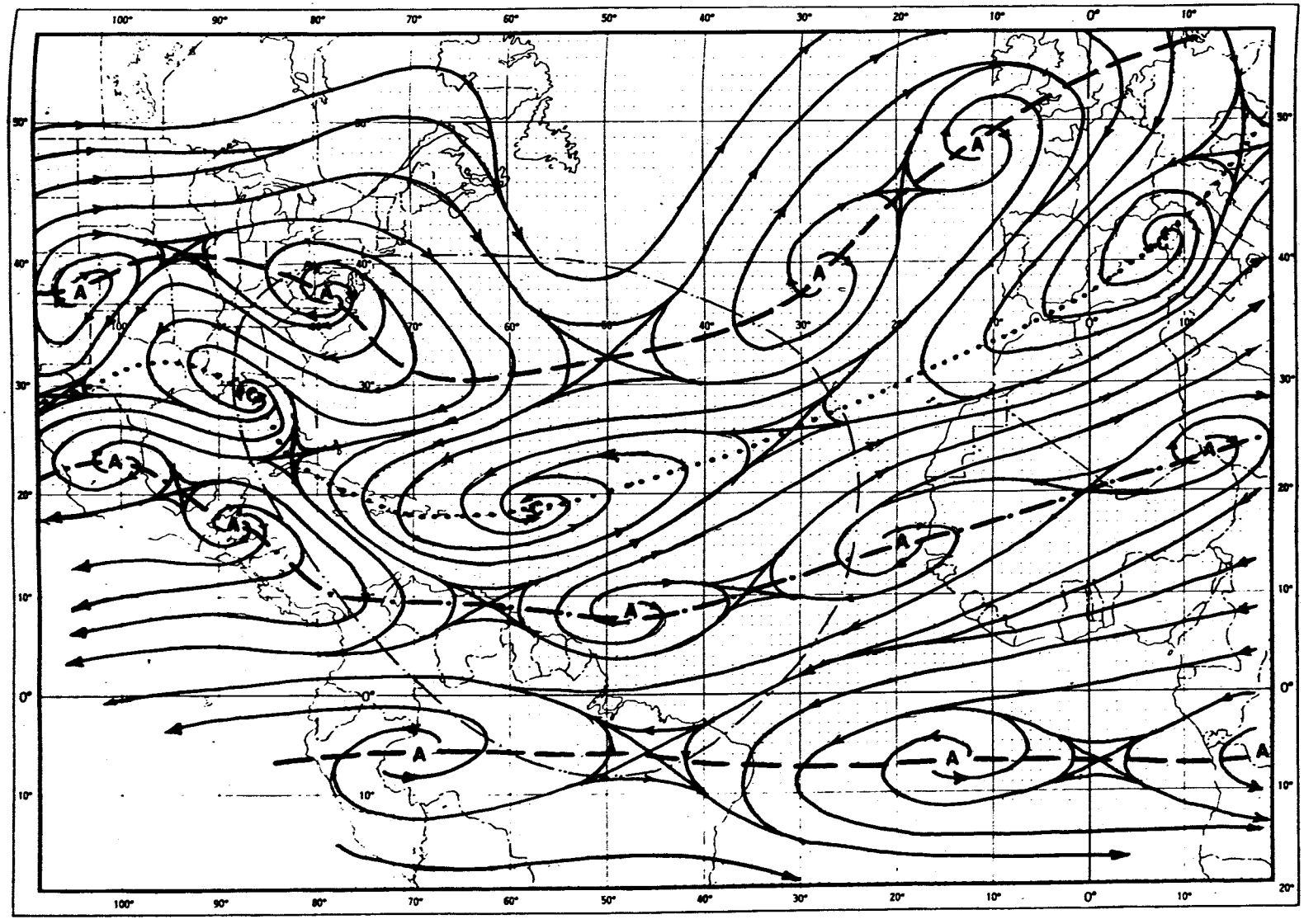

Fig. 4 250 mb (35,000 feet) streamline chart, 1200Z, 24 August 1959

the Western Atlantic is a quasi-stationary east-west frontal trough. The charted position of this front is that of 16Z based on the best possible continuity of maps and interpolation. South of the ridge over the Caribbean and Central Atlantic, trade flow exists to approximately 10°. The equatorial low-pressure trough between 5° and 10°N over South America extends eastward and then northeastward entering Africa at about 20°N. At 2000 feet there is a monsoonal circulation associated with this trough over West-Central Africa that is further complicated over North-West Africa by a reflection of the upper-level trough system.

2.3.2 High-level

In the pattern of Fig. 4 the Northern Hemisphere subtropical ridge has a slightly northward slope with height. The Sourthern Hemisphere subtropical ridge is oriented east-west at approximately 10° South. What might appear to be a complicated circulation pattern lies between these ridges; however, the pattern is believed typical for this season. A sharp tropical cold trough extends from the Southern United States southeastward across the Caribbean, then eastward across the Atlantic, and northeastward into the Mediterranean Sea. Throughout most of its length, the bottom of this trough does not penetrate much below the 500-mb level. Only over the Mediterranean does an intense cell penetrate into the very low levels and actually reach the surface. South of the trough is an associated tropical anticyclonic belt.

2.3.3 Photographic

The rectification shown in Fig. 5 is the result of transferring by hand the positions of clouds in respect to a perspective grid overlaying the photo to a corresponding grid which is seen

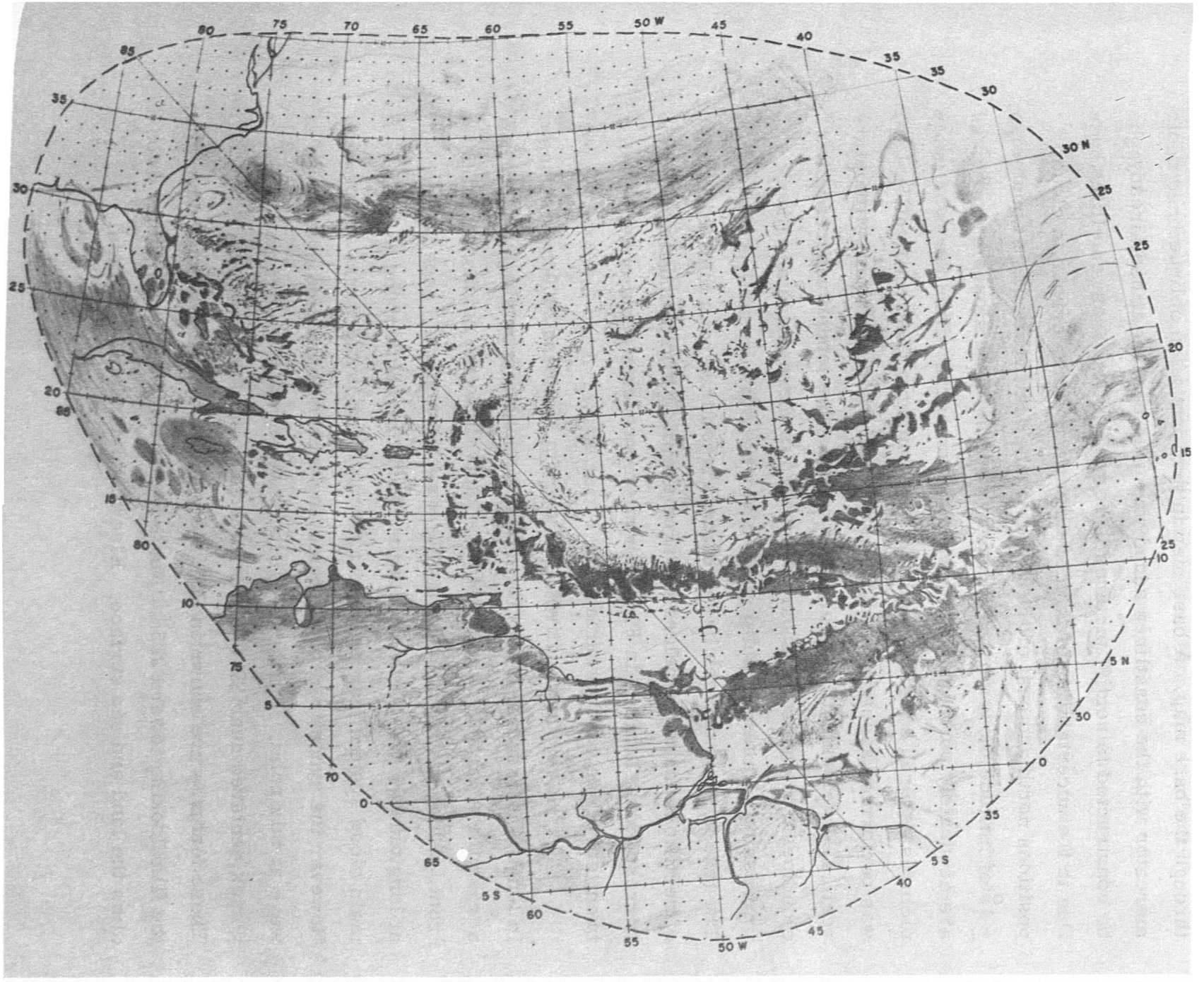

Fig. 5 Cloud distribution, 1600Z, 24 August 1959

through the base map. A base map in the form of an oblique mercator with the coastlines added was used because it had already be constructed to rectify pictures to be transmitted from satellites. Due to the uncertainties of frame number vs. time, errors in cloud positions north and east of the center of the rectification are about $\pm 1^{\circ}$ of latitude; however the relative postions of the clouds are accurately portrayed. Elsewhere, landmarks within the pictures assured a higher degree of positioning. The rectification was performed assuming that the clouds were horizontal and without vertical development. Toward the horizons this tends to increase the cloudiness; therefore less care was taken in these areas and the impression of a nearly solid cloud cover is not necessarily correct. The true horizon as seen by the camera was far beyond the limits of rectification; nevertheless the area shown in Fig. 5 and its corresponding location in Figs. 3 and 4 represents about one-twentieth of the earth's surface.

A very distinctive cloud system, at least 2000 miles in length, is associated with the quasi-stationary frontal system across the Atlantic. In general the clouds lie to the north of the front. Along it the pattern suggests wave formations, especially at longitude 66°W. At this point the cloud line south of the main cloud system may represent a squall line in the warm sector. However the synoptic reports which are rather sparse indicate no wave at this point. Further west the eastern half of a circular vortex centered near 32.0°N, 74.5°W is faintly discernible. These features are shown in Fig. 6 which is an enlargement from the film looking toward 325°. North of the vortex, cirrostratus dims the land and sea surface. Elsewhere north of the frontal

cloud bands the clouds show no organization. Along the southern edge of the frontal band, bands spaced roughly 15 miles apart appear to merge with the main cloud system as they slant eastward.

Two distinct cloud systems exist between 5° and 12°N extending from near the coast of South America eastward. A hasty interpretation might indicate a double intertropical convergence zone; however, only the southernmost system is associated with the low-level circulation of the intertropical convergence zone, while the northernmost one is attributed to the high-level trough. These two cloud systems are shown in Fig. 7 looking toward 151°. The intertropical convergence-zone cloud system had developed to the rain and thunderstorm producing stages as shown by the reports. The northern system exhibits a repetitive cellular structure with concentrations of cloud about every 100 miles for a distance of 700 miles. The system curves northward to the west, and a series of five north-south bands can be seen from longitude 58° to 67°W between latitude 15° and 20°N. Reports under this system east of the West Indies are completely lacking, but a few stations within the island chain observed middle and high clouds. It is suspected that this system lies in the 20,000 to 30,000 foot altitude zone and that it yielded rain in the developed areas. Stereo-views of these clouds place them above the low-level trade cumulus. Their relation to the 35,000 foot wind field shown in Fig. 4 suggests that they are moving from the north and west.

The circular vortex over the Gulf of Mexico is clearly shown in Fig. 6. This system is precisely tied to the pattern shown in Fig. 5. Surface reports show that it was composed of

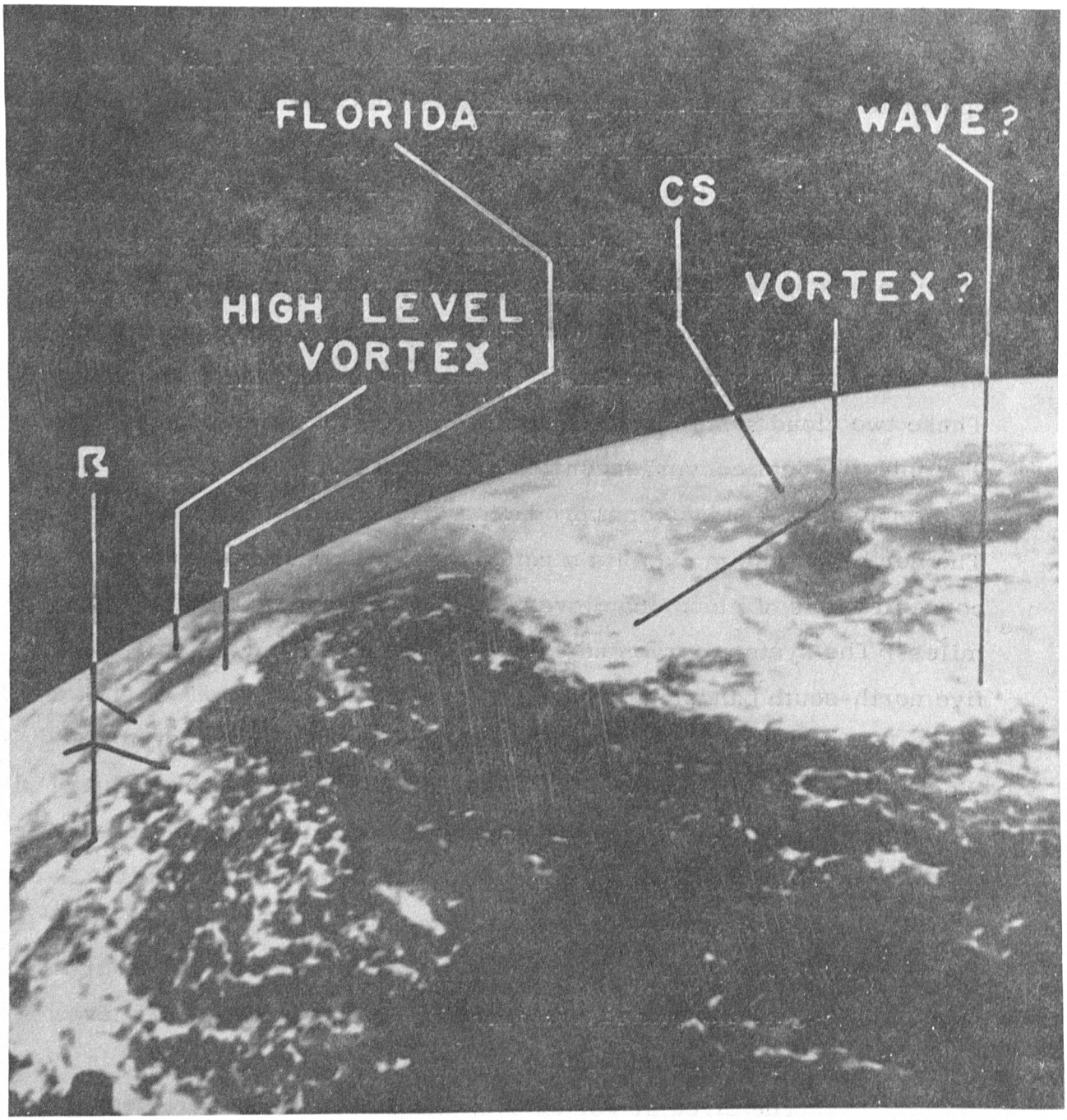

Fig. 6 Photo toward 325° from an altitude of 484 miles

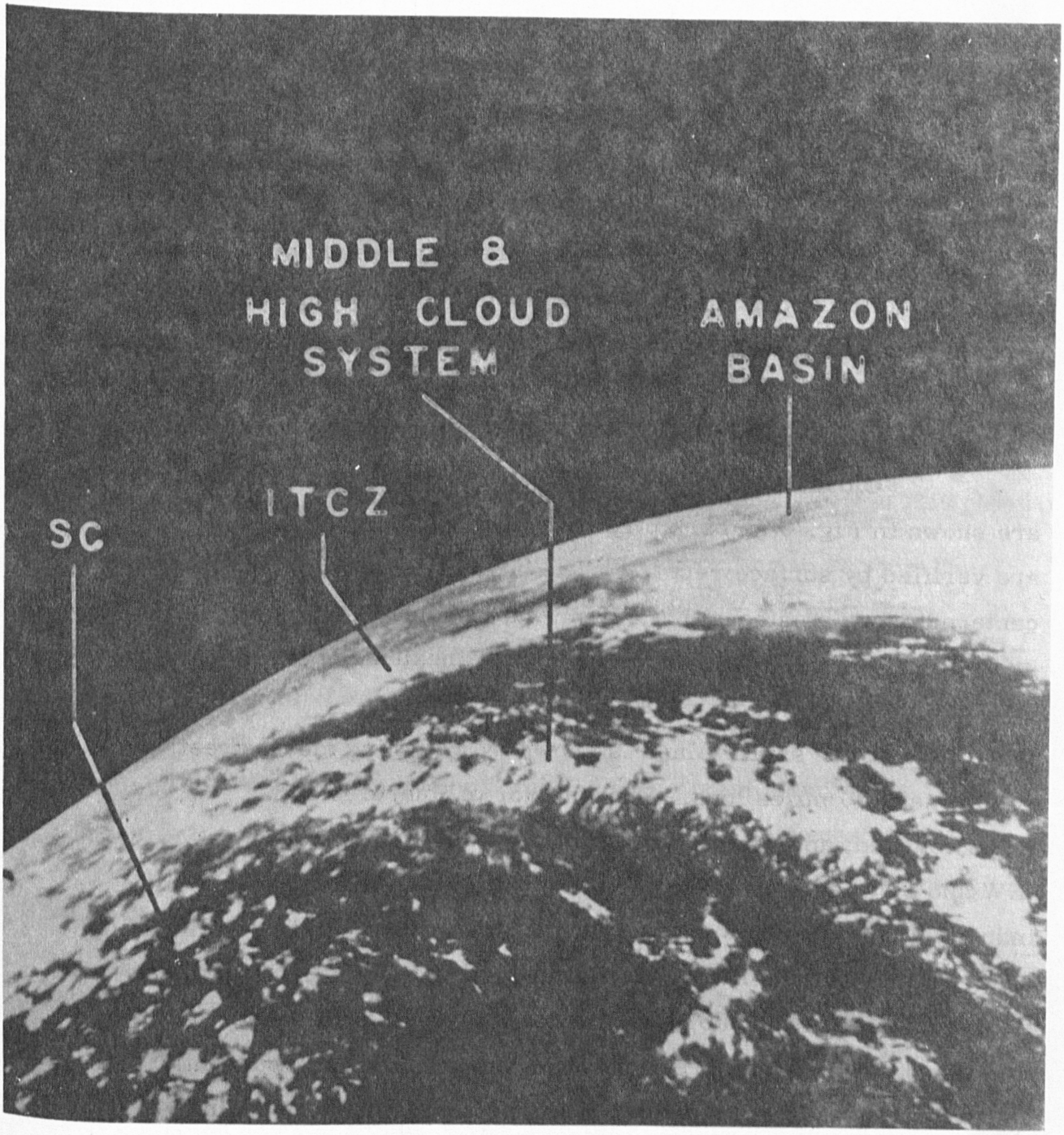

Fig. 7 Photo toward 151° from an altitude of 690 miles

high, middle and low clouds, thunderstorms and squalls. No. circulation exists in the levels below 500 mb.

The sharply-curved bands along the south coast of Cuba at 19.5N, 77.5W may also be a part of a similar high-level circulation.

It is of interest to note that the major cloud systems attributed to the upper cold trough are south of the trough line, probably within the westerly current. This agrees well with observations in the Central Pacific where such troughs are more common and persistent.

Clouds of thunderstorm proportions in the Caribbean area are shown in Fig. 5 as dark circles or ovals. Many of these are verified by surface reports. The huge cloud system centered over Jamaica, 18°N, 78°W was reported from the ground as a few cumulonimbi embedded in anextensive layer of altocumulus and altostratus.

Each small island is shown by a trailing cloud street, sometimes 100 miles long. The interior of Puerto Rico is cloud covered; and, streaming from its downwind corners (NW and SW), are large vortices of clouds which are apparently induced by the stronger winds over the sea. These vortices are about 10 miles in diameter. Downwind and spreading laterally from Puerto Rico and Hispaniola for distances equalling the length of the island, clear areas are found over the sea. These apparently correspond to areas of subsidence which complement the rising motion over the islands. In this case, when the prevailing wind at cloud levels was 15 - 20 kt, a "pie-shaped" area of clear sky was formed downwind. The apex of the area was near the windward

end of the island, and the angle between the mean wind direction and edge of the "pie-shaped wedge" was 20°. These areas extended downwind about twice the length of the islands or, in the case of Puerto Rico and Hispaniola, 90 and 360 miles, respectively. Similar effects appear along the north shore of South America where the easterlies have crossed northward peninsulas of land. These patterns were found in other nose-cone films; and in one case there was convergence between the subsiding outflow, at the edge of the pie-shaped area, and the general flow was sufficient to cause a cloud band more intense than over the adjacent waters.

To the east of the high-level pattern (15° - 25°N, 55°W) disorganized patterns which thicken toward the east are observed. These represent stratocumulus according to two aircraft reports from that area. Near 60°N, 26.5°W a vortex was plotted; this apparently corresponds to the low-level vortex which was placed slightly further east on the chart in Fig. 3.

A broken-to-continuous, slightly curved, narrow line of cloud was observed between Trinidad and a point about 450 miles to the ENE. This is clearly shown in Fig. 5 between 10.8°N, 60.0°W and 11.8°N, 55°W; the eastern end of the line also shows on the extreme right-hand side of Fig. 7. This line is presumed to have been initiated by one or more contrails which developed a cloud of visible proportions, or one several miles wide in this case.

Over some areas of the oceans, cloud patterns in the form of crescents or scallops with clear areas inside were observed. These were first observed by Dr. R. Cunningham, of GRD's Cloud Physics Branch, from an airplane. They are about 20 miles

in diameter and there are indications that the general wind is in a direction from the center of the crescent toward its thickest part. The cause of this pattern is unknown.

Almost all of the visible portion of South America was cloud covered. Cirrostratus clouds could be distinguished from other clouds along the coast at 71°W. Between the equator and 6°N near 34°W cumuliform bands were prominent. Heavy cloud bands of cumulus congestus proportions were observed along all coastlines experiencing a general onshore flow. Over parts of South America, bands parallel with the wind were prominent. They appeared to be deep and probably were yielding rain. Although the land is flat over the Amazon Basin the rivers are apparently large enough to suppress convection, as shown by the pattern of clouds over that area. Smudges in the photography at the mouth of the Amazon apparently are caused by silt-laden water; while northwestward along the coast the silt, shallow water, or their combination shows as a smudge to a distance of about 30 miles from the shoreline.

In regard to the identification of cloud forms, the construction of a cloud Atlas is planned which will show cloud forms under different conditions of solar altitude, light filtering, distance away, and effective magnification. At this stage the following forms have been identified from the nose-cone films:

a. Cumulonimbus
b. Cirrus or cirrostratus
c. Altocumulus (tentative)
d. Cumulus (tentative)
e. Cumulus congestus (tentative)
f. Stratocumulus (tentative)

The use of stereo has been attempted to distinguish different levels of clouds. Vertical separation of the clouds has been achieved in areas where the slant distances are as large as 900 miles and altitudes as great as 500 miles. The ratio of the base line to distance was approximately 1:80.

2.4 Acknowledgements

Allied Research Associates, Inc., performed analyses of the frame rate and camera orientation. They also provided the oblique mercator chart, produced photographic prints, programmed and ran the computations for the grids, and drafted the grids on transparent overlays.

Blank page retained for pagination

CHAPTER III (Continued)

SECTION 3

ON THE POSSIBILITY OF MEASURING CLOUD VELOCITIES FROM A SATELLITE*

J. J. Aiken and W. K. Widger, Jr.
Geophysics Research Directorate

3.1 Introduction

One of the primary uses of satellite observations that one would like to make would be the detection and measurement of cloud movements. In many cases this knowledge of cloud velocity would provide some measure of the wind at the cloud level and, if enough such observations can be obtained over an area, a general picture of the flow pattern. The importance of atmospheric flow patterns to an analysis of present weather conditions and the forecasting of future conditions cannot be stressed too heavily. [1]

A satellite 350 miles above the earth's surface would be traveling at about 17,000 mph. From this satellite it is at least theoretically possible to photograph cloud movements. By using these photographs we would like to be able to determine the speed of a cloud to an accuracy of $\pm$ 10 mph.

Three cases are presented here for discussion. Cases I and II, which use ground distance and angle measurement respectively in determining cloud velocity, are special cases in that the cloud is

---

* Originally prepared as a Technical Memorandum to the Director, GRD, GRD-TM-57-34, 16 September 1957.

assumed to be moving in the same vertical plane as the satellite orbit. Case III is the more general case which occurs when the cloud is not moving in the plane of the satellite orbit.

3.2 Case I, Two Dimensional CAse

The cloud and the satellite are traveling in the same vertical plane. Cloud velocity will be determined by measuring the ground distance "b" between two distinguishable points on the earth's surface Fig. 8*.

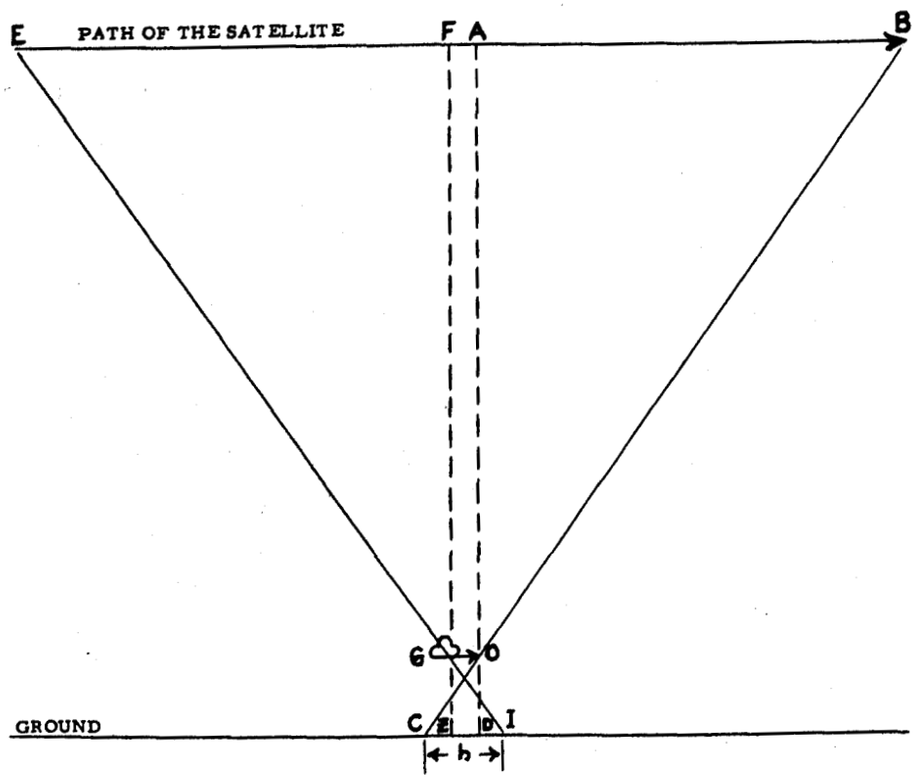

Fig. 8 Measuring cloud velocity "v" by using ground distance

* In all of the figures scale accuracy is sacrificed for clearer drawings.

Given:

V = velocity of the satellite = 17,000 mph

H = Height of the Satellite = 350 miles

t = time between two observations = 2 minutes

$\overline{EB} = Vt$

$\overline{AB} = \overline{EB}/2 = Vt/2$ (by construction)

b = measurable ground distance

v = velocity of the cloud

h = height of the cloud

3.2.1 Deriving a Formula for "v" by using Ground Distance

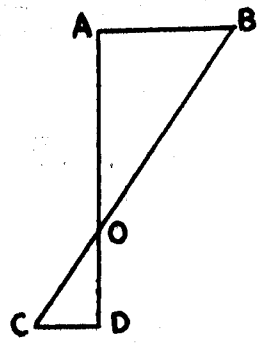

Fig. 9 Similar triangles

used in deriving "v" for Case I

$\Delta AOB \sim \Delta COD$ (Fig. 9)

$$\frac{\overline{AB}}{\overline{CD}} = \frac{\overline{AO}}{\overline{OD}}$$

$^*\overline{AB} = Vt/2$ *(by construction)

$\overline{AO} = H-h$

$\overline{OD} = h$

$$\frac{Vt/2}{\overline{CD}} = \frac{H-h}{h}$$

$$\overline{CD} = \frac{(h)\ (Vt/2)}{H-h}$$

$\Delta EGF \sim \Delta ZGI$ (Fig. 10)

$$\therefore \frac{\overline{EF}}{\overline{ZI}} = \frac{\overline{FG}}{\overline{GZ}}$$

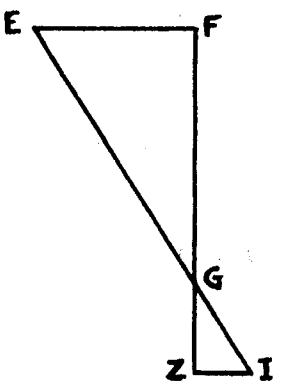

Fig. 10 Similar triangles used in deriving "v" for Case I

$$\overline{EF} = \overline{EA} - \overline{AF}$$

$$* \quad \overline{EA} = Vt/2 \qquad *\text{(by construction)}$$

$$\overline{AF} = vt$$

$$\overline{EF} = Vt/2 - vt$$

$$\overline{ZI} = b - \overline{CD} + \overline{AF}$$

$$= (vt + b) - \frac{Vth}{2(H-h)}$$

$$\overline{FG} = H-h \ , \quad \overline{GZ} = h$$

$$\frac{\overline{EF}}{\overline{ZI}} = \frac{\overline{FG}}{\overline{GZ}} = \frac{\dfrac{Vt - 2vt}{2}}{(vt + b) - \dfrac{Vth}{2(H-h)}} = \frac{H-h}{h}$$

Solving for "v" we find:

$$v = \frac{bh}{tH} + \frac{Vh}{H} - \frac{b}{t}$$

3.2.2 Error Analysis Computations

In the original statement of the problem the probable error in velocity "dv" must lie in the range between + 10 mph and - 10 mph.

$$dv = \frac{\partial v}{\partial b}\, db + \frac{\partial v}{\partial t} + \frac{\partial v}{\partial h}\, dh + \frac{\partial v}{\partial H}\, dH + \frac{\partial v}{\partial V}\, dV$$

and the most probable value of the resultant error "dv" is

$$dv = \sqrt{(d\,v_b)^2 + (d\,v_t)^2 + (d\,v_h)^2 + (d\,v_H)^2 + (d\,v_V)^2}$$

where

$$d\,v_b = \frac{\partial v}{\partial b}\, db \qquad d\,v_h = \frac{\partial v}{\partial h}\, dh \qquad d\,v_V = \frac{\partial v}{\partial V}\, dV$$

$$d\,v_t = \frac{\partial v}{\partial t}\, dt \qquad d\,v_H = \frac{\partial v}{\partial H}\, dH$$

We have derived a formula for "v" the velocity of the cloud where [19]

$$v = \frac{bh}{tH} + \frac{Vh}{H} - \frac{b}{t}$$

Taking partial derivatives of each of our variables with respect to "v" and assuming;

V = 17,000 mph

h = 2 miles, a typical middle cloud height ("h" could range from the surface to 40,000 ft for all types.)

H = 350 miles

t = 2 minutes = $\frac{1}{30}$ th of an hour (for a longer period the depression angle would be too small and cloud identification improbable.)

b = 2.25 miles ("b" will range from 1.25 miles when v = 60 mph to 3.25 miles when v = 0 mph. The 2.25 miles is an average value and occurs when v = 30 mph.)

We find:

$$\frac{\partial v}{\partial b} = \frac{h}{tH} - \frac{1}{t} = -29.8\,, \quad \frac{\partial v}{\partial h} = \frac{1}{H}\left(V + \frac{b}{t}\right) = 48.8\,, \quad \frac{\partial v}{\partial V} = \frac{h}{H} = 0.006$$

$$\frac{\partial v}{\partial t} = \frac{b}{t^2}\left(1 - \frac{h}{H}\right) = 2013.4\,, \quad \frac{\partial v}{\partial H} = -\frac{h}{H^2}\left(V + \frac{b}{t}\right) = -0.3\,,$$

If we let our error in "v" be equal to 10 mph(the maximum allowable error), we will then be able to compute the maximum errors db, dt, dh, dH, and dV that can be tolerated in each of our measured quantities while maintaining the relationship that dv $\leq$ 10 mph.

$$\therefore \text{let } dv = 10 \geq \sqrt{(-29.8\,db)^2 + (2013.4dt)^2 + (48.8dh)^2 + (0.3dH)^2 + (.006dV)^2} \tag{1}$$

In solving for "db" we let

$$dt = dh = dH = dV = 0$$

In doing this we assume that we have perfect measurements in our variables t, h, H, and V. By making this highly idealized assumption, we are able to compute the maximum allowable error in "b" while maintaining the relationship expressed in Eq. (1).

We can now see that the total error in our resultant "dv" is due only to the error in the measurement of ground distance, that is, "db".

$$10 \geq \sqrt{(-29.8db)^2}$$

$$db \leq \frac{10}{29.8} = \pm 0.3 \text{ miles}$$

In the same manner as above we solve for dt, dh, dV and dH finding

$dt = \pm 17.8$ sec, $\quad dh = \pm 0.2$ miles $= \pm 1082$ ft

$dH = \pm 36$ miles, $\quad dV = \pm 1751$ mph

3.2.3 Conclusion

The values computed above are the maximum probable errors in each term of Eq. (1) which permits the cloud speed to be determined to within ± 10 mph. The accuracy required in determining the cloud height "h" appears to be too stringent for practical application. Obviously the individual accuracy requirements must be even more stringent if the total of their effect is not to exceed ± 10 mph.

3.3 Case II, Two-Dimensional Case

Case II occurs when the cloud and the satellite are traveling in the same vertical plane (the same as in Case I), only now cloud velocity is determined by measuring the angles of depression from the satellite to the cloud.

3.3.1 Deriving "v" by the Use of Angle Measurement (See Fig. 11)

$$\tan \theta = \frac{\overline{GZ}}{\overline{ZI}} = \frac{h}{\overline{ZI}}, \qquad \tan \phi = \frac{\overline{OD}}{\overline{CD}} = \frac{h}{\overline{CD}}$$

$$\overline{ZI} = h/\tan \theta \qquad \overline{CD} = h/\tan \phi = Vth/2(H-h) \qquad (2)$$

$$\overline{ZI} = (vt+b) - \frac{Vth}{2(H-h)} \qquad \text{(derived in Section 3.2.1)} \qquad (3)$$

$$= vt+b - \overline{CD}$$

Equating Eqs. (2) and (3) and solving for "b" we find

$$b = h(\cot \theta + \cot \phi) - vt$$

substituting this expression for "b" in the equation

$$v = \frac{bh}{th} + \frac{Vh}{H} - \frac{b}{t} \qquad \text{(derived in Section 3.2.1)}$$

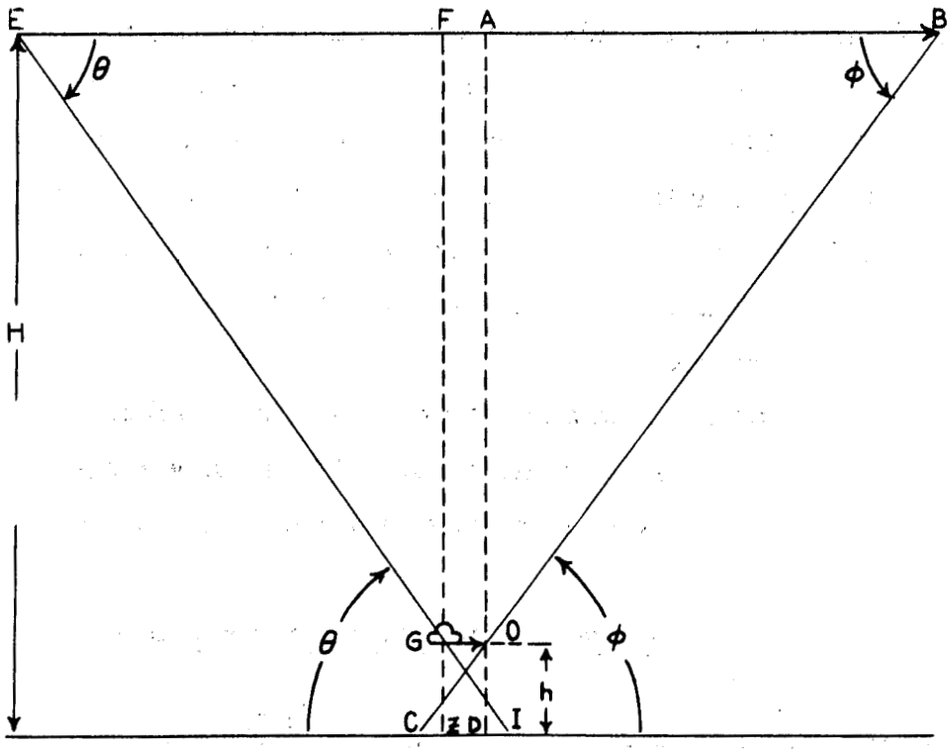

Fig. 11 Measuring cloud velocity by using angle measurement

we find:

$$v = V - \left(\frac{H-h}{t}\right) (\cot \theta + \cot \phi) \ .$$

3.3.2 Error Analysis Computations

Requiring once again that "dv", the error in cloud velocity, be less than ± 10 mph and assuming:

$V = 17,000$ miles $\qquad AB = \frac{Vt}{2}$ (by construction)

$h = 2$ miles

$H = 350$ miles

$t = 2$ minutes $= \frac{1}{30}$ hour

$$\tan\phi = \frac{H-h}{\overline{AB}} = \frac{H-h}{Vt/2} = 1.22824$$

$$\phi = 50^{\circ}\ 50'\ 55''$$

let v = 30 mph

distance $\overline{GO}$ = 1 mile , $\tan\Theta = \frac{H-h}{Vt/2} - 1.2326$

$$\Theta = 50^{\circ}\ 56'\ 51''$$

We find:

$$\frac{\partial v}{\partial V} = 1\ , \quad \frac{\partial v}{\partial t} = -\left(\frac{h-H}{t^2}\right)(\cot\Theta + \cot\phi) = 509{,}094$$

$$\frac{\partial v}{\partial H} = -\frac{1}{t}(\cot\Theta + \cot\phi) = 48.8\ , \quad \frac{\partial v}{\partial\Theta} = \frac{h-H}{t}(-\csc^2\Theta) = 17{,}312$$

$$\frac{\partial v}{\partial h} = \frac{1}{t}(\cot\Theta + \cot\phi) = 48.8\ , \quad \frac{\partial v}{\partial\phi} = \frac{h-H}{t}(-\csc^2\phi) = 17{,}360$$

$$dv = \sqrt{\left(\frac{\partial v}{\partial V}dV\right)^2 + \left(\frac{\partial v}{\partial H}dH\right)^2 + \left(\frac{\partial v}{\partial h}dh\right)^2 + \left(\frac{\partial v}{\partial t}dt\right)^2 + \left(\frac{\partial v}{\partial\Theta}d\Theta\right)^2 + \left(\frac{\partial v}{\partial\phi}d\phi\right)^2}$$

To solve for "dV", set $dH = dh = d\Theta = d\phi = 0$.

We then have $dv \leq 10$ mph $\leq \frac{\partial v}{\partial V}\ dV$, $dV = \pm 10$ mph.

In a similar manner we solve for our remaining variables and find:

$dH = \pm 0.2$ miles $= \pm 1082$ ft; $d\Theta = \pm 01'\ 59''$;

$dh = \pm 0.2$ miles $= \pm 1082$ ft; $d\phi = \pm 01'\ 59''$;

$dt = \pm 0.07$ sec.

3.3.3 Conclusion

Once again we see that the limits of tolerance in our measurements are much too stringent for practical application.

3.4 Case III, The General Case in Three Dimensions

Case III is the more general case and occurs when the cloud is moving in a plane not parallel to that of the satellite. (See Figs. 12 and 13)

3.4.1 Data Given

AB = path of satellite

DC = path of cloud

ϕ and Θ are measured angles of depression

α and β are horizontal angles between the path of the satellite and the cloud at the time t = 0 and t = 2 minutes respectively.

t = time between two observations = 2 minutes

V = 17,100 mph

3.4.2 Deriving "v" from the Given Data

$$\overline{CD} = vt = \sqrt{(\overline{CO})^2 + (\overline{OD})^2}$$

where $\overline{CO} = st$, $\overline{OD} = ut$

$$\overline{CO} = \overline{EF} = (\overline{AG} - \overline{EG}) - (\overline{AB} - \overline{BI} + \overline{FI})$$

$$\overline{OD} = \overline{DF} - \overline{OF}$$

$$\overline{GE} = M, \quad \overline{FI} = M'$$

$$\tan \alpha = \frac{\overline{DF}}{\overline{AF}} , \qquad \tan \phi = \frac{H}{\overline{AG}} = \frac{h}{M}$$

$$\tan \beta = \frac{\overline{CE}}{\overline{BE}} , \qquad \tan \Theta = \frac{H}{\overline{BI}} = \frac{h}{M'}$$

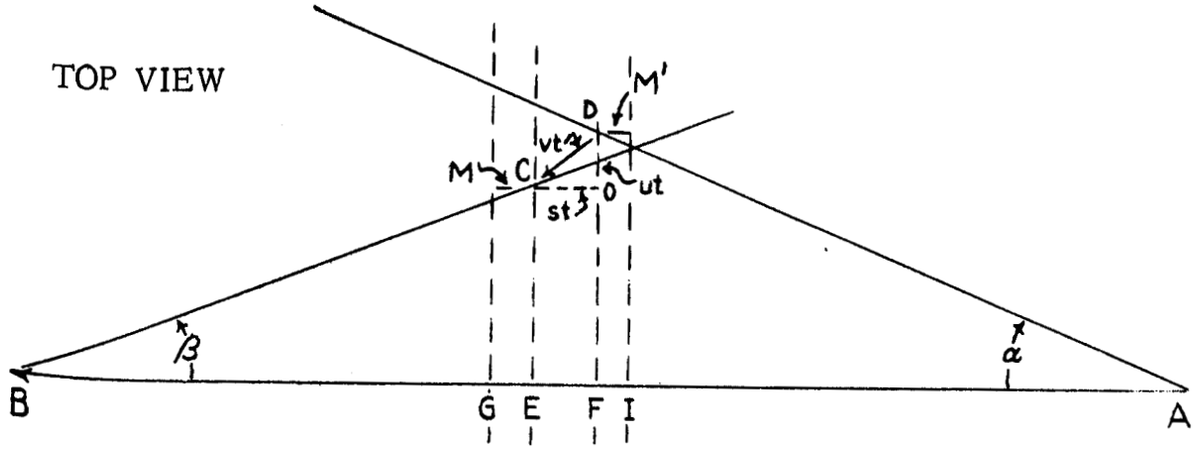

Fig. 12 Top view of cloud and satellite in Case III

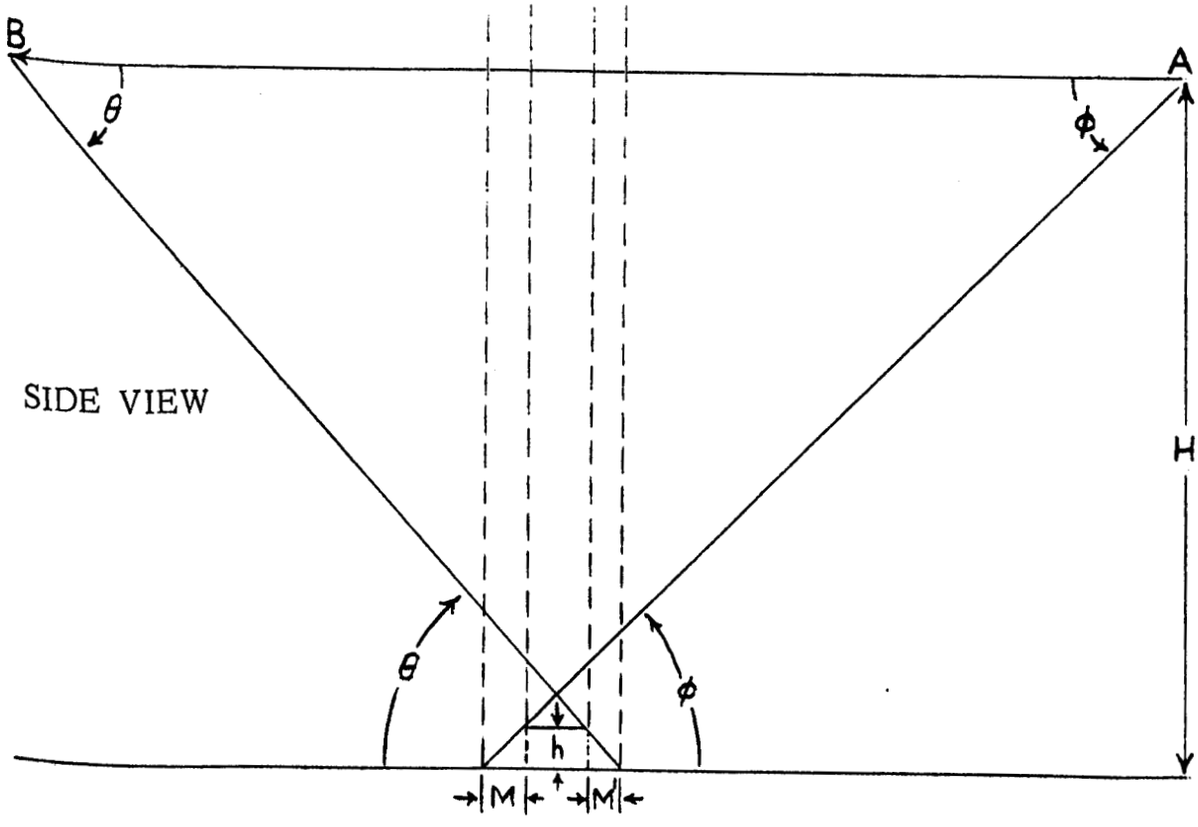

Fig. 13 Side view of cloud and satellite in Case III

$$\overline{CO} = \frac{H}{\tan\phi} - \frac{h}{\tan\phi} - \left(Vt - \frac{H}{\tan\Theta} + \frac{h}{\tan\Theta}\right)$$

$$\overline{OD} = \overline{BF}\ \tan\beta - \overline{AE}\ \tan\alpha = (\overline{BI}-M')\ \tan\beta - (\overline{AG}-M)\ \tan\alpha$$

$$\overline{CO} = st = (H-h)\ (\cot\phi + \cot\Theta) - Vt$$

$$\overline{OD} = ut = (H-h)\ (\cot\Theta + \tan\beta - \cot\phi\ \tan\alpha)$$

Solving these equations individually for "st" and "ut" respectively, we can then solve for "v" where,

$$v = \frac{\sqrt{(st)^2 + (ut)^2}}{t}$$

3.4.3 Error Analysis Computations

Once again we have the requirement that "dv", the error in measuring the velocity of the cloud, must be less than ± 10 mph.

Assuming again:

V	$= 17,100$ mph	Θ	$= 50^\circ\ 41'\ 04''$
H	$= 350$ miles	ϕ	$= 50^\circ\ 36'\ 13''$
h	$= 2$ miles	α	$= 20^\circ\ 00'\ 00''$
t	$= 2$ minutes	β	$= 19^\circ\ 54'\ 47''$
$\cot\Theta$	$= 0.81895$	$\csc\Theta$	$= 1.29254$
$\cot\phi$	$= 0.82130$	$\csc\phi$	$= 1.29405$
$\tan\alpha$	$= 0.36397$	$\tan\beta$	$= 0.36214$
$\sec\alpha$	$= 2.92381$	$\sec\beta$	$= 2.93608$

$$\overline{CO} = st = (H-h)\ (\cot\phi + \cot\Theta) - Vt$$

$$s = \frac{(H-h)}{t}\ (\cot\phi + \cot\Theta) - V$$

where "s" is a function of H, h, ϕ, Θ, V, and t.

Taking partial derivatives with respect to "s" and computing their numerical value with the above information we find:

$$\frac{\partial s}{\partial H} = -\frac{1}{t}(\cot\theta + \cot\phi) = 49.2 \qquad \frac{\partial s}{\partial \theta} = -\left(\frac{H-h}{t}\right)(\csc^2\theta) = -17,441.7$$

$$\frac{\partial s}{\partial h} = -\frac{1}{t}(\cot\theta + \cot\phi) = -49.2 \qquad \frac{\partial s}{\partial V} = -1$$

$$\frac{\partial s}{\partial} = -\left(\frac{H-h}{t}\right)(\csc^2\phi) = -17,482.5 \qquad \frac{\partial s}{\partial t} = -\left(\frac{H-h}{t^2}\right)(\cot\theta + \cot\phi) = -513,726.3$$

$$\overline{OD} = ut = (H-h)\ (\cot\theta\tan\beta - \cot\phi\tan\alpha)$$

$$u = \frac{H-h}{t}\ (\cot\theta\tan\beta - \cot\phi\tan\alpha)$$

where "u" is a function of H, h, t, θ, α, ϕ, and β.

$$\frac{\partial u}{\partial H} = \frac{1}{t}(\cot\theta\tan\beta - \cot\phi\tan\alpha) = 0.071$$

$$\frac{\partial u}{\partial h} = \frac{1}{t}(\cot\theta\tan\beta - \cot\phi\tan\alpha) = 0.071$$

$$\frac{\partial u}{\partial t} = -\left(\frac{H-h}{t^2}\right)(\cot\theta\tan\beta - \cot\phi\tan\alpha) = -739.2$$

$$\frac{\partial u}{\partial \theta} = -\left(\frac{H-h}{t}\right)(\csc^2\theta\tan\beta) = -6316.3$$

$$\frac{\partial u}{\partial \alpha} = \left(\frac{H-h}{t}\right)(\cot\theta\sec^2\beta) = 70,598.2$$

$$\frac{\partial u}{\partial \phi} = \left(\frac{H-h}{t}\right)(\csc^2\phi\tan\alpha) = 6363.1$$

$$\frac{\partial u}{\partial \beta} = - \left(\frac{H-h}{t}\right) (\cot\phi \ \sec^2 \alpha) = - 73,299.3$$

$$\overline{CD} = \sqrt{\overline{(CO)}^2 + \overline{(OD)}^2}$$
$$= \sqrt{(st)^2 + (ut)^2}$$

To find the maximum allowable errors possible in each measurement while fulfilling the requirement that "dv" must be less than ± 10 mph, we isolate each variable and assume that we have perfect measurements in the remaining variables. Assuredly, this is a very idealized condition but it provides us with the varest minimum of limits which must be met in our measurements to satisfy the relationship, "dv" $\leq \pm 10$ mph.

Let $st = 0$, $\therefore v = u$

$$dv = du \leq \pm 10 \text{ mph}$$

$$du = \sqrt{(du_H)^2 + (du_h)^2 + (du_t)^2 + (du_\Theta)^2 + (du_\alpha)^2 + (du_\phi)^2 + (du_\beta)^2}$$

To solve for du_H, let the remaining terms be equal to zero. We then have: $10 \text{ mph} \leq du = du_H = \frac{\partial u}{\partial H} \ dH$

$$10 \text{ mph} \leq .071 \ dH$$

$$dH \leq 140 \text{ miles}$$

In a similar manner we solve for the remaining variables and find:

$$dh = \pm 140 \text{ miles}$$
$$dt = \pm 48.7 \text{ sec}$$
$$d\Theta = 00^\circ \ 05' \ 25''$$

$d\alpha = 00^{\circ}\ 00'\ 28''$

$d\phi = 00^{\circ}\ 05'\ 23''$

$d\beta = 00^{\circ}\ 00'\ 26''$

If we set "ut" = 0 , we then have the special Case II (discussed earlier) where the maximum allowable error possible in each variable, while maintaining the requirement that dv $\leq$10 mph, are as follows:

$dH = 10/49.2 = \pm 0.2$ miles

$dh = \pm 0.2$ miles $= \pm 1073$ ft

$d\phi = \pm 00^{\circ}\ 01'\ 57''$

$d\theta = \pm 00^{\circ}\ 01'\ 58''$

$dV = \pm 10$ mph

$dt = \pm 0.07$ sec

3.5 Concluding Remarks

We have shown that the degree of accuracy of measurement necessary to measure the velocity of a cloud to within $\pm$ 10 mph is much too stringent for practical application; and, unless some new methods of measurement can be devised, the outlook for measuring cloud speeds by the exemplified methods will remain very bleak.

The accuracy required with regard to the height of the cloud, in particular, is beyond that expected to be obtainable unless only the zonal component of velocity is needed. If the satellite revolves in a polar orbit the error in the height of the cloud turns out to be insignificant in computing the zonal component of the wind.

The measurement of cloud velocity in the three-dimensional case by using ground distance has been investigated and no gain was realized in the limits of our required accuracies, and the method was more complex in its application than by angle measurement. Two other methods have been suggested for measuring cloud speed from a satellite vehicle but at the time of this writing they need further investigation before any comment can be made on their full worth. The two methods are (a) by use of parallax and (b) by taking three or more sightings over a small increment of time.

It is the authors' opinion that the problems which arise in regards to the stringent requirements of measurement may be intrinsic to the basic problem of trying to measure cloud velocity from a satellite vehicle traveling at a speed approximately 570 times that of the cloud and some 348 miles above it.

Any criticism of the work presented in this paper or suggestions as to new methods of attack are welcomed.

CHAPTER IV

SECTION 1

A SYSTEM FOR THE METEOROLOGICAL USE OF SATELLITE TELEVISION OBSERVATIONS

Arnold H. Glaser
Allied Research Associates, Inc.*

1.1 Introduction

1.1.1 General

Plans exist for the orbiting of meteorological satellites of moderate sophistication. The principal observational sensor on such satellites will be a television camera of near-convertional design. Early satellites will be spinstabilized, so that the axis of rotation will remain fixed in inertial space over at least moderate intervals of time.

In one set of plans the axis of the principal camera will be directed along the spin axis. The camera is outfitted with a wide-angle lens of 105° coverage. Continuous pictures are not taken; instead, snapshot pictures are to be taken by a shutter mechanism. at regular, programmable intervals. The photosensitive surface of the image tube is of long persistence, so that the snapshot image is retained on the screen as an electrostatic charge. The image is "read" off the screen by a scanning

---

* This work was sponsored under Contract No. AF19(604)-5581, under ARPA Order No. 26-59.

beam at a relatively low scan rate. The corresponding signals are stored in a small tape recorder.

When the satellite passes over the data acquisition stations, and interrogating signal is sent from the ground station to the satellite. This causes the contents of the tape recording to be telemetered to the ground station, where the signals are recorded both on magnetic tape and in reconstructed picture form by photography of a video monitor. At the termination of the satellite tape readout, the satellite may be instructed to directly telemeter pictures of the environs of the data acquisition station and may receive instructions for the picture-taking program of the next orbit or orbits.

The camera will have a 500-line noninterlaced format. Then looking straight down from the intended orbital altitude of 380 miles, this will give a resolution somewhat poorer than one mile. Lens distortion introduced to avoid exposure difficulties caused by the falling-off of illumination at the picture corners will result in a deterioration of this resolution toward the picture boundaries.

In addition to the television system the satellite will contain the usual beacons for tracking purposes. To help establish orientation, a set of infrared horizon sensors is provided. Also, a set of slit photocells is provided which, when the picture is exposed, records the relative azimuth of the sun in the picture plane. This quantity can be used to establish the rotary orientation of the picture around the spin axis.

Satellite position and horizon sensor data will be channeled into the computation center. There, short-term forecasts of satellite

position and axis orientation with respect to terrestrial coordinates will be issued. These will serve to permit programming of future picture-taking activities and also to establish locations of recently taken pictures. Under optimum conditions this information will be available at the data acquisition stations at least 24 hours in advance of the actual picture taking.

According to the most recent advices the intended orbital parameters of the satellite are a height of 380 miles, and orbital inclination of 47.7°, and an initial spin axis orientation such that the camera will be pointing vertically in the region of 20°N latitude, 43°E longitude.

Pictorial material from the meteorological satellite will be made available on film and will contain information of value for meteorological analysis and forecasting. The experiment will explore techniques of recognition of pictorial features, abstraction of pertinent meteorological information, data transmission, and data utilization.

The experiment is visualized as being performed as follows. After each telemetering of pictorial data to the data acquisition station, a filmed reconstruction of each picture will be delivered to the meteorological group. Aided by additional information on the satellite orbit and attitudes, the meteorological group will establish the locations of the pictures and of features contained therein. Significant meteorological features will be transferred to maps and interpretations of the significance of the features will be made.

The attempt to derive results from this experimental satellite system will considerably accelerate the realization of a practical operational meteorological satellite system for world-wide use.

1.1.2 Objectives of the Program

The objectives of the program are to provide a fund of knowledge on the design and operation of future satellite meteorological systems. In a negative sense, the misadventures experienced during this first experiment will prevent their repetition in later, more extensive, operations.

Techniques will be generated for the effective handling of the pictorial material contained in the telemetered pictures. These will provide a measure of initial guidance to the scientists who will late study the same picture in a more leisurely fashion.

Techniques will also be developed for the effective utilization of the type of information that can be expected from a meteorological satellite. It is anticipated that the forecaster will experience some initial difficulties in the integration of the satellite material into his normal forecasting procedures. For example, the satellite material will not be synchronous with convenient observations. In addition, various parts of the satellite field of coverage will be acquired at different times.

Perhaps one of the largest gains to be expected from the program is a rational evaluation for the scientific and meteorological community, as well as for the public at large, of the potentialities of the meteorological satellite as a tool for increasing the scope of observation and for improving forecasting. Any contributions that satellites may make toward forecasting in any part of the globe will mark a significant step forward in meteorology.

1.1.3 Scope of the Program

The program involves the setting up of methods and systems for processing the information received from the television cameras of the satellite that will enable meteorologists to

make use of the pictures. Methods are to be developed for the extraction of meteorological information from these pictures. Also included is the design of a system or systems for determination of orientation of the satellite in cases where other information may not be available.

1.1.4 General View of Procedures

As an aid in understanding the various procedures to be described in detail, the following quick resume of the chain of events at the data acquisition station is presented.

The satellite, programmed from ground commands, takes a series of snapshot pictures along a part of one orbit. These are stored in the internal memory of the satellite until the satellite passes within appropriate telemetering distance of one of the readout stations. Here, the signals are recorded both on film and on video tape. A secondary film copy is prepared from a playback of the video tape; this copy is processed, then delivered to the meteorological group. There the film is placed in a special enlarger and projected onto a perspective grid. The perspective grid will have been chosen from a library of such grids precalculated to give an approximate representation of the perspective and lens distortion of the picture. Each quadrilateral of the perspective grid matches an equivalent square of a rectified grid which can be superimposed on an appropriate map to permit relatively facile mapping of the material contained in the pictures. Pertinent detail is marked on the expendable perspective grids and then transferred to the map. Mosaics are not prepared except in the map form. A certain amount of calculation may be required to utilize the satellite position and orientation data to permit the

selection of the appropriate perspective grid and to enable appropriate orientation of the rectified grid with respect to the map.

Log books and other records will be maintained to permit future evaluations of both the operations and of the pictorial material.

1.2 Perspective Rectification

1.2.1 The Problem

The meteorological information to be obtained from satellite pictures can be put to use only if the locations of the observed phenomena can be established reasonably well. The required accuracy of location depends upon the use to which the meteorological information is to be put. Such an application as very short range terminal forecasting would require accuracy of location to within single miles. But since a single satellite will scan the same area in daylight at best once each 24 hours, a more probable application of such satellite information will be for the analysis of large-scale meteorological systems for purposes of forecasts of the order of 24 hours. Here the requirements for accuracy of location can be considerably relaxed. Assuming that a meteorological system moves at speed of 20 knots and that its progress can be predicted to an accuracy of 10 per cent (perhaps an optimistic estimate), then the error of estimated position will be of the order of 50 nautical miles for a 24-hour forecast. This then is an estimate of the maximum magnitude of location error that can be tolerated without materially adding to the uncertainties of forecasting.

Establishing locations within the satellite pictures to even this degree of accuracy is not completely simple. A spin-

stabilized satellite, orbiting about the earth, represents a dynamic system of six degrees of freedom. The six coordinates necessary to establish location and orientation of the satellite will be listed for our purposes as: (1) the latitude and (2) longitude of the satellite subpoint, (3) the height of the satellite above the geoid, (4) the nadir angle measured between the axis of rotation and the vertical through the satellite, (5) the azimuth of the projection of the axis of rotation onto the earth's surface, and (6) the rotary angle between some fiducial direction in the picture and the direction of the image of a line on the earth. For convenience the latter line will be taken as the projection of the axis of rotation. The six coordinate parameters define a coordinate transformation from the two-dimensional representation of the picture tube image to the two-dimensional location on the earth. If it is further desired to map the image, the elements of the map projection used will also enter.

Essentially, then, the problem becomes one of finding corresponding points in the pictures and on a map. The correspondence should be presented in a fashion that makes the location of features in the picture readily obvious.

1.2.2 Facilities for Picture Location

As outlined earlier, the satellite internal system plus external tracking and computing facilities provide information that will aid in the location of pictures. The successful functioning of the system will provide the following information:

a. Latitude and longitude of the satellite subpoint

b. Latitude and longitude of the principal point (the principal point is defined as the intersection of the camera axis with the earth)

c. The nadir angle

d. Satellite height

e. Azimuth of the line joining subpoint and principal point

f. The angle between the projection of the sun line on the satellite image plane and the intersection of that plane with a vertical plane containing the camera axis

g. Time of picture taking

All of these quantities must be made available as functions of time. It will be seen that sufficient, even redundant, information is given to permit the transformation of location in the picture to map location. The technique used to perform this transformation is described below.

1.2.3 Perspective Grids

1.2.3.1 General Description

The method established to locate features in the pictures is based upon the "Canadian Grid" system of photogrammetry. The perspective grid is a network of lines constructed for an oblique photograph, the lines representing corresponding lines of an imaginary rectangular grid on the ground. The perspective grid is superimposed on the picture while the corresponding rectangular grid is superimposed in the proper location and orientation on the map. A one-to-one correspondence then exists between lines and intersections of lines in the picture and on the map. A typical perspective grid is shown in Fig. 1, and a corresponding rectangular grid is shown in Fig. 2.

The starting point for the gridding system is taken as the principal point of the picture. The principal point of the picture is defined as the intersection of the camera axis with the image plane. A corresponding principal point in the object space exists at the intersection of the camera axis with the earth's surface. This point

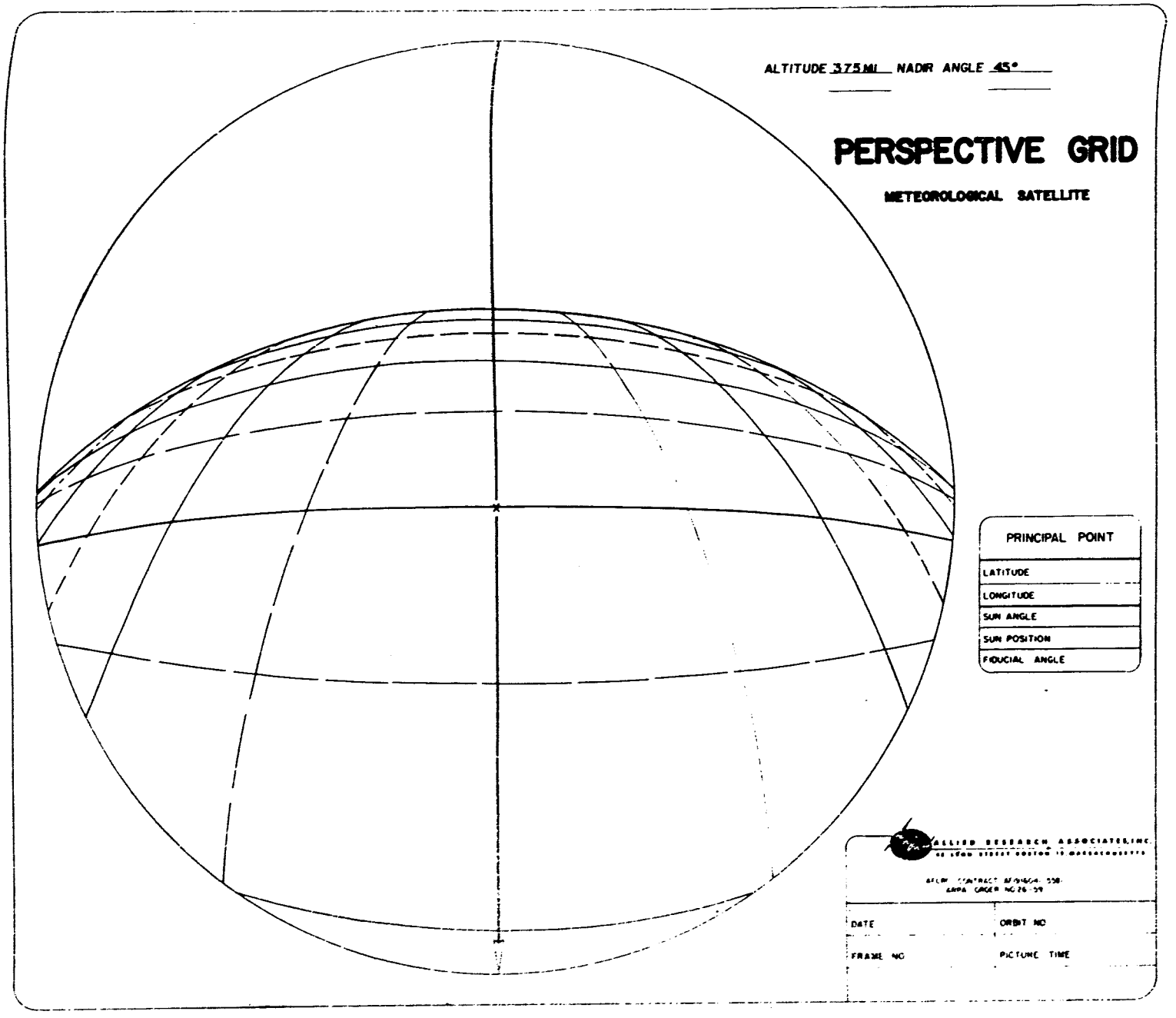

Fig. 1 · Perspective Grid

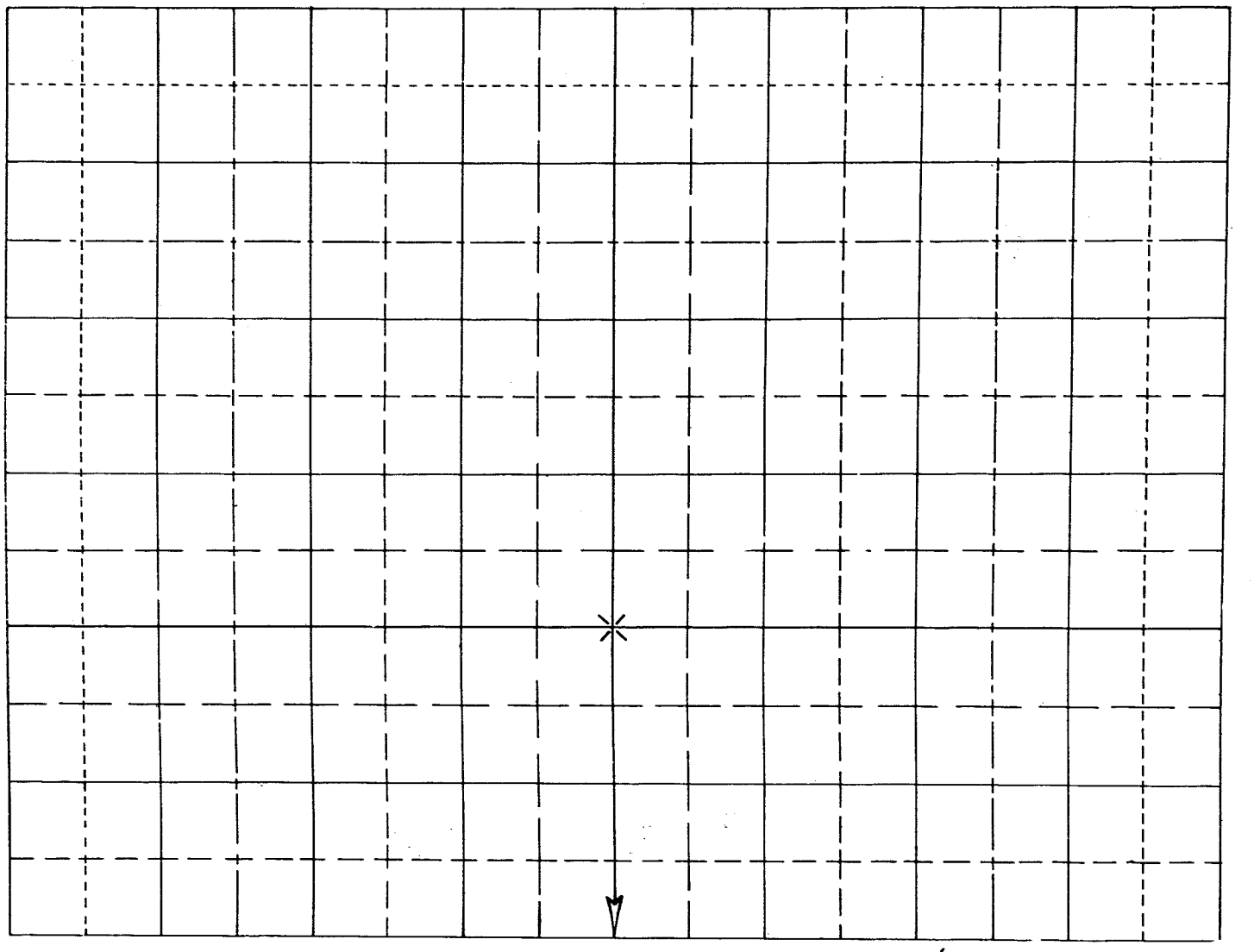

DATE _____
ORBIT NO. _____
FRAME NO. _____
FRAME TIME _____

ANALYST _____

PRINCIPAL POINT
LAT. _____
LONG. _____

SUBPOINT
LAT. _____
LONG. _____
AZIMUTH FROM
PRIN. PT. _____

AFCRC Contract AF 19(604)-5581
ARPA Order No. 26-59

TRANSFER GRID

METEOROLOGICAL SATELLITE

FOR USE WITH TRANSVERSE
MERCATOR MAP, SCALE 7,500,000 : 1
ONE INCH = 118 STATUTE MILES

Allied Research Associates, Inc.
43 Leon St., Boston 15, Mass.

PROPERTY OF THE UNITED STATES AIR FORCE

Fig. 2 Transfer Grid

corresponds more or less exactly with the intersection of the spin axis of the satellite with the surface of the earth. If prediction of satellite attitude is successful, the predicted position of the principal point on the earth's surface should be reasonably accurate. For the sake of further argument, the position of this point will be taken as accurately determined.

If a perspective grid is inaccurately drawn, it will be seen that the errors in position resulting from a scale error in the grid will increase with distance from the center of the picture (see Appendix B). But since the location error at the principal point is by definition zero, tolerable errors may occur even though the grid was computed for a somewhat different set of satellite parameters than those actually prevailing. This leads to the concept of the pre-computation of a library of perspective grids. In the mathematical development in Appendix A, it is shown that the only parameters controlling the form of the perspective grid, once the camera geometry has been established, are the nadir angle and the height of the satellite. It thus becomes feasible to establish a relatively restricted library of perspective grids for various combinations of these two parameters. Further transformations, such as those for the position of the subpoint and the azimuth of the principal line, are handled by the placing of the rectilinear grid on the map.

1.2.3.2 The Grid System--Use of Transfer Grid

A "quadrilateral" grid is constructed, in principle, on the surface of the earth. A great circle is passed through the principal point (the intersection of the camera axis with the surface) oriented so that it crosses the horizon seen from the satellite perpendicularly.

This will be called the principal line. Another great circle is passed through the principal point perpendicular to the principal line. Small circles are drawn parallel to the two great circles, forming a grid of near-squares.

This quadrilateral grid is mathematically projected onto the image plane of the satellite for several satellite heights and inclinations of the camera axis from the vertical. The number of such projections required will depend on the range of heights and angles anticipated and on the accuracy to which points are to be located. A limit to this accuracy occurs in the nonlinearities, noise, and jitter occurring in the reconstituted vertical and horizontal scans presented at the data acquisition stations.

The horizon will appear in the picture at most angles of view. It can be used to establish both the inclination of the camera axis, the height being known, and the rotation of the camera about its axis. It is not believed that sufficient accuracy can be achieved in the measurement of the apparent radius of the horizon circle to permit establishing the height of the satellite. The horizon is to be projected onto the image plane along with the grid.

The image of the grid and horizon gives the perspective view of the grid as it would be seen at the satellite. The following procedure is envisaged for the use of these perspective grids: the proper grid is selected from information provided on satellite height and inclination; a check is provided by horizon position (if present). The perspective grid is superposed on the picture with the principal point of the grid at the center of the picture. The grid is rotated about this point until the horizon is in its proper position. If the horizon is not available, the proper rotation can be established by reference to solar position data to be supplied with the pictures.

Simultaneously, a corresponding quadrilateral transfer grid of the appropriate scale is placed on a map which is used as a location guide and transfer medium. The principal point of the transfer grid is placed on the map at its correct geographical location as determined from the satellite subpoint and axis orientation. The principal line of the transfer grid is oriented along the azimuth from the principal point toward the satellite subpoint. Then the transfer grid corresponds, point by point, with the perspective grid on the satellite picture. It is a relatively easy operation to transfer significant points on the picture to their corresponding points on the map.

It is recognized that a transfer grid, constructed as described, will not "fit" properly on any real plane map of the earth's sphere. The errors incurred in the use of such a grid with various map projections has been evaluated. It is found that the minimal errors will occur with the use of a Mercator chart in low latitudes, or an appropriate transverse Mercator at higher latitudes.

1.2.4 Procedures for Perspective Rectification

The actual procedures to be used in the location of information in the satellite pictures are keyed to the characteristics of the particular system. Assume pictorial information will be obtained in the form of developed, positive 35 mm film strips. Each double frame will contain one picture and the images of signal lights indicating the picture number and the angle between the sun and the fiducial direction in the image plane. The film is placed in a special projector. The image is focused on a special focusing sheet which permits the adjustment of the enlarged image to the appropriate size. Provision exists for the partial compensation of any distortion that may have occurred between the original television camera lens and the projector. To enhance the psychological perception of

perspective, the picture is rotated so that the observer will be looking in a direction essentially perpendicular to the horizon, right-side up. For near-vertical pictures, it may be convenient to place North at the top.

The focusing sheet is replaced by the appropriate perspective grid, chosen to correspond as closely as possible with the reported height and nadir angle of the satellite. The center mark of the perspective grid is made to coincide with the center mark of the picture. Where a horizon is present, the perspective grid is rotated until the picture horizon and the grid horizon are parallel. In general, they will not quite coincide. The lack of coincidence is caused by inexact nadir angle. Where radical discrepancies are found, error is indicated.

If no horizon is present, it will be necessary to use the sun angle information to orient the perspective grid. The sun angle is read from the signal lights recorded on the film and entered in the appropriate space on the perspective grid sheet. Also entered is the angle between the picture vertical and the sun line. These are added (or subtracted) and the result is used to orient the fiducial direction of the picture with respect to the principal line of the perspective grid; a large protractor will be provided for this purpose.

The projected picture is now ready for analysis. The transfer grid, drawn to the scale of the map to be used, is the plane counterpart of the perspective grid. For convenience the transfer grid is permanently mounted on a small, flat light table. The map to be used is moved about over the light table until the center point of the grid coincides with the principal point geographically located on the map, and the azimuth line drawn on the map coincides with the principal line of the transfer grid.

It will now be possible to sketch on the map features observed in the projected picture.

1.3 Mapping

1.3.1 Map Selection

The cloud images seen in the telemetered pictures must be represented on a map to permit the integration of images seen in several pictures and to permit the ready definition of the location of meteorological features. The grid system that has been adopted for perspective rectification places certain requirements on the map to be used.

The "rectilinear" transfer grid is fundamentally a grid of mutually perpendicular families of small circles inscribed on the surface of the earth, the central circles being great circles. The rectilinear transfer grid as actually used on a plane surface is then a mapping of this system of circles onto a plane tangent to the earth at the principal point. It is desirable that this mapping coincide with the projection of the final map even though the transfer grid may be oriented at any azimuth and may be centered upon almost any parallel.

The qualities required of the map are macroscopic conformality and constancy of scale. Patently, no global map can have these features. It was originally believed that a suitable compromise could be reached by the use of maps having the appropriate characteristics over certain parts of the earth's surface. Thus, a polar stereographic chart might be suitable for high latitudes, a Lambert conformal projection suitable for middle latitudes, and a Mercator chart would be suitable for lower latitudes. More detailed investigation of this concept revealed that the use of a multiplicity of projections would be, at best, confusing. Even worse, it was found difficult to provide for overlap between areas to be covered by the various projections. The Lambert conformal chart, while preserving

microscopic conformality, was found to perform rather poorly over the substantial areas to be covered by a single picture. The best representation seemed to be provided by the Mercator map in the equatorial regions. These virtues vanished abruptly at latitudes greater than about 22°. A complete development of the mapping problem is contained in Appendix C.

These considerations led to the investigation of the transverse Mercator chart which is similar in principle to the conventional Mercator. However, the cylinder upon which the map is developed is skewed with respect to the poles. The chart is defined by the inclination of the great circle of contact between the cylinder and the earth's sphere.

The use of the transverse Mercator is attractive because the satellite orbit approximates a great circle, at least in inertial space. The rotation of the earth under the satellite orbit makes the actual path of the satellite about the earth somewhat different from the great circle. However, for the purposes of mapping, the deviation for a rapidly orbiting satellite is not sufficiently great to invalidate the concept.

While the complete transverse Mercator completely encircles the globe, it was found convenient to split the chart into three sections. Because of symmetries, these actually represent about 1/6 of a great circle each. By simple inversion, the same section can be used for the maximum northern and southern excursions of the satellite orbit. Similarly, the same section that is used to map the southbound leg of the orbit from the middle latitudes to the equator can be used to continue the southbound leg below the equator by inversion. The three sectional charts, then, correspond to the maximum excursions, the northbound and the southbound legs respectively.

Longitude is arbitrary on these charts. A set of longitudes is chosen which will satisfactorily map an appropriate section of the satellite orbit. Space is provided on the charts for the designation of these longitudes. Except for north and south ambivalence, latitudes are fixed.

As a result of this generalization to but three charts, continental geography cannot be shown. It is recognized that, under some conditions, this may be somewhat of a handicap. However this shortcoming can be minimized by having conventional maps for reference.

Fig. 3 shows a greatly reduced example of one of the transverse Mercator charts to be used. The original scale is 1:7,500,000. This scale was chosen as a compromise between a minimum number of charts and the ability to transfer the information on a convenient scale.

1.3.2 Mapping Procedures

The method of use of the transverse Mercator charts is dictated in great measure by the details of the satellite system. At some time in advance of the actual receipt of the photographs, predictions will be available of the geographic position of the successive principal points on the earth's surface and of the azimuth of the satellite from those points. Accordingly, the chart section may be selected and the appropriate range of longitudes assigned. The placing of the principal points on the map will depend somewhat on expected coverage of the pictures. Also, it will be determined to a certain extent by the number of parallel orbits to be recorded on the same chart; a practical limit is three orbits.

The use of the quadrilateral transfer grid with the map has been described earlier.

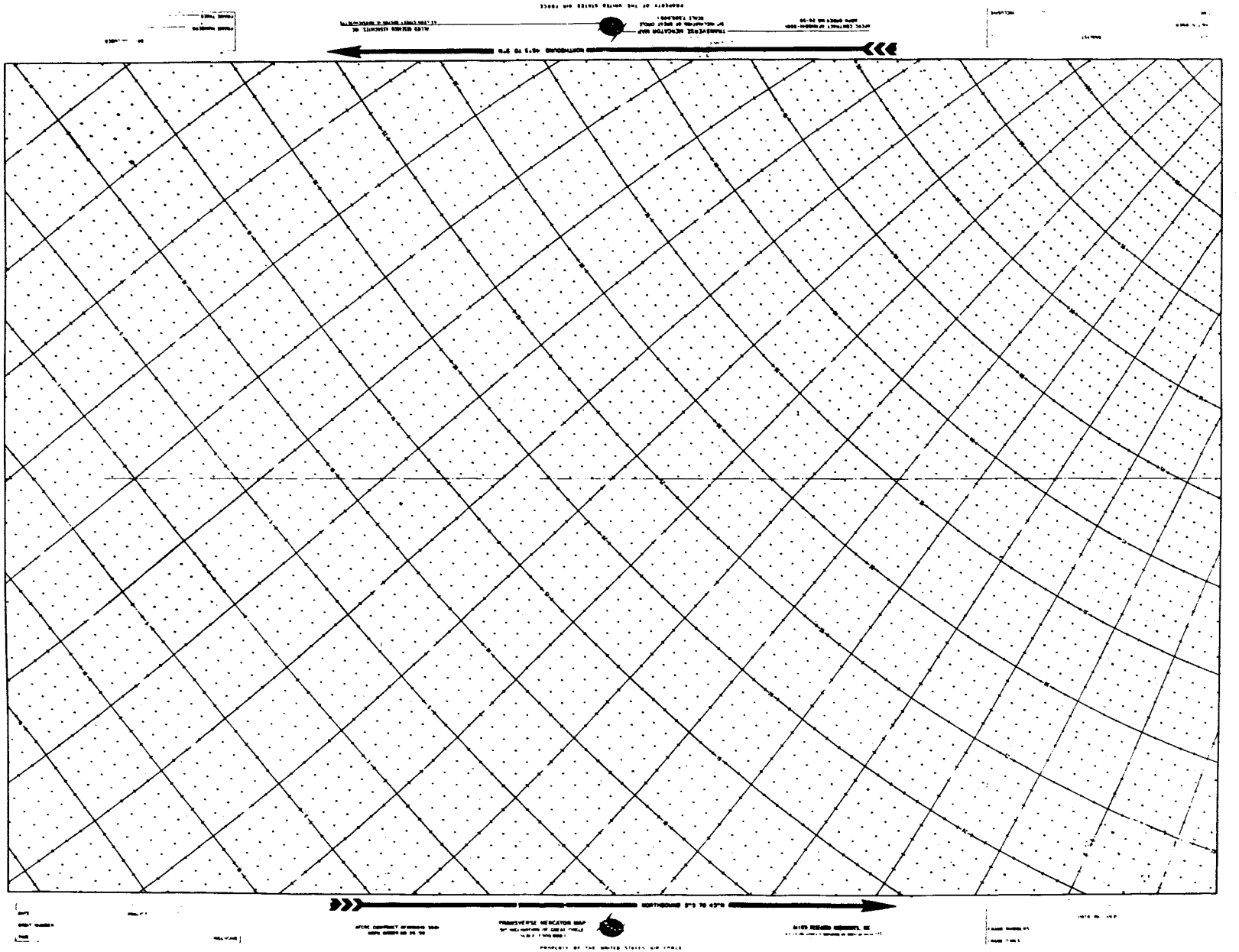

Fig. 3 Transverse Mercator Chart

The transfer of information from the photograph to the map will be done in a conventionalized symbolism, some of which will follow standard meteorological practice. Other parts will probably be more pictorial in nature. An attempt will be made to maintain as great simplicity as possible and to develop standarization.

The mapped information is then ready for the users of meteorological information.

1.4 Equipment

1.4.1 Projectors

A number of Simmon Omega DM-3 microfilm projectors have been acquired and modified for use as projectors of the film transparencies obtained from the satellite readout system.

Basically the projector is a 35 mm autofocus enlarger, modified to accept a point light source as opposed to the diffused light source typical in enlarging. Conventional enlargers were not useable for the present purposes because of inadequate light output. The modified Omega DM-3 combines the advantages of horizontal display, automatic focusing and a rotatable film holder with approximately 60 times the light output of the conventional condenser enlarger. Its use is shown in Fig. 4.

The nominal lamp rating is five amperes at 20 volts. The intensity of illumination is controlled by a variable transformer permitting overloading of the lamp by some ten per cent. With the lamp thus overloaded the light intensity is ample, even with fairly dense film projected at 15 times enlargement and with fairly high ambient illumination.

The DM-3 lamphouse was apparently not designed for continuous operation at such high illumination; under such conditions, the level of heating becomes dangerous to the life of the film. The pro-

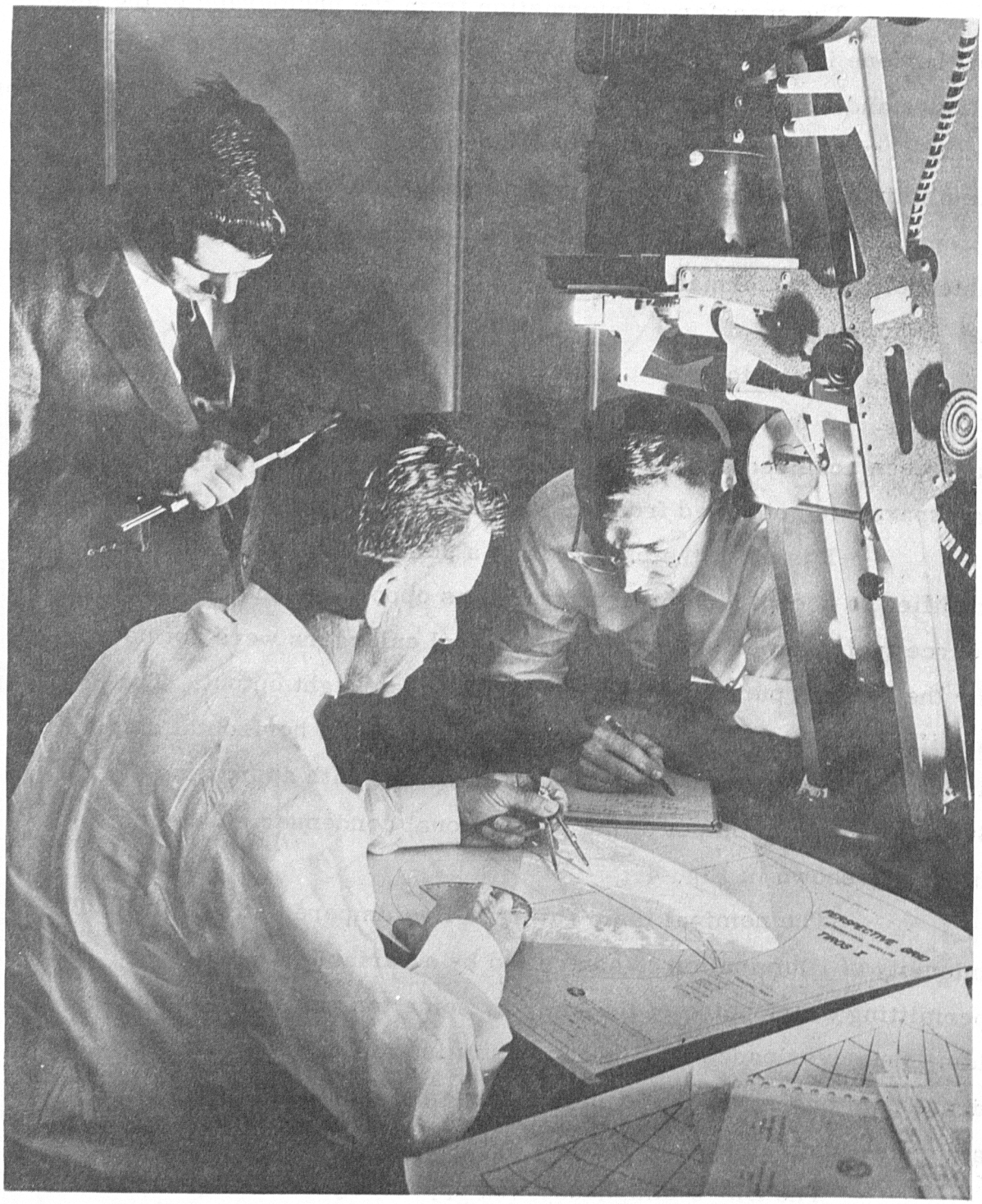

Fig. 4 Use of Projector for Superimposition

of the Image on the Perspective Grid

jector was modified to accept a squirrel-cage blower of 100 cubic feet per minute capacity. The draft is directed on the lamp assembly. Air passage channels were drilled through the condenser assembly to direct a cooling stream of air onto the film itself.

A final modification was to arrange for direct mounting of the projecton on a 36" X 72" library table. This permits free use of large perspective grids and convenient transfer of information to the adjacent map.

1.4.2 Light Box

A portable fluorescent light box is provided as a means of superimposing the image of transfer grid on the transverse Mercator map. At the possible expense of some clumsiness of handling, the box has not been sunk into the table top; this permits ready motion of the transfer grid, permanently affixed to the light box, with respect to the Mercator chart.

1.5 Data Abstraction and Interpretation

1.5.1 Recognition

In previous sections mention was made of transferring pertinent detail from the satellite pictures to a mapping medium. This calls for recognition of such detail. Unfortunately, the relatively low resolution and scan line pattern of the television pictures will make it difficult at best to identify individual cloud types. There may even be difficulty in separating cloud from terrestrial reflections.

Experience in cloud recognition can only be gained through practice. Currently a limited amount of material is available from high-altitude photography which can be adapted to provide at least a certain familiarity with the general aspects of the view from above. Some work has been done with conversion of this material to a form similar to that which might be televised from a satellite; these

attempts have been only partially successful because of the photographic shortcomings of the original material.

There is considerably more hope for successful recognition of cloud systems. The principal difficulties to be encountered here are likely to be in the interpretation of the observed cloud systems. Here experience and knowledge on the part of the photo-interpretor of the optical and electronic processes by which the pictures were made, of the optical properties of clouds, and of the synoptic associations of cloud forms and cloud patterns will help in the synoptic interpretation of the pictorial material.

1.5.2 Abstraction

1.5.2.1 Introduction

Once the meteorological nature of the images in the field of view has been more or less completely established, it remains to describe these images in an abbreviated form that will permit their transfer to the mapping medium.

Two alternate philosophies of abstraction can be presented, each of which has obvious virtues and drawbacks. The eventual system will probably represent an appropriate compromise based on experience.

1.5.2.2 Descriptive Abstraction

Here the photo-interpreter would present a description of the cloud field, being careful not to interject any subjective interpretation of what he sees. Where cloud forms are unambiguous, their nature and location is presented. Where ambiguity is present, the cloud location is given with whatever description of the cloud field is possible. Lines, sheets, broken areas, and clear spaces are described as fully as facilities permit. Then the user of satellite information performs his own analysis and interpretation, and

integrates the satellite data with the other conventional information at his disposal.

Advantages of this purely objective system are obvious. The user, having as full a description of the cloud field as circumstances permit, is free to make his own interpretation to fit his own needs. There is no danger that a misinterpretation generated at some intermediate point in the chain may cause an erroneous decision on the part of the ultimate consumer. On the other hand, there is the real possibility that a remote analyst, who may not see the original picture, may completely miss an interpretation patently obvious to the data abstractor viewing the original picture. In practice this may occur only infrequently, as the data abstractor, upon recognition of a particular situation, is almost sure to "slant" his description in such fashion that the consumer of the information is forced to concur with his unexpressed analysis of the situation.

Disadvantages of the strictly objective system are:

a. The relatively large amount of information required to provide an adequate description of the cloud field even if compressed codification is used.

b. The additional workload placed upon the already harried user who is forced to transform the involved codified descriptive material into a form that can be analyzed and interpreted

c. The difficulty of combination of the purely descriptive satellite information with other meteorological intelligence

1.5.2.3 Interpretative Abstraction

Here the photo-interpreter is charged with performing as complete an interpretation as may be legitimate of the meteorological

occurrences in the pictures. In this case he should be provided with all available conventional meteorological information in an analyzed, readily assimilable form. Making full use of this material as well as of the satellite photographs, he would prepare essentially a combined analysis taking into account time discrepancies, etc. This analysis would then be reduced to a form suitable for transmission to the consumer. Sufficient pure description would also be included to satisfy any needs.

1.5.3 Early Trials

Since early meteorological satellites will constitute an experiment, provisions are being made for both forms of information abstraction. Data abstractors will be trained meteorologists, provided with a reasonably assimilable amount of conventional meteorological information. Where interpretation of the meteorological occurrences in the field of view is possible, this is to be encouraged. Where recognition and interpretation fail, a more objective description of the field of view will be permitted.

Hopefully, as the experiment progresses, experience and capability in recognition and interpretation will increase.

1.6 Codification and Data Transmission

1.6.1 Codification

Following the philosophy of the data abstraction presented in Section 1.5, two code forms have been developed for concise data transmission. Allied Research Associates, Inc., has been concentrating on an abbreviated "plain language" code, styled after the RAREP and analysis codes, which lends itself to quick assimilation by both encoder and decoder. It is particularly suited to the interpretative mode of data abstraction. A description of the code is contained in Appendix D.

A somewhat more elaborate five-digit numerical code prepared by the Meteorological Satellite Section. U.S. Weather Bureau, has been published by them in a manual along with the Allied Research code [20]. The choice between the two codes can be made on the site by the meteorological data-abstraction team after due consideration has been given to data quantity and quality, and to the time available to personnel and on the data transmission links. Both codes use the same preamble but differ in their internal structure.

1.7 Emergency Procedures

1.7.1 Establishment of Location with Certain Data Missing

The successful operation of the data-abstraction system depends upon the provision of adequate information establishing satellite location and attitude for each picture. The information will normally be provided in forecast form from the satellite computation center.

The possibility exists, however, that the necessary data may be missing or erroneous. Such features may stem from several sources. Satellite attitude is to be determined by the output of infrared horizon sensors. If the attitude is rapidly changing for any reason, or if any defect develops in the sensing or communication chain, it is possible that attitude information will be unavailable. Simple communications failures such as teletype garbling might also result in a temporary failure of attitude information.

The pictures themselves can be used to establish the attitude of the satellite with respect to the earth. The easiest operation is the determination of the nadir angle of the camera axis, the angle between the vertical and the axis. This can be accomplished by measuring the horizon position on the picture. In case of no horizon, the same operation can be performed with recognizable landmarks. A further piece of information needed to establish the angle is the

height of the satellite. This can be obtained from the curvature of the horizon, but it is anticipated that the combination of lens distortion and nonlinear scans likely to be present will make effective measurements of the horizon curvature quite difficult.

If the sun sensor equipment is functioning properly, it is also possible to establish the azimuth of the picture from the indication provided from the sun sensor. Here, in addition to the nadir angle (obtainable from the horizon) and the height (best obtained from the tracking forecast), the elevation and azimuth of the sun must be known. These are obtainable from standard navigation-type computations using the Air or Nautical Almanac.

Other emergency computational procedures may be required where defective data is provided or it is found desirable to verify data.

A manual of emergency calculations has been prepared for field use; it is reproduced as Appendix E to this report. The procedures given can be performed with reasonable speed with a desk calculator and trigonometric tables. Forms are being established to facilitate computation.

If circumstances make it necessary to perform these computations on a routine basis to salvage any worthwhile data, it would be possible to use an Allied Research-generated program with a Bendix G-15 computer. The important output would then be readily transmitted via existing teletype networks.

1.8 Recommendations for Future Activities

1.8.1 Suggestions as to Improved Techniques

Detailed recommendations for future activities must await the outcome of the first experiment which is scheduled to occur near the release of this report. However, some areas of weakness that have

become apparent in developing the present system may bear further attention. Most of these problems center around the data location and abstraction areas.

The problem of picture perspective rectification cannot be considered solved in final form by the grid library technique. If the grid technique is found to be convenient in practice, the possiblity of automatic generation of the grid should be considered. A typical possibility is the generation of the grid by analog circuitry with a presentation on the face of a cathode-ray oscilloscope. This presentation could be projected onto the picture to provide a set of superposed lines. If reasonably dependable satellite locations could be provided, it might be feasible to extend this method to the inscription of the latitude and longitude grid lines on the picture. Rough experiments with this type of presentation have suggested however, that it may be somewhat confusing, particularly it lens distortion is present.

Various optical methods of image rectification or map projection onto the image may also be considered. One of the most attractive is the camera lucida or "sketchmaster" system. Here, the picture and the map are viewed simultaneously through a single eyepiece. A beam-splitting prism causes the map to appear superposed on the picture. Adjustments for perspective are easily made where a plane earth is involved. However, from satellite altitudes, the earth is hardly a flat plane, so that more elaborate optical features would be required to appropriately superpose the image of the curved earth on a flat plane map.

This leads to the problem of map projection. While the transverse Mercator chart described in this report is a significant step, it is felt that further advances are available in charting that will

facilitate the data-abstraction process. As an example, a Mercator-type chart whose arc of contact with the earth's surface spirals about the earth directly under the satellite orbit might prove even more useful than the transverse Mercator.

Because of the extreme perspective effects present in most pictures taken from a satellite with attitude not stabilized to always look downward, it is not felt to be profitable to attempt direct picture rectification--that is, to reproject the picture optically onto an appropriate map projection. This is particularly true of television line-scanned pictures, as the scanned lines would be projected into widely varying widths. Other effects of perspective, such as the variation of brightness of clouds with angle of view and the apparent heavy cloudiness of the horizons, would become unrecognizable in a rectified projection.

In the area of meteorological interpretation of the satellite pictures, it is believed that considerable progress will be made in defining cloud systems. This is partially a semantic problem, since much of meteorological thinking is directed around meteorological systems defined by pressure or circulation patterns. Some cloud systems may be identifiable which have no direct counterpart in pressure patterns. These recurring patterns will eventually be recognized and named.

The problems associated with the integration of cloud patterns with more conventional analytical models will not be readily solved. This is particularly true when attempts are made to combine cloud analysis with such quantitative analyses as those used for numerical weather prediction. The authors of this report would like to caution against premature attempts to fully integrate satellite observations. Much work must be done on the synoptic causes of cloud manifestations before such integration can give encouraging results.

It should be recognized, however, that the observations of the meteorological satellite, by themselves, can be of extreme value in the under-observed areas of the globe.

Blank page retained for pagination

CHAPTER IV (Continued)

SECTION 2

A PHOTOGRAMMETRIC METHOD OF OBTAINING THE CAMERA AXIS AND ITS APPLICATION IN DETERMINING THE TIME OF PHOTOGRAPHS TAKEN FROM A SPACE VEHICLE

R. J. Boucher

Allied Research Associates, Inc.*

2.1 Introduction

Presently planned meteorological satellite systems, whose purpose is to obtain cloud photographs, are designed to provide considerable auxiliary information to be used in locating the photographed region. Various techniques for obtaining the map coordinates of the pertinent weather features observed on the photographs have been worked out by Allied Research Associates, Inc., under Contract No. AF19(604)-5581, and have been reported in Section 1 of this chapter. To appreciate better the problems of data processing and interpretation, photographs of weather features taken during a ballistic flight of an Atlas missile were examined. During this examination, it was found that lack of sufficient documentation made it impossible to apply directly the techniques for obtaining the map coordinates of weather features. A procedure was devised to develop the necessary data to permit application of the mapping techniques. This procedure is presented here.

---

* This work was sponsored under Contract No. AF19(604)-5582, under ARPA Order No. 26-59.

The technique which will be described below was devised specifically to provide data necessary for the interpretation of pictures taken from the Atlas Missile 11C. However this technique, or a slightly modified version may be applied to pictures received from any missile or satellite vehicle for the purpose of providing or verifying data on the azimuths of the principal lines, or camera axes and the times of the pictures.

2.2 Description of the Techniques

It is assumed that the missile or satellite will be tracked with sufficient accuracy to establish the position of its subpoint and its height at any given time. The satellite vehicles will also telemeter data independent of the picture information, which should suffice to determine the angle of the camera and/or spin axis with respect to the subpoint at any given time. It is possible, however, that the orientation of the camera axis and the timing of the pictures, either television or direct photographs, may be in doubt at times due to several possible factors affecting the rate of picture taking and the start of picture taking sequences, difficulties in transmission of pictures and other data, or partial or temporary failure of one or several components in either the satellite or read-out stations. This may necessitate determining the relation between the time and space coordinates of the vehicle and its orientation from the pictures themselves.

The first step in the technique is to find pictures with recognizable landmarks such as islands, coastlines, or land features which can be identified on a map and which can yield latitudes and longitudes of at least two points along the principal line (the projection of the principal axis on the film plane) of the photograph.

To facilitate establishing accurately the principal point and principal line of the photographs, permanent fiducial marks in the

optical system are highly desirable. Should these be absent, it may still be possible to establish, with reasonable accuracy, the principal point of the picture. This requires that the square or rectangular boundaries of each picture be determined. Assuming the camera lens to be centered, the principal point is then the intersection of diagonals from opposite corners. This point may be above or below the horizon, depending on the height and nadir angle.

The principal line is drawn, which is defined as a line passing through the principal point and perpendicular to a tangent to the horizon at a point where the principal line intersects the horizon. The second point needed to draw this line can be found by locating two points on the horizon equidistant from the principal point. The desired point defining the principal line will then be the intersection of two more arcs from each of the horizon points. (See Fig. 5.) This procedure can be repeated for as many pictures as needed which have recognizable land freatures falling under the principal line. For the Atlas 11C, suitable pictures were selected from each of the five scans of the camera that were recorded on film, and principal points and principal lines drawn on each.

The next step is to establish the geographical location--that is, latitude and longitude--of the two or more recognizable landmarks intersected by the principal line, using a set of high-quality maps such as may be found in the Times Atlas of the World.

On a Mercator or Transverse Mercator map on which has been plotted successive positions and times of the vehicle subpoint, the landmarks positions are plotted and a line connecting them is extended until it intersects the locus of the vehicle subpoints. The intersection point then furnishes an estimate of the time of this picture and also the subpoint of the vehicle at the time of the picture. There

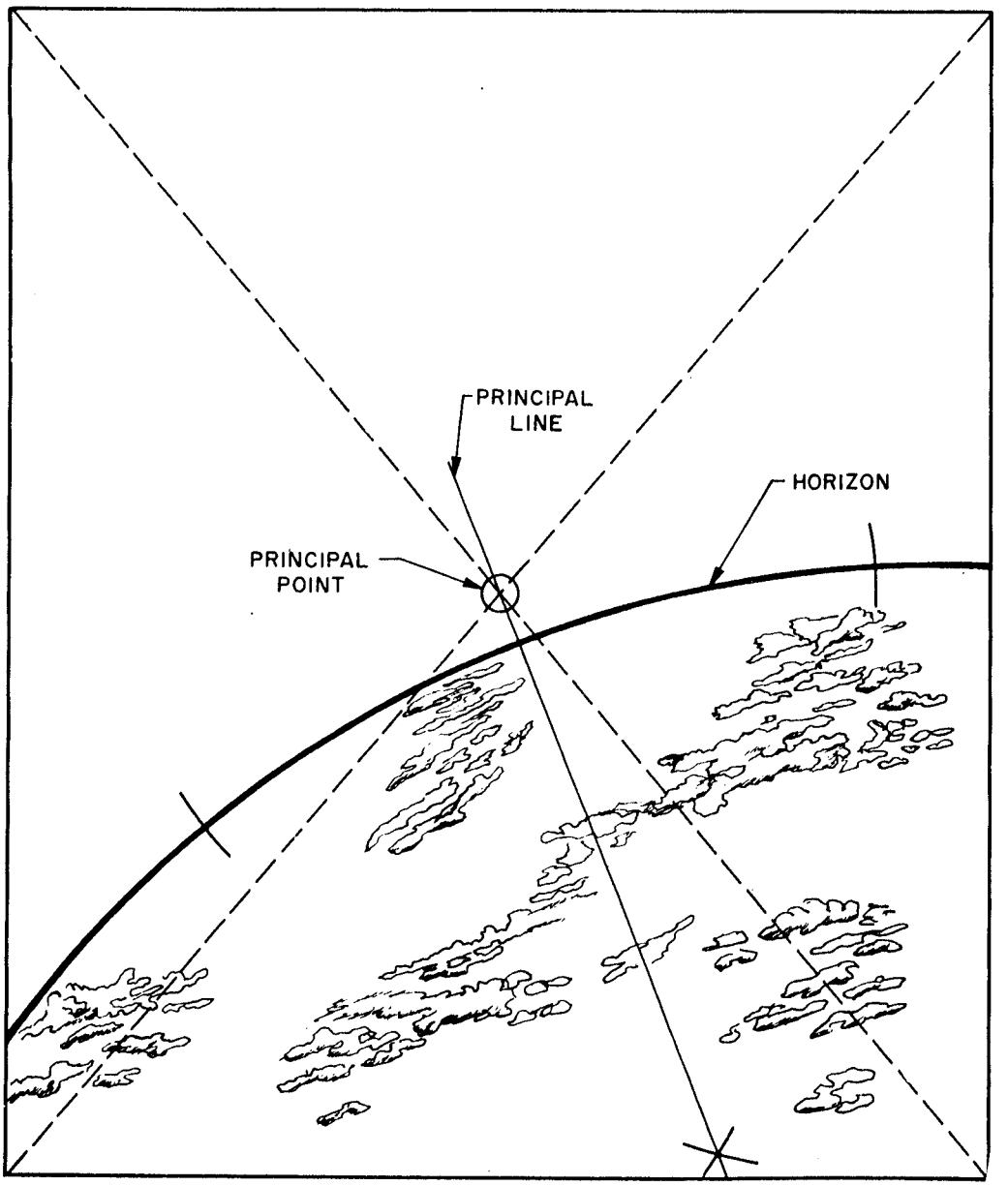

Fig. 5 Sketch showing method of locating principal line on space vehicle photograph

is an obvious source of error in this approximate technique because of the map projection used. A gnomonic projection would result in correct bearings; but this projection is virtually useless for other purposes. However there is a simple method of correcting for the fact that a bearing line (great circle) on a Mercator map should be a curved and not a straight line. This method, shown in detail in Reference 21, consists of adding or subtracting the "convergency" to the azimuth or bearing. The convergency, C, is computed as follows:

$$C = \Delta \Theta \sin \frac{\phi_1 + \phi_2}{2}$$

where

$\Delta \Theta$ = difference in longitude between end-points of the bearing or azimuth line,

ϕ_1 and ϕ_2 are the latitudes of the end points.

The sign of C will be positive if the vehicle is east of the landmarks used or negative if west. Obviously, C will be zero or near zero when the line crosses the equator and zero when the bearing is along a meridian.

For the Atlas 11C missile pictures, the maximum bearing error was 4° for an E-W bearing at about 27°N. Most errors were of the order of 1° to 2° which is considered within the magnitude range of other errors.

Using the method described above, it then becomes possible to plot frame number vs. time for the pictures for which lines can be plotted, as illustrated in Fig. 6. If enough reference points are available, a curve can be drawn allowing the determination of time for any frame number.

In a similar manner the azimuths of the bearings can be plotted against frame number and another curve drawn giving azimuth vs. frame number, as shown in Fig. 7, which is necessary in establishing the location of clouds observed in the pictures.

2.3 Conclusion

The method described above, while devised specifically for use with the Atlas 11C pictures, may be adapted for use with pictures obtained from other vehicles, including satellites. The successful application will hinge on obtaining sufficient pictures with recognizable landmarks. The pictures must have the horizon visible, otherwise the principal line cannot be established.

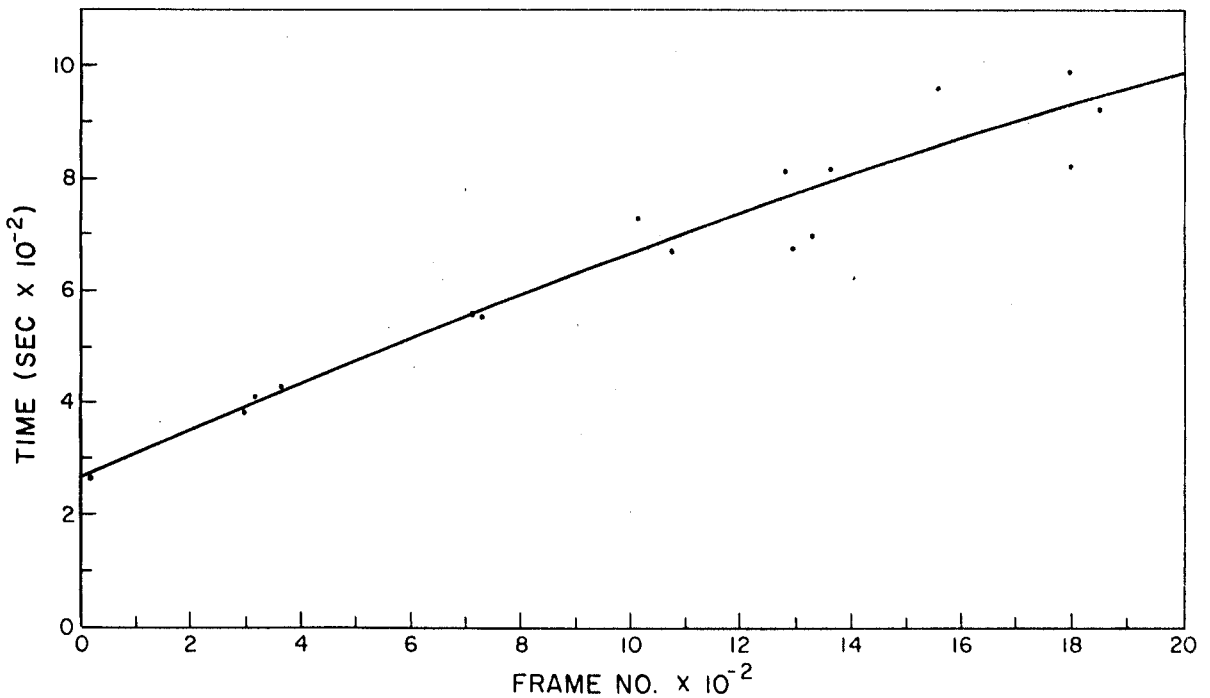

Fig. 6 Frame number vs time for Atlas 11 c photographs

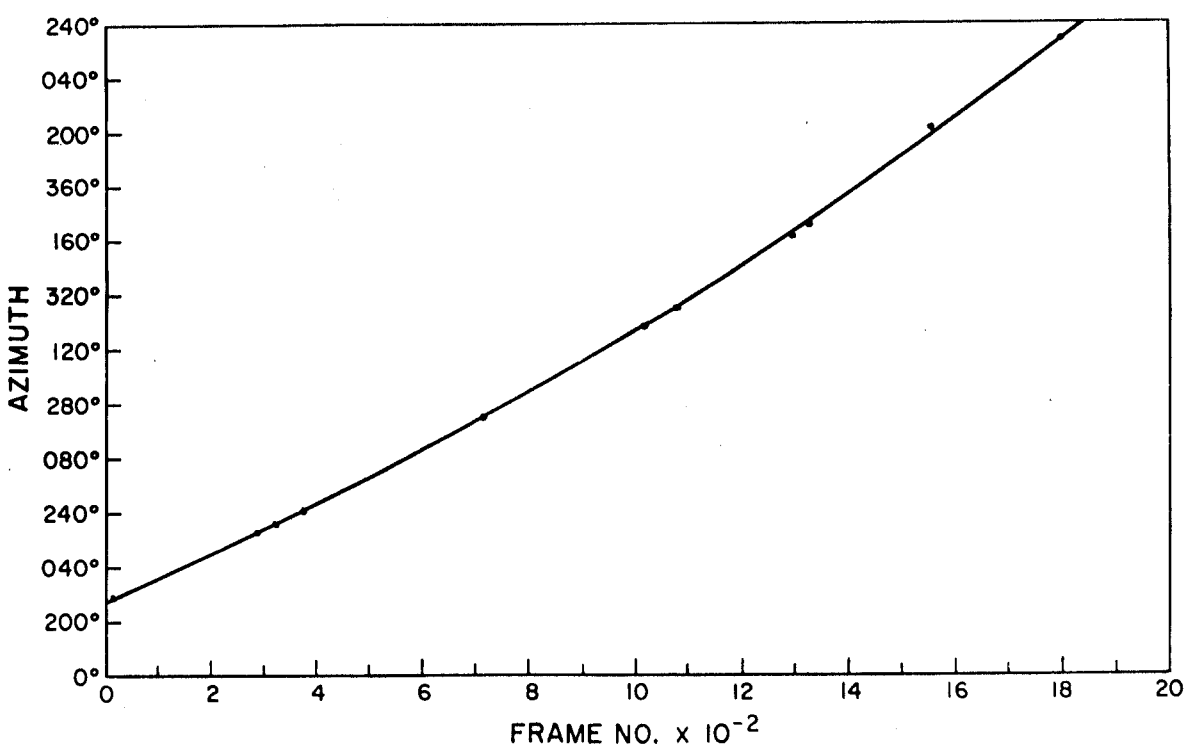

Fig. 7 Frame number vs azimuth for Atlas 11 c photographs

Blank page retained for pagination

CHAPTER V

SECTION 1

SYNOPTIC-SCALE RADIATION PROCESSES

K. L. Coulson

Stanford Research Institute* †

1.1 Introduction

The energy balance of the atmosphere is determined mainly by three energy-transfer processes: (1) the transfer of sensible heat, (2) the transfer of latent heat in the hydrologic cycle, and (3) the transfer of energy by both long-wave and short-wave radiation. The relative importance of the processes varies with time and location, but they are each of great importance in the atmospheric heat engine. It is known that the radiative processes generally act more slowly than do either of the other processes, and that for a period of the order of a day or so the radiative exchanges can be neglected in considerations of the over-all energy balance. However, for longer periods the radiative effects, being of a systematic nature, become relatively more important, and in the final analysis the energy for driving the atmosphere must be furnished by radiation.

---

* This work was sponsored under Contract No. AF19(604)-5965, under ARPA Order No. 26-59.

† Further details on the research summarized here are being published as Scientific Report No. 1, Contract No. AF19(604)-5965, Atmospheric Radiative Heating and Cooling, by K. L. Coulson, Stanford Research Institute.

110 876

The radiational energy budget is receiving the maor emphasis in the present study. Computations of the radiation emerging from the upper reaches of the atmosphere and the measurements accomplished by properly instrumented satellites will serve as valuable mutually independent checks. Of the energy-transfer processes the radiational regime is more amenable to study because (1) radiative exchanges are probably more influential in the development of large-scale circulations and their subsequent evolution than are the other processes, (2) the theoretical tools for studying radiation are more advanced than those for the other processes, and (3) observational data for computing radiative transfers are more complete than those for either latent or sensible heat transfers, although even here there remains much to be desired.

The atmosphere divides itself in the vertical into four more-or-less distinct radiation regions, a division that seems appropriate for the present investigation as well:

a. The uppermost region extends from the top of the atmosphere down to the top of the ozonosphere at roughly 65-70 km above the surface. It is a region of many very interesting phenomena such as the aurorae, noctilucent clouds, ionized gases, and others, but the mass density is so low that it does not enter significantly into the large-scale atmospheric energy budget.

b. The second region is the region of ozonosphere, extending from 70 km down to the base of the ozone maximum at about 22-25 km. Despite the low density of the air in the layer, important radiation effects are produced, principally by the absorption of ultraviolet solar radiation by ozone and the emission of infrared radiation by the 15-micron band of carbon dioxide.

c. Radiation effects in the third region, namely the region from the base of the ozone maximum down to the tropopause, are of relatively minor importance. For practical purposes they can be neglected until such time as further refinements can be utilized. Any ozone present is protected from the short-wave ultraviolet coming from the sun by the ozone above. Emission of infrared radiation by carbon dioxide, and by the small amount of water vapor, is balanced by absorption of the radiation emitted from

the warmer layers above and below, establishing a condition of radiative quasi-equilibrium for the layer.

d. The fourth region, the troposhere, extends from the tropopause to the earth's surface and is by far the most important region from a radiation standpoint. It is here that atmospheric water vapor makes itself felt in the radiation regime; absorption and emission effects of ozone, carbon dioxide, and other atmospheric gases are dwarfed by comparison with those of water vapor. The complicated absorption spectrum and the great variability of the amount of water vapor combine to make the tropospheric radiation problem a very difficult one. The problem is further enhanced by the large effects of tropospheric cloudiness on both the incoming solar radiation and the outgoing terrestrial radiation.

The major part of the present radiation study has been, and continues to be, an evaluation of the radiant energy entering the troposphere and the ozonosphere, the amount of energy leaving those layers, and the amount and distribution of the net radiation which goes to heat or cool the respective regions.

1.2 Radiation Budget of the Ozonosphere

Because the radiation contributed by the ozonosphere to the total radiation emerging from the top of the atmosphere is a relatively small fraction of that supplied by the troposphere, only the broad features of the radiation regime of the ozonosphere need be taken into account here. For this part of the investigation, recourse to the literature provided a very adequate evaluation for present purposes. Much effort has been expended by different groups in determining the physical characteristics of the ozone layer, and in studying the absorption and emission spectrum of carbon dioxide, Of particular value is the extensive work of Plass on the radiative cooling of the ozone layer. Plass's computations were based on the radiative

properties of ozone and carbon dioxide as determined experimentally by Summerfield and Cloud, respectively. More recent transmission data have been supplied by Howard, et al, and used by London, et al, to give a general picture of the flux divergence in the layer between the tropopause and 55 km for various latitude belts. Important contributions have been made by many other authors, including Kaplan, Craig, Curtis and Goody, Elsasser and King, Gowan and Callender. Present knowledge of the short-wave absorption in the ozonosphere is limited largely by lack of knowledge of the ozone distribution in the critical 35-60 km region. The spectrographic measurements by high-altitude rockets, performed by the Naval Research Laboratory, provide the most precise data available on both the ozone distribution and the ultraviolet portion of the solar spectrum; but more such measurements at various locations and times are badly needed. The work of Pressman and London give an over-all view of the energy absorbed by ozone at various latitudes and seasons.

The radiation balance in the ozonosphere may, within the framework of present knowledge, be summarized as follows:

a. Carbon dioxide is the most important agent for cooling the ozonosphere; ozone plays a secondary but not unimportant role.

b. Heating of the ozonosphere by solar radiation is accomplished almost entirely by ozone absorption.

c. The maximum rate of cooling and the maximum rate of heating, both of the order of a few degrees Centigrade per day, occur in the 45-50 km region, although the maximum ozone concentration is at a much lower altitude.

d. Photochemical equilibrium amounts of ozone are quickly established in the region above 45 km, but radiative production and dissociation of ozone at lower levels are so slow that the ozone concentration is a conservative property of an air parcel.

e. Although the divergence of radiative flux is an order of magnitude smaller in the stratosphere than in the troposphere, the heating and cooling rates are often larger because of the much lower air density at high levels.

f. There is a large seasonal variation of short-wave absorption by ozone; the maximum occurs in high latitudes in summer and the minimum in high latitudes in winter.

g. The diurnal temperature variation caused by absorption of solar radiation is of the order of 3-5°C at the maximum, which occurs in the 40-50 km region.

h. The extent to which day-to-day radiative equilibrium is established in the ozonosphere is still a matter of controversy; but it seems clear that, in the main, the ozonosphere acts as a heat sink in high latitudes and a heat source in low latitudes. However there is no reason to believe that a direct circulation is established at high levels for bringing the low-latitude energy excess to high latitudes.

i. The region of the temperature maximum near 50 km probably has a net radiation excess, necessitating a circulation for transporting energy, in the form of sensible heat, away from that level.

Work is largely complete on summarizing the ozonospheric radiation balance as a function of latitude, season, altitude, and ozone distribution, and determining (1) its effect on the total radiation flux proceeding to space from the top of the atmosphere, and (2) a heating function appropriate for introduction into the dynamical-numerical models.

1.3 Radiation Budget of the Troposphere

In contrast to conditions in the ozonosphere, the radiation characteristics of the troposphere are determined almost entirely by atmospheric water, either in the form of water-vapor or the liquid water of clouds. As pointed out above, the complete absorption spectrum of water-vapor and the great variability of the amount of water-vapor and clouds in both space and time make the problem

difficult indeed. The broad features of the radiation balance were outlined in Simpon's classical investigations. More recent developments have been provided by Baur and Phillips, Mugge and Moller, Elsasser, Moller, Elsasser and King, Hales, London, to mention only a few. It is necessary, however, to interpret these works in terms of the present problem and to fill the gaps as much as possible. In the interest of brevity, a review of the literature will not be given here. Instead, the method of attack being applied on this project to the tropospheric radiation problem will be outlined.

1.4 Vertical Profile of the Infrared Radiation Balance

There is generally more long-wave radiant energy leaving the troposphere than entering it, representing a mean net cooling. The cooling of the total troposphere has been studied by several investigators and is fairly well understood. However the vertical profile of the radiation balance is important in the present problem, and this aspect has received scant attention so far. Work is underway to determine the radiation balance at various levels in an actual synoptic weather situation which was chosen as being typical. The study is just getting started and has yielded no results as yet, but it is expected that the effects of the vertical moisture distribution, cloudiness at different levels, and other characteristics will be brought into focus. Results obtained by previous authors on the over-all radiation balance will serve as a valuable check on the total flux divergence obtained by integration of our vertical profile through the entire troposhere.

1.5 Cloud Distribution and its Effects on Atmospheric Radiation

Most clouds radiate essentially as black bodies, so their influence on the infrared radiation regime can be assessed if the amount, height, thickness, and temperature of the clouds themselves are known. The

amount of the incoming solar radiation which is reflected back to space from the clouds can also be estimated if the cloud characteristics are known.

Unfortunately much of this information is seldom available, and some approximations become necessary. Average cloud characteristics as obtained from climatological data are usually used in lieu of more definite information, but this obliterates many of the important details of the radiation regime. One of the advantages of concentrating on a particular weather system is that a more comprehensive study of the cloud patterns can be made, as is being done at the Stanford Research Institute.

1.6 Effect of Surface Temperature on the Atmospheric Radiation Balance

Because of the fourth-power dependence of energy emission on temperature, the amount of radiant energy introduced at the bottom of the atmosphere is critically dependent on surface temperature. The temperature of the radiating surface, that is, the ground itself, is not measured in standard meteorological observations, and the instrument shelter temperature reported may be very different from the ground temperature. Consequently the computations do not give an accurate value for the energy radiated by the ground surface. An evaluation of the errors introduced can be made by assuming a given error in the surface temperature and computing the effect this has on the radiation regime. These determinations are anticipated in the present study but have not been started as yet.

Current plans for case studies and calculation thus include a determination of the upward and downward radiative fluxes, and the resulting flux divergence, as a function of height in the troposphere, as well as an evaluation of the effects of both cloudiness and surface temperature on the tropospheric radiation balance.

1.7 Use of Radiation Data Obtained by Satellites

The great potential of radiation data obtained by measurements from satellites makes it desirable to tailor the present work as much as possible toward the interpretation of such data, which will become available shortly. Although the details of the radiative heating and cooling within the atmosphere will still have to be determined by conventional means, efforts will be made in the present case to estimate just how well the atmospheric radiative balance can be approximated from only the radiation directed outward from the top of the atmosphere. By this means a preliminary estimate of the relation between measurements made by satellites and by existing methods can be made, and an indication of the extent to which they will serve as valuable independent checks will be obtained.

CHAPTER V (Continued)

SECTION 2

STUDIES OF ATMOSPHERIC RADIATION AS OBSERVED FROM SATELLITES

Julius London
New York University*

2.1 General

Until quite recently most of the computations of atmospheric radiation were based on theoretical studies rather than atmospheric observations. It is therefore of utmost importance that planned meteorological satellites are now being designed to observe the basic components of the radiative balance of the atmosphere (a fundamental quantity for understanding the major large-scale processes of the atmosphere). In complementing theory with observations, however, it is necessary that they both operate on a consistent set of parameters. That is, the theory even when limited by assumptions still represents at least a part of the real atmosphere; and the observations can be so interpreted as to give meaning to that same real atmosphere. Unfortunately this has not always been the case. (See, for instance, Moller, [22].)

Studies of the atmospheric heat balance are of importance in at least two particular stages. First, the large-scale seasonal and annual distributions of the heat sources and sinks provide us with the basic quantities for determining the driving forces of the general circulation of the atmosphere. Second, the short time variations of these

---

* This research was conducted under Contract No. AF19(604)-5955, under ARPA Order No. 26-59

quantities can give some additional insight as to how the circulation systems develop.

If the solar constant is known, the local heat input and output to the earth-atmosphere system is a function only of the local planetary albedo and the outgoing infrared radiative flux of this system. Both of these quantities have been determined from theory (Houghton, [23]; London, [24]) for averaged seasonal and latitudinal conditions. Suitably instrumented meteorological satellites could provide the type of observations needed to check these theoretical calculations.

At the outset there are many problems in applying the satellite observations in terms of the theory. For instance, in computing the total outgoing infrared flux from the earth-atmosphere system, it is always assumed (with great validity for the purpose of this computation) that the atmosphere is plane and stratified. As a result, one can interpret the total computed flux as equivalent to an assumed black-body flux from some level in the atmosphere. This effective emitting level would in general vary with latitude and season. However results show that the variations of the "effective" emission level in the atmosphere is quite small indeed and is almost always found between about 6-7 km (see Fig. 1). This would not be true for any particular satellite observation of total atmospheric emission since in that case the "effective" emission level would be lowest at the sub-satellite point and be concave upwards (with respect to the earth's surface) at increased angle from the vertical. Obviously, then, the radiation reaching the satellite sensors cannot be treated as coming from a plane, stratified, terrestrial atmosphere.

To apply the results of forthcoming radiation measurements from satellites, one must reformulate the radiative flux problem so that it is consistent with the various observations.

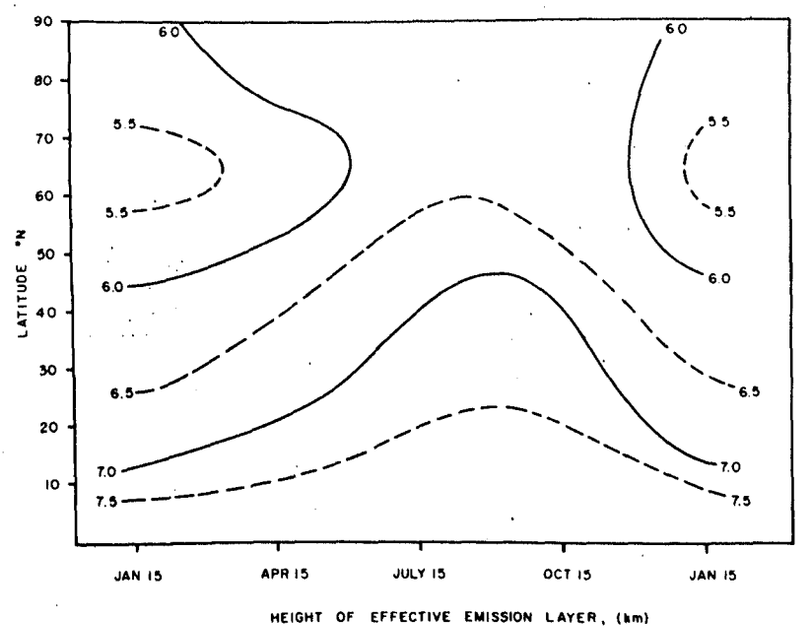

Fig. 1 The calculated height of the effective emission layer

2.2 The Fundamental Radiative Transfer Equation

The fundamental differential equation governing atmospheric radiative transfer is given for a monochromatic vertical beam by

$$dI = - k(I - I_b)du \tag{1}$$

where I is the radiative intensity per unit solid angle (I_b, then, is the black-body intensity), k is the monochromatic absorption coefficient per unit optical thickness, and u is the optical thickness of the absorbing gas. The only atmospheric gases of any importance for radiative transfer in the earth's atmosphere are H_2O, CO_2, and O_3. The absorption spectra of these gases are not completely mutually exclusive. However, the transfer problem can be simplified, and there is no great error made if they are so treated.

The solution for the vertical beam arriving at the top of the atmosphere (level of the satellite) is simply

$$I(z) = I(0)\ \tau(0,\ u_z) + \int_0^{u_z} I_b(T_u) k\, \tau(u,\ u_z) du \qquad (2)$$

where I(0) is the upward directed intensity from the ground, I_b is the black-body intensity corresponding to the temperature found at the level u, and τ represents the specific transmission function for the gas and spectral interval involved. For any particular case in the real atmosphere the integral must be evaulated numerically (or graphically) since, in general, the relationship between T and u in the atmosphere cannot be specified.

The quantity most easily observable from a satellite is the total radiation flux at the satellite level. However, in that case, the corresponding solution for Eq. (1) involves integration over all angles of the incoming beam and over all frequencies of the received radiation. The former presents additional difficulties because at these heights the upwelling beam can no longer be assumed to traverse a plane, stratified atmosphere. The latter integration requires suitable approximations for the transmissivities of the various absorbing gases and suitable temperature and pressure corrections to these transmissivities. Since these difficulties are quite substantial, it is of some instructive use to adopt the solution given by Eq. (2) to the simplest nontrivial case. It is planned that additional procedures will be adopted, in due course, in order to have the theoretical computations correspond as closely as possible to the observational program of satellite radiational measurements.

2.3 Case I

Assume the case of a vertical beam and consider only the spectral interval 10.5-11.5 microns (the so-called atmospheric window region). In this region the only significant absorption is the wing continuum due to the distant water-vapor rotational lines.

Eq. (2) now takes the form

$$I_z = I(0) \exp[-\bar{k}_o u_z] + \int_0^{u_z} I_b(T_u) \bar{k}_0 \exp[-\bar{k}_o (u - u_z)] \, du \qquad (3)$$

where $\bar{k}_o$ is average absorption coefficient in the interval 10.5-11.5 microns at STP. If $\bar{k}$ is assumed independent of temperature, we can write

$$k = k_o \frac{\bar{p}}{p_o} \qquad (4)$$

since we are concerned only with the region far removed from the absorbing line centers. The value for $\bar{p}$ is the average pressure of the absorbing gas (water vapor) from any level u up to the top of the atmosphere. For the vertical beam, $\bar{p} \approx 700$ mb for the entire column of water vapor. This value varies slightly from place-to-place and with season and should be evaluated specifically for each computation.

Computations for an average atmosphere, with the ground temperature of 20°C containing 2 cm precipitable water, and assuming a value of $\bar{k}_o = 0.3$, give for the total intensity at the top of the atmosphere

$$I_z \approx 0.011 \text{ ly min}^{-1} .$$

Since the ground beam has an intensity of $I_o \approx 0.0125$ ly min^{-1}, the intensity received at the top of the atmosphere represents approximately 80 per cent. of the surface beam. It is also interesting to note that of the 80 per cent. received at the top, approximately 65 per cent. comes from the surface beam and 15 per cent. from the atmosphere chiefly in the layers below 700 mb. If clouds were interposed between the ground and the satellite level, a larger proportion of cloud radiation would be received by the satellite in comparison to the remaining atmospheric beam.

Use of this simple radiation model for the "transparent" portion of the spectrum also permits some approximations for the intensity reaching the satellite from some nonvertical direction.

A satellite at a height of 300 km can accept a collimated beam of radiation from any angle from the vertical up to 72° before it is pointed to the horizon. Thus a radiating beam originates at the earth's surface at distances as great as 4000 km away as the satellite turns on its axis from horizon to horizon. At this distance the total intensity reaching the satellite is reduced to less than one quarter of its vertical value with the ground, and atmospheric beams each contribute about one-half of this amount.

The above figures are quoted for illustrative purposes only. Individual values must and will be computed to indicate the variation of intensity as received at satellite levels for this spectral interval under various ground and atmospheric conditions. A more complete set of computations can then be used to determine the relationship between the vertical beam and the intensity at any angle from the vertical. It will then be possible to compute the flux of radiation reaching satellite levels in the "transparent" portion of the spectrum.

CHAPTER V (Continued)

SECTION 3

A PRELIMINARY INVESTIGATION OF THE NATURE OF THE INFRARED VIEW OF THE EARTH'S ATMOSPHERE FROM A SATELLITE

A. H. Glaser and S. N. Milford

Allied Research Associates, Inc. *

3.1 Introduction

One proposed use of the satellite for meteorological purposes is to scan the atmosphere at an infrared wavelength in which water strongly absorbs and emits. The varying intensity of radiation at this wavelength would give an indication of the temperature at which the emission is taking place and of a part of the total heat balance. A preliminary investigation was executed to find the nature of the view that might be obtained from a scanning device that would create pictures as seen by infrared light. The present discussion will be limited to water-vapor emission.

For the sake of simplification, it will be taken that the atmosphere is viewed at a wavelength such that the water vapor is quite opaque. Such wavelengths are found in the 6.3μ band. It may be found more convenient to use wave lengths somewhat longer than this, say 7.5μ, to take advantage of the greater water-vapor emission which occurs near the peak of the black-body radiation. Differing choices of wavelength also affect the region of the atmosphere from which most of the radiation will be emitted as will become apparent later.

---

* This research was conducted in part under Contract No. AF19(604)-5582, under ARPA Order No. 26-59, and in part under Contract No. AF19(604)-3881.

The view of the atmosphere as seen in an intense emission (and absorption) band of water will be that of a glowing fog. The intensity of glow will be related to the temperature of the top layer of the visible fog. The outer layers of the fog are somewhat transparent and, in general, the inside of the fog will be of a higher temperature than the outside. This presents a problem in the calculation of radiative transfer familiar to astrophysicists. A simplified approach yielding approximate numerical results will be presented here to demonstrate the behavior of the radiation. A heuristic approach is then adopted to investigate the meteorological significance of the radiation. Finally, a discussion of some applications is presented.

3.2 Radiation Source in the Atmosphere

3.2.1 Background

The intensity of radiation emitted normally from the top of an absorbing medium can be written

$$I_\lambda = \int_0^\infty K_\lambda B_\lambda (T) e^{-\tau_\lambda} ds \quad (\text{erg cm}^{-2} \text{ sec}^{-1} \text{ sterad}^{-1} \text{ micron}^{-1}) \quad (1)$$

where K_λ = absorption coefficient per length L, where the length ds in the atmosphere is measured in the same units as L. Calculations are often made in terms of K'_λ, the absorption coefficient per cm of water vapor, and w, the water content in cm of water vapor per length L of the atmosphere. In this notation, $K_\lambda = K'_\lambda w$.

$$\pi B_\lambda (T) = \frac{2\pi hc^2}{\lambda^5} \left(\frac{e^{hc}}{\tau kT} - 1 \right)^{-1} \quad \text{is the Planck function.} \quad (2)$$

$$\tau_\lambda = \int K_\lambda ds \quad \text{is the optical depth.} \quad (3)$$

By choosing different wavelengths in the micron range, one will effectively see different levels of the atmosphere, since the absorption coefficient ranges over a factor of about one thousand in going from the depths of the water-vapor band at 6.5μ to the "window" near 11μ. For simplicity, it is advisable to choose regions of the spectrum which have only water-vapor bands present (avoid O_3, CO_2, etc. bands).

To observe high levels in the atmosphere (to avoid confusion with the ground) the calculations here concentrate on the wavelength regions where the water-vapor absorption is large-- for example, in the range $K'_\lambda = 30$ to $300\ cm^{-1}$ of water vapor at STP.

3.2.2 Calculations

All quantities and calculations here are approximate. The parameters of the atmosphere on 19 January 1954 were obtained from the measurement of Murgatroyd et al [25]; these parameters are the pressure, temperature, and water content as a function of height and appear in Table 1.

Now the absorption coefficient K'_λ is a function of temperature and pressure; here only the pressure dependence is approximately included by setting $K'_\lambda = (p/p_s)\ k_\lambda$, where k_λ is the absorption coefficient per cm of water-vapor measured in the laboratory at pressure p_s, and p is the ambient pressure. While there is some question about the form of the pressure dependence, Kaplan [26] and Taylor and Yates [27] have been followed in assuming the absorptivity is directly proportional to pressure.

To integrate Eq. (1) the atmosphere is divided into 2000-foot elements of height and the change in optical depth in each is then approximately given by:

TABLE 1

PARAMETERS OF ATMOSPHERE OF JANUARY 19, 1954 AND CALCULATIONS OF RADIATION INTENSITY FOR VARIOUS ABSORPTION COEFFICIENTS

h (1000 ft)	T (°C)	$\frac{p}{p_s}$	H_2O (cm/1000 ft)	$\frac{(\Delta\tau_\lambda)\,\pi B_\lambda}{2.7\times10^7 k_\lambda}$	$\frac{\tau_\lambda}{k_\lambda}$	$e^{-\tau_\lambda}$			Integrand = $\frac{(\Delta\tau_\lambda)\,\pi B_\lambda\, e^{-\tau_\lambda}}{2.7\times10^7 k_\lambda}$		
						$k_\lambda = 300$	30	3	300	30	3
30	-45	0.30	0.0005	3×10^{-8}	0.0003	.91	.91	.99	28×10^{-9}	3×10^{-8}	0×10^{-7}
28	-39	0.33	0.0006	5.4	0.0007	.85	.98	.99	46	5	1
26	-34	0.36	0.0009	10.0	0.0014	.66	.96	.99	66	10	1
24	-28	0.39	0.0012	18.2	0.0023	.50	.93	.99	92	17	2
22	-23	0.43	0.0017	26	0.0038	.32	.89	.99	116	32	4
20	-19	0.47	0.0038	98	0.0074	.109	.80	.98	108	78	10
18	-15	0.50	0.0076	234	0.0150	.0111	.64	.96	26	148	22
16	-10	0.54	0.014	540	0.0302	.00012	.41	.92	1×10^{-9}	220	50
14	-6	0.60	0.027	1280	0.062		.156	.89		200	114
12	-3	0.65	0.048	2720	0.125		.0235	.69		64	186
10	+1	0.70	0.08	5240×10^{-8}	0.24		.00075	.59		4×10^{-8}	316×10^{-7}

$$\Delta \tau_\lambda \ (2000 \text{ ft}) = \frac{p}{p_s} \ k_\lambda \ w \tag{4}$$

where k_λ is in cm^{-1} and w is in cm of H_2O per 2000 ft of atmosphere at the particular level considered.

Rewriting Eq. (1) as

$$I_\lambda = k_\lambda \int_0^\infty \left[\frac{\Delta \tau_\lambda}{k_\lambda} \ B_\lambda \ (T) \right] e^{-\tau_\lambda} \ ds \tag{5}$$

with ds in units of 2000 ft, the quantity $\Delta \tau_\lambda \ B_\lambda / k_\lambda$ can be tabulated as a function of height (independent of k_λ).

Calculations for k_λ = 300, 30, 3 cm^{-1} of water-vapor are given in Table 1. Because of the relative flatness of the black-body radiation curve in this region, a value of $\lambda = 6.75\mu$ was used to compute B_λ for each k_λ. Note also that τ_λ / k_λ for any height is obtained by adding together the tabulated values of $\Delta \tau_\lambda / k_\lambda$ for all higher levels.

To find the intensity at the satellite, assume that its height h above the ground is much greater than the height of any water vapor which contributes appreciably to the intensity. Let A be the area of atmosphere from which radiation is received and $\Delta \lambda_\mu$ be the width of the filter in microns. Then the energy in this band received at this satellite is

$$E_\lambda (\Delta \lambda_\mu) = \frac{A \ \Delta \lambda_\mu}{4\pi \ \underline{\underline{h}}^2} \ I_\lambda \ (\text{erg cm}^{-2} \ \text{sec}^{-1}) \tag{6}$$

For A = 10,000 km^2 and a receiving area of 1000 cm^2, and $\underline{\underline{h}}$ = 200 km, the energy received is

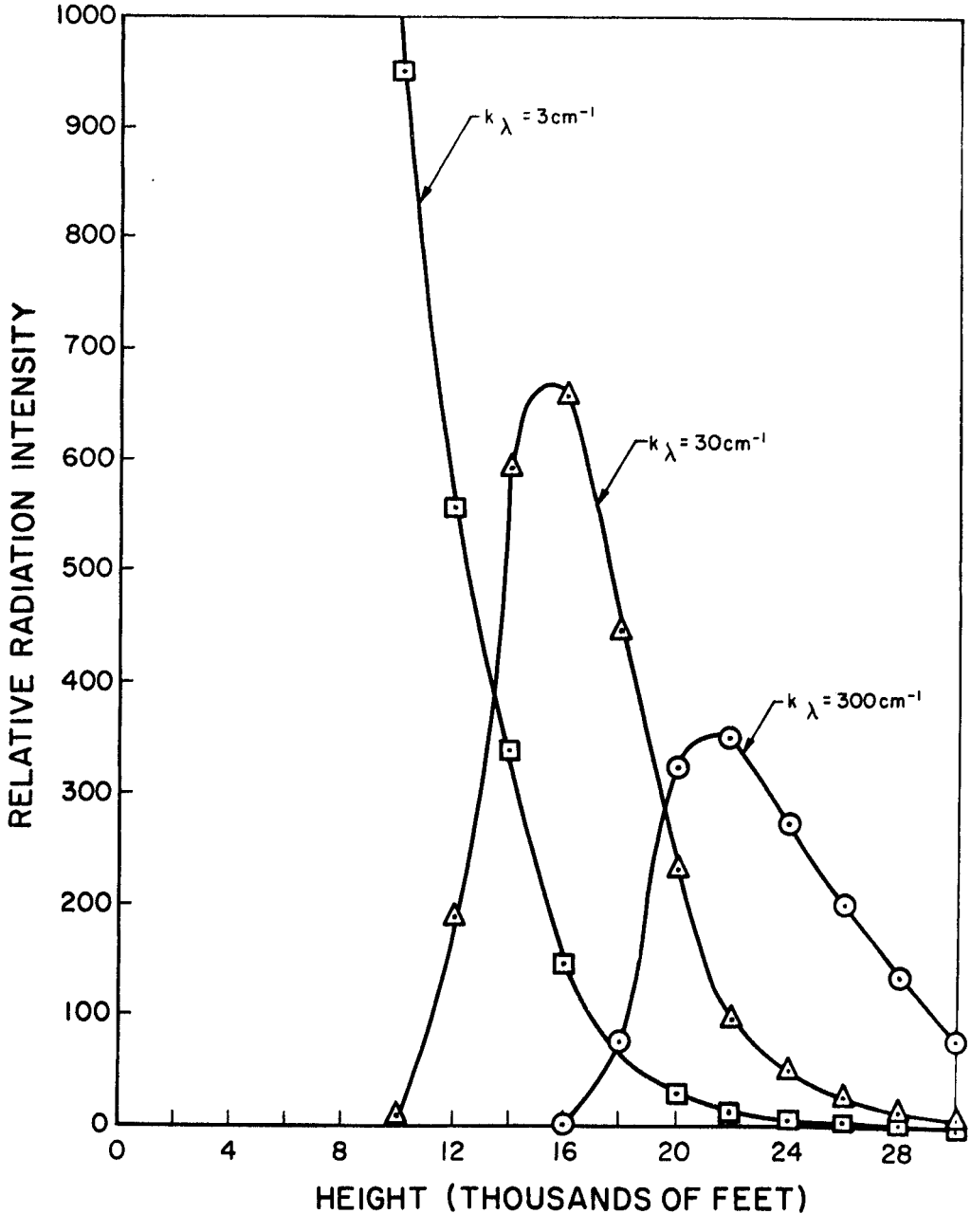

Fig. 2 Calculated distribution of intensity of radiation from water vapor in the atmosphere over Southern England, 19 January 1954

$4.1 \times 10^4 \ \Delta\lambda_\mu$ erg sec^{-1} for $k_\lambda = 300\ cm^{-1}$ ($4.1 \Delta\lambda_\mu$ mw)

$2.2 \times 10^4 \ \Delta\lambda_\mu$ erg sec^{-1} for $k_\lambda = 30\ cm^{-1}$ ($2.2 \Delta\lambda_\mu$ mw)

For radiation in the region $\lambda = 6.75\mu$, these represent about 10^{17} photons sec^{-1}.

From Table 1, part of which is plotted in Fig. 2, it is seen that the major contribution to the integral, Eq. (1), and, therefore, to the total intensity received at the satellite, comes from a slice of the atmosphere of small thickness. For example, the 14,000 to 18,000-ft region contributes about 70 per cent of the intensity at $k_\lambda = 300\ cm^{-1}$.

3.3 An Heuristic Approach

3.3.1 Introduction

The results of the previous section indicate that the bulk of the radiation departing the outside of the atmosphere at any given wavelength emanates from a relatively thin atmospheric stratum. We will now proceed to examine the meteorological significance of this localized source of the radiation. In the interests of lucidity of argument, a very approximate approach will be used, with specific numerical values chosen ad-lib for illustration. The objective will be to find the meteorological parameters that define the stratum from which the radiation originates.

3.3.2 Background

Let us examine the path that the infrared must traverse on its way through the atmosphere to the satellite. The absorptivity of water vapor is greater at higher pressures than it is at lower, as a result of pressure broadening of lines. As in Section 3.2.2 we assume that the absorption coefficient is directly proportional to

pressure. Standard absorptivity will be considered to occur at 1000 mb.

The water equivalent path length is defined by

$$du = \frac{p}{1000} \, adz \tag{7}$$

where u is the equivalent water path length in cm, p is the pressure in millibars, a is the absolute humidity or vapor density in gm cm^{-3}, z is the geometric path length in cm (here assumed to be in the vertical). Note that a is also the number of cm of water per cm of path length since the density of water is 1 gm cm^{-3}. Various hydrostatic and gas law substitutions may be made, resulting in such forms as

$$du = 6.4 \times 10^{-4} \, edp \tag{8}$$

or

$$du = \frac{.0217 \, pe}{T} \, dz \tag{9}$$

Here e is the vapor pressure in millibars, and T is the absolute temperature in degrees Kelvin.

Results of calculations of equivalent water path length from the top of the atmosphere (or rather, the top of the flight), taken from the data collected with a frost-point hygrometer by Murgatroyd et al [25] are shown in Fig. 3. The increase of equivalent water path length with depth going down through the atmosphere is seen to be roughly exponential. The slope is such that the increase of equivalent water path length in about 2000 ft of geometric path is about the same as the total equivalent water path length above the 2000-ft increment.

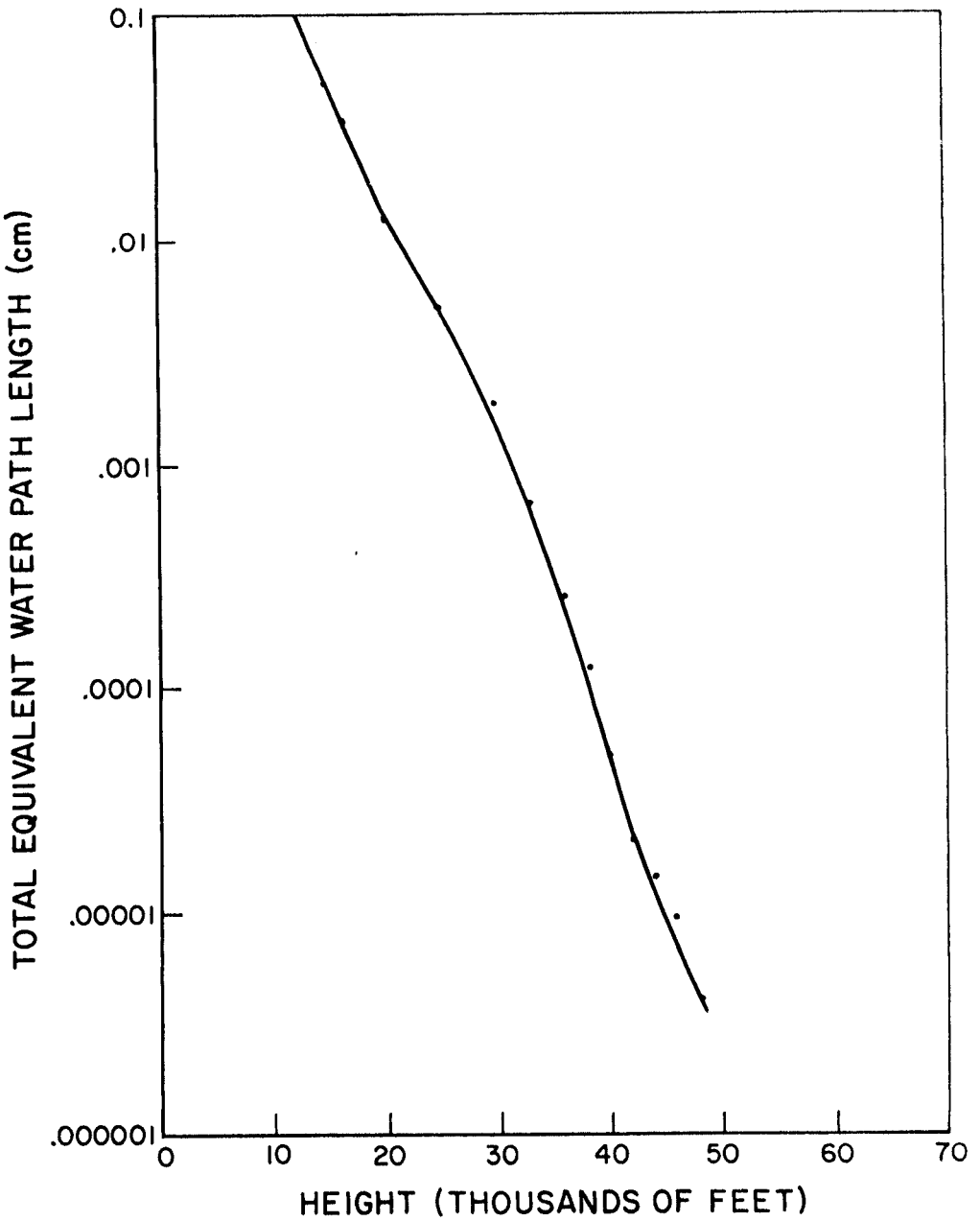

Fig. 3 Total equivalent water path length vs altitude in the atmosphere over Southern England, 19 January 1954

The same data plotted on a linear scale of path length is shown in Fig. 4. A sharp bend occurs in the curve, the position of the bending being dictated somewhat by the choice of the scale of plotting. This bend marks the altitude at which the absorption begins to increase markedly. Noting that the bend occurs at about 0.05-cm path length, the view of the atmosphere at a wavelength such that the absorption is essentially total in a 0.05-cm equivalent water path length will not penetrate appreciably below the corresponding altitude. Plotting dewpoint temperature vs. altitude on Fig. 4 it is found that this path length corresponds to a dewpoint temperature of $-30^{\circ}C$. In the present case this corresponds to an air temperature of $-9^{\circ}C$.

The water equivalent path in the 2000 foot immediately surrounding the $-30^{\circ}C$ dewpoint position is, as has been illustrated above, about the same as the total water equivalent path down to that point. Since the temperature at the $-30^{\circ}C$ dewpoint is materially higher than temperatures at higher elevations, the radiant intensity emanating from the $-30^{\circ}C$ region will be greater than that emanating from the regions above. Admittedly, part of the $-30^{\circ}C$ radiation will be absorbed on its way out, but this absorption will be partly replaced by radiation at a lower temperature from the reaches above. Essentially, then, the $-30^{\circ}C$ dewpoint marks the outside of the glowing fog, as seen at the appropriate wavelength. A change in wavelength would make possible the definition of another dewpoint temperature as the outside of the fog.

It remains to be demonstrated that the dewpoint temperature is an adequate description of the outside of the glowing fog. A scatter plot of dewpoint temperature against the rate of increase of path length with depth--that is, corresponding to the slope - du/dh

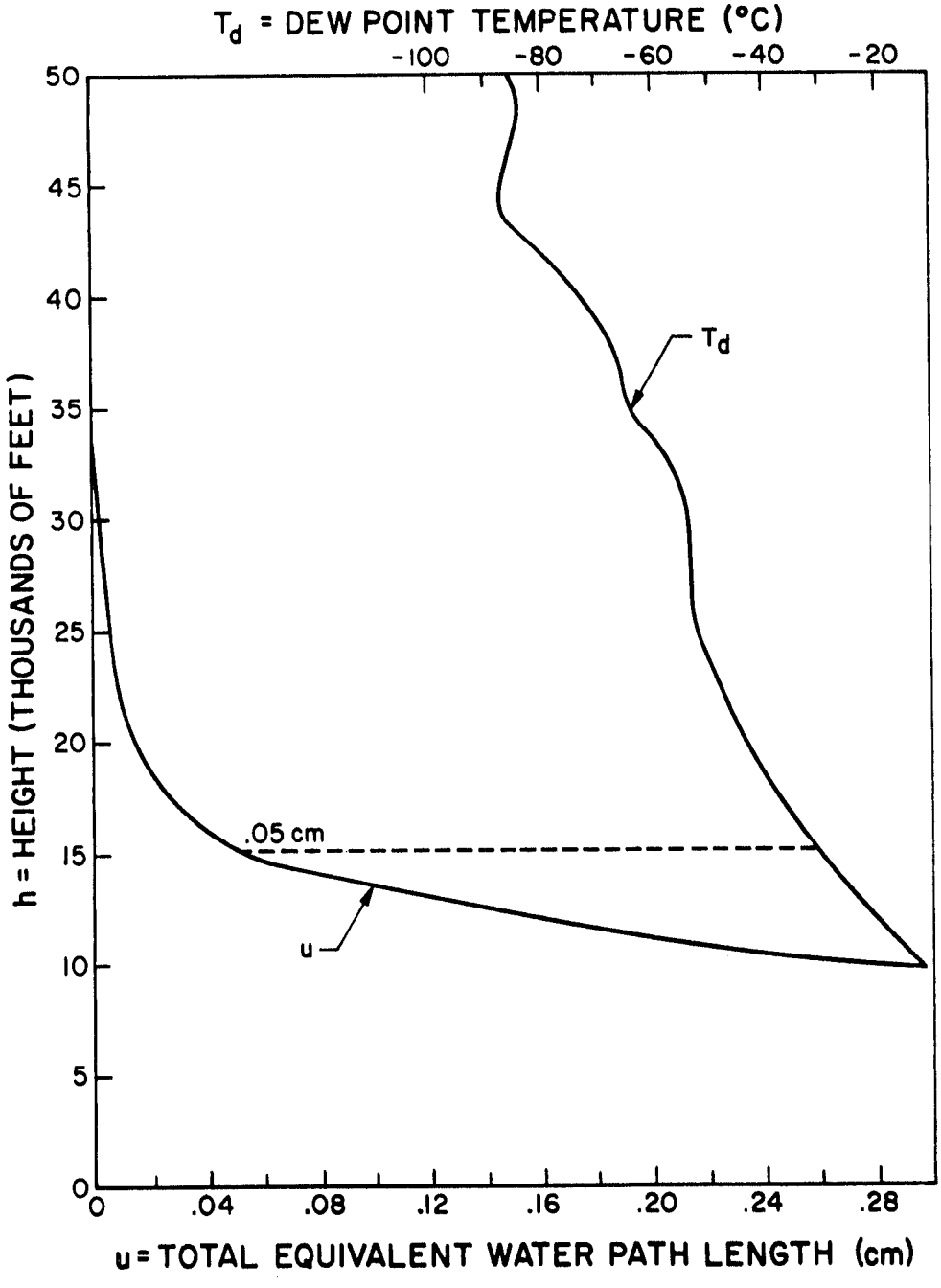

Fig. 4 Total equivalent water path length and dewpoint temperature vs. altitude in the atmosphere over Southern England, 19 January 1954

of the equivalent water path length curve of Fig. 4--taken from random samplings of radiosonde data over the North American continent from Alaska through Mexico and Central America is shown in Fig. 5. The actual heights of the various iso-dewpoint surfaces varied considerably. It will be seen that there is very small scatter in the data, so that any dewpoint that may be chosen as characteristic of the outside of the glowing fog for a given wavelength will represent a constant value of increase of optical depth wherever it is met.

The radiation from the constant dewpoint surface is a function of the temperature of that surface. As might be expected, the temperature range associated with a given dewpoint is not very large. The temperatures associated with the same data plotted in Fig. 5 are shown in Fig. 6. The spread of temperatures is somewhat greater than that of dewpoints, having a maximum scatter in the 240° to 270°K region corresponding to dewpoints of the order of -40° to -10°C. Results of a statistical tabulation of the temperature associated with the -30°C dewpoint from radiosonde reports over the North American continent on a single day are shown in Fig. 7. The curve has a mode at about -16.3°C, a mean at -19.4°C, and a standard deviation of 4.6°C. (The mode was determined by fitting a parabola to the points at -20°, -17°, and -14°. The range of temperatures associated with a given dewpoint, and thereby the outside of the glowing fog, is not very great.

It may be more instructive to cast these data over to the amount of radiation corresponding to the temperatures of the atmosphere at the -30°C dewpoint. The result of this transformation is shown in Fig. 8. Radiation amounts and number of cases are now

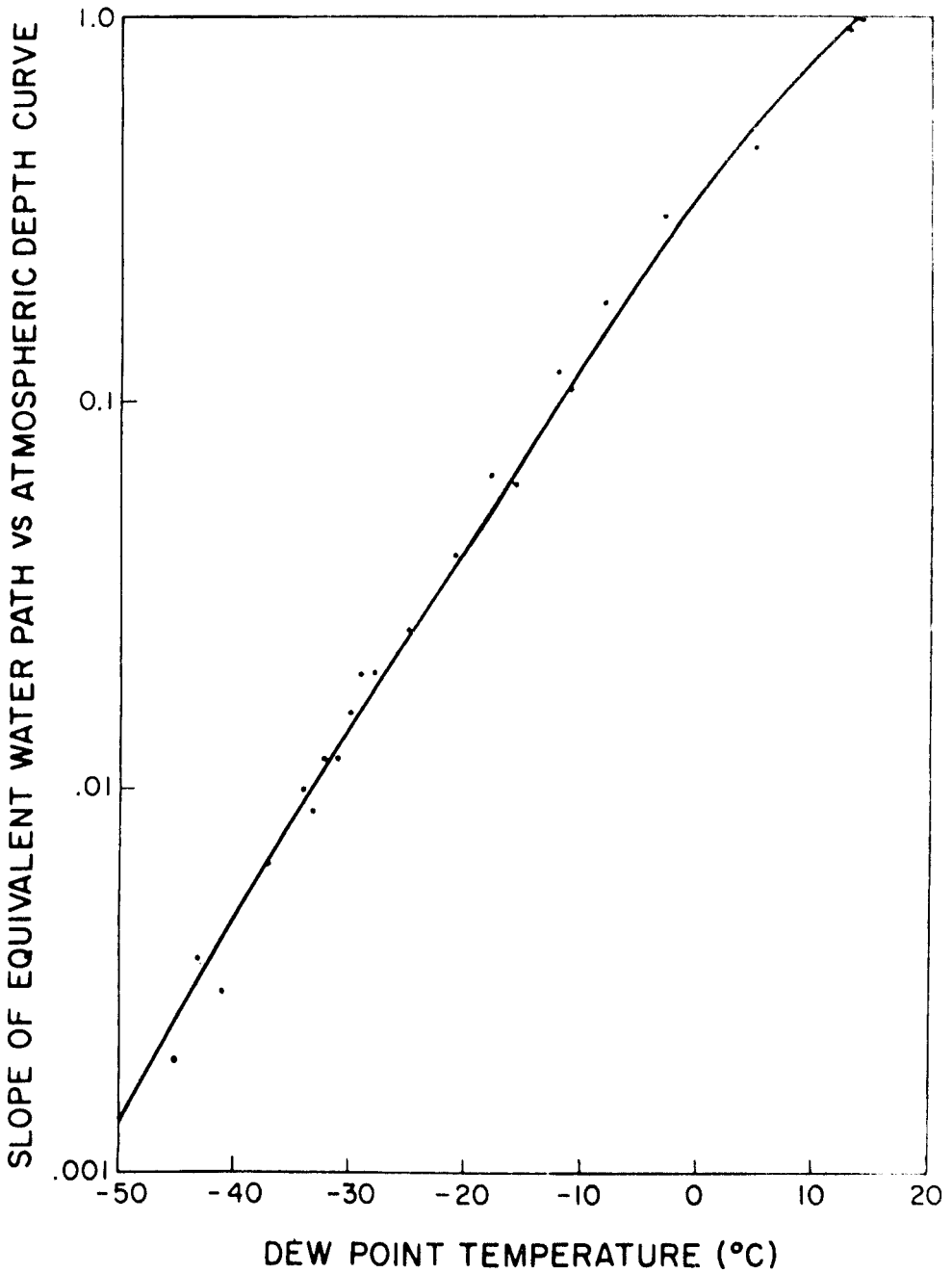

Fig. 5 Observed rate of increase of equivalent water path length with depth vs dewpoint temperature

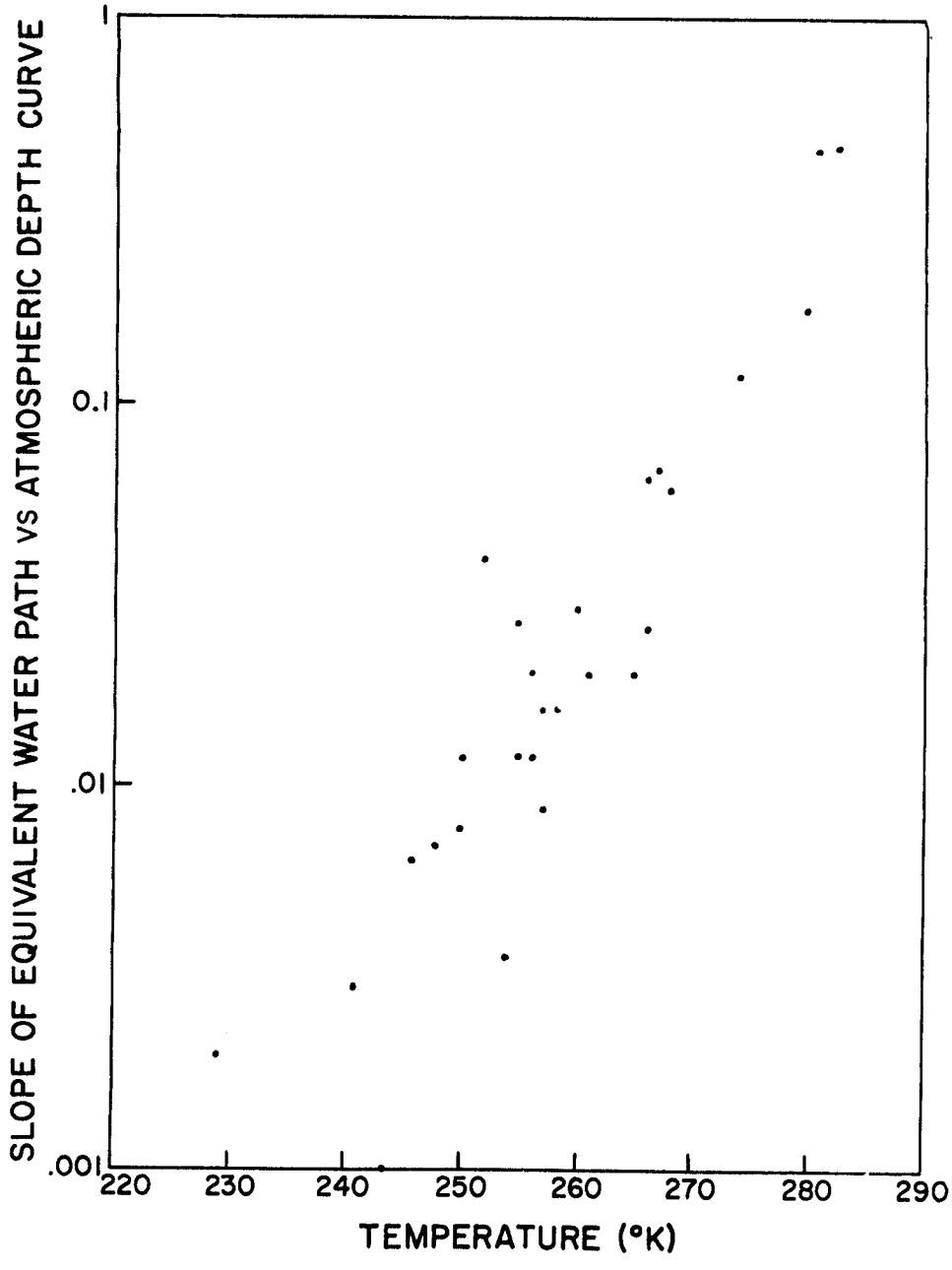

Fig. 6 Observed rate of increase of equivalent water path length with depth vs. temperature corresponding to data on Figure 5

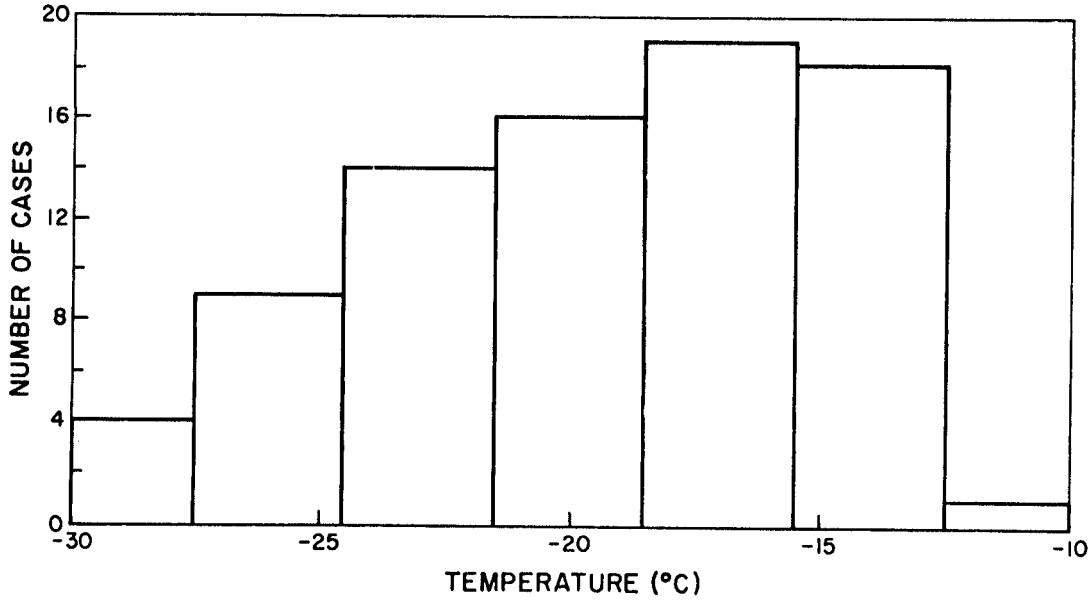

Fig. 7 Distribution of Temperatures associated with the -30°C dewpoint

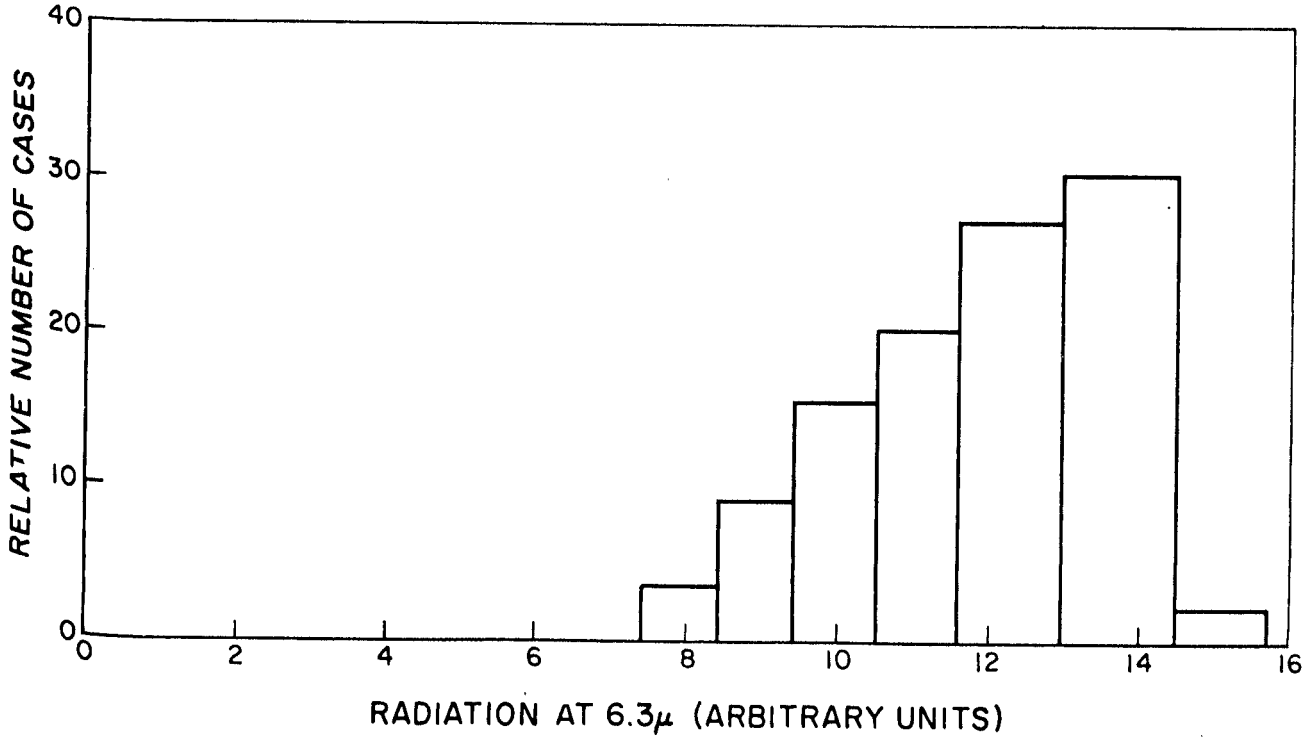

Fig. 8 Distribution of Radiation associated with the -30°C dewpoint

shown in arbitrary units, avoiding the need to normalize. The curve has a fairly sharp mode, and the standard deviation is found to be only 15 per cent of the value of the mean. (In arbitrary units, the mean is at 11.8 and the standard deviation is 1.77.) The total spread of radiation covers about a 2 to 1 ratio.

This apparently indicates that a relatively limited amount of variation will be found in the radiation emerging from the glowing fog at the strong emission bands. The amount of emission will not depend on the height in the atmosphere at which the water "ends", but rather on the relative humidity at the -30°C (or other appropriate to the wavelength) dewpoint temperature. While the meteorological significance of this quantity is not immediately apparent, it will be seen (in the next section) to have some interesting properties.

3.4 Synoptic Behavior of Water Vapor Infrared Emission

3.4.1 Introduction

Sections 3.2 and 3.3 point out that the vast bulk of the emission in the dense sections of the water-vapor emission bands emanates from relatively thin strata of the atmosphere. It was shown that these strata are characterized by being surfaces of essentially constant dewpoint. The amount of emanation is controlled by the temperature of this constant dewpoint surface. In this section an attempt will be made to develop the synoptic significance of the temperature of a constant dewpoint surface.

Synoptic charts of the temperature of constant dewpoint surfaces were prepared for successive days. The period was chosen essentially at random and two surfaces were used, the zero-degree dewpoint and the -20°C dewpoint surface. Isotherms have been drawn upon these surfaces, a 4°C interval being used as a matter of convenience. Analysis was performed by personnel unfamiliar with

the conventional weathermap analyses of those days.

Two difficulties attended the preparation of these charts from radiosonde data. In warm areas, that is, areas of great difference between the temperature and the dewpoint--it was frequently found that "motorboating" was reported, making it difficult to assign rational temperatures. In other cases the dewpoint surface was found to intersect the ground, indicating that even the relatively small quantities of water vapor required for ground obscuration were not present. This latter hazard, of course, would also be present in real observations from a satellite.

3.4.2 26 April 1955, 0300 Z

The temperature map of the $0^{\circ}C$ surface presented in Fig. 9 shows interesting similarity to many of the features of the surface analysis for that day shown in Fig. 10. The cold band extending from the Los Angeles region through Idaho toward the Dakotas corresponds reasonably well with the band of precipitation associated with the complex frontal system in the West. The warm tongue invading the southern Rocky Mountains is found to correspond quite well with the anticyclone in that region. A cold region is found to occupy the same area as the band of precipitation and cloudiness extending from northern New England to the northern Georgia region. The rather flat high between the Great Lakes and Louisiana is relatively poorly marked by a warm band. There is believed to be little reality to the cold stripe covering the Gulf and Caribbean Islands.

At the -20° dewpoint surface shown in Fig. 11, the pattern is less clearly marked. The principal cold band extends over the northern tier of states. On the Atlantic side separate cold centers appear to correspond to lows over Pennsylvania and off the New England coast, respectively. The warm tongue over the southern

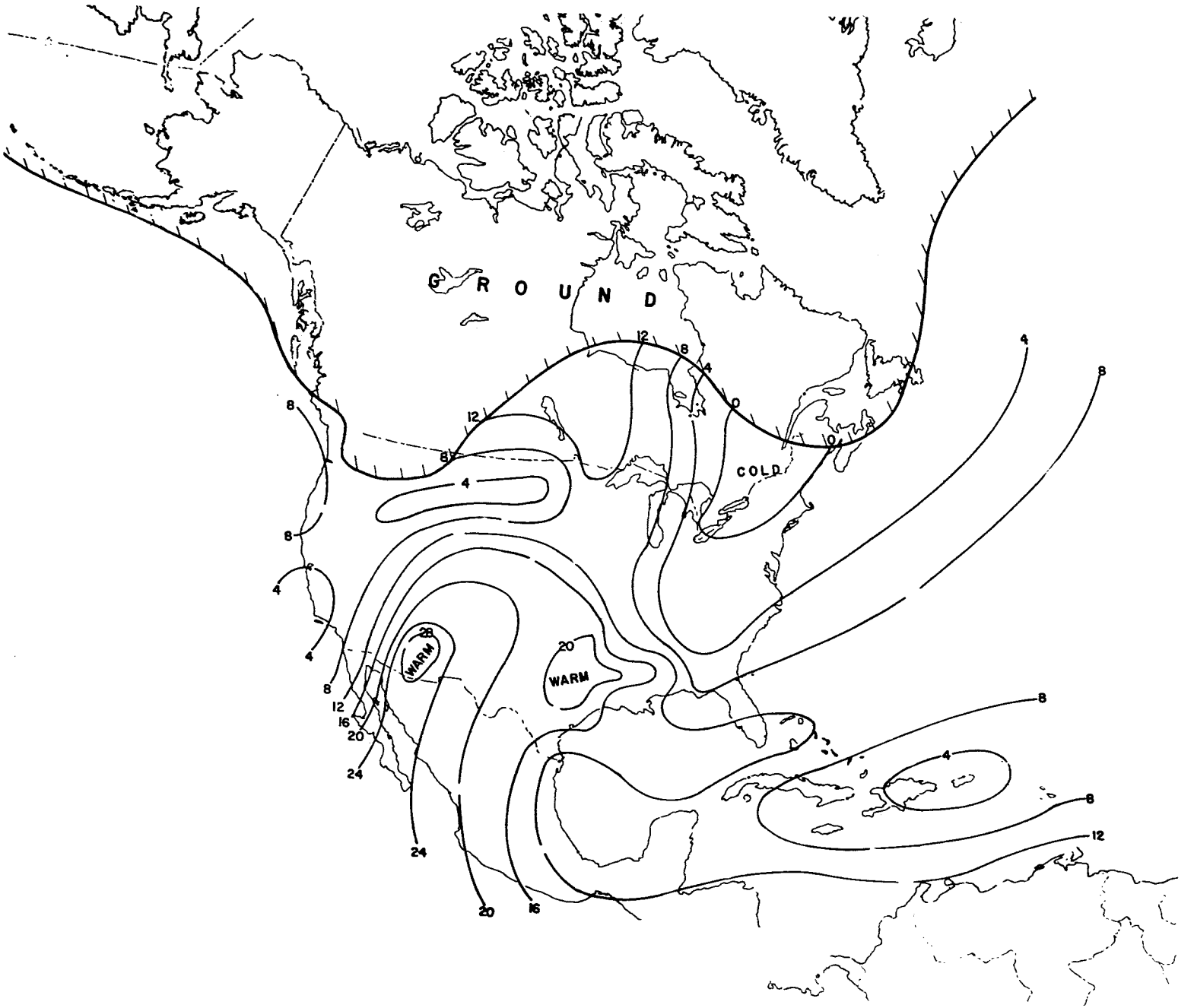

Fig. 9 0300Z, 26 April 1955, temperature at 0° dewpoint surface

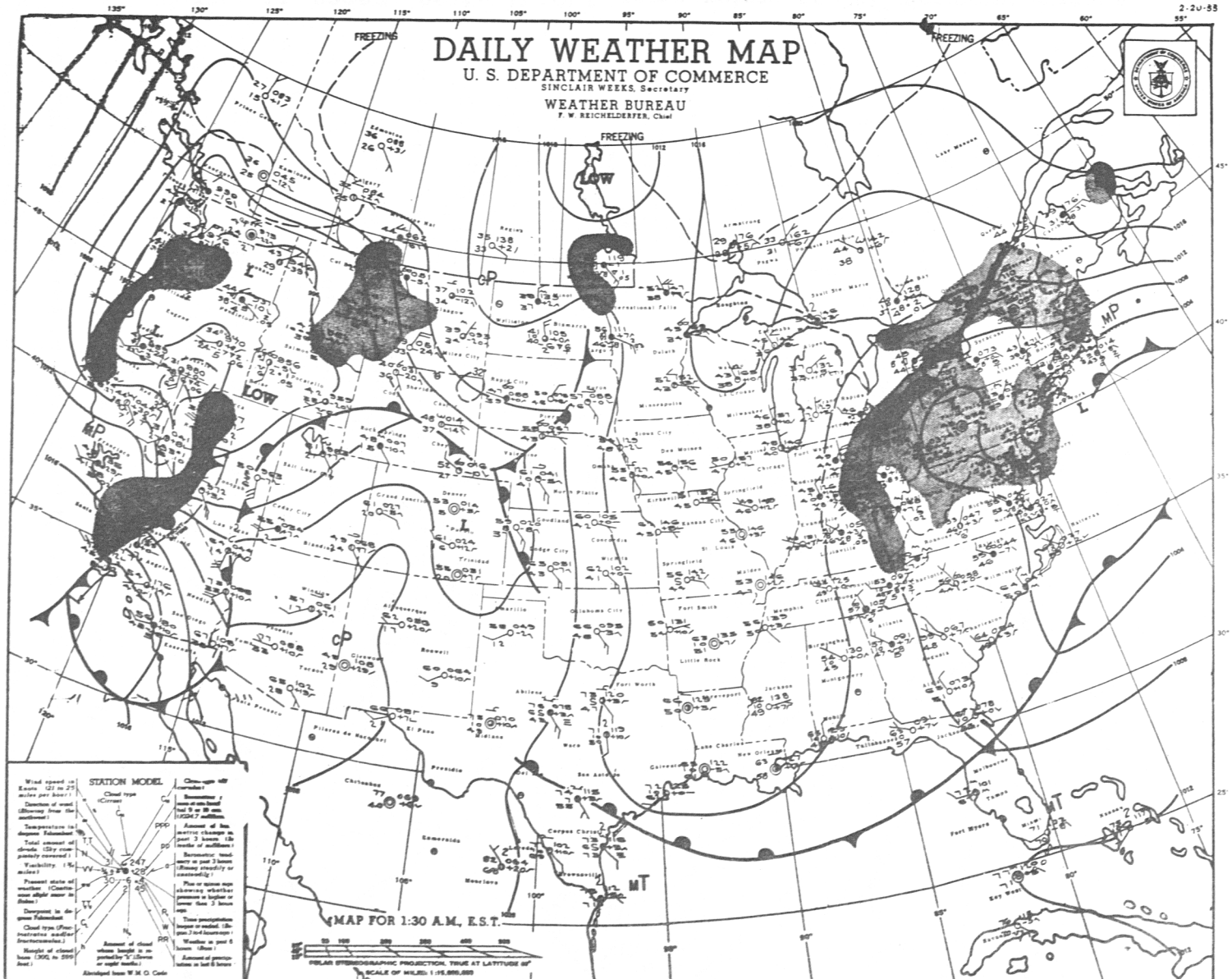

Fig. 10 Surface map, 0630Z, 26 April 1955

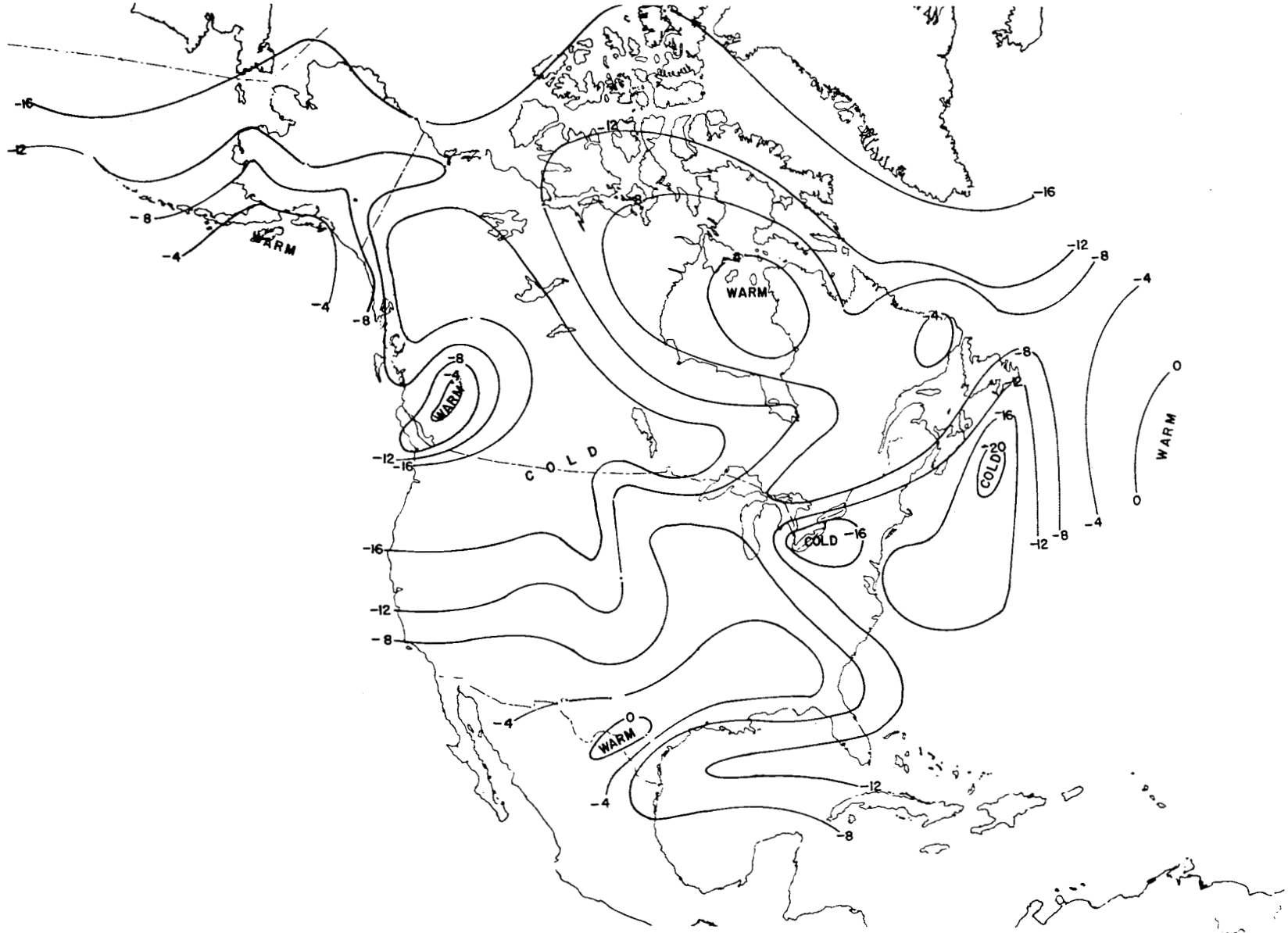

Fig. 11 0300Z, 26 April 1955, temperature at -20° dewpoint surface

United States is now shifted eastward. Any correspondence of the band over the Gulf and Florida with the indicated cold front is probably fortuitous.

The upper-air chart given in Fig. 12 shows that the strong gradient of temperature on the constant dewpoint surface across the northern tier of states delineates on the position of the jet stream at 500 mb. It follows such features as the abrupt southward bend of the jet stream over the Great Lakes area and its curvature about the low over Pennsylvania.

The warm incursion in the southern part of the country is seen to correspond to the anticyclonic area observed there at 500 mb, and similarly, the warm pocket in British Columbia corresponds to a small wedge in that area. Since the delineation of this warm area depends essentially upon a single observation, it may be somewhat over-emphasized.

3.4.3 27 April 1955, 0300 Z

The 0° dewpoint map of Fig. 13 has assumed a noticeable meridional nature in keeping with the development seen on the surface chart of Fig. 14. The major significant features are a warm band now extending from the southwest to the Great Lakes and a cold band from New England down through the middle South. This corresponds to an observed band of cloudiness which does not correspond to any particular manifestation on the surface chart. Representation of the principal features of the cyclonic system in the West has been disrupted by insufficient quantities of water vapor in the mountain states.

On the -20° dewpoint surface shown in Fig. 15, the central United States is dominated by a bifurcating warm tongue. While this bifurcation does not find any complete counterpart on the

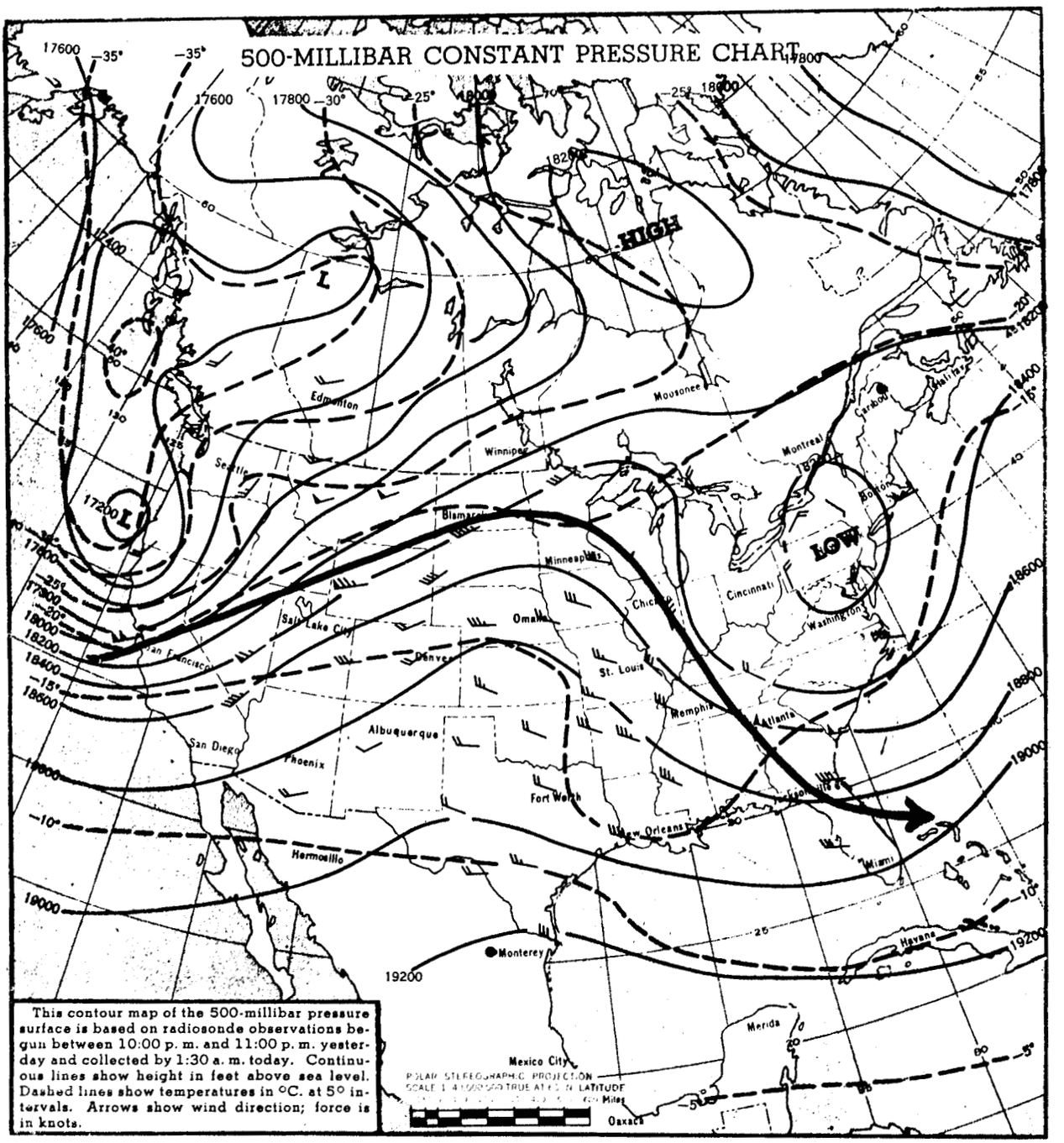

Fig. 12 500 mb chart, 26 April 1955, 0300Z

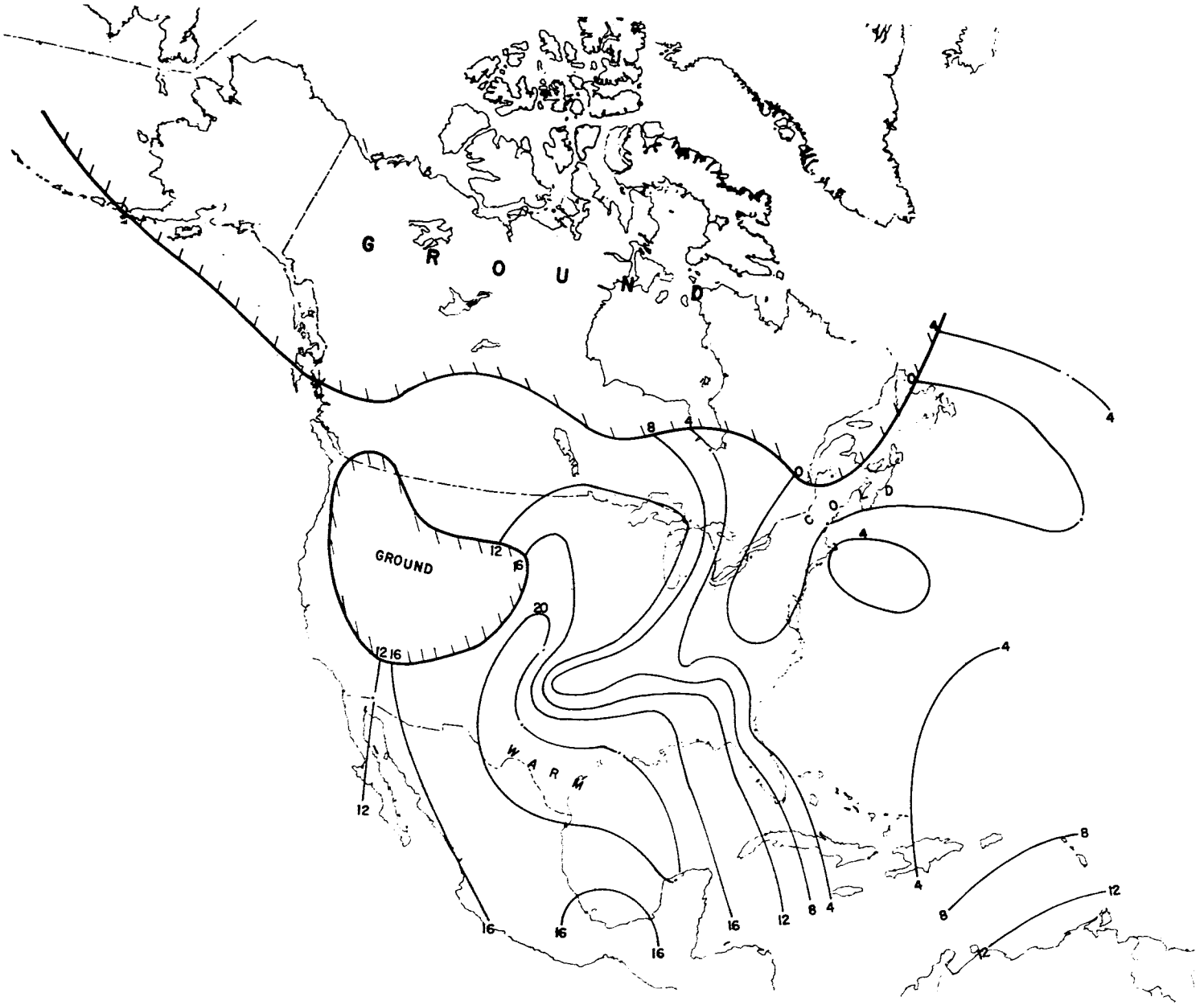

Fig. 13 0300Z, 27 April 1955, temperature at 0° dewpoint surface

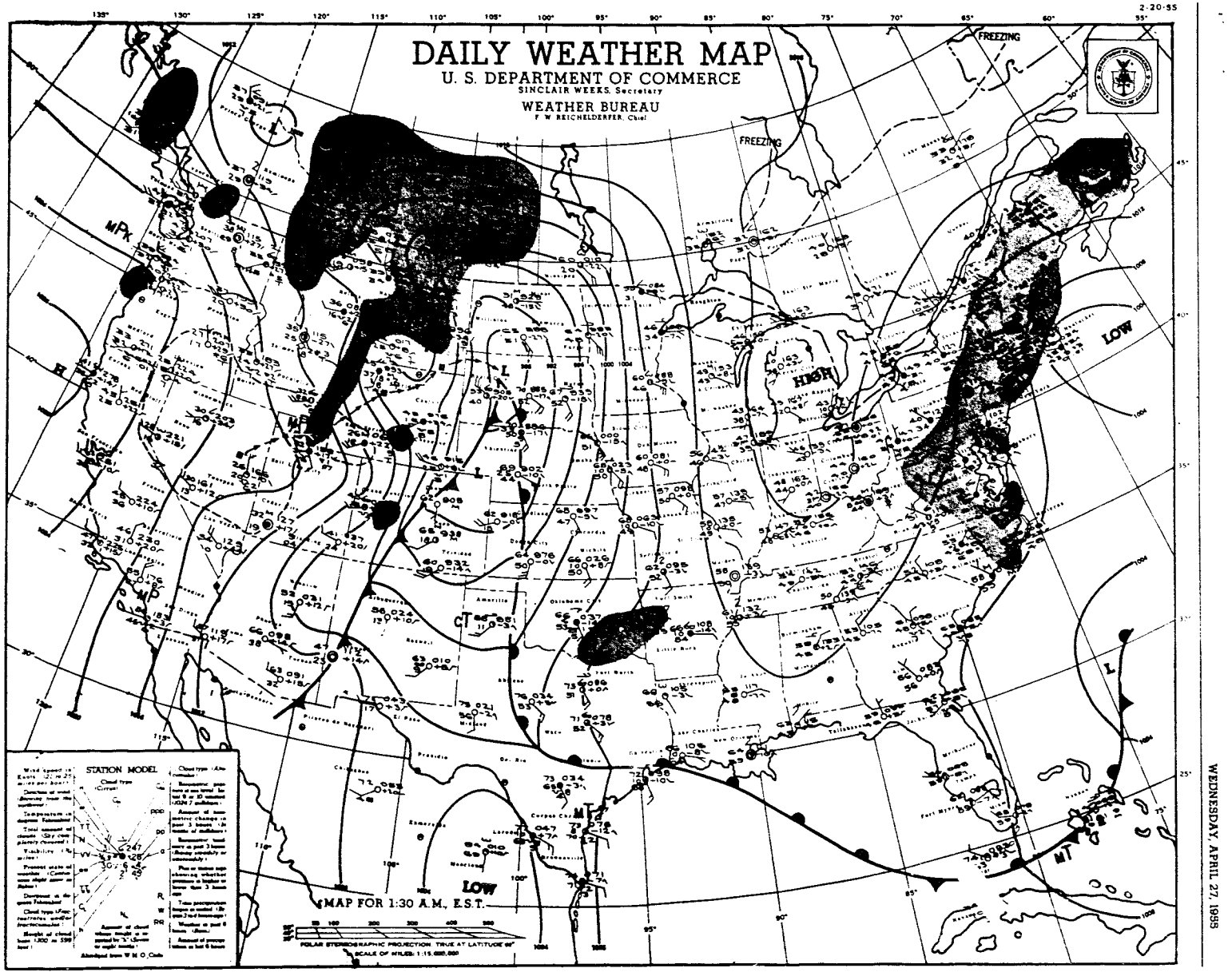

Fig. 14 Surface map, 0630Z, 27 April 1955

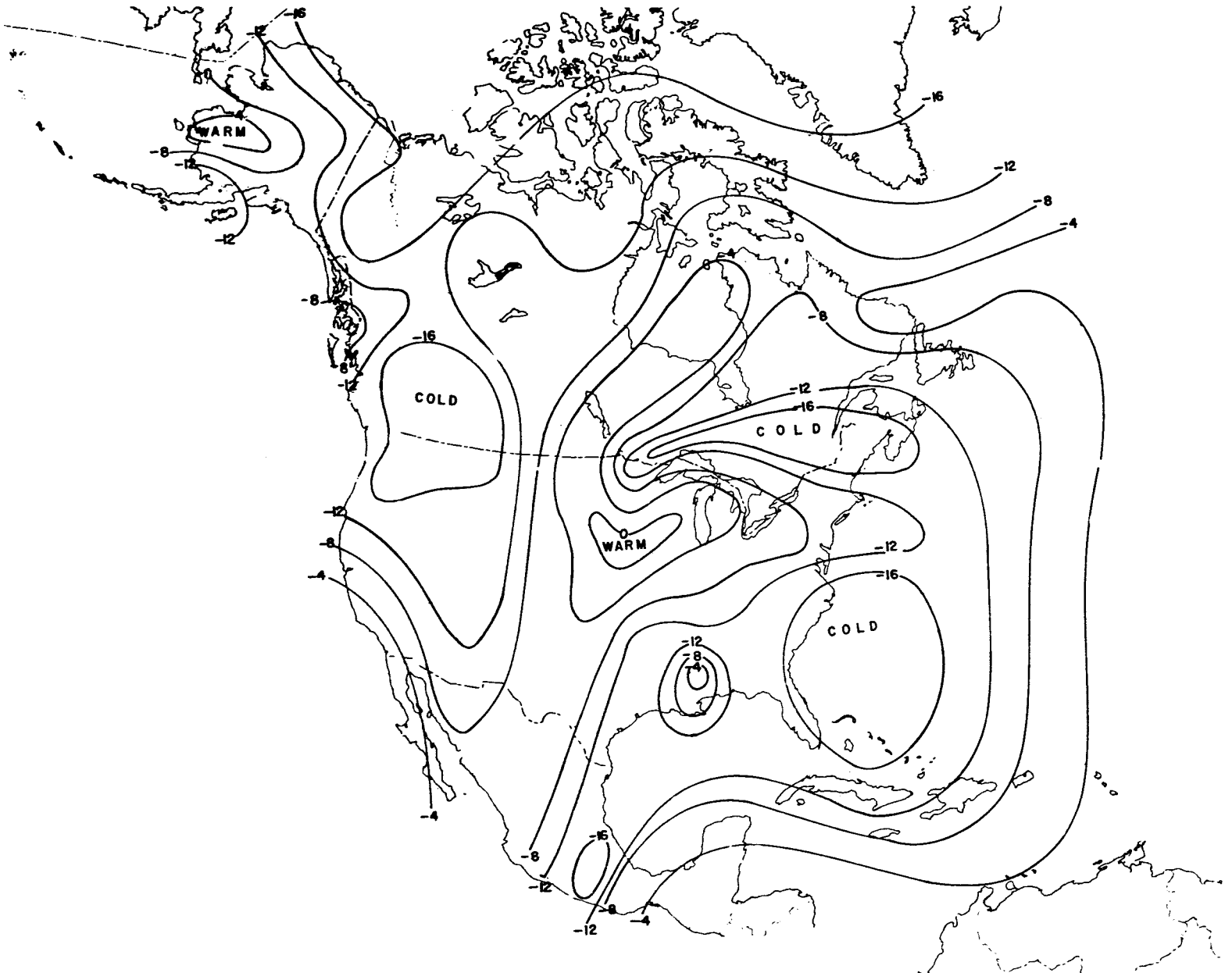

Fig. 15 0300Z, 27 April 1955, temperature at -20° dewpoint surface

500 mb chart of Fig. 16, it is in fact a precursor of later developments. It does, in general, correspond to the expanding ridge in the Central States extending up through Canada toward Hudson Bay. Delineation of the jet stream by the gradient areas does not appear to be as good on this chart as previously. This is probably due to the increasingly meridional nature of the circulation which has made jet-stream curvatures and meanderings too great to be followed by the loose network available for our analysis.

3.4.4 28 April 1955, 0300 Z

The pattern on the 0° dewpoint surface presented in Fig. 17 has ceased to bear any very significant relationship to the surface chart of Fig. 18. A cold area extending from Manitoba southward corresponds to the position of the low center and some of its attendant precipitation. The warm axis lies materially to the west of the surface high position. The cold area extending from New England down the Atlantic Coast apparently coincides with the areas of rain and cloudiness in those regions.

On the other hand, the 0° dewpoint surface temperature seems a strikingly good representation of the 500-mb chart given in Fig. 20. The warm ridge corresponds quite nicely with the extremely sharp ridge found in the Great Lakes area. The deep trough off the coast is equally well represented. The coincidence of the Rocky Mountain trough with the ground intersection is probably fortuitous.

The -20° dewpoint surface chart of Fig. 19 provides, in this case, an interesting synthesis of surface and upper-air features. The same gross features that existed on the 0° chart are repeated. However the bifurcation that was present earlier in the warm area is still marked, corresponding to the bifurcating nature of the ridge

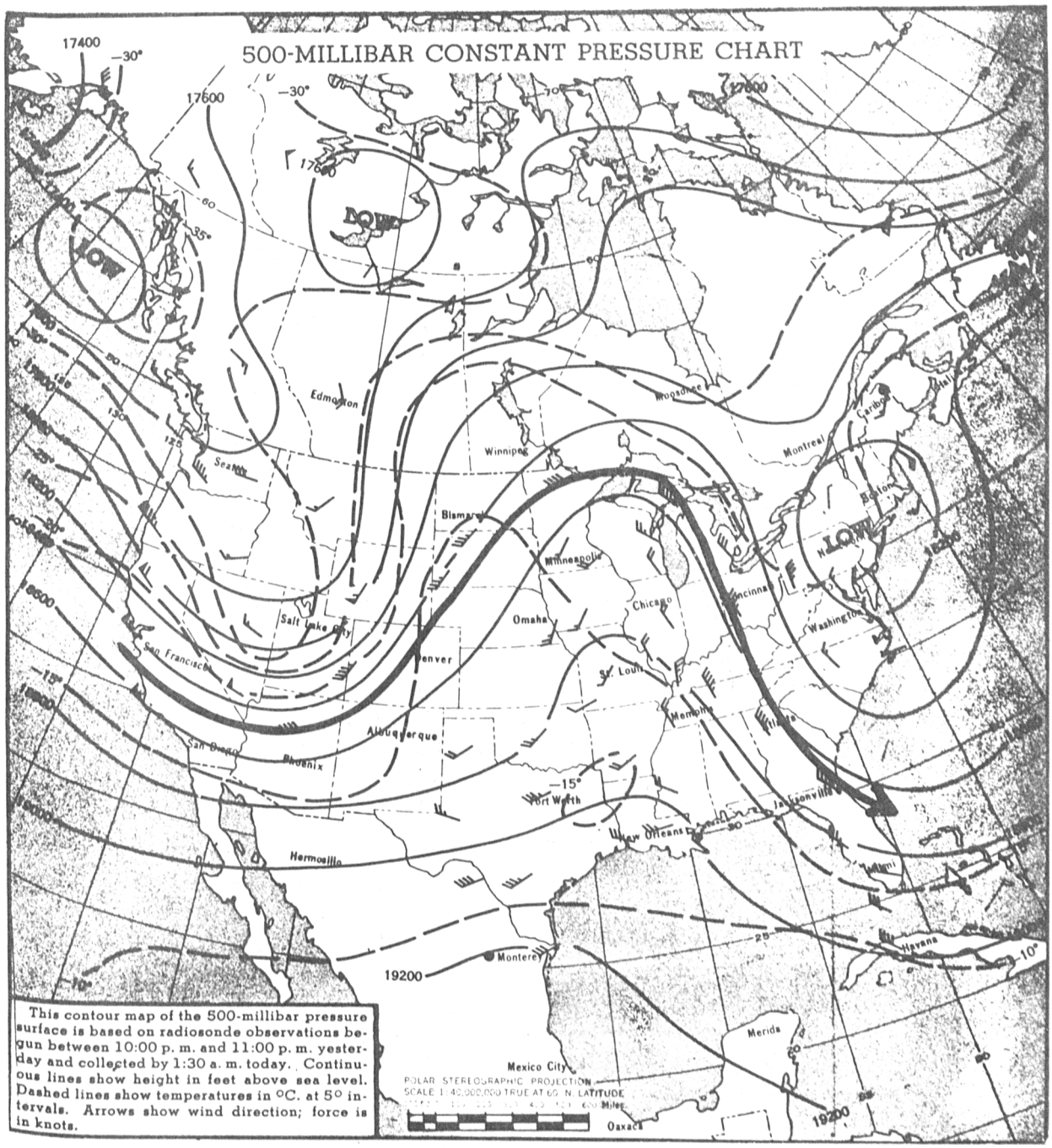

Fig. 16 500 mb chart, 27 April 1955, 0300Z

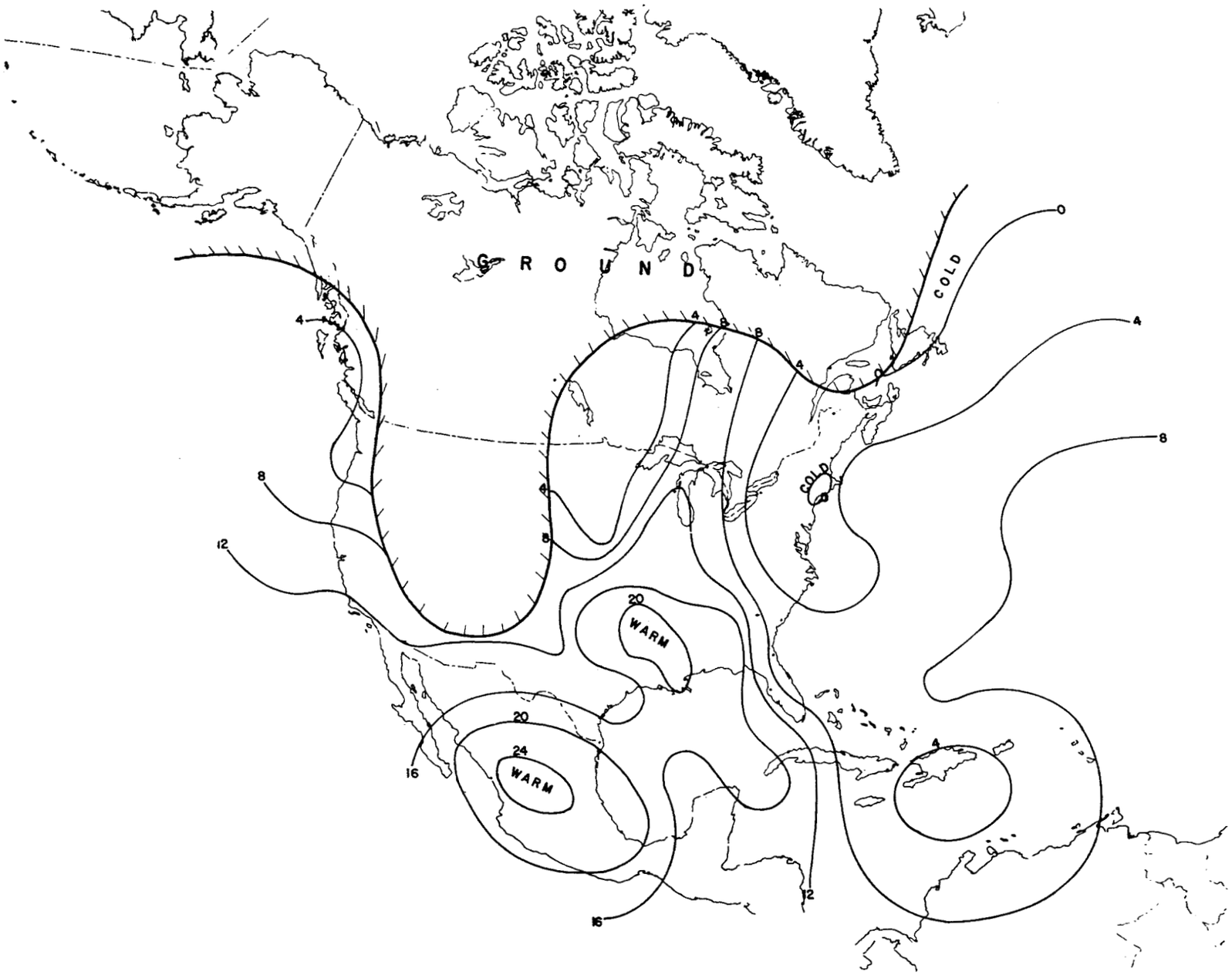

Fig. 17 0300Z. 28 April 1955, temperature at 0° dewpoint surface

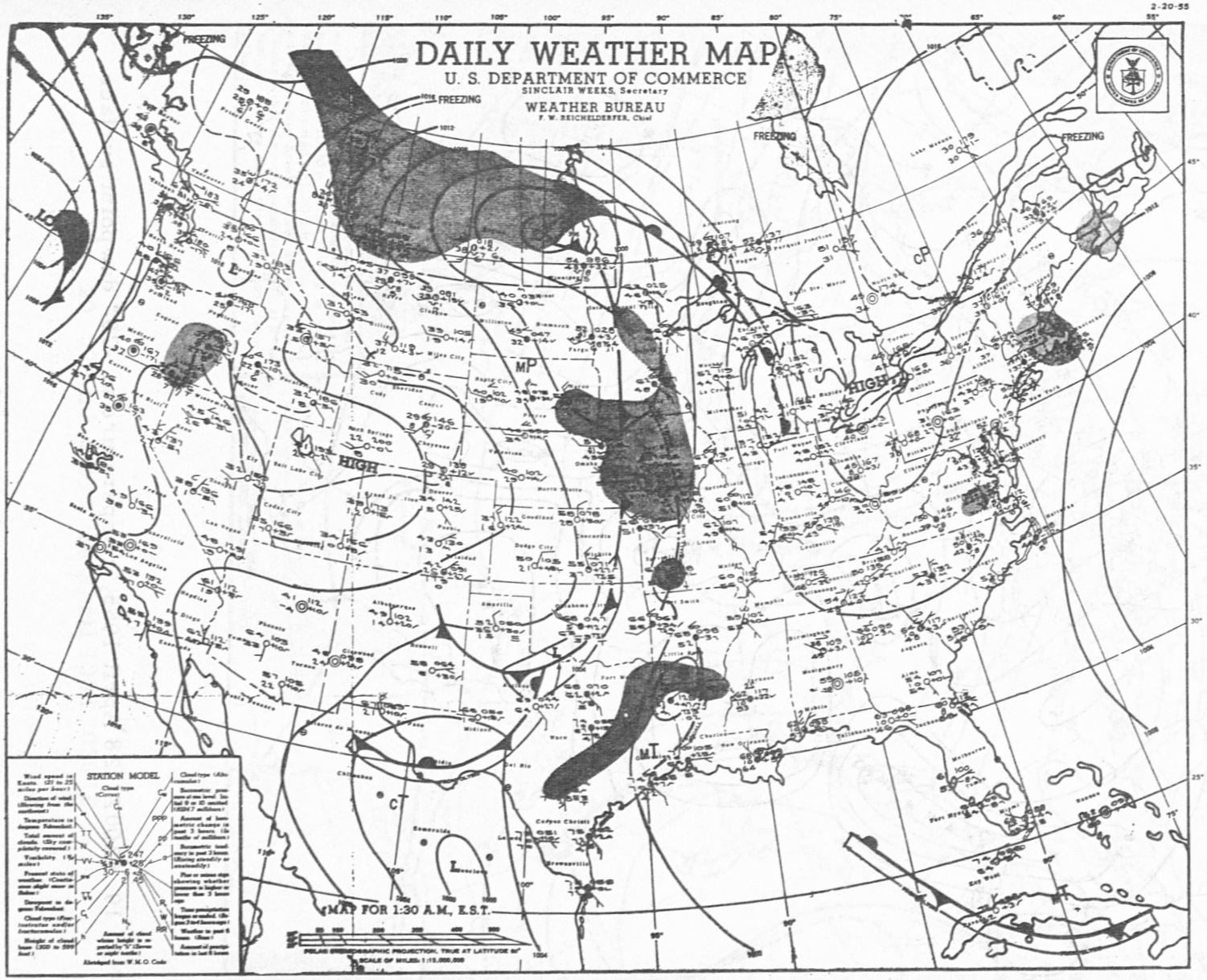

Fig. 18 Surface map, 0630Z, 28 April 1955

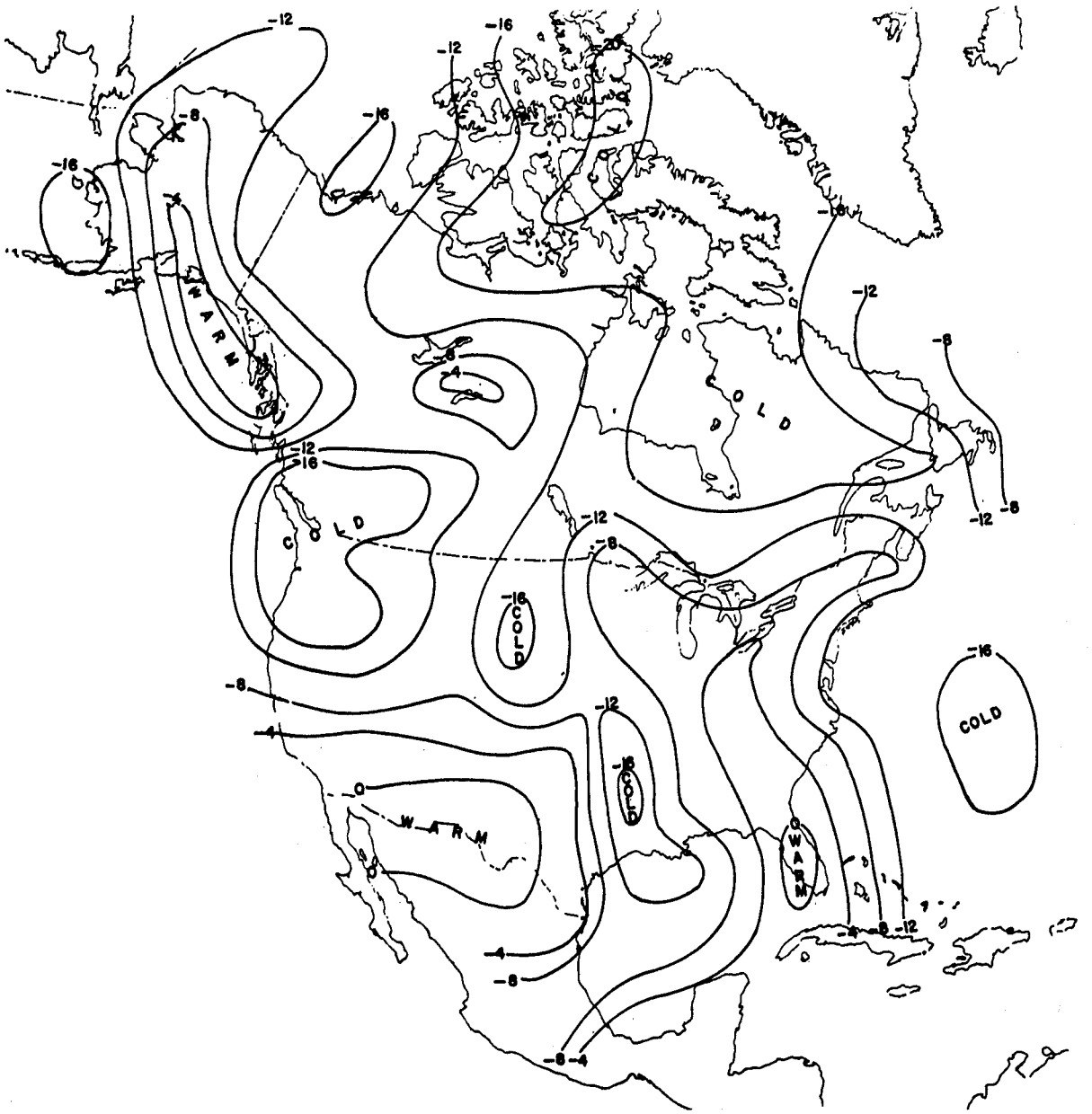

Fig. 19 0300Z, 28 April 1955, temperature at -20° dewpoint surface

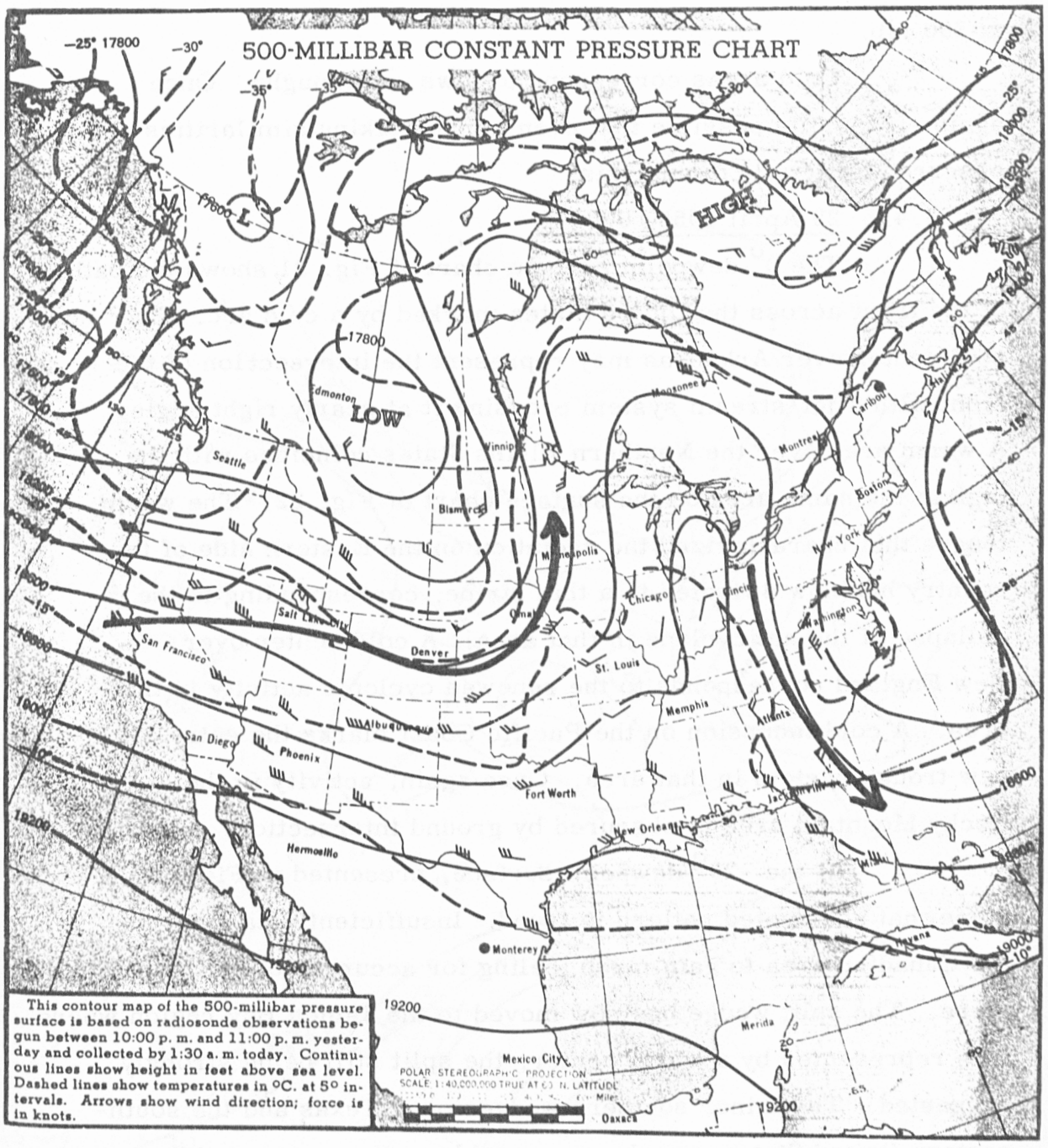

Fig. 20 500 mb chart, 28 April 1955, 0300Z

at 500 mb.

Cold areas correspond to lows and troughs. Once again, it is quite possible that even more striking similarities are obscured by details of analysis.

3.4.5 29 April 1955, 0300 Z

The 0° dewpoint surface chart of Fig. 21 shows the path of the front across the United States marked by a cold arc. The cold center over Arkansas may represent the intersection of the front with a jet-stream system crossing it at nearly right angles. A warm area over the Northern Plains States coincides with the high in the same area on the surface chart of Fig. 22. The warm tongue that characterized the radiation on the Eastern side of the country has now dwindled to a thin stripe, corresponding to the collapse of the anticyclone in that area. A cold center over New England corresponds to the renewed cyclonic activity in that area. A cold incursion on the Pacific Coast marks the entry of a new trough system in that area. Once again, activity in the Rocky Mountain area is obscured by ground intersection.

At the -20° dewpoint surface, presented in Fig. 23, a somewhat accidented pattern is found. Insufficient data exist in the Canadian area to gain much feeling for accuracy of representation there. The split wedge has now moved to the James Bay region where it is represented by a warm center, the split still being strongly suggested. The minor southern wedges over Texas and the southeastern United States are also reasonably well represented by warm areas. The cold stripe over New England and the Maritimes is apparently related to the complicated convergent situation occurring in that area. The significance of the details over southern Florida and the Caribbean is not obvious.

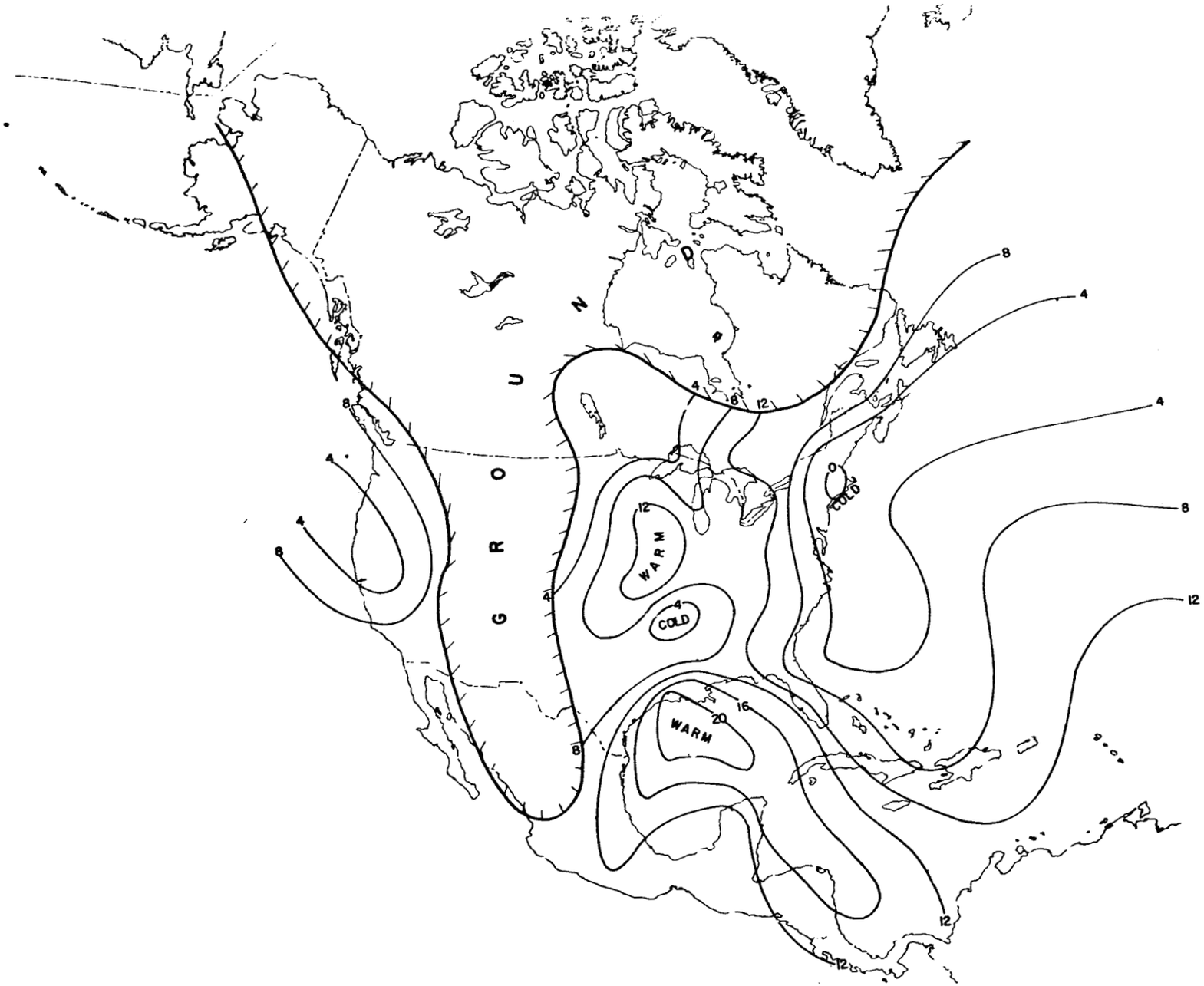

Fig. 21 0300Z, 29 April 1955, temperature at 0° dewpoint surface

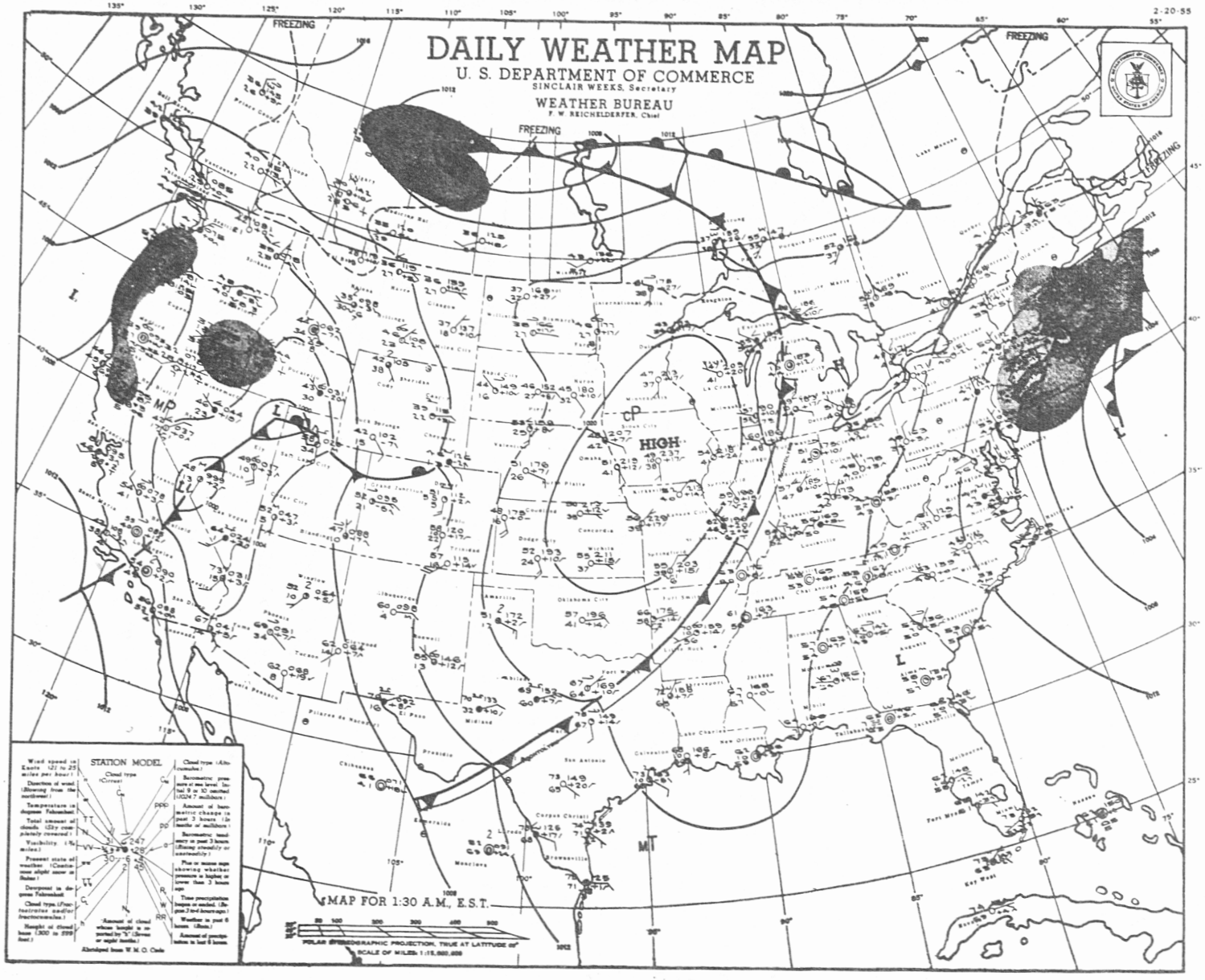

FRIDAY, APRIL 29, 1955

Fig. 22 Surface map, 0630Z, 29 April 1955

Fig. 23 0300Z, 29 April 1955, temperature at 20° dewpoint surface

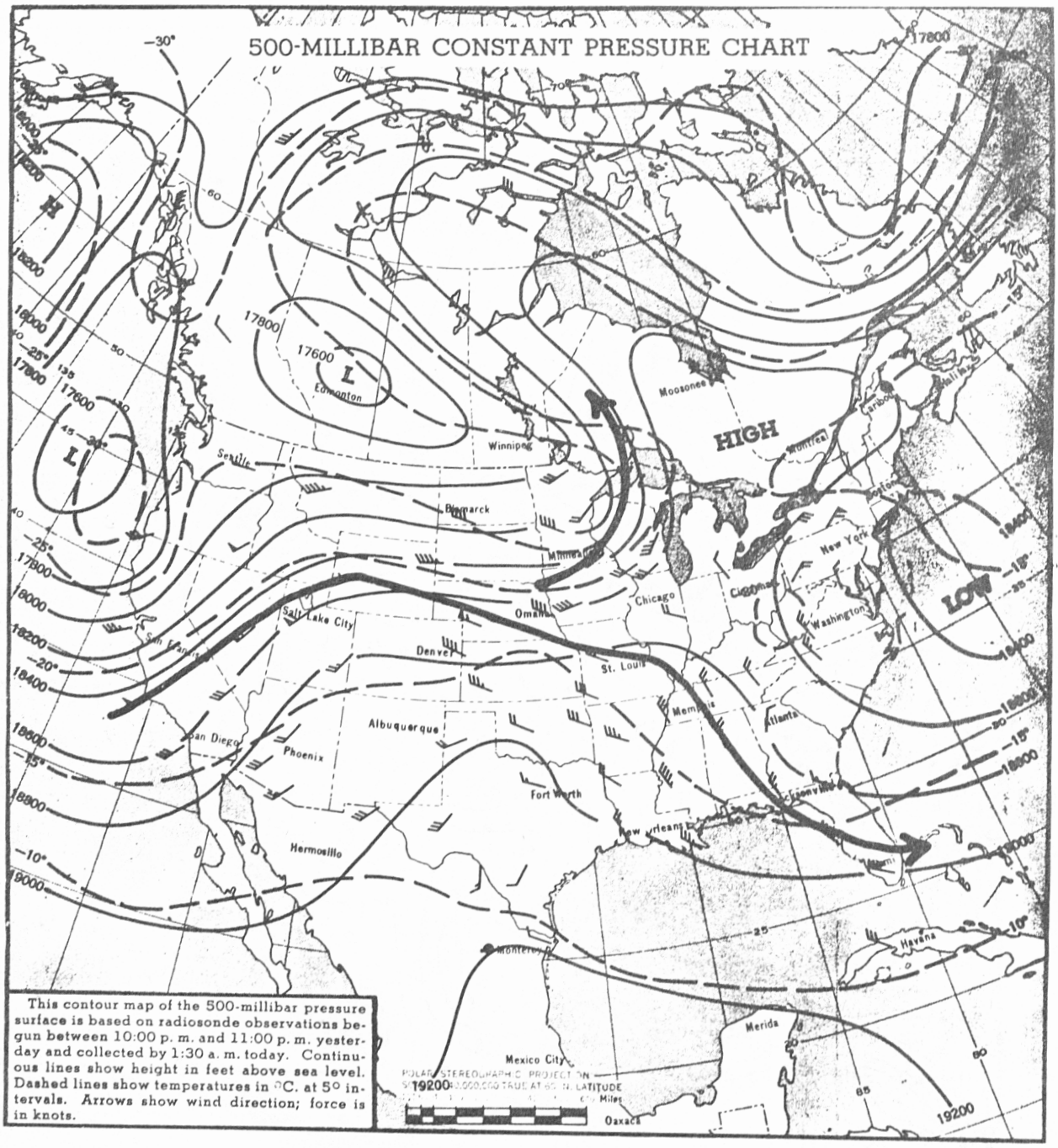

Fig. 24 500 mb chart, 29 April 1955, 0300Z

3.4.6 Discussion

The correlation between the conventional analyses and the simulated radiation temperature maps is quite interesting. In a general sense the high temperatures appear to be associated with anticyclonic activity; the low temperatures, with cyclonic activity. Furthermore, there does seem to be a tendency for the jet-stream areas to be marked by bands of strong temperature gradient.

These finding are qualitatively similar to those obtained from accurate calculations of the radiation from the entire 6.3μ band. This work was performed at Allied Research Associates, Inc., under Contract No. AF 19(604)-5968, and is discussed in Section 4.

Lack of experience in the analysis of these charts led to the delineation of structures which, in some cases, do not well correspond to features observed on the conventional charts. This lack of experience made necessary the unquestioning use of all data points, resulting in the construction of what may be absurd gradients based on single observations. But even with these difficulties, the interrelations between conventional analyses and the temperature structure of a constant dewpoint surface seem evident.

Explanation of most of the observed features is not difficult. A high temperature at a constant dewpoint surface represents a low relative humidity, which must be the result of subsiding motion in the atmosphere. Similarly, low temperatures correspond to high relative humidities where water vapor is brought up into higher (and colder) regions by upward motion. Thus a representation of the vertical motion field is obtained, bearing the appropriate relationship to the horizontal fields of motion.

It is probably not highly profitable to pursue further the type of analysis that has been presented here. The relationships involved can be better explored by methods that consider more of the parameters that control the amount of radiation.

The results of this analysis are interesting because they show that observation in the infrared from a satellite vehicle can provide information that would not be available from inspection of pictures made by visible light. The analysis also apparently demonstrates that useful results can be obtained with an infrared sensing device of extremely poor resolution.

3.4.7 Conclusions

To the extent that the assumptions and logic that have gone into the development of the use of constant dewpoint surfaces as surfaces of origin of radiation may be valid, it is clear that the radiating temperature of the atmosphere seen in a dense part of the water-vapor emission band is a significant meteorological parameter. High temperatures appear to correspond to regions of divergence or sinking air; and low temperatures, to regions of convergence or rising air. This relationship is obscured somewhat by the tendency of the dewpoint surfaces to slope upward toward the south.

The results thus far obtained indicate that meteorologically useful information can be obtained from satellite observations of the infrared emission in the 6.3μ water-vapor band. A considerable amount of experience and of analysis will be required before the maximum utility can be extracted from such satellite observations.

CHAPTER V (Continued)

SECTION 4

SATELLITE OBSERVATIONS OF INFRARED RADIATION

Raymond Wexler
Allied Research Associates, Inc. *

4.1 Introduction

The use of statellites for photographic (television) observations and infrared measurements of the earth's atmosphere may ultimately contribute significantly to our knowledge of the atmospheric structure, global circulation, and heat balance. Proposed meteorological satellites will carry several infrared sensing elements intended to provide information on the infrared radiative properties of the atmosphere. The sensors will be directional, accepting infrared radiation from a relatively narrow angle of view. They will be mounted on the satellite in such fashion that their field of view will sweep across the earth as the satellite spins. Sensor outputs will be telemetered back to earth, along with sufficient additional information to permit establishing the location of each observation. Thus, in a single sweep, the sensor will scan across a substantial part of the earth, taking in angles of view of the atmosphere ranging from glancing angles at the horizons to near vertical below the satellite.

The infrared radiation emerging from the top of the atmosphere is known to be nonisotropic; that is, the atmosphere does not radiate as a diffuse radiator. As a result, observations taken at differing angles of view are not directly comparable. Nor is it

* This research was sponsored under Contract No. AF19(604)-5968, under ARPA Order No. 26-59.

possible, without further analysis, to infer the total amount of radiation emerging in all directions from a measurement of the radiation in but one direction. Thus it becomes desirable to determine the variation of the radiation which may be expected at different angles of view.

The most important information which may be expected from such observations is the determination of a spatial pattern which may thereby be associated with synoptic conditions. From such patterns, it may be possible to determine large-scale vertical motions, which together with photographic observations, may give a three-dimensional aspect to synoptic disturbances. By the use of infrared windows it may be possible to determine the temperature of the radiating surfaces (cloud or ground). The use of other bands may give qualitative information concerning the temperature structure and the distribution of water vapor in the atmosphere.

In this report atmospheric transmissions in the infrared have been determined from available experimental data on absorptions by atmospheric gases. The actual amounts of radiation which may be expected to leave the top of the atmosphere over the United States on a specific occasion (6 March 1959, 0000Z) were mapped for the "window" regions, the 6.3μ H_2O band, the 15μ and 4.3μ CO_2, and ozone bands. For the H_2O band, computations were made at air masses (secant of the zenith angle) of 1, 2, and 3, that is, for zenith angles of 0°, 60°, and 81.5°. The results of this study should facilitate the interpretation of future measurements of infrared radiation made from satellites.

The dependence of atmospheric absorption on temperature is not considered as yet. The effect of temperature dependence deduced from theory together with a more complete analysis of the infrared

spectrum will be considered in a future report.

4.2 Atmospheric Transmission in the Infrared

4.2.1 Division of the Spectrum

The earth's surface or a cloud radiates essentially as a black body. A portion of this radiation is transmitted through the atmosphere and the remainder is absorbed by atmospheric gasses--principally CO_2, H_2O, and O_3. In addition the atmosphere itself reradiates energy. The amount of energy in the different infrared bands which reaches the satellite is dependent on the atmospheric temperature at and above the surface or cloud top and the distribution and temperature of absorbing gas between the surface and the satellite. For computation purposes, convenient spectral regions have been chosen as shown in Table 1. The third column shows the absorbing gas in these regions and the wavelength (inverse of wave number) of the band center.

TABLE 1 DIVISION OF INFRARED SPECTRUM

Wave Number (cm^{-1})	Wave-length (μ)	Absorption
250-560	17.9 - 40	H_2O
560-800	12.5-17.9	$15\mu CO_2$
800-1000	10 - 12.5	window
1000-1100	9.1 - 10	9.6μ O_3
1100-1200	8.31 - 9.1	window
1200-2000	5 - 8.3	6.3μ H_2O
2000-2200	4.6 - 5	4.8μ CO_2
2200-2460	4.1 - 4.55	4.3μ CO_2

Absorption by CO_2 is associated with changes in the rotation-vibration energies of the molecule with strong bands centered at 15 and 4.3μ, and the weaker band at 4.8μ. Absorption in the 1000 to 1100 cm^{-1} region is due to the rotation-vibration ozone band centered at 9.6μ and a rotation band in the region 0 to 560 cm^{-1}. In the window regions absorption is small (except for the lower layers in tropical regions with high humidity) and the outgoing radiation from the underlying cloud or surface is not much different from black-body radiation, according to its temperature.

4.2.2 Radiation Theory

For a given wave-number interval the outgoing radiation at the top of the atmosphere from a radiating surface may be put in the form

$$R = B' + \int_{B'}^{B} \tau \, dB \tag{1}$$

where τ is the transmission between a level and the top of the atmosphere, B' is the black-body radiation from the top of the atmosphere, or from a level above which absorption is negligible, and B is the black-body radiation at the radiating surface. For relatively thin atmospheric layers where the lapse rate is constant and the temperature change is about 10°C or less, the integration in Eq. (1) may be carried out in the form $\Sigma \tau \Delta B$ where τ is now the transmission from the middle of the layer to the top of the atmosphere, and ΔB is the difference in black-body radiation between the bottom and top of the layer. For any wave-number interval, B may be calculated from the Smithsonian Meteorological Tables [42] (Table 129).

According to the Curtis approximation [28] the transmission depends on the amount m of absorbing gas, between a level at pressure p and the top of the atmosphere, and a mean pressure P which, without temperature dependence, may be defined by the equation

$$mP = \int_{o}^{m} p \; dm \tag{2}$$

For an absorbing gas like CO_2 where m is proportional to p, then $P = \frac{p}{2}$. For O_3 or H_2O, integration must be made according to the vertical distribution of m.

In a small wave-number interval D, Kaplan [29] has shown that the transmission by a gas having an irregular spectrum (such as H_2O) is given by

$$\tau = e^{-\frac{m}{D}} \Sigma S_i e^{-xi} [I_o(x_i) + I_1(x_i)] \tag{3}$$

where

$$x_i = \frac{m S P_o}{2 \pi \alpha_{oi} P} \tag{4}$$

and S_i is the line intensity of the line i, α_{oi} is the line half-width, and I_o and I_1 are Bessel functions of imaginary argument. At large x_i, Eq. (3) converges to

$$\tau = e^{-k \sqrt{mP}} \tag{5}$$

If x_i is not large, τ will be dependent on both mP and P. If Eq. (5) is valid for all intervals of a band, then the whole band transmission is also a function of mP.

4.2.3 6.3μ H_2O Band

Excellent data on the absorption due to 6.3μ H_2O have been obtained by Howard et al [30] who derived from them empirical absorption formulae. However, Benedict [31] finds that a more satisfactory representation can be found from theoretical considerations. In particular, Benedict points out that the effect of pressure broadening due to collisions between H_2O molecules is considerably greater than the effect due to air-H_2O collisions. As a result the pressure P in the experiments should be redefined as:

$$P = p + np' \tag{6}$$

where p is the total pressure and p' is the partial pressure of water vapor. In the atmosphere np' is generally negligible compared to p, but in laboratory experiments it is not. Benedict found that a value of n between 4 and 6 fitted the various H_2O bands.

Using n = 6 in Howard's data for 6.3μ H_2O, points were plotted on a log τ vs $\sqrt{mP}$ graph(Fig. 25)* Note that the transmission of this band can be represented quite adequately as a function of mP. A line of best fit (by eye) has been drawn. The data for $\sqrt{mP} > 5$ fits the straight line (solid in Fig. 25):

$$\tau = 0.665e^{-0.715\sqrt{mP}} \tag{7}$$

where m is in cm of precipitable water and P in mb.

---

* Not all of Howard's data are included in Fig. 25 because of crowding, especially at low values of $\sqrt{mP}$.

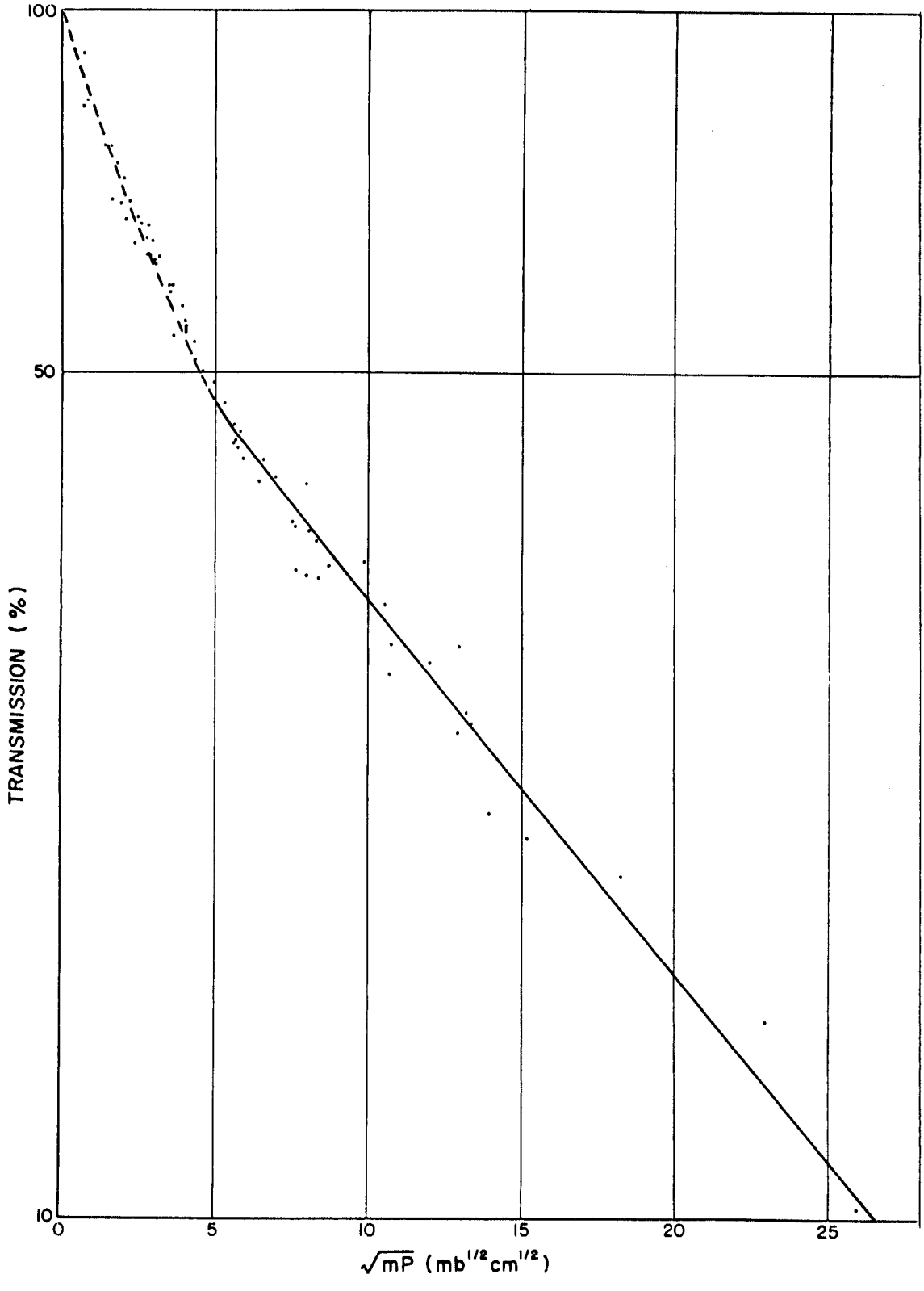

Fig. 25 Transmission for 6.3μ H_2O from Howard's data

4.2.4 Rotational Water

Palmer [32] measured the absorption due to rotational water in the region 250-500 cm^{-1} under varying conditions of P and m. A plot of his absorption data over intervals 30 to 60 cm^{-1} in width shows that at constant m, log τ vs $\sqrt{mP}$ are straight lines. These lines, however, differ as m changes. A considerable portion of his data include cases where the partial pressure of water is a significant if not major portion of the total pressure. In the atmosphere the partial pressure is usually negligible compared to the total pressure. Since there is no reason to suppose that a constant value of n can be used in this region [33], it was decided to use the upper envelope of Palmer's data, thus effectively using only those data in which np' is relatively small compared to the total pressure. In this case it does not much matter what value of n is chosen; it was taken as 6 as for the case of 6.3μ H_2O. The coefficient K of the exponent in Eq. (5) was derived in this manner for the various spectral intervals and the results are shown in Table 2. The coefficient for the 560-500 cm^{-1} band was derived by extrapolation.

TABLE 2 TRANSMISSION FOR ROTATIONAL WATER

Band (cm^{-1})	Transmission (m in cm, P in mb)
560-500	$e^{-0.046\sqrt{mP}}$
440-500	$e^{-0.08\sqrt{mP}}$
380-440	$e^{-0.145\sqrt{mP}}$
310-380	$e^{-0.31\sqrt{mP}}$
250-310	$e^{-0.51\sqrt{mP}}$

4.2.5 mP for H_2O

For water vapor the optical depth m may be determined from the distribution of specific humidity q:

$$dm = \frac{qdp}{g} \tag{8}$$

Frequently the specific humidity may be approximated over a considerable pressure-interval by the relation:

$$q = q_o \left(\frac{p}{p_o} \right)^c \tag{9}$$

where c is a constant. Inserting Eq. (9) in Eq. (8) and then in Eq. (2) we obtain after integrating from o to p:

$$mP = \frac{p^2 q}{c + 2} \tag{10}$$

where, by omitting g, p is in mb and m in cm. If the exponent in Eq. (9) is c_i between p_i and p_{i+1}, then Eq. (10) becomes:

$$mP = \sum_i \frac{p_{i+1}^2 q_{i+1}^2 - p_i^2 q_i}{c_i + 2} \tag{11}$$

Frequently radiosonde data on humidities are missing above 400 mb. Murgatroyd et al [25] measured the distribution of q at levels above 400 mb in southern England. His values are marked by crosses in Fig. 26. Above 150 mb he found that q was constant with elevation at about 0.002 g/kg. Figure 26 also shows the distribution of q from 450-150 mb using $q_o = 0.2$ g/kg at $p_o = 400$ mb and c = 5 in Eq. (9). In view of the good agreement and the fact that q = 0.2 g/kg at 400 mb was a frequent value over northern and western

United States on 6 March 1959, the distribution of q in Fig. 26 was chosen as a "standard" atmosphere. A portion of the curve for mP is also shown in Fig. 26.

For tropical soundings like Miami on 6 March 1959, q is 0.4 g/kg at 400 mb. In this case the q-distribution from 400 to 150 mb is assumed to be exactly double that in Fig. 26, and then to approach the same constant value of 0.002 g/kg above the 125-mb level. The mP distribution for the tropical atmosphere is essentially double that for the "standard" atmosphere at 300 to 400 mb.

Using curves for mP for the "standard" and tropical atmospheres, transmissions were computed from 0 to 400 mb for both the 6.3μ and rotational water bands for air masses of 1, 2, and 3. The result for air mass 1 of the 6.3μ H_2O band is shown in Fig. 27. For those stations in which the observed value of q at 400 mb was different from 0.2 to 0.4 g/kg, values of the transmissions above 400 mb were interpolated (or extrapolated) from Fig. 27. At lower levels, where q could be determined from the sounding, mP was computed directly using Eq. (11). The transmissions could then be determined from either Eq. (7) or Fig. 25.

4.2.6 15μ CO_2

In the atmosphere the amount of CO_2 is essentially proportional to the pressure and for air mass 1 is about 260 cm (NTP) at 1000 mb [34, 35]. Transmissions at p = 1000 mb (P= 500 mb) are thus required for m = 260, 520, and 780 cm (air masses 1, 2, and 3) and proportional values for other pressures.

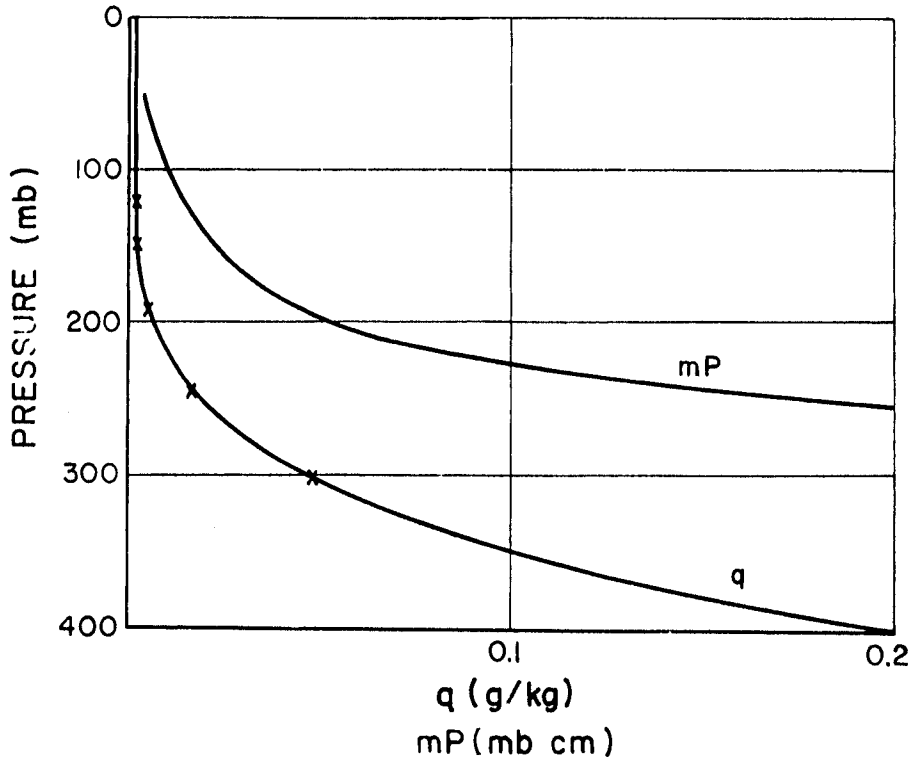

Fig. 26 Distribution of q and mP for standard atmosphere above 400 mb.

(Murgatroyd's observations are indicated by x).

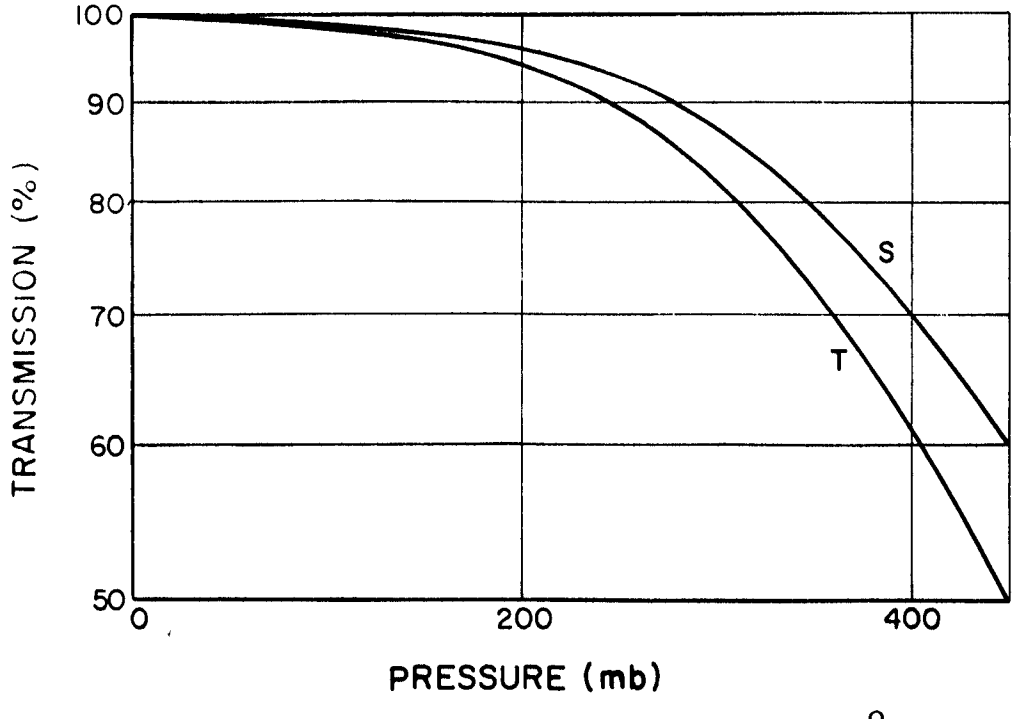

Fig. 27 Transmissions for 6.3μ H_2O above 45°mb

for standard (S) and tropical (T) atmosphere of air mass 1

Howard's data [30] on 15μ CO_2 shows that, unlike the 6.3μ H_2O band, a universal curve of τ vs mP could not be used. It was necessary, therefore, to draw curves of the absorption vs m at different pressures. The relatively sparse data for m>200 cm indicated a levelling off of the absorptions converging to values near 80 per cent. The values of the transmissions calculated for the three air masses at atmospheric pressures are shown in Fig. 28. At p = 50 mb transmissions range from 54 to 70 per cent while at 1000 mb they range from 18 to 24 per cent.

4.2.7 4.3 and 4.8μ CO_2

Howard's data for 4.3μ CO_2 also shows pressure dependence at constant mP. Interpolation was made for different pressure levels in a similar manner to 15μ CO_2. The derived transmissions for the three air masses at atmospheric pressures are shown in Fig. 29. At low pressures the transmissions are considerably lower than for 15μ CO_2, but at high pressures they are somewhat higher.

Absorptions for a weak CO_2 band centered at 4.8μ are also given by Howard. The derived transmissions are shown in Fig. 30. For air mass 1, the band is essentially a window with 92 per cent transmission from 1000 to 0 mb. Transmissions were found to be approximately linear with atmospheric pressure.

4.2.8 Ozone Band

Distributions of ozone for different seasons have been summarized by Paetzold [36]. According to his curves, the optical depth m of ozone is approximately linear with pressure at levels higher than about 20 km (50 mb) where it has a value of 0.20 cm (NTP). From 50 to 1000 mb the further increase is relatively small with m = 0.27 cm at 1000 mb for spring and summer. For lack of better information,

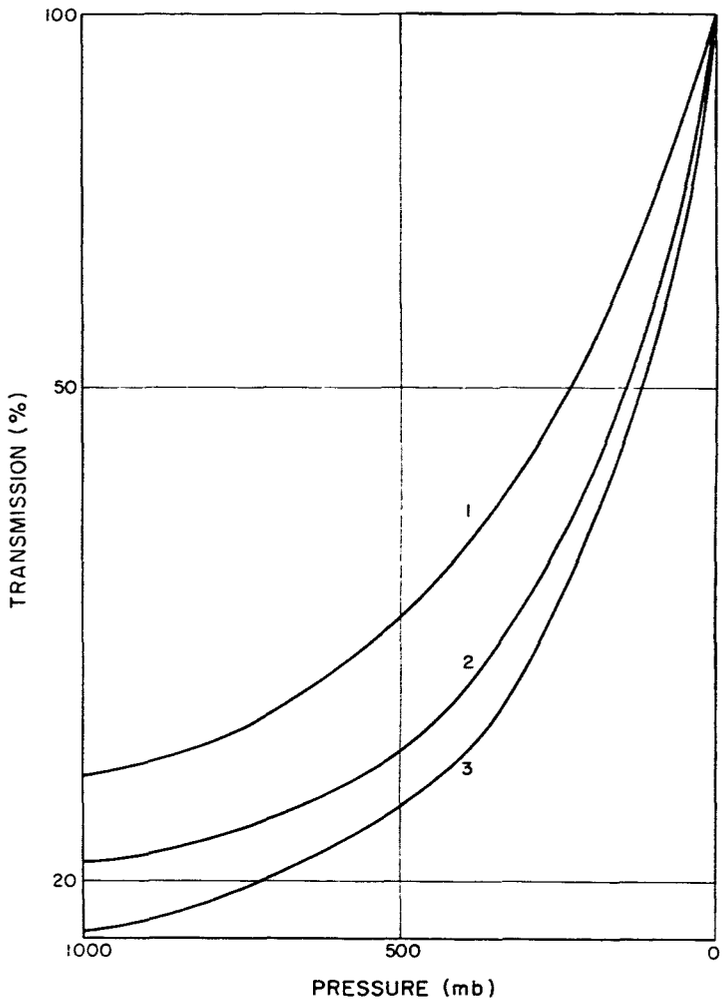

Fig. 28 Transmissions for 15μ CO_2

for air masses 1, 2, and 3.

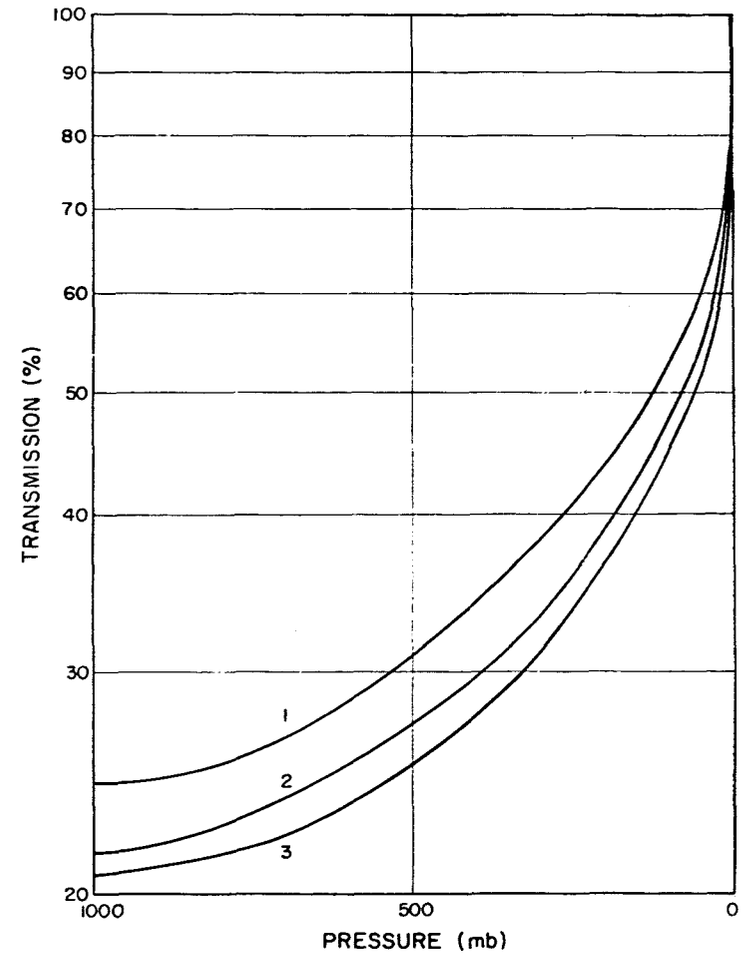

Fig. 29 Transmissions for 4.3μ CO_2

for air masses 1, 2, and 3

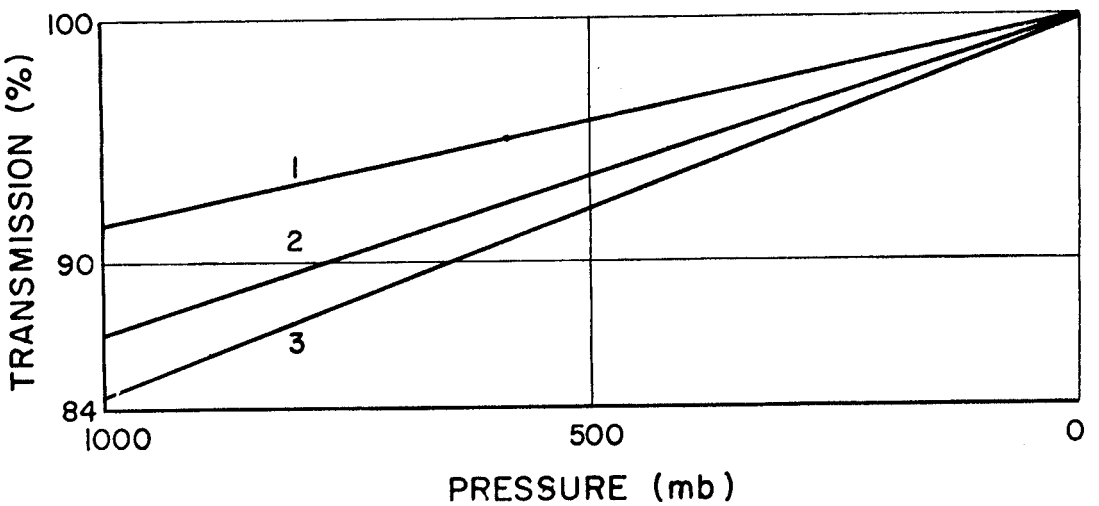

Fig. 30 Transmissions for 4.8μ CO_2 for air masses 1, 2, and 3

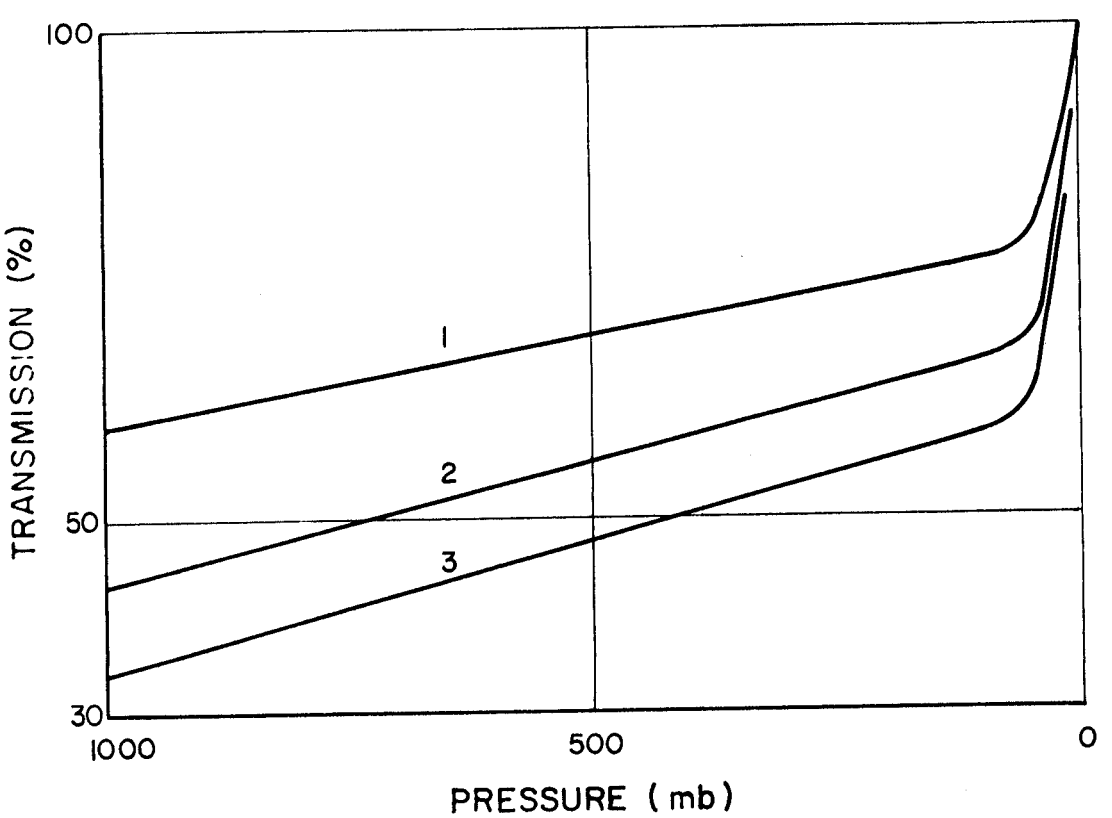

Fig. 31 Transmissions for O_3 (1100-1200 cm^{-1})

this distribution of ozone was assumed for all stations on 6 March 1959, although it is likely that there was considerable variation relative to the upper levels of the deep cyclone on that day (see Section 4.3.1).

The absorption due to O_3 has been measured experimentally by Walshaw [37]. His data were plotted as isopleths of absorption on a graph of m/P vs P. From this graph the transmissions for Paetzold's O_3 distribution of m and P were computed. The result is shown in Fig. 31 which shows that the greatest absorption occurs between 0 and 50 mb.

4.3 Infrared Maps for 0000Z, 6 March 1959

4.3.1 Weather Map

At 0000Z, 6 March 1959, a deep cyclonic storm was centered over western Illinois (Fig. 32). Widespread moderate-to-heavy snow extended from Lake Michigan westward into North Dakota and southward around the low into Kansas. A sharp cold front accompanied by heavy showers and thunderstorms extended southward to Mobile, Alabama. Tropical air in advance of the front convered the southeastern states. A thunderstorm in the past hour at Jacksonville and heavy rain at Charleston indicated a squall line along the southeastern coast. Cirrus overcast extended far to the east of the low into southern New England, but northern New England was clear. Variable high cloudiness extended from Washington state over the mountains as far east as Denver.

On the 300-mb chart (not shown) a closed cold low was centered over western Iowa and a deep trough extended southward into Texas. A jet of 100 to 150 knots extended from Louisiana northward to Lake Ontario and then eastward into southern New England.

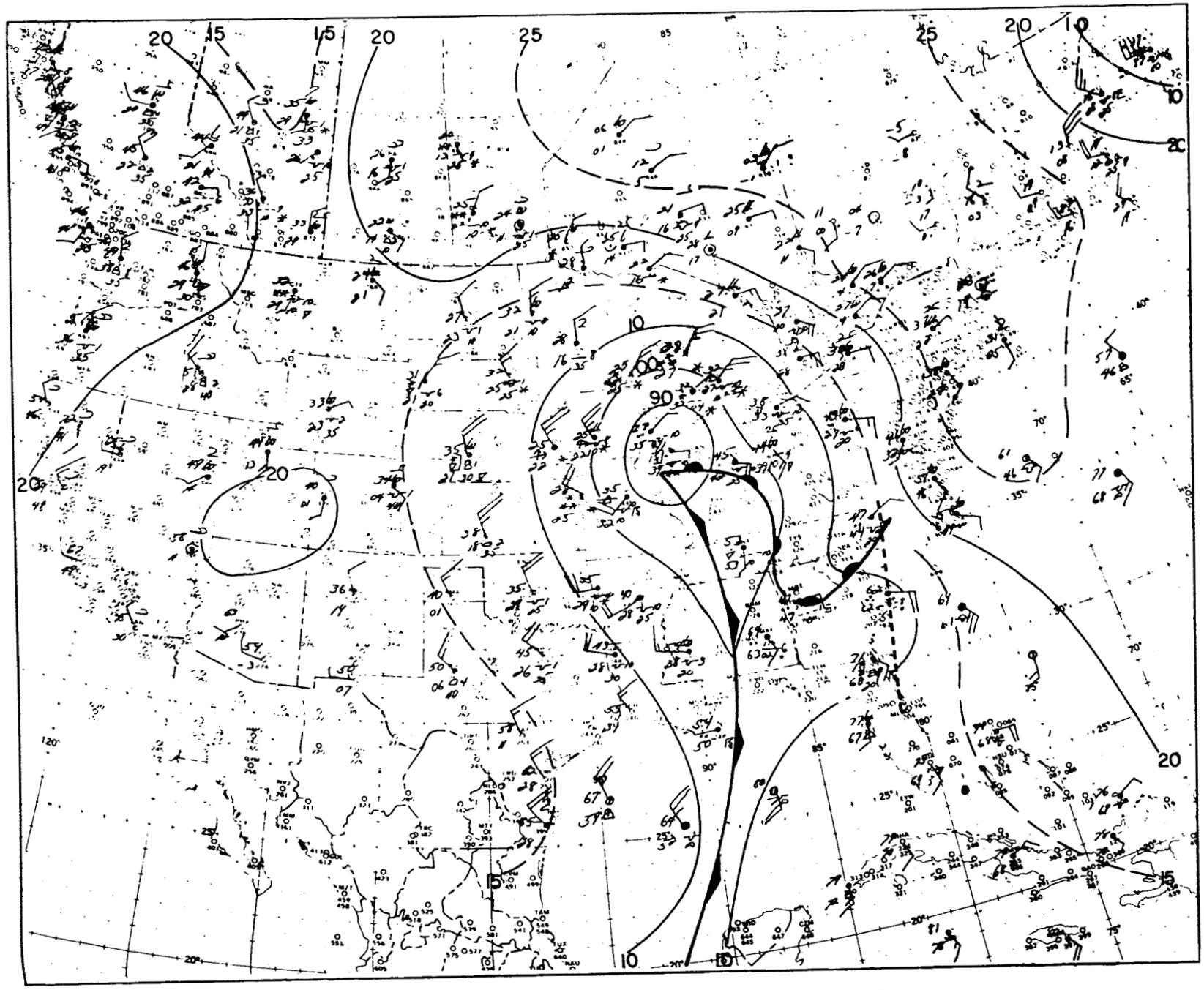

Fig. 32 Surface Map for 0000Z, 6 March 1959

4.3.2 The Window Map

Figure 33 shows the window map prepared with the aid of Fig. 32 and plots of the radiosonde data on adiabatic charts. The actual temperatures and pressures of the cloud tops or, in the case of clear skies, of the surface are plotted. The temperatures are those which would be approximately equivalent to the radiation in the window regions 800-1000 cm^{-1} and 1100 - 1200 cm^{-1}. However, observations by Taylor and Yates [38] indicate that some absorption by water vapor occurs in these window regions. The transmission is given approximately by

$$\tau = e^{-\frac{4}{3} \times 10^{-4} mP} \qquad \text{(m in cm, P in mb)} \tag{12}$$

Using this formula for the Miami sounding, it is found that the equivalent temperature in the window region would be 21.5°C at air mass 1 instead of the 24°C plotted in Fig. 33 for air masses 2 and 3, the temperatures are 19.3° and 17.3°C respectively. For other stations, corrections are much smaller. For the relatively dry air of El Paso with an actual surface temperature of 10°C, the equivalent temperatures are 9.6°, 9.2°, and 8.8°C for air masses 1, 2, and 3.

It was assumed that the cloud tops radiate as a black body, although this may not be strictly true for cirrus. The effect of this assumption is to give somewhat higher contrast between warm and cold areas than may actually exist. The location of cloud top temperatures required some judgment. The tops of middle or low clouds were chosen at levels where, according to the sounding, the lapse rate became more stable. Occasionally these levels coincided

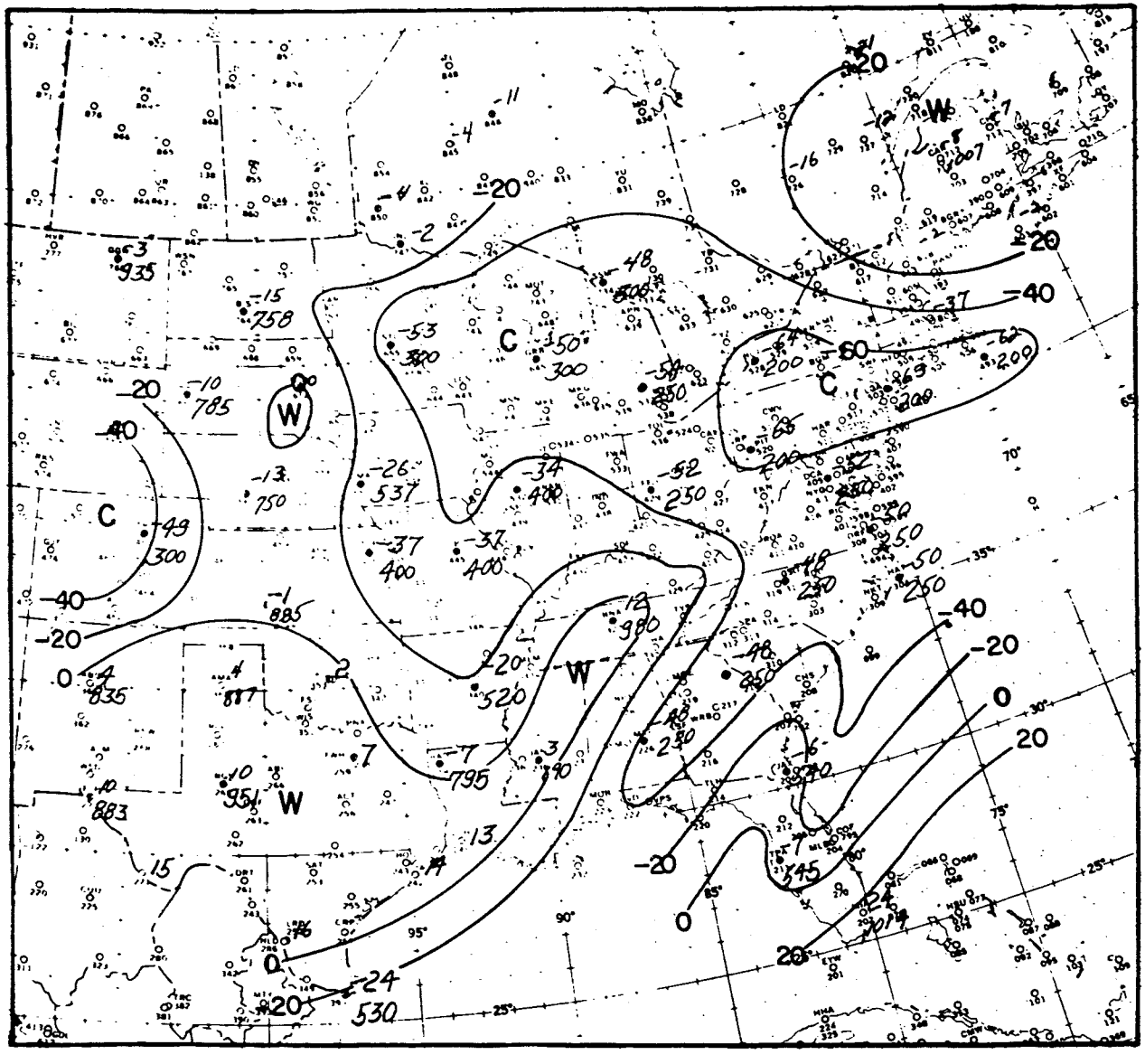

Fig. 33 "Window" Map for 0000Z, 6 March 1959, showing Temperatures at Cloud Top or at the Surface (for clear skies)

with the tropopause. The locations of the tops of cirrus chosen in this manner agree with observations by French and Johannsen [39] who found that cirrus tops were frequently either at the tropopause or within a few thousand feet below.

Six radiosonde stations had cloud covers ranging from 0.2 to 0.8. In these cases the amounts of radiation reaching the top of the atmosphere were computed from the formula

$$R = CR_c + (1 - C) R_s \tag{13}$$

where C is the cloud cover, and R_c and R_s are the respective radiations from the cloud top and the surface. An equivalent temperature for R, using black-body radiation for the 800-1000 cm^{-1} band, was then computed. Use of the 1100-1200 cm^{-1} window gave almost identical values. The formulation of Eq. (13) is valid only at air mass 1. For air masses 2 and 3, the radiation reaching the top of the atmosphere is a complicated function of cloud shape and vertical extent in addition to cloud cover. For stratiform clouds, the use of Eq. (13) for air masses 2 and 3 is probably reasonably accurate; but for cumuliform clouds appreciable error may result. Hence, Fig. 33 is strictly valid only for air mass 1. However at larger air masses only regions involving a rapid change of equivalent temperature with distance will be appreciably affected.

The window map, Fig. 33, shows that the coldest temperatures below -60°C, lie far to the east of the surface cyclone and coincide with a region of high tropopause in a westerly jet which extends from Pennsylvania through southern New England. An extensive cold area of -40°C or colder extends from Minnesota eastward to the Atlantic and southward to the Gulf, the latter portion coinciding

with the heavy rain area just ahead of the cold front. Another indentation of the -40°C line has been drawn to coincide with the line squall at Charleston and just past Jacksonville. Warm surface air is seen over most of Texas and a pocket of this warm (drier) air has extended towards the northeast as far as Nashville, coinciding with the clearing conditions west of the cold front. Beyond the cold temperatures to the west of the low lies a narrow clearing area of warmer temperatures in the Dakotas. The cold temperatures in Colorado are associated with the penetration of cirrus from the Pacific northwest. The entire map gives the appearance of a marked circulation pattern associated with the deep cyclone.

4.3.3 Temperatures in the Stratosphere

Since absorption may be appreciable at levels above the tops of soundings (usually 100 to 150 mb), some extrapolation was necessary to higher levels. For this purpose soundings were connected to a standard or tropical atmosphere [40], the characteristics of which are given in Table 3.

TABLE 3 STANDARD (S) AND TROPICAL (T) ATMOSPHERES
(Adapted from Air Force Handbook [40])

Pressure (mb)	Temperature (°C)	
	S	T
200	-56	-51
95	-56	-80
25	-56	-50
5	-24	-24
1	10	10

The standard stratosphere is isothermal at -56°C from 225 to 25 mb. Since most soundings above the tropopause were isothermal or nearly so, isothermalcy under these conditions was assumed above the top level until it intersected the standard atmosphere above the 25-mb level or its extension below 25 mb. Above the intersected level the standard atmosphere was assumed. For those soundings with tropical characteristics (such as Miami on 6 March 1959) the existing lapse rate near the top of the sounding was extended until it intersected the tropical stratosphere in Table 3.

4.3.4 The 6.3μ H_2O Band

Figure 34 shows the equivalent isotherms for radiation of the 6.3μ H_2O band for air mass 1. Equivalent temperatures (hereafter T_E) for air masses 1, 2, and 3 are plotted at the various radiosonde stations. Although a pattern similar to the window map is evident, the contrast between warmest and coldest regions (center of gravity Miami and New York) is reduced from about 90°C in Fig. 33 to 54°C in Fig. 34 (47°C for air mass 3). For the high clouds near the tropopause, T_E is about the same as the window temperature; for clear skies, T_E is colder than the surface temperatures by about 35°C (for air mass 1) over Miami, 20° to 25°C over the arid regions of Texas, and 15°C colder for the cold dry air over Bangor. For air masses 2 and 3 the contrast is further reduced, largely because of a reduction of T_E over clear areas by 3° to 10°C (compared to air mass 1).

4.3.5 The 15μ CO_2 Band

Fig. 35 shows the equivalent isotherms for air mass 1 in the 15μCO_2 band. The pattern is also similar to the window map, except that the contrast is further reduced to a maximum of

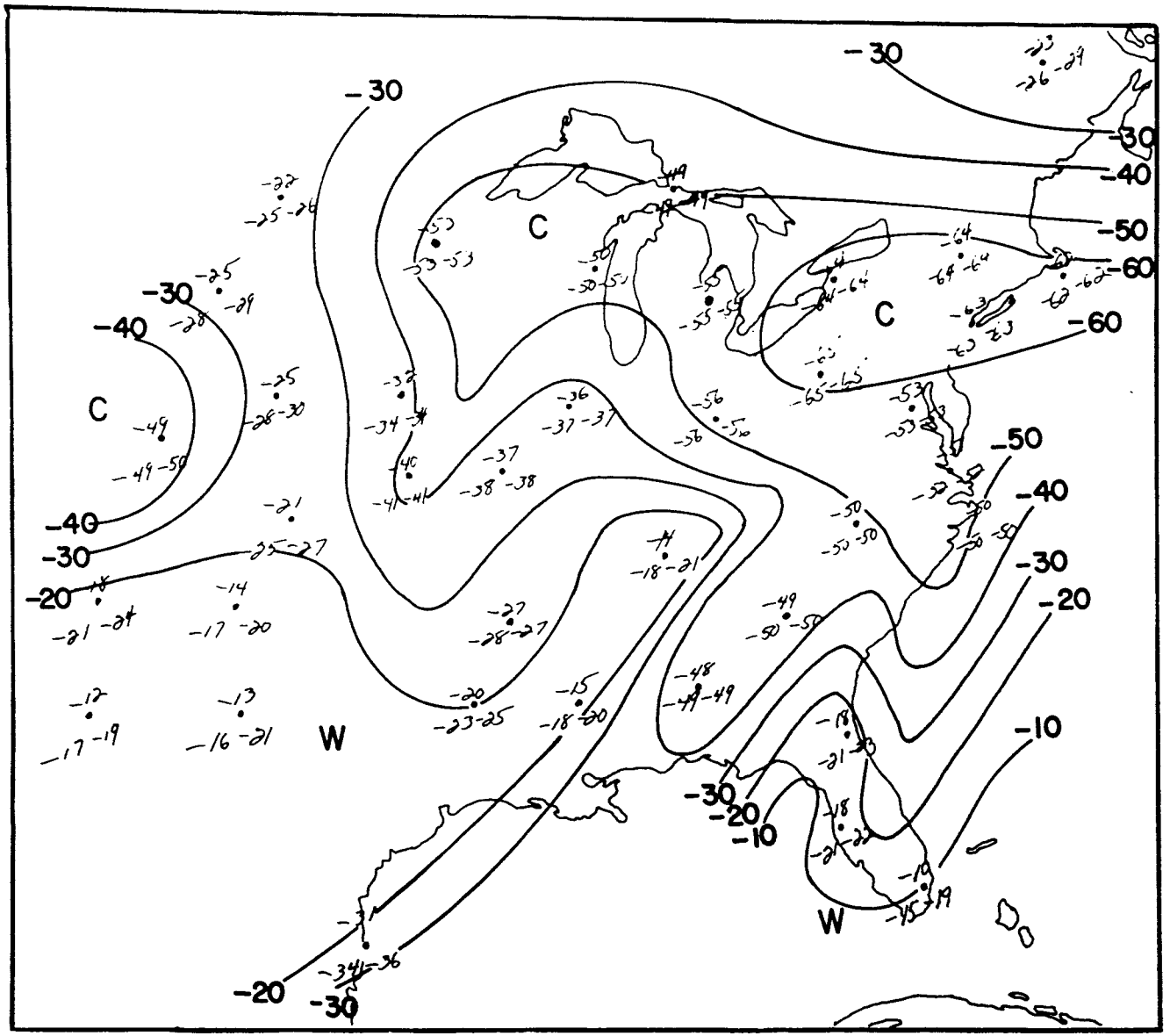

Fig. 34 Equivalent Isotherms for 6.3μ H_2O Band, Air Mass 1, 0000Z, 6 March 1959.

Equivalent Temperatures for Air Mass 1, 2, and 3 are plotted according to the model: 1 2 3

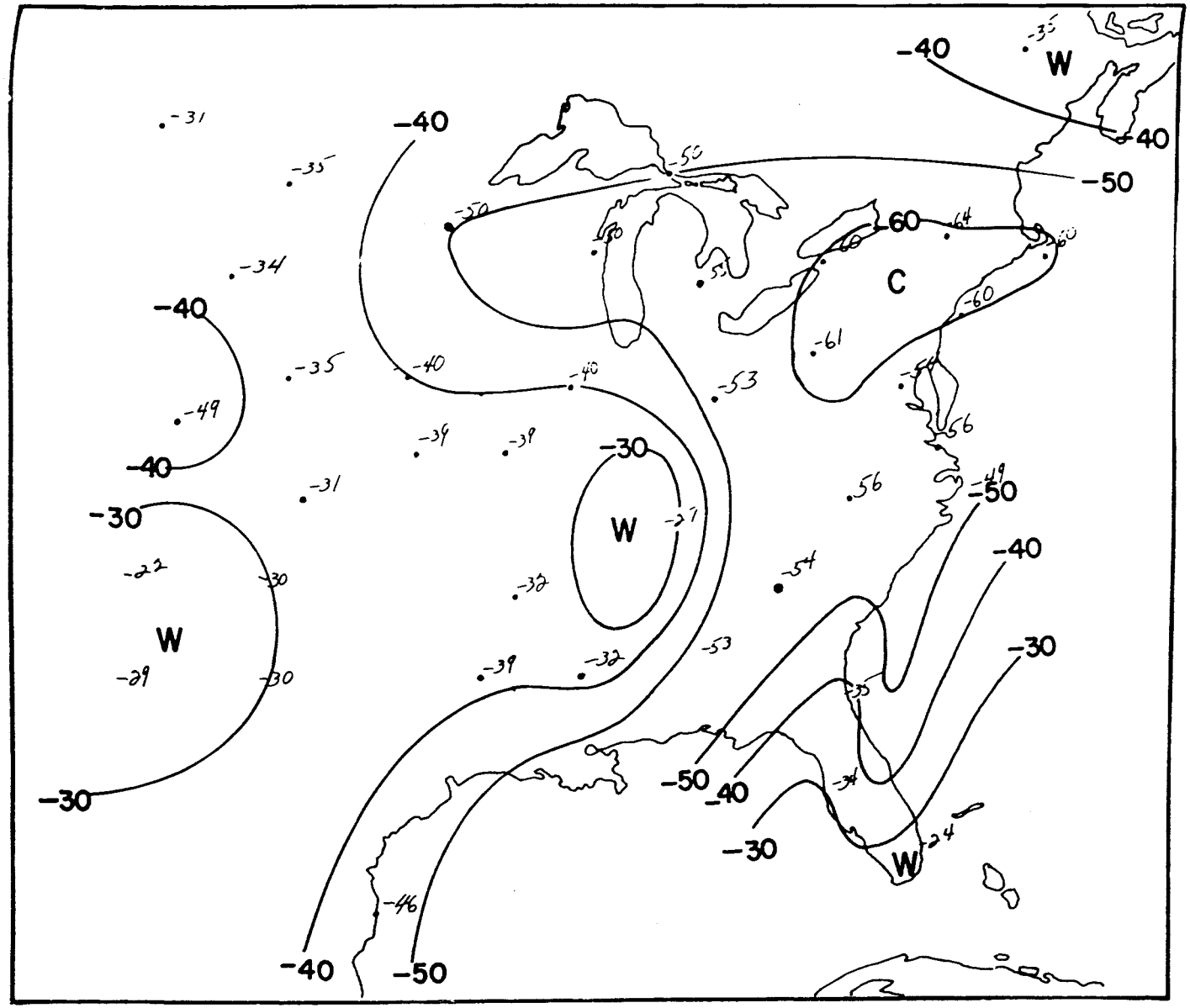

Fig. 35 Equivalent Isotherms 15μ CO_2 Band, Air Mass 1, 0000Z, 6 March 1959

about 40°C. T_E is somewhat warmer than the high-cloud top temperatures, because of stratospheric absorption. For clear skies, T_E is 50°C colder than the Miami surface temperature, and 25°C colder over Bangor.

4.3.6 The 4.3μ CO_2 Band

Fig. 36 shows the equivalent isotherms for air mass 1 in the 4.3μ CO_2 band. The most remarkable aspect of the diagram is the increase in T_E by about 30°C over the actual temperatures at the top of the high cold clouds in the northeast. This curious result is due entirely to high absorption in the stratosphere at levels generally above 25 mb where the temperature of the standard atmosphere rises sharply. Between 10 and 17 mb, for example, the average absorption of the 4.3μ CO_2 band is about 25 per cent at air mass 1; between 1 and 5 mb it is 10 per cent. In this region of the spectrum at cold temperatures, a relatively small increase in radiation produces a relatively large increase in T_E. Hence the T_E for the high clouds is markedly dependent on the temperature of the mesosphere for which we have no data.

The contrast between warmest and coldest regions in Fig. 36 is further reduced about 30°C. Over clear areas, T_E is about 25°C colder than the surface temperature.

4.3.7 The Ozone Band

Fig. 37 shows the equivalent isotherms for the O_3 band (air mass 1). This band also has the characteristic of high stratospheric absorption, which causes the T_E over the high-cloud areas to be 20°C warmer than the cloud top temperature. The absorption at low levels, however, is relatively small. These two effects cause T_E over clear areas to be only 10°C colder than the surface temperature. The contrast between coldest and warmest T_E is about 55°C, which is greater than

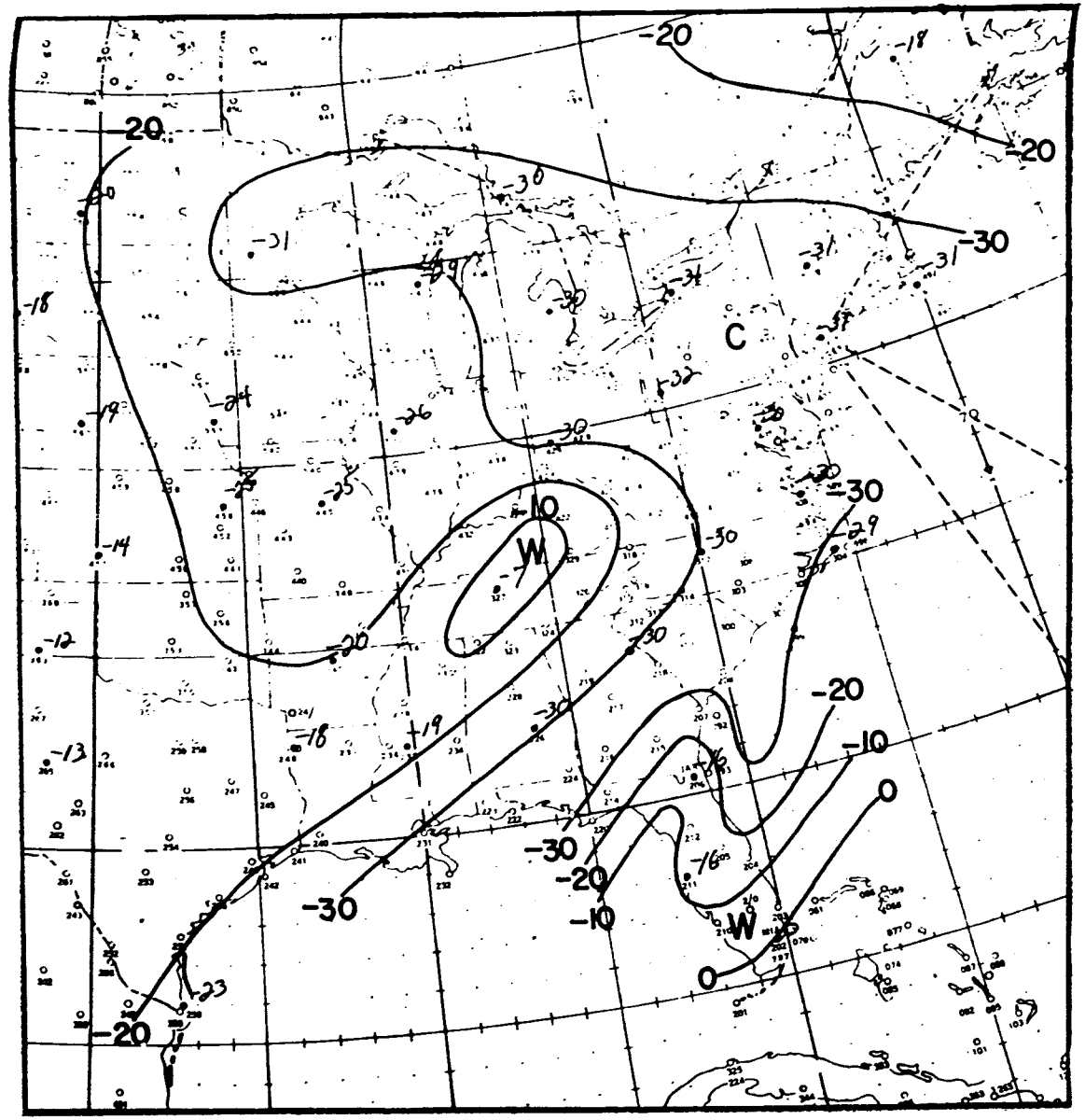

Fig. 36 Equivalent Isotherms 4.3μ CO_2 Band, Air Mass 1, 0000Z, 6 March 1959

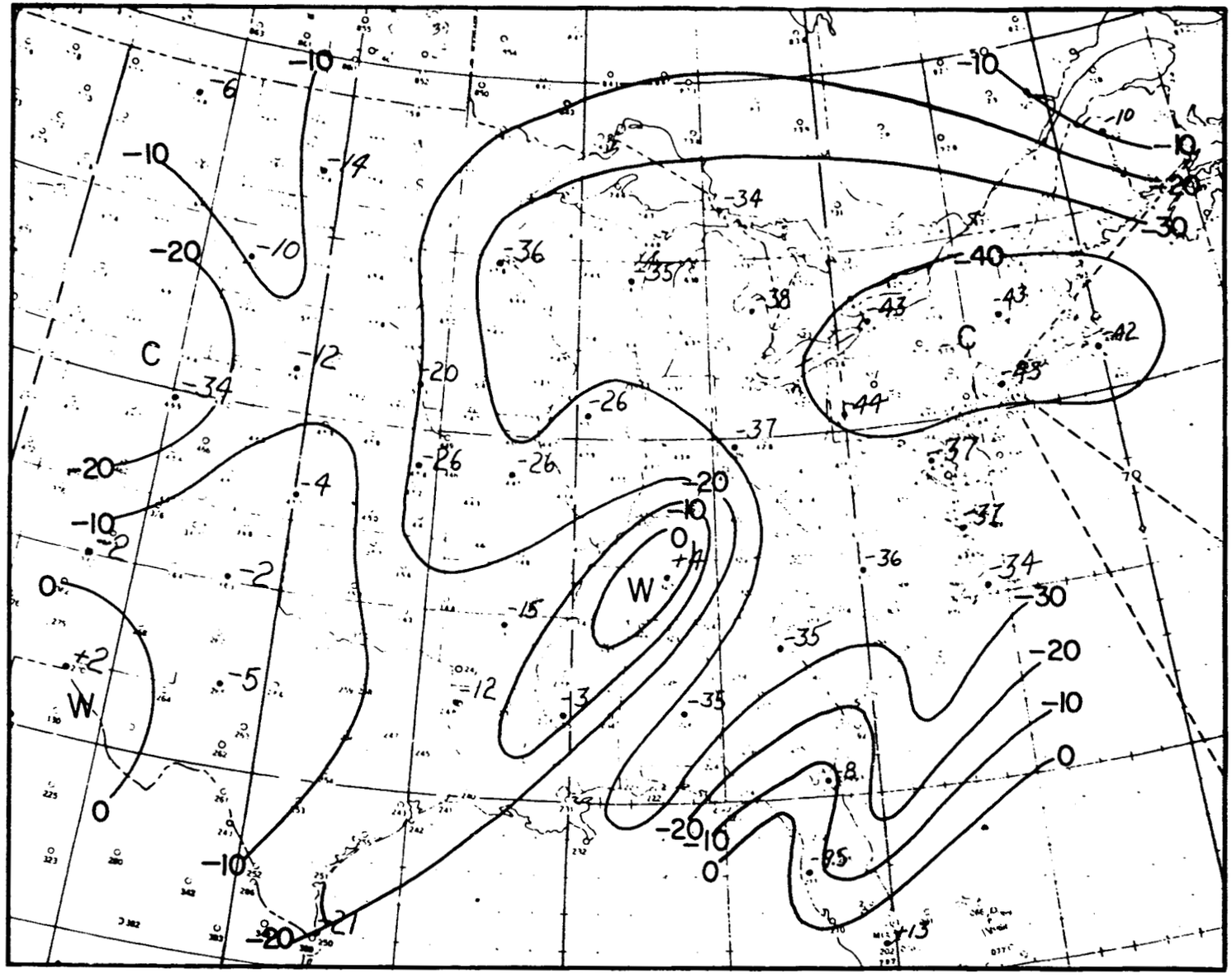

Fig. 37 Equivalent Isotherms 9.6μ O_3 Band, Air Mass 1, 0000Z, 6 March 1959

those of the CO_2 bands and the 6.3μ H_2) band.

4.4 Conclusion

Measurements of the infrared radiation from the atmosphere by a satellite gives a pattern which is dependent on the distribution of temperature at cloud tops or at the surface, and on the distribution of temperature and absorbing gases in the atmosphere. Such measurements enable the determination of the large-scale pattern of vertical motions: low T_E signifies cloud and therefore updraft, while high T_E signifies clear skies implying subsidence. A similar result was found in the other study (Section 3 of this chapter) using an opaque portion of the 6.3μ H_2O band. Over polar regions there may be some confusion between the cloud-top temperatures of 40°C or colder and similar surface temperatures. However, since such surface temperatures are generally associated with a shallow inversion, this confusion may be resolved by observation in the 15μ CO_2 band where the surface temperature has a relatively small effect.

The pattern of clear and cloudy areas would be best observed in the window regions: 800-1000 cm^{-1} where contrasts of T_E may be as great as 80°C. Although some absorption does occur in the window regions, the effect is relatively small except in tropical regions, of high moisture, where it may produce a T_E of 3° to 7°C lower than the surface temperature.

The effect of viewing the atmosphere in other infrared regions is to give a pattern which looks very much like a blurred version of the window map. Even greater blurring occurs when viewed through larger air masses. Use of the 6.3μ H_2O band reduces the contrast between coldest and warmest areas to about 50°C but gives a similar pattern. The amount of reduction from the window temperature may give a very

rough measure of total water vapor contents in the atmosphere. Thus, at Miami the reduction in T_E from the window (surface) temperature is about 25°C while in drier regions it is 15° to 20°C. A better measure of the total water-vapor content may be obtained by use of more opaque portions of the water-vapor band thus giving greater contrast between dry and moist areas.

Use of the 15μ or 4.3μ CO_2 bands reduces the contrast between coldest and warmest regions even further. For high clouds the T_E for 15μ CO_2 is slightly greater than cloud-top temperatures, but the T_E for 4.3μ CO_2 exceeds it by some 30°C largely due to absorption in the high stratosphere. It appears possible that use of a more opaque portion of the 4.3μ CO_2 band may give a rough measure of exosphere temperatures.

Absorption by O_3 in the upper stratosphere also causes the T_E in that band to be some 20°C warmer than the temperature at the top of high clouds. A rough measure of the ozone content also appears feasible by use of a narrower portion of the O_3 band.

Use of the 4.8μ CO_2 band gives a distribution of T_E only slightly less than surface temperatures, so that this band can be treated essentially as a window.

These maps of equivalent isotherms for the deep cyclonic storm of 6 March 1959 appear very promising for an interpretation of storm patterns from satellite observations in the infrared. Used in conjunction with photographs of cloud tops from a satellite, it appears possible to determine a cloud topography, representing essentially a three-dimensional structure of a synoptic disturbance. Useful supplementary information would thus be provided to the weather analyst and forecaster.

CHAPTER V (Continued)

SECTION 5

DETECTION OF OZONE AMOUNTS FROM SATELLITE MEASUREMENTS

Raymond Wexler
Allied Research Associates, Inc. *

5.1 Introduction

One of the methods used to measure the amount of ozone in the atmosphere is the determination of the intensity of direct solar radiation at two different wavelengths in the ultraviolet, frequently 0.311μ and 0.329μ. The former wavelength is strongly absorbed and the latter very weakly absorbed by ozone. Measurements at the surface are generally made at different zenith angles, which allows a rough determination of the heights of the ozone layer.

Another method involves measurements of the intensities of the scattered radiation at these wavelengths. Such measurements, generally made with the sun at large zenith angles, result in the well-known "umkehr" effect when the ratio of the intensities of the strongly-absorbed to that of the weakly-absorbed wavelengths reaches a maximum at about sunrise or sunset.

The determination of ozone amounts from a satellite by measuring the scattered radiation from an atmospheric column at two different wavelengths was suggested by Singer [11]. In this note, this method is discussed in an effort to determine the theoretical ratios of radiation intensities to be expected at the two wavelengths.

---

* This research was conducted under Contract No. AF 19(604)-5582, under ARPA Order No. 26-59.

5.2 Theory

Let the sensor on the satellite be directed at an angle ϕ from the zenith. The solar radiation at angle Θ from the zenith and of intensity I_o at the top of the atmosphere will undergo scattering and absorption in the atmosphere. The scattered radiation towards the satellite will also undergo this attenuation.

Singer [11] has shown that the amount of radiation incident at the satellite is theoretically independent of range, although the volume of atmosphere being sampled is directly proportional to the square of the range. The intensity of the solar radiation at depth h from the top of the atmosphere is given by

$$I_{o\lambda}\, e^{-\int_0^h (k_a + k_s) \sec \Theta \, dh} \qquad (1)$$

where k_a and k_s are the absorption and scattering coefficients respectively. The intensity I_λ of scattered light reaching the outside of the atmosphere is given by the equation

$$\frac{I_\lambda}{I_{o\lambda}} = \int_0^h S\, e^{-\int_0^h (k_a + k_s)\, X\, dh} \sec \phi \, dh \qquad (2)$$

where S is the ratio of scattered to incident radiation from a unit volume of air in the direction ϕ , and $X = \sec \Theta + \sec \phi$ is the slant-path-length correction factor.

Assume now that the absorption due to ozone takes place outside the atmosphere and so is independent of H. This is not a serious restriction since the ozonosphere is located above about 95 per cent of the atmosphere. Then

$$\frac{I_\lambda}{I_{o\lambda}} = e^{-k_a m X} \int_0^h S\, e^{-\int_0^h k_s X dh} \sec\phi\, dh \tag{3}$$

where m is the ozone mass (in cm) in a vertical column. From reference 41, the molecular scattering coefficient k_s is given by

$$k_s = \frac{32\pi^3 M (n-1)^2}{3 N \rho \lambda^4} \tag{4}$$

where M is the molecular weight of air, N is Avogadro's number, ρ is the air density, n is the index of refraction, and λ is the wavelength. Also from Reference 41, the scattering function S is

$$S = \frac{2\pi^2 M (n-1)^2}{N \rho \lambda^4} \tag{5}$$

From the Lorenz-Lorentz relation [42]

$$\frac{n^2 - 1}{n^2 + 2} \frac{1}{\rho} = c \tag{6}$$

where c is a constant. We note that for n close to 1, Eq. (6) may be written

$$\frac{2}{3} \frac{n-1}{\rho} = c \tag{7}$$

Substituting sea-level values of $n = 1.00028$ and $\rho = 1.25 \times 10^{-3}$, obtained from Reference 42, and solving for the constant we find $c \approx 0.15$, whence

$$\frac{n-1}{\rho} \approx 0.05\rho \tag{8}$$

Hence both k_s and S are a function only of ρ

$$k_s = c_1 \rho \tag{9}$$

$$S = c_2 \rho$$

where for $\lambda_1 = 0.311\mu$

$$c_1 = 8.6 \times 10^{-4} \text{ cm}^2 \text{ g}^{-1}$$

$$c_2 = 5.2 \times 10^{-5} \text{ cm}^2 \text{ g}^{-1} \tag{10}$$

and for $\lambda_2 = 0.329\mu$

$$c'_1 = 6.8 \times 10^{-4} \text{ cm}^2 \text{ g}^{-1}$$

$$c'_2 = 4.1 \times 10^{-5} \text{ cm}^2 \text{ g}^{-1} \tag{11}$$

Note that the ratio c_2/c_1 is $\frac{3}{16\pi} \approx .06$ regardless of wavelength.

Substituting Eq. (9) in Eq. (3) and using the hydrostatic relation, we may integrate with the result:

$$\frac{I_\lambda}{I_o^\lambda \sec\phi} = e^{-k_a m X} \frac{c_2}{c_1 X} \left(1 - e^{-\frac{c_1 X p}{g}} \right) \tag{12}$$

where p is the pressure.

Substituting Eqs. (10) and (11) into Eq. (12) we find

$$\frac{I_\lambda}{I_{o\lambda}} = 0.06 \quad \frac{\sec\phi \, e^{-k_a m X}}{\sec\theta + \sec\phi} \left(1 - e^{-\frac{c_1 X p}{g}} \right) \tag{13}$$

The ratio of intensities at wavelength 1 to that of wavelength 2 is then given by

$$\frac{I_{\lambda_1}}{I_{\lambda_2}} = \frac{I_{o\lambda_1}}{I_{o\lambda_2}} \quad \frac{e^{-k_{a_1} m X}}{e^{-k_{a_2} m X}} \quad \frac{\left(1 - e^{-\frac{c_1 X p}{g}} \right)}{\left(1 - e^{-\frac{c_1' X p}{g}} \right)} \tag{14}$$

Since $I_{o\lambda_1}$ and $I_{o\lambda_2}$ are known, if I_{λ_1} and I_{λ_2} can be measured, then an estimate of the mass m of ozone may be made.

5.3 Calculations

For reasonable values of p, θ, and ϕ the ratio of the expressions in the parentheses of Eq. (14) varies from about 1.1 to 1.2. The ratio $I_{o\lambda_1} / I_{o\lambda_2}$ for an 0.01μ wavelength interval is about 0.67. Hence, without the ozone absorption factor, the ratio given by Eq. (14) is about 0.8.

Let us define the principal factor as

$$\psi = \frac{e^{-k_{a_1} m X}}{e^{-k_{a_2} m X}} \tag{15}$$

According to the Handbook of Geophysics [40] for temperatures of $18^{o}C$ and $-44^{o}C$, K_{a_1} varies from 2.42 to 2.20 and k_{a_2} from 0.140 to 0.08. Using mean values of 3.2 and 0.11, the factor ψ is shown in Table 1 for various values of m X:

TABLE 1 RELATIVE SCATTERING OF 0.311μ TO 0.329μ RADIATION

m X (cm)	0.2	0.4	0.6	0.8	1.0	2.0
ψ	0.64	0.42	0.27	0.175	0.11	0.012

Plots of the ratio $I_{\lambda_1} / I_{\lambda_2}$ versus m for X = 2.0, 2.5, 5.0, and 10.0 have been derived from Table 1 and are shown in Fig. 38. The value of X depends on both the zenith angle of the solar radiation, Θ, and the zenith angle of the satellite sensor, ϕ. For Θ and ϕ moderately small, the value of X is very nearly 2, so that the plot for X = 2 of Fig. 38 will apply in most cases. Should larger zenith angles be involved, values of X may be obtained from Fig. 39.

It is seen from Fig. 38 that the value of $I_{\lambda_1} / I_{\lambda_2}$ varies appreciably with the mass of ozone present in the atmosphere. Hence the measurements of scattered solar radiation for the two wavelengths could be used to give an estimate of the total mass of ozone. Corrections would have to be made for the value of X if the zenith angles of either solar radiation or satellite sensor direction become large.

5.4 Discussion

The total ozone amount, or a number closely related to it, apparently can be determined by a measurement of relative absorption of scattered ultraviolet light. There are some complications that must

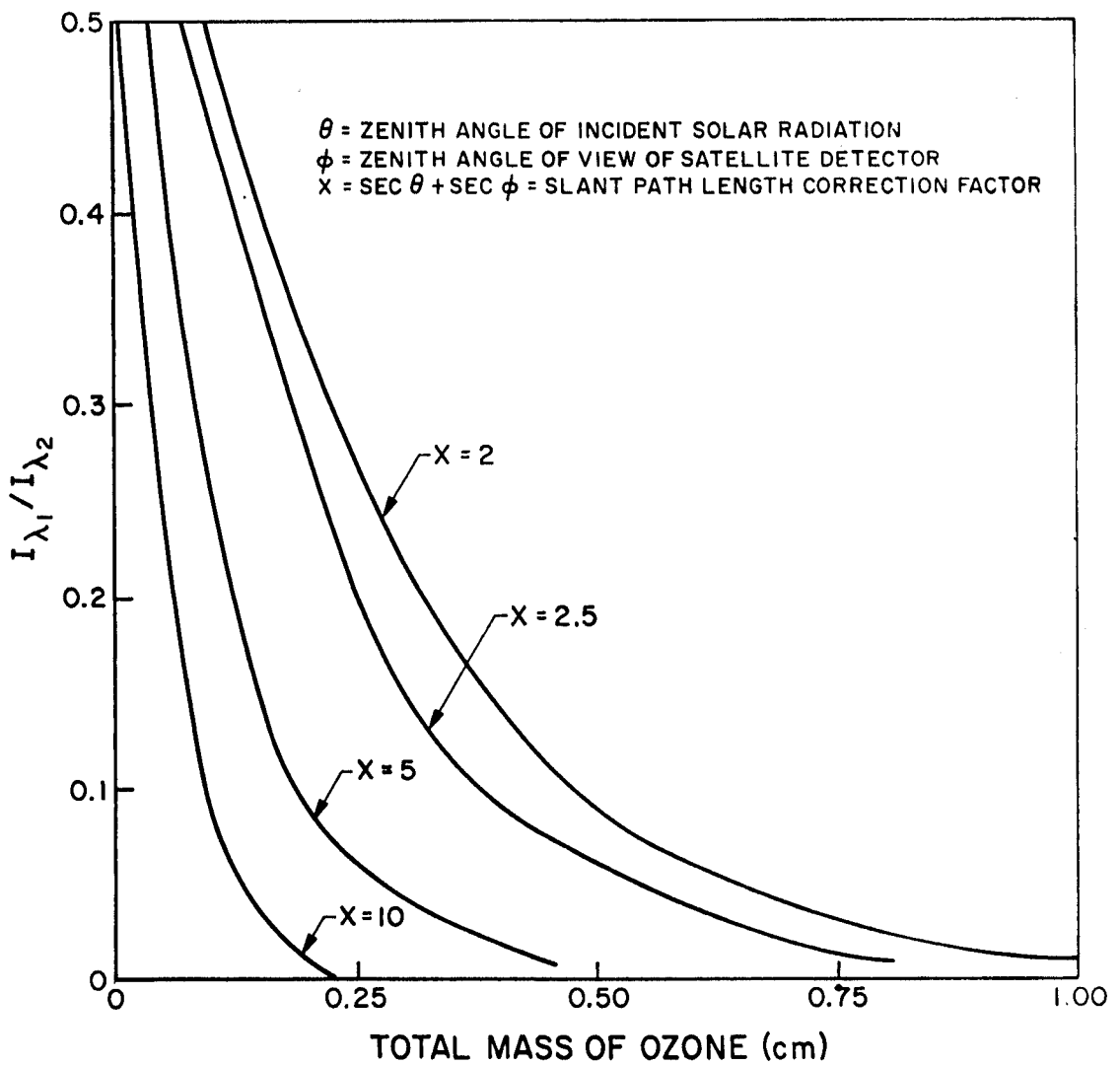

Fig. 38 Variation of ratio of scattered radiation at .311μ to that at .329μ vs. total mass of ozone in the atmosphere

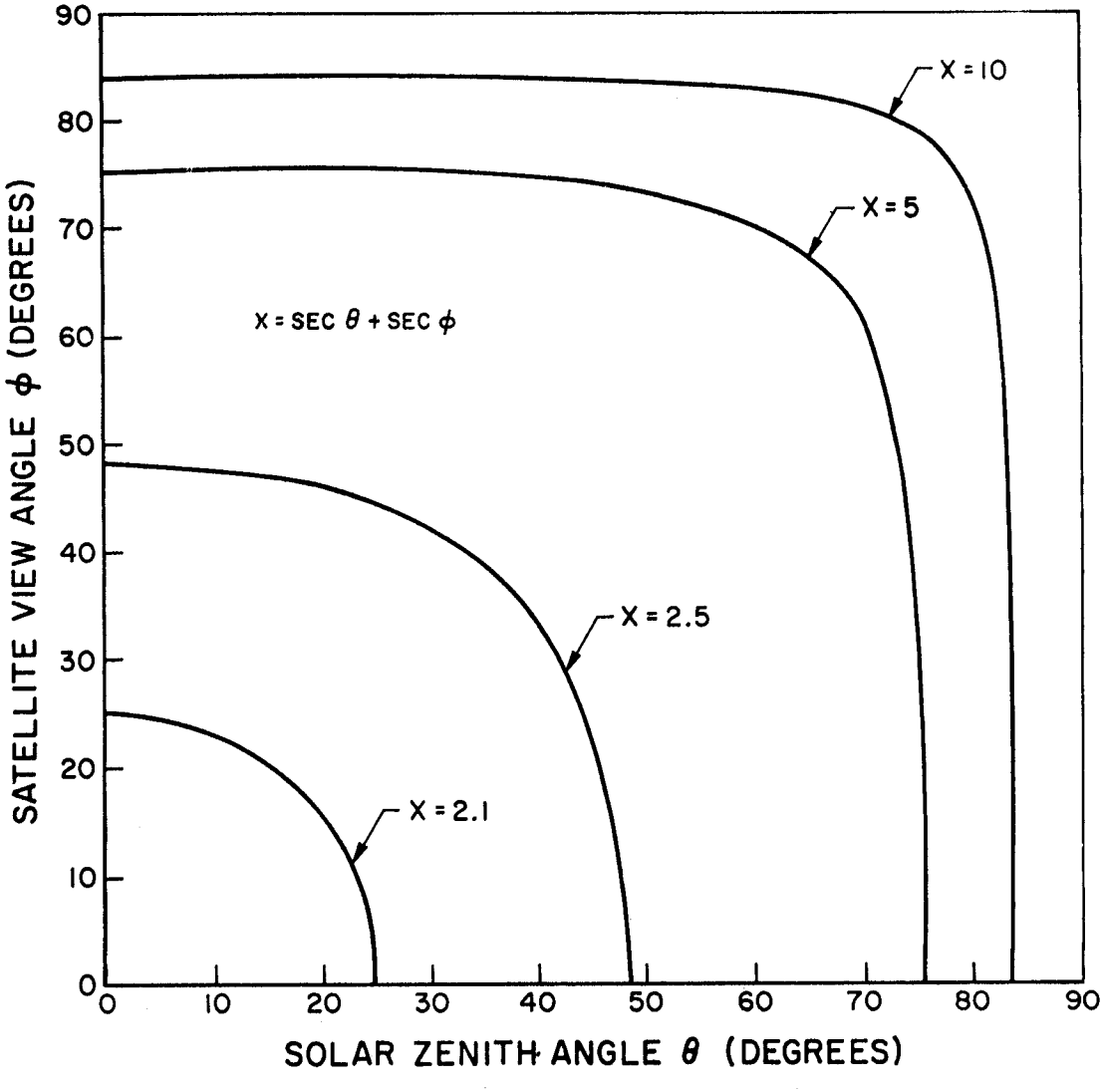

Fig. 39 Slant path length correction factor (X)

be considered, however.

The back-scattering does not necessarily follow the Rayleigh law, particularly if the possibility of cloud-scattering enters. Thus a further group of observations is necessary to establish the "law" of scattering and the intensity of scattering. Since ozone absorption would occur at (at least) some of the wavelengths used to establish the scattering "law", rather complex equation-solving methods would be required.

Even with such additional complexities, it would seem that a well-designed satellite system could provide an excellent tool for the determining global distribution of total ozone.

Blank page retained for pagination

CHAPTER VI

SECTION 1

A GENERALIZED, SCHEMATIC FLOW-CHART FOR THE REDUCTION AND PROCESSING OF SATELLITE METEOROLOGICAL DATA

William K. Widger, Jr.
Geophysics Research Directorate

1.1 Introduction

A most significant problem in satellite meteorology, and one whose importance and complexity it would be difficult to over-estimate, is that of the reduction and processing of the data to be obtained. As used here, the terms reduction and processing include essentially all handling and treatment of the data from the time observations are made by the satellite until the data are presented to the meteorologist in optimum forms for use in weather analysis and forecasting--or for the purposes of meteorological research or climatology. Ultimately, as numerical prediction techniques (especially those applicable to the parameters observable from satellites) are perfected, the area of reduction and processing may in some cases be extended to include the application of such techniques and the presentation of required weather conditions and forecasts directly to the operational user.

The significance of the data reduction and processing problem stems from two causes:

a. Satellites will produce data in quantities and at rates far in excess of those with which the meteorologist, already

swamped by the amount of available normal weather data, is used to coping. In most cases the satellite data will be in addition to present normal weather data.

b. Much of the data, particularly the pictorial presentations of clouds and the radiation parameters, will be in forms or of types relatively foreign to past and present experience.

Specific systems for the reduction and processing of satellite meteorological data can be usefully designed only in terms of both the established configurations of meteorological satellites and known or anticipated requirements and practices of the consumers of the data. Neither are sufficiently well determined at present. (Certain specific reduction techniques for the geographical location of satellite cloud pictures have, nevertheless, been presented in Chapter IV.) Consequently, the discussion here will be towards a general and rather inclusive consideration of steps that might be considered but not all of which would be incorporated in any one system. This can hopefully serve as a basis for the design and development of specific operational systems or research programs.

The remainder of the discussion will center around the block diagram or flow chart in Fig. 1.

1.2 Types of Data and Initial Recording

1.2.1 Types of Data

The types of data to be obtained from the satellite may be broken down as follows:

a. Orbit and position data which locate the satellite in three-dimensional space (longitude, latitude, and altitude) at the time other data are taken; and attitude data which indicate the direction of view of the sensors in the satellite.

b. TV or pictorial data.

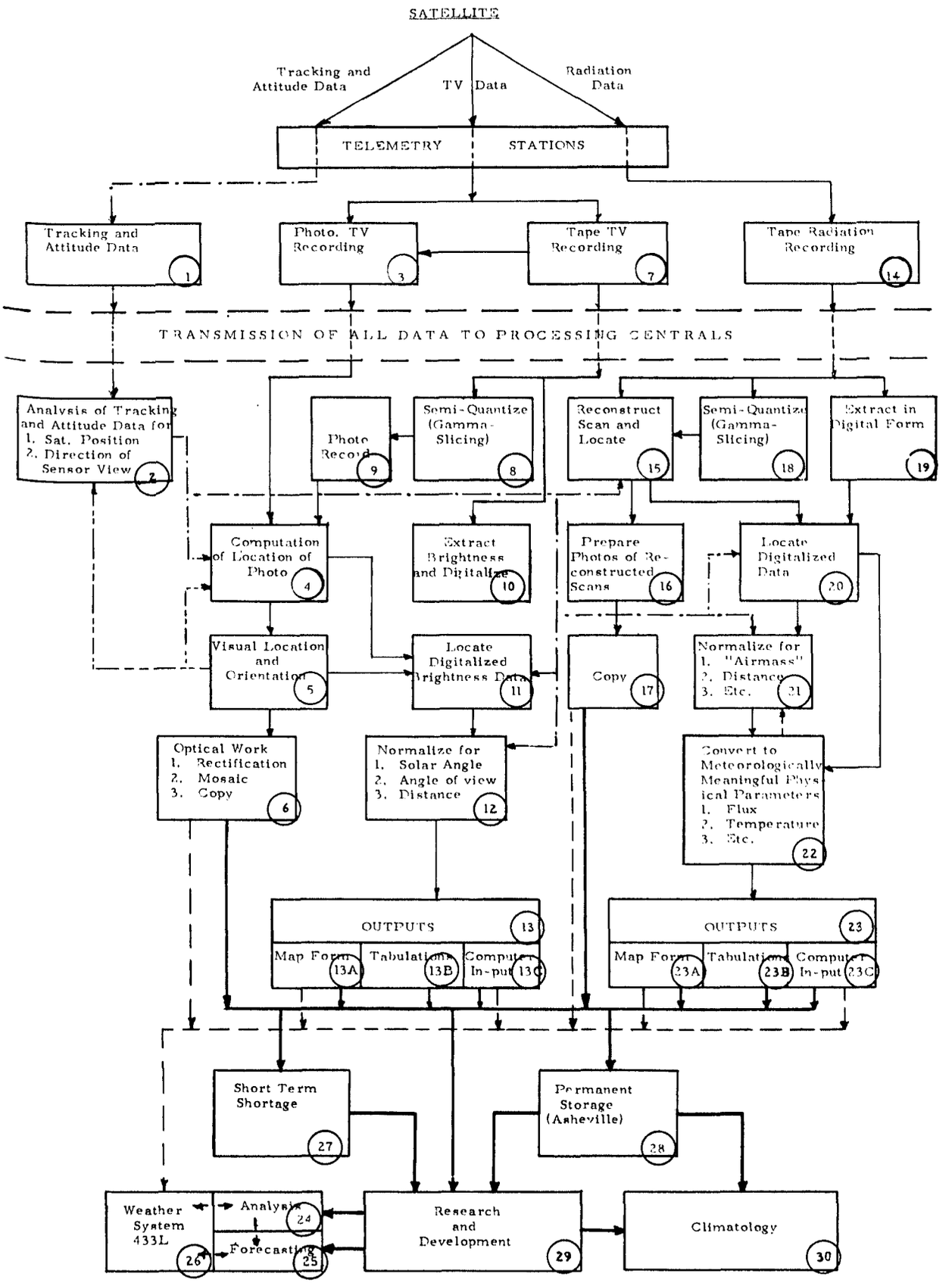

Fig. 1 Block Diagram - Schematic Data Reduction and Processing System

c. Radiation data, which is used here as embracing all radiometric type data, whether observed by radiometers or spectrometers, and whether in the IR, the UV, or the visible portion of the spectrum.

Later, more sophisticated meteorological satellites may be expected to contain other sensing subsystems such as radar, spherics, and those measuring solar radiation. As far as can be foreseen at this time, reduction and processing procedures for such data will be analogous to those described here, or some combination thereof.

1.2.2 Orbit Tracking and Attitude Data

1.2.2.1 Orbit data

Data from which the position in space of the satellite can be determined or forecast will probably be obtained at other stations besides those at which sensor data are read-out, telemetered, and recorded.

1.2.2.2 Attitude data

For spin-stabilized satellites, data from which the orientation of the axis of spin can be determined will probably also be obtained at other stations in addition to the data acquisition stations for the sensor readings. The same will be true of data with regard to the phase of rotation about the axis of spin.

For earth-stabilized satellites, the data on satellite and/or sensor attitude or orientation may be expected to be stored and telemetered in associated with the sensor data.

1.2.3 TV Data

Data from TV or similar systems will be telemetered to selected major data-acquisition stations. It may be recorded in two ways: by direct photography of a video monitor and by magnetic tape.

Other conceivable methods, that is, flying spot recorders or electrostatic tape, etc. will produce recordings comparable to photographic or tape storage.

1.2.4 Radiation Data

Radiometric data will be telemetered to the same stations as the TV data and will be recorded on magnetic tape or equivalent media.

1.3 Transmission to Processing Centrals

Figure 1 contemplates, for simplicity of depiction, that all data will be transmitted to a central point for reduction and processing. This will almost certainly be true for the orbit computations, which require data from widely-spaced points for accurate determination of the location of the satellite. To a lesser degree this is also true of the attitude data for a spin-stabilized system.

For other data, reduction and processing is possible--perhaps even probable--right at the data-acquisition stations, based on orbit and attitude computations to be transmitted from a central to those sites. Then the reduced and processed data would be transmitted to an analysis central for synergistic combination and general use. This would reduce the bandwidth that would be required for transmission if all raw data were to be sent from the telemetry stations to a central. Adverse consequences are the need for the provision of any necessary data-processing equipment at each site, and the possible masking of significant detail during the local processing central in a single, near polar, site.

Regardless of where located, the scope of the operations to be performed will remain essentially the same.

1.4 Analysis and Use of Tracking and Attitude Data (1), *(2)

Data relating to the position of the satellite in space (longitude, latitude, altitude) and to the attitude of the satellite or its sensors, from wherever obtained (1)*, will be transmitted to a central where the geographical position and altitude of the satellite and the direction of view of each sensor will be computed for the time of each observation (2). This information will then be used to:

a. Compute the location of each cloud photograph and of significant features within the photographs (4).

b. Determine the location of any quantitative values that may be derived from the TV observations (11).

c. Determine various factors, such as the angle of view and the distance from the point being observed, which will be required for any normalization of the photographic data (12).

d. Locate the geographical positions of the radiation observations (15) (20)

e. Determine the various factors, such as the angle of view and the distance from the point being observed, which will be required for any normalization of the IR data (21)

1.5 Reduction and Processing of Visual Data (3) - (13)

1.5.1 Photographically Recorded Data (3), (4)

The satellite position and attitude data (2) will be applied to the photographic record of the video monitor (3) to determine the location and orientation of the picture and the location of specific features within it (4). The locations may be depicted by the use of relative grids, such as the methods described in Chapter IV, Section 1.2 (p. 65) and then transferred to maps as described in Section 1.3 (p. 73). Alternatively, grids of absolute longitude and latitude (or other equivalent grid systems) may be superimposed

---

* Circled numbers, as (1), referred to equivalent-numbered blocks in Fig. 1.

on the pictures, as suggested in Section 1.8 (p. 84).

1.5.1.1 Improvement of location by visual and photogrammetric methods (5)

It is not expected that, in the near future, satellite positions and attitudes can be determined, from tracking data alone, with as great precision as would be desired. Using visually recognizable geographical features (5), it should be possible to improve on the locations initially determined in (4), not only for a specific frame itself but also for adjacent frames when sufficient overlap exists. Furthermore, using photogrammetric techniques, these identified landmarks can provide improved data on the position and attitude of the satellite which, when fed-back into (2), will provide greater precision in the location of both other photographs and of the radiometric data. One simplified method towards this objective has been discussed in Section 2, Chapter IV.

1.5.1.2 Optical processing and presentation (6)

Once the locations of the pictures and the features therein have been determined as precisely as is either necessary or practicable, consideration must be given to various techniques that will improve their usefulness (6). These may include rectification to give an approximation to a vertical view over the picture as a whole (for some of the associated problems, see Section 1.8, Chapter IV) or combination of several individual frames into a mosaic*. In any event, copies of the output of the processed pictures must be provided, in suitable sizes and scales, for the use of the forecaster of research worker.

---

* For an example of the results of such rectification and mosaic preparation, see Chapter III, Section 2.

1.5.2 Semi-quantitative Photographic Data[7], [8], [9]

It may be desirable to have the TV pictures presented in the form of discrete rather than continuous grey levels to make possible studies or analyses of actual data along the lines of those of Glaser [2] for simulated satellite data. In that event the TV tape-recorded data[7] would be passed through a suitable quantizing technique, such as electronic gamma-slicing[8], and photographed using a video monitor[9]. From there, the photographed using a video monitor[9]. From there, the photographs would pass along the same chain as described in Section 1.5.1 above. Of course, by the use of proper digitalization equipment in the satellite, the equivalent of the steps described here can, alternatively, be accomplished prior to telemetry.

1.5.3 Quantitative TV Data[7], [10] - [13]

If desired, it would be possible to obtain fully quantitative brightness data directly from the tape-recorded TV signals[7]. One use of such data would be the types of analysis made by Glaser [2] for simulated satellite data. It must, however, be mentioned that consideration should be given as to whether such brightness data are required at resolutions of the order of those the TV provides. If not, while it would be possible to space-average the TV signal prior to the reduction and processing to be discussed below, it would probably be more efficient to consider special albedo-measuring radiometer equipment in the satellite which would make direct brightness measurements at the grosser degree of resolution desired.

Assuming that is decided to use the TV signal, the tape recorded data[7] would be processed to extract the brightness of each point (or unit area) and digitalize it[10]. The geographical

locations of these points is then determined (11), either directly from the satellite position and attitude computations (2), or by reference to the located pictorial presentations (4), (5).

For such brightness data to be meaningful, it must be normalized to eliminate differences due solely to the sun's inclination, the angle of view from the satellite, "limb darkening" effects, and the varying distances between the satellite and the point under observation (12). (For a summary discussion of some of these problems, see Glaser [2].) These corrections will require data on the satellite position and the sensor direction of view (2).

The outputs of this processing may be presented in at least three possible ways (13):

a. Isoline maps of brightness (13A) for either research use or forecasting.

b. Tabulated values (13B) which would be primarily used by research workers.

c. Direct inputs into high-speed computing equipment (13C) for use on either research programs or in predetermined numerical weather prediction computations.

1.5.4 IR TV Data

While the discussions above have been oriented around visual spectrum data, similar reduction and processing operations would be applicable to IR TV data used to observe nighttime cloudiness, that is, observations in the 4-micron or 8 to 12-micron water-vapor windows.

1.6 Reduction and Processing of Radiation Data (14) - (23)

1.6.1 Pictorial Presentations (14) - (17)

In some cases, due either to the lack of precise accuracy in

the basic observations or the applications to be made of them, semi-quantitative, pictorial presentations may be sufficient, with the degree of grey shading being an indicator of the intensity of the radiation observation. In such cases the tape-recorded radiation data (14) would be processed to reconstruct the scans of the instruments (15) and, using values of the satellite position and attitude (2), to locate geographically the observed values (15). The reconstructed and located data presentations are then photographed (as from an oscilloscope presentation) (16), and copies of the proper size and scale prepared (17).

1.6.2 Semi-quantitative Presentations (18)

In case slightly more quantitative data presentations (that is, discrete grey levels) are desired, the tape-stored radiation data (14) will first be run through gamma-slicing or some similar semi-quantitative processing (18) before scan reconstruction and geographical location (15). The remainder of the processing is identical to that described in Section 1.6.1 above.

1.6.3 Quantitative, Digital Presentations (14), (19) - (23)

Where fully quantitative presentations are required, the tape-recorded radiation parameters (14) are run through an analogue to digital converter (19), unless conversion to digital values was performed in the satellite prior to telemetry. The data are then geographically located, either by reference to the located pictorial presentations (15) or directly from the computations of satellite position and sensor attitude (2). Then, if desired, the data are normalized as regards such parameters as angle of view (which is related to the "air mass" depth under observation) and distance of the satellite from the observed point (21). (In the present state-of-the-art there is not sufficient knowledge to permit such normalization corrections to be built into early data reduction and processing

systems.) The required satellite position and attitude data will again come from (2).

The values are then converted to meteorologically meaningful parameters and dimensions, (that is, radiation flux, temperature, amount of water-vapor, amount of ozone). (22) In some cases the results of these conversions may be required in making the normalization corrections for the same or other parameters (21).

The forms of output presentations (23) will be analogous to those described in Section 1.5.3 of this chapter for visual data, that is:

a. Isoline maps or geographically plotted values (23 A)

b. Tabulated values (23 B)

c. Direct inputs into high-speed computer (or recording on tapes to be used by such computers) (23 C)

1.7 Distribution and Use of the Processed and Presented Satellite Meteorological Data (24) - (30)

1.7.1 Research Use (29)

In the earlier stages of a project the various forms of output described above ((6), (13), (17), (23)) may be expected to go essentially directly to the research meteorologists (29). Later, it is to be expected that the data will go either into specialized short-term storage for relatively immediate use (27) or into permanent weather-records storage (presumably as part of the National Weather Records Center at Asheville, North Carolina) (28), with the research worker (29) drawing the data he requires from the appropriate storage. Short-term storage (27) will presumably be an ad hoc unit directly associated with a specific satellite or research project.

1.7.2 Weather Analysis and Forecasting Use (24), (25), (26)

The various types of output appropriate to analysis and forecasting use ((6), (13 A), (13 C), (17), (23 A), (23 C)) will be transmitted to the analysis center (24). (Note that outputs in the form of tabulations -- (13 B), (23 B) -- do not enter in here because such a form is seldom appropriate to the rate of use required in weather forecasting.) The analyzed data and/or the forecasts derived from it (25) are then fed into the operational weather analysis and forecasting system, here represented by Weather System 433L (26). Standard weather data required in analysis and forecasting use of the satellite data (24), (25) are provided by the weather system [26]. The techniques used in the analysis and forecasting (24), (25) have, of course, been provided from the research and development effort [29].

1.7.3 Climatological Use (30)

Data for climatological purposes (30) are drawn from permanent storage (28). The techniques used are provided from research and development (29).

1.8 On-Board Analysis

The discussion above contemplates little or no reduction nor processing on-board the satellite. In early systems this will doubtless be true. However, considerations of available radio bandwidth dictate that any possible methods of reducing the telemetry bandwidth requirements must be fully explored. One possible approach to this problem has been proposed by Glaser [2].

A single example of what would be desired is illustrated by considering the case of an area of cumulus cloud streets covering some hundreds of square miles. Recognition of the cumulus clouds probably requires resolutions of the order of a few tenths of a mile; determination of the cloud street pattern makes resolutions of the

order of a mile or so mandatory. Transmission of data at either of these resolutions demands bandwidths of the order of hundreds of kilocycles, at a minimum. Yet all the meteorologist really desires to derive is of the nature of the following information: (a) type of cloud (that is, cumulus); (b) size, or distribution of sizes, of individual clouds; (c) type of pattern (that is, cloud streets); (d) orientation of pattern; (e) distances between individual clouds and individual pattern elements; and (f) geographical area uniformly covered by the clouds and cloud patterns described by Items a-e.

Data beyond what is necessary to determine such information are redundant, wasteful of telemetry bandwidth, and a burden to the weather analyst. If the analysis necessary to remove such redundancy can be practicably performed in the satellite, it would be of obvious advantage to do so. Even if the equipment necessary is not suitable for use in an orbiting vehicle, similar mechanical or electronic analysis on the ground would be of significant assistance to the meteorological user.

1.9 Conclusion

It seems desirable to re-emphasize, in closing, that the intent of the above discussions has <u>not</u> been to design a specific system for the reduction and processing of satellite meteorological data. Rather, it is to describe the various types of steps and of transformations that must be considered in carrying out such a system design.

APPENDIX A

PERSPECTIVE GRIDS

1 Introduction

The principle of the perspective grids to be used in satellite programs has been described in Section 1, Chapter IV, of this report. This appendix is concerned with the detailed description of the techniques involved in the generation and preparation of the perspective grid system.

2 Computation of Grids

A relatively simple method for computing perspective grids has been devised. It has the advantages of relative simplicity of vi xualization and equivalent simplicity of digital programming. Geocentric axes are set up, x toward the principal point on the earth's surface, y in the satellite -- principal point -- geocenter plane, and z at the right angles to the plane. We work with a latitude-latitude (small circle) grid on the surface of the earth, closely approximating a grid of squares. The parametric representation of the grid is

$$\begin{aligned} x &= r\sqrt{\cos^2\psi - \sin^2\Omega} \\ y &= r \sin\Omega \\ z &= r \sin\psi \end{aligned} \tag{1}$$

where ψ and Ω are angular parameters describing the distance from the equator and prime meridian (both great circles) in degrees of latitude, and r is the radius of the earth. One grid circle is described by holding one parameter constant and permitting the other to be the independent variable. Perpendicular circles are described by reversing constant and variable parameters.

A new set of axes is set up at the satellite. x' is now along the (negative) camera axis, y' in the original $x\,y$ plane, and z is unchanged. Let h be the satellite height, α the zenith angle of the satellite from the principal point on the ground, and n the nadir angle of the camera axis. Then the transformation of coordinates gives the following expressions for the small circles on the earth.

$$\begin{aligned} \alpha &= \arcsin \frac{r+h}{r} \sin n \\ x' &= x \cos \alpha - y \sin \alpha - (r+h) \cos n \\ y' &= x \sin \alpha + y \cos \alpha - (r+h) \sin n \end{aligned} \tag{2}$$

The image plane of the satellite camera is defined by $x' = -f$, the focal distance of the camera focussed at infinity. Let us erect a $y'' - z''$ coordinate system in the image plane, y'' and z'' being parallel to y' and z. The projection of the small circles on the image plane is given by

$$\begin{aligned} y'' &= -\frac{f}{x'} y' \\ z'' &= -\frac{f}{x''} z \end{aligned} \tag{3}$$

Finally, the distortion produced by the wide-angle lens may be compensated on the image plane. Each coordinate is multiplied by a factor depending on the radius of the image point.

$$\begin{aligned} y''' &= y'' \ell \\ z''' &= z'' \ell \end{aligned} \tag{4}$$

where

$$\ell = \ell \left(y''^2 + z''^2 \right)$$

The image of the horizon may also be reproduced on the image plane. The horizon is a small circle around the satellite subpoint. Let us define new coordinates, where x^{IV} is along the radius from the center of the earth to the satellite, y^{IV} is in the same plane as the other y coordinates, and z is perpendicular to this plane. The horizon circle is given by

$$
\begin{aligned}
y^{IV}_h &= \frac{r}{r+h} \sqrt{h(h+2r)} \cos \xi \\
z_h &= \frac{r}{r+h} \sqrt{h(h+2r)} \sin \xi
\end{aligned}
\tag{5}
$$

where ξ is a parameter.

Transformation to our satellite coordinates is accomplished by

$$
\begin{aligned}
x'_h &= x^{IV} \cos n + y^{IV} \sin n - (r+h) \cos n \\
y'_h &= y^{IV} \cos n\,\phi - x^{IV} \sin n + (r+h) \sin n
\end{aligned}
\tag{6}
$$

From this point, projection to the image plane and distortion correction follow through Eqs. (3) and (4).

These formulae were programmed for digital computation on the Allied Research Associates, Inc., Bendix G-15 D computer. The computations establish the intersections of the two sets of grid lines.

A grid interval of 3° was selected as a compromise between simplicity of grid and presentation of a sufficient number of grid lines to properly delineate the perspective. Logical provisions were included to stop computation as each line went beyond the 105° coverage of the lens and when lines became too crawded for usefulness at the horizon. The program for the horizon provides the intersection of each "meridian" line with the horizon.

A modified program was written for use in the case where the forward camera axis does not intersect the earth's surface. Here a "starting point" is defined as the origin of the grid system. It is located along the arc of intersection of the earth's surface with the vertical plane containing the camera axis, at a point determined by a fixed angle of depression below the camera axis. This angle has been specified as 40.0°. A somewhat modified coordinate transformation procedure is used for this case.

The lens distortion function is approximated by a fifth-degree polynominal, providing rather more accuracy of reportuction of lens characteristics than the empirical calibration justifies.

3 Preparation of Grids

Computations of grids were performed for height intervals of 25 statute miles from 200 to 500 miles and 50-mile intervals to 800 miles. Nadir angles were computed at 5-degree intervals to 60°. Justification of these intervals is contained in Appendix B.

The intersection points were hand-plotted on graph paper, careful control being exercised to assure accuracy. The grid lines were traced with drawing ink on Ozalid process master sheets, which had been preprinted with guide lines, computation areas, and identification provisions. A small supply of working perspective grids was Ozalid printed for the expected range of heights and angles.

Less probable situations were left in Ozalid master form, to be printed as needed. Grids representing situations not expected in the planned experiment are available in computed form, to be plotted as required.

APPENDIX B

ACCURACY REQUIREMENTS FOR PERSPECTIVE GRID LIBRARY

1 Introduction

The utilization of a discrete number of perspective grids for locating clouds or other features in the televised pictures necessitates the selection of appropriate intervals for both satellite heights (h) and nadir angles (δ) of the camera axis. Substitution of discrete values for the continuous variables "δ" and "h" generates errors in object location except for those cases where the satellite height and nadir angle are precisely the same as the values for which a grid was computed.

To facilitate handling at the data-acquisition stations, the number of grids should be kept to a minimum. By choosing appropriate height and nadir angle intervals, it is possible to maintain the location errors within limits, thus minimizing the library of grids.

The method of determining an optimum number of grids is described here. An estimate of the maximum permissible errors was based on the technical limitations of the satellite instrumentation.

2. Accuracy Criteria

The principal point is assumed as being accurately located; then, errors of 15 miles or 5 per cent of the true distance from the principal point, whichever is greater, are established as the minimum accuracy tolerable. The former is based on a desired accuracy, the latter on practical consideration of the linearity of the scanning system which apparently may be in error by some 5 per cent.

3. Nomenclature

Figure 1 illustrates the notation used here for the angles and distances involved. In the plane containing the camera axis and the subpoint,

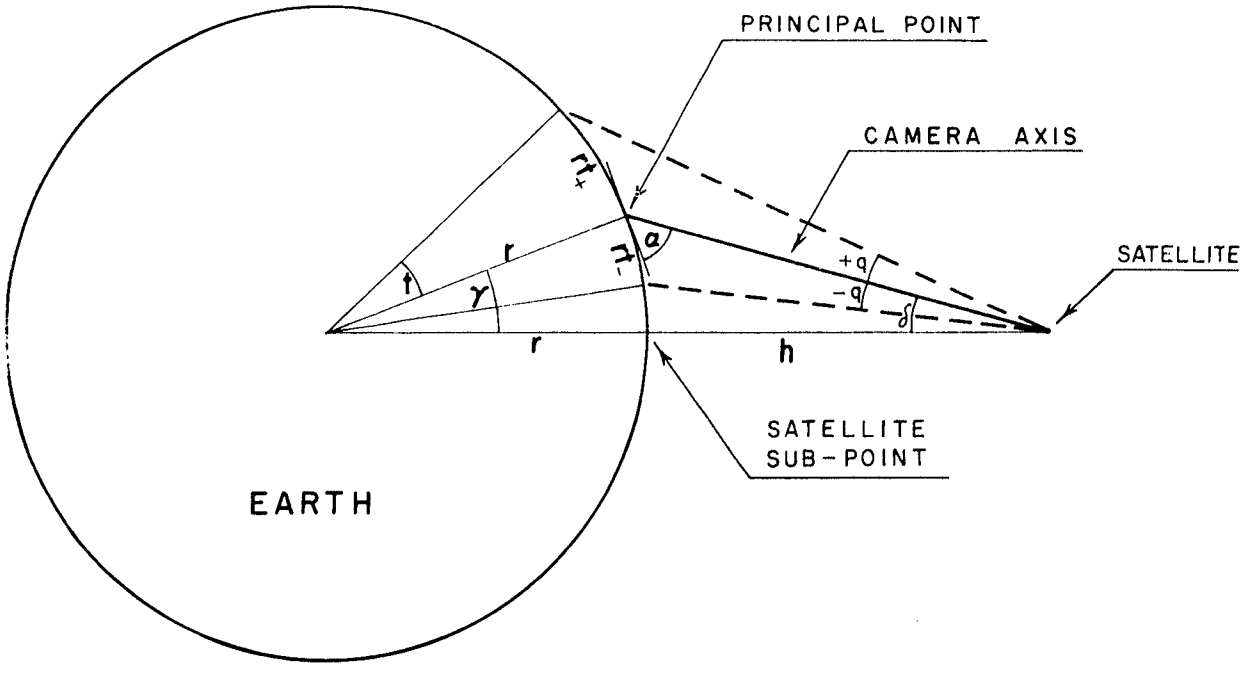

Fig. 1 Schematic of Nomenclature

r t + and r t - represent distances subtended on the earth's surface by lens angles q and -q, respectively. r is the radius of the earth and

$$t = \arcsin\left[\frac{r+h}{r}\sin(\delta+q)\right] - \arcsin\left[\frac{r+h}{r}\sin\delta\right] - q \qquad (1)$$

is the corresponding angle at the center of the earth. h is the height of the satellite and δ is nadir angle of the camera axis.

4. Computational Formulae

The fundamental assumption of the grid system is that the position of the principal point is known with respect to the subpoint. Essentially, then, the angle γ defined by these points and the center of the earth (see Fig. 1) is a constant. The angle γ may also be defined in terms of α (the elevation angle of the satellite measured from the principal point) and δ .

$$\gamma = \frac{\pi}{2} - \alpha - \delta \tag{2}$$

So

$$d\,\alpha = -\,d\,\delta \tag{3}$$

Also,

$$\cos\alpha = \left(\frac{r+h}{r}\right) \sin\delta \tag{4}$$

So, with substitution from Eq. (3),

$$\left(\frac{d\,\delta}{d\,h}\right)_{\gamma} = \frac{\frac{1}{r}\sin\delta}{\sin\alpha - \left(\frac{r+h}{r}\right)\cos\delta} \tag{5}$$

From Eq. (1)

$$\frac{\partial t}{\partial h} = \frac{\frac{1}{r}\sin(\delta+q)}{\sqrt{1-\left(\frac{r+h}{r}\right)^2 \sin^2(\delta+q)}} - \frac{\frac{1}{r}\sin\delta}{\sqrt{1-\left(\frac{r+h}{r}\right)^2 \sin^2\delta}} \tag{6}$$

and

$$\frac{\partial t}{\partial \delta} = \frac{\left(\frac{r+h}{r}\right)\cos(\delta+q)}{\sqrt{1-\left(\frac{r+h}{r}\right)^2 \sin^2(\delta+q)}} - \frac{\left(\frac{r+h}{r}\right)\cos\delta}{\sqrt{1-\left(\frac{r+h}{r}\right)^2 \sin^2}} \tag{7}$$

Finally, the errors committed in the determination of the angles t by error in choice of h and δ are, respectively,

$$\frac{dt}{dh} = \frac{\partial t}{\partial h} + \frac{\partial t}{\partial \delta} \left(\frac{d\delta}{dh}\right)_{\gamma} \tag{8}$$

and

$$\frac{dt}{d\delta} = \frac{\partial t}{\partial \delta} + \frac{\frac{\partial t}{\partial h}}{\left(\frac{d\delta}{dh}\right)_{\gamma}} \tag{9}$$

These equations, with appropriate substitutions, may be used to determine the maximum intervals d h and d δ leading to acceptable values of d t.

5 Error Determinations

5.1 Height Errors

The relative position error 1/t dt/dh was computed for a range of satellite heights h, nadir angles δ, and lens angles $\pm$ q. Figures 2 through 6 show the results of the computations. In each case the solid curves represent computational results, and the dashed curves are the envelopes representing errors of $\pm$ 15 miles on the surface of the earth for 25-mile errors in satellite height. Two vertical lines are drawn at $\pm$ 0.2 per cent error per mile increase of h (these represent the $\pm$ 5 per cent for a 25-mile height error previously discussed).

Computed (solid) curves that fall inside the outermost limit satisfy the accuracy criteria.

From the samples chosen, it would appear that the location of objects on the earth's surface can be accomplished to the desired

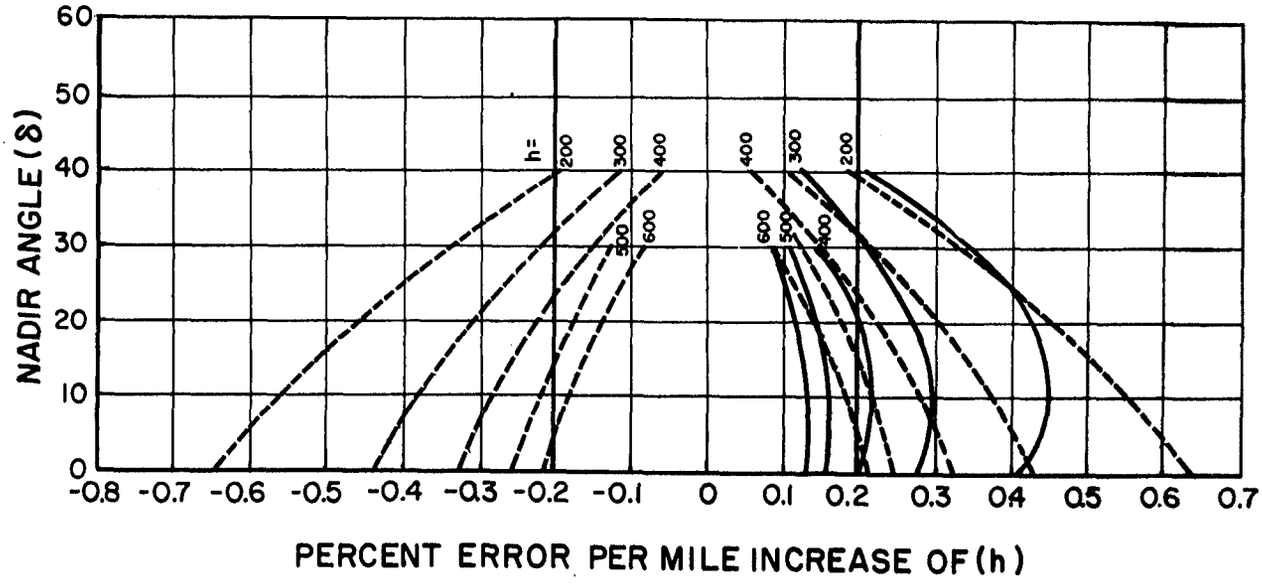

Fig. 2 Location Errors for Lens Angle of + 25°

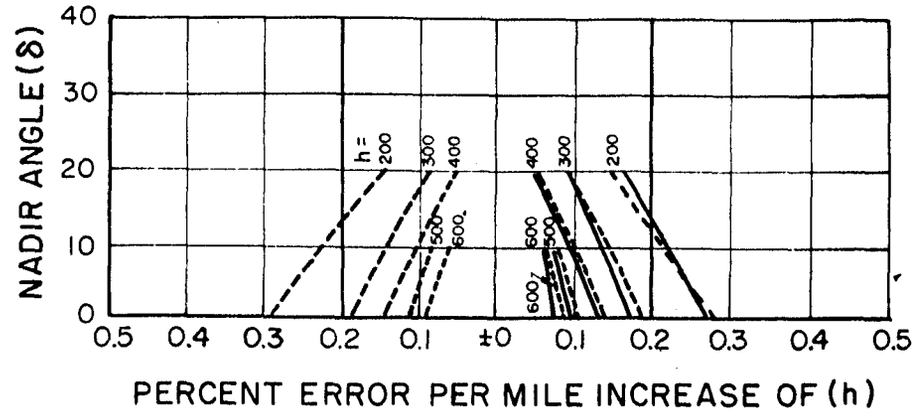

Fig. 3 Location Errors for Lens Angle of + 45°

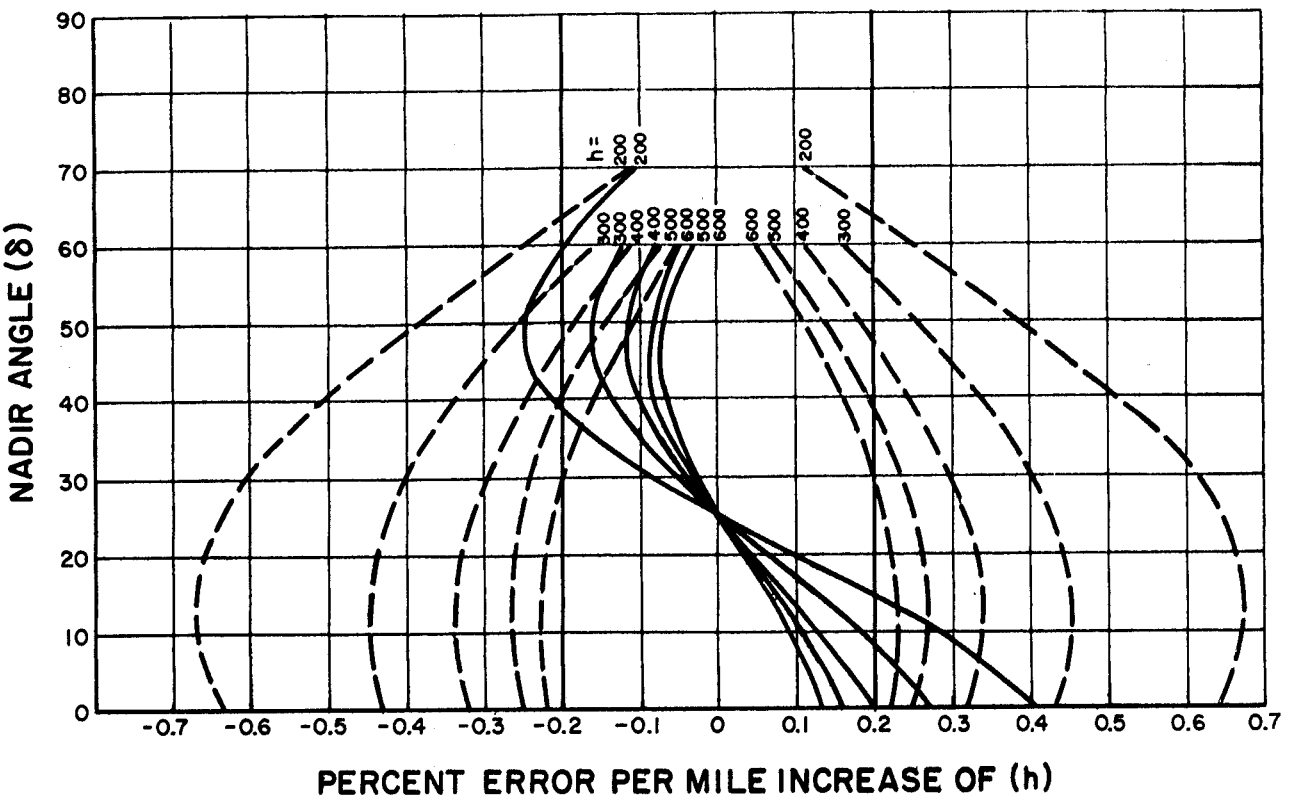

Fig. 4 Location Errors for Lens Angle of - 25°

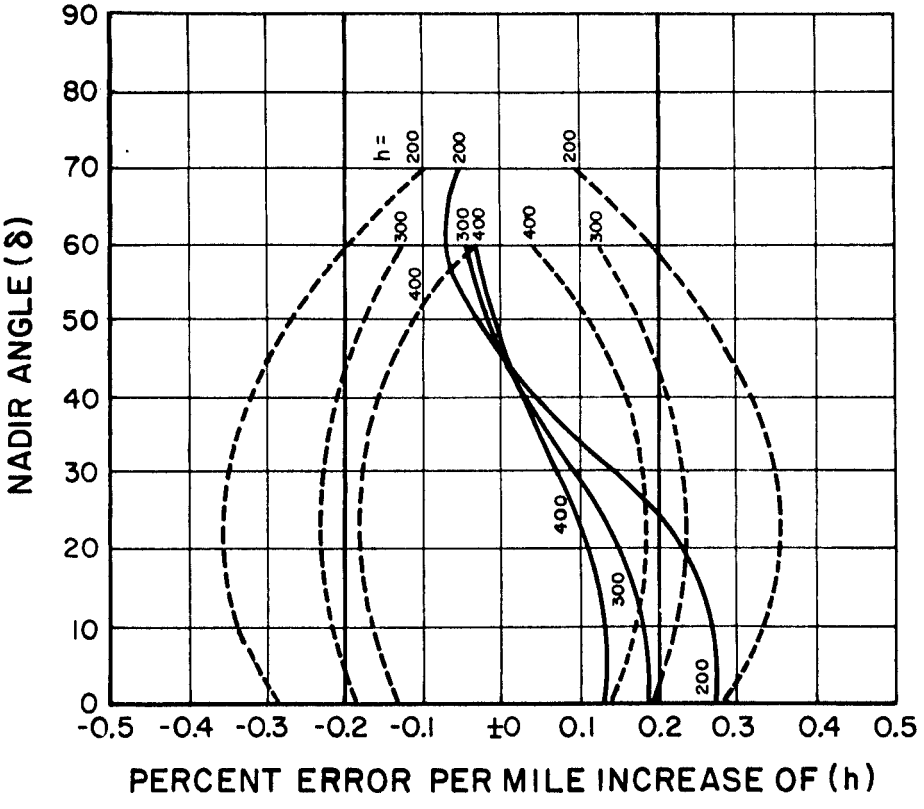

Fig. 5 Location Errors for Lens Angle of - 45°

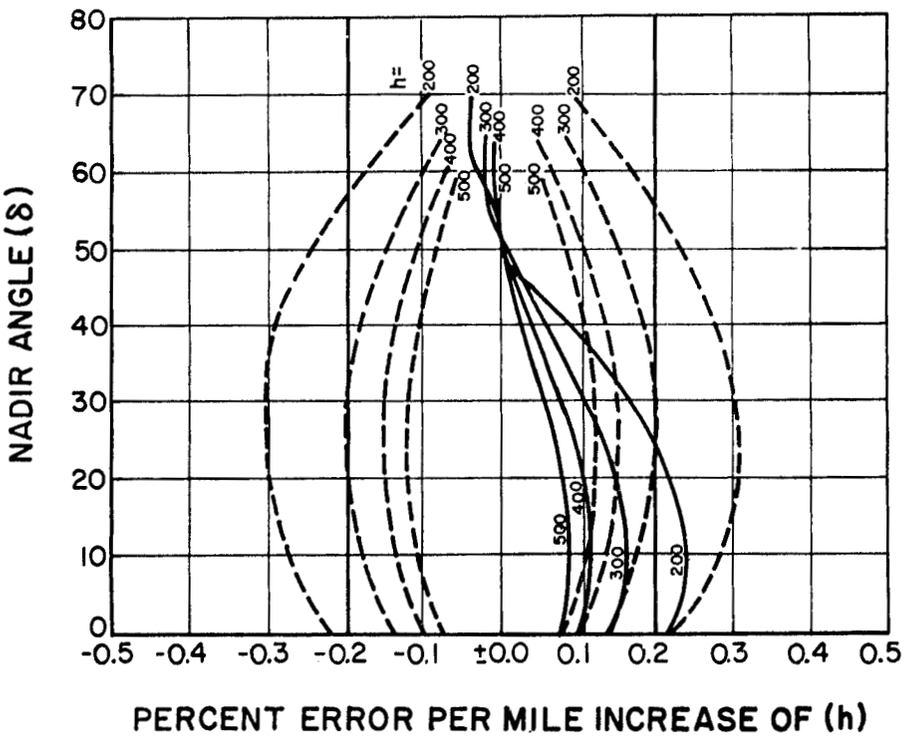

Fig. 6 Location Errors for Lens Angle of - 52.5°

accuracy with height errors of 25 miles or less. At heights above 500 miles, height errors of 50 miles are permissible.

Closer inspection of Fig. 2 (lens angle = + 25°) shows that the arbitrary limits are exceeded at a satellite elevation of 200 miles with $27^{\circ} < \delta < 40^{\circ}$. Figure 3 shows such passing of the limits at 200 miles with $6^{\circ} < \delta < 14^{\circ}$. Perigee is expected at about 300 miles, so that these errors will be found only in limited parts of the picture at improbable satellite heights.

5.2 Nadir Angle Errors

The relative position error $1/t\ dt/d\delta$ was computed for a similar range of satellite heights h, nadir angles δ, and lens angles. Figures 7 through 12 present the results of the computations. On each of the curves two sets of error limits are shown, one corresponding to a 5 per cent position error for a 5° error in the nadir angle δ, the other corresponding to the same error for a 10° error in δ.

In general, it is found that satisfactory intervals of δ are 5°, or even 10° for small values of δ. Toward the horizon, position errors increase abruptly, extending far beyond acceptable limits. Fortunately, little meteorological information can be recognized in these regions, so that these errors are not important.

6. Conclusion

On the basis of this analysis and empirical trials, it was decided to base the grid library on height intervals of 25 miles from 200 to 500 miles height, with 50-mile intervals above. Nadir angle intervals of 5° were used throughout.

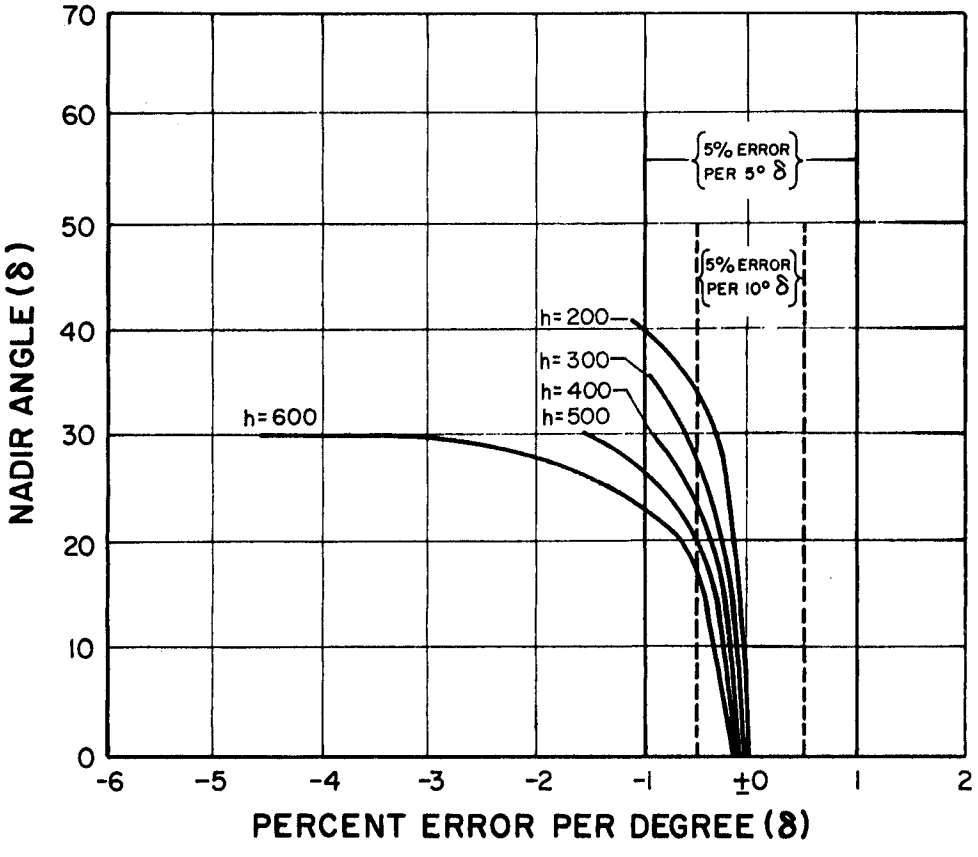

Fig. 7 Location Errors for Lens Angle of + 30°

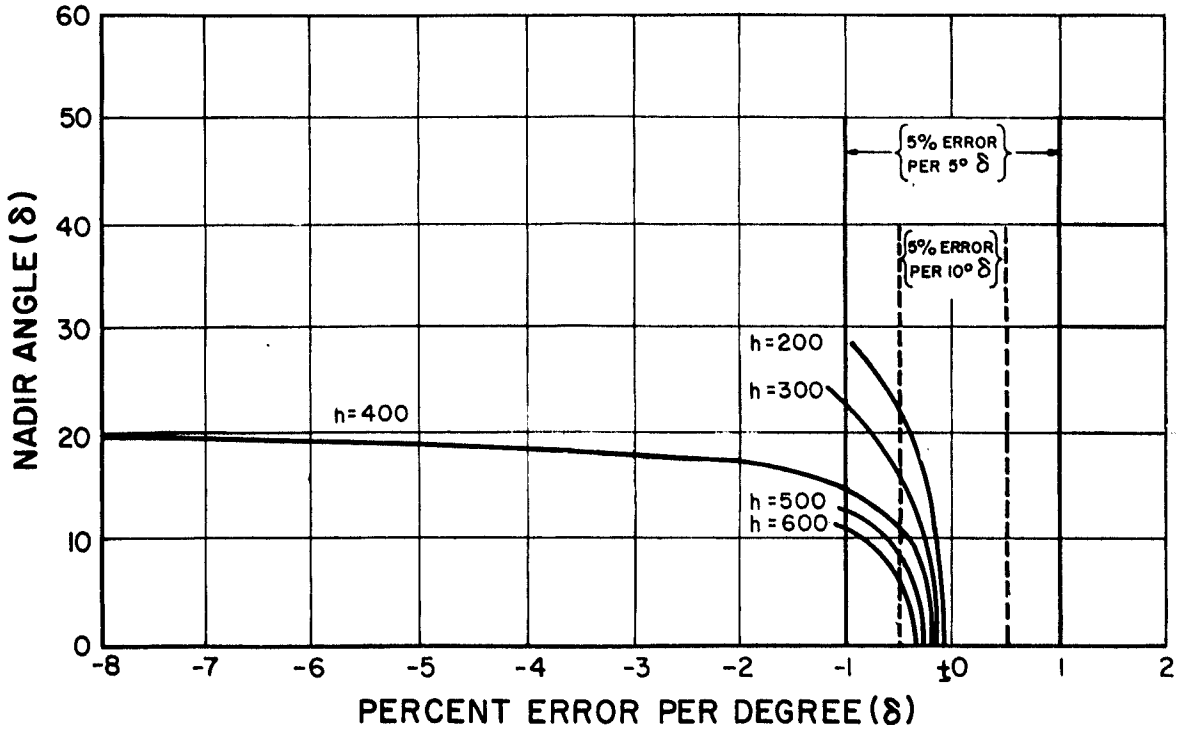

Fig. 8 Location Errors for Lens Angle of + 45°

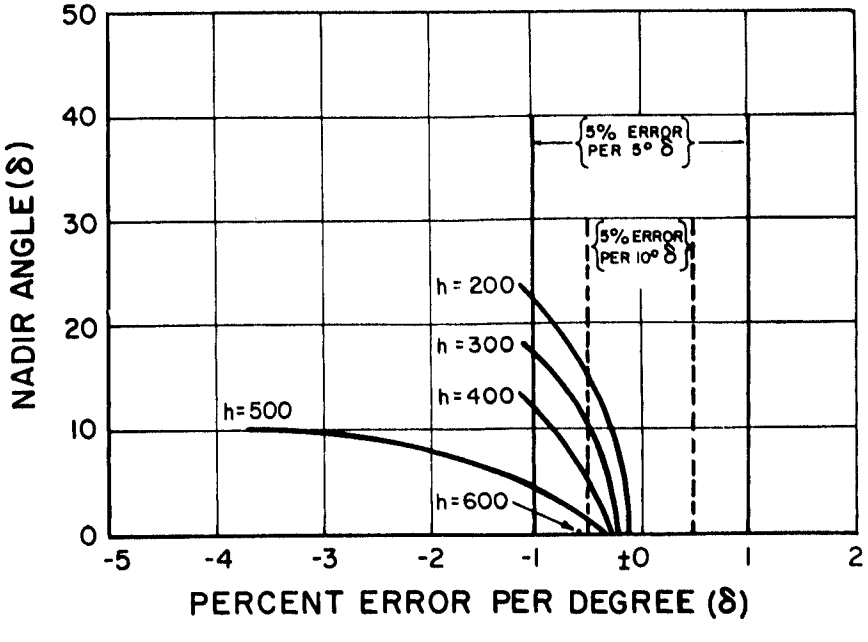

Fig. 9 Location Errors for Lens Angle of + 52.5°

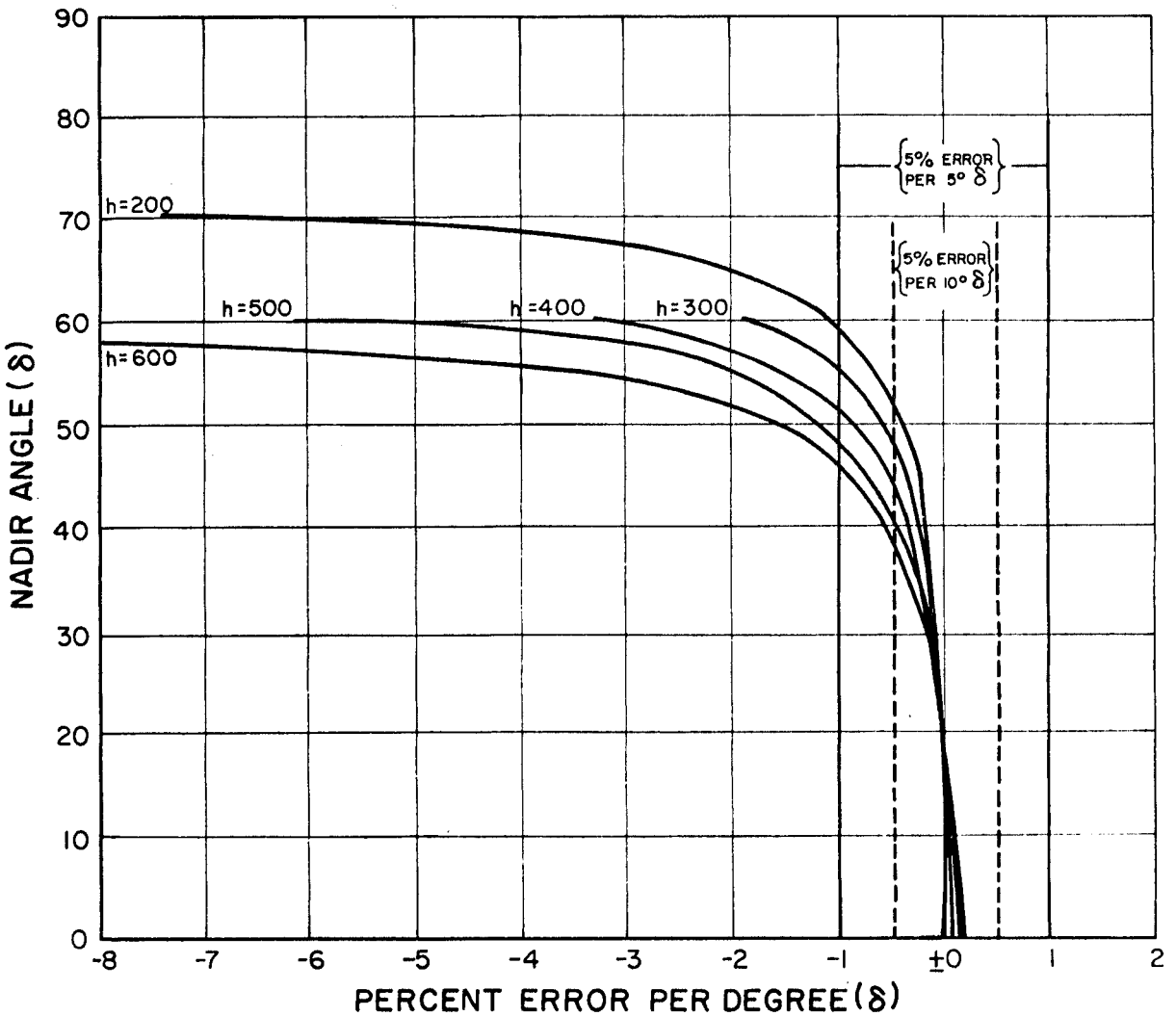

Fig. 10 Location Errors for Lens Angle of - 30°

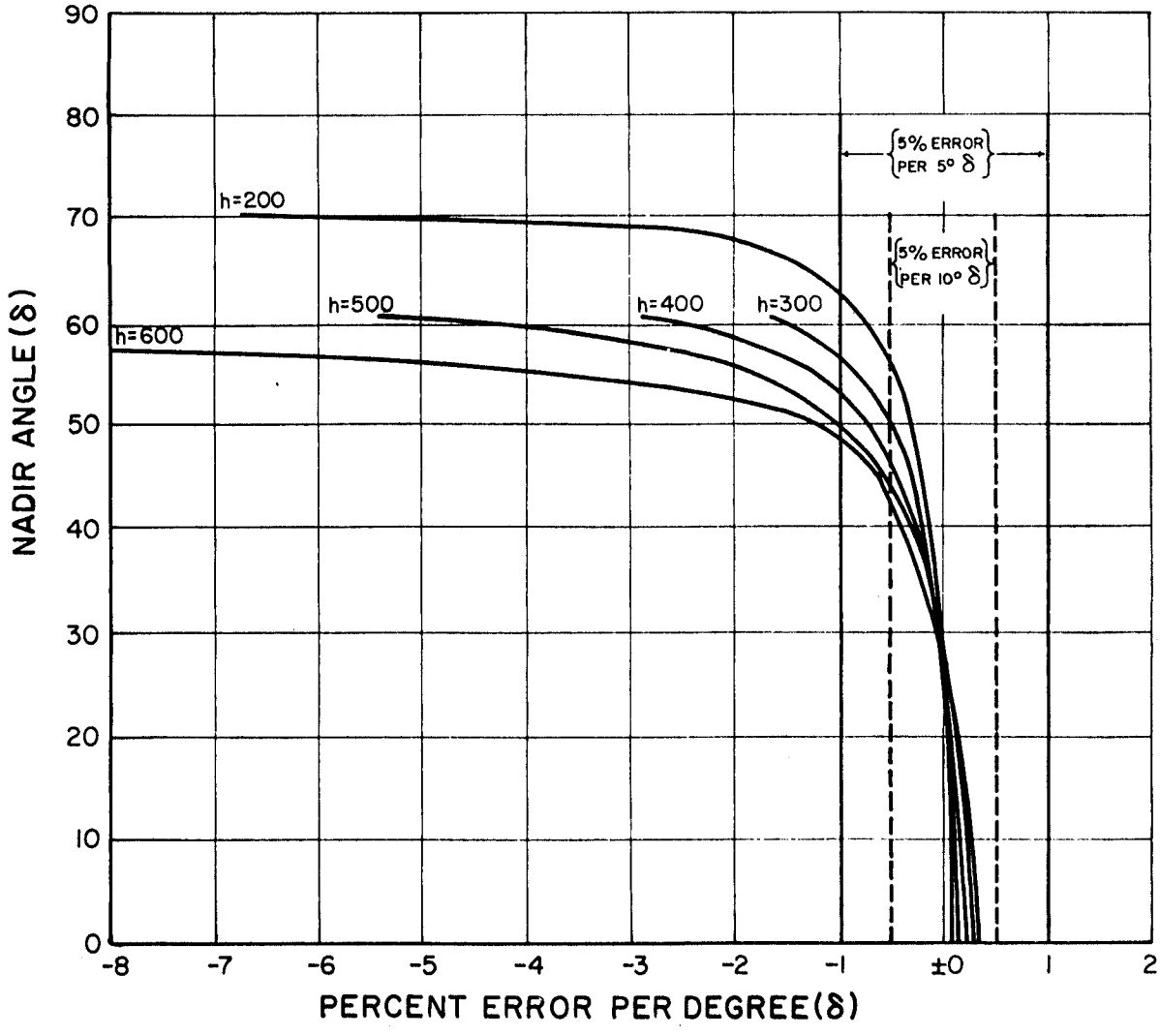

Fig. 11 Location Errors for Lens Angle of - 45°

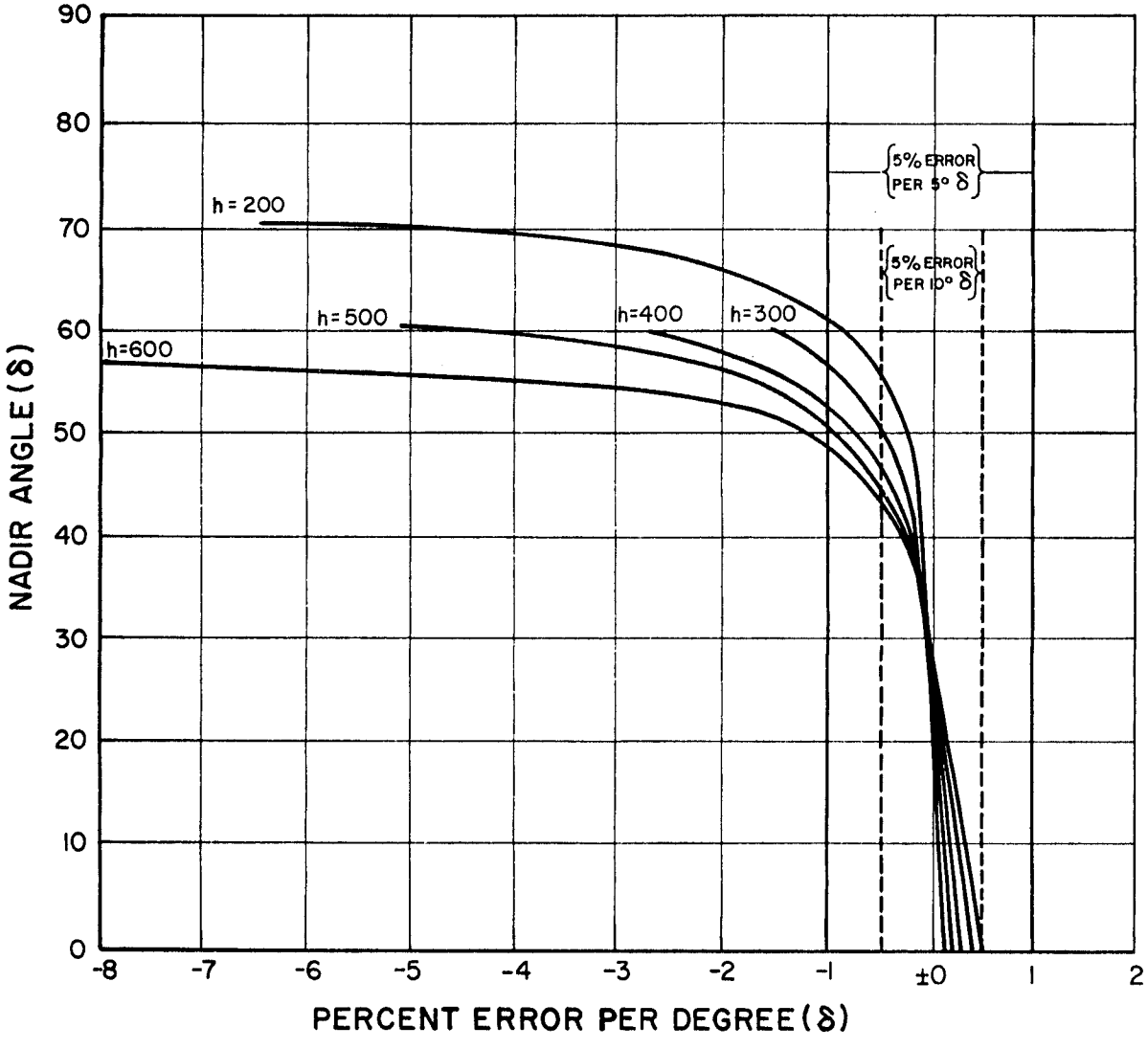

Fig. 12 Location Errors for Lens Angle of - 52.5°

APPENDIX C

MAPPING

1. Introduction

In order to locate observed cloud areas and indicate interrelations, they must be represented on a map of some sort. The map (or maps) must adequately cover the area to be scanned by the satellite. Various requirements are put on the maps by the nature of the use for which they are intended.

2. Conformality

The cloud material is to be transferred from uniform but unoriented "transfer" grids to the maps by tracing or other direct copying. The random orientation of the transfer grid imposes the requirement of conformality.

A conformal map is one that preserves the shape of infinitesimal areas. Here, with a single picture, we are covering areas that are far from infinitesimal. It is thus necessary to verify carefully the applicability of any given map projection, particularly with respect to its macroscopic conformality.

One measure of the rotability of the rectangular transfer grid is the arc-to-chord correction on the map. In Fig. 1, if a straight line is drawn on the map between the principal point and the position of an arbitrary point, it will in general not coincide with the great circle path between the points. (An exception is the gnomonic projection which, however, departs seriously from conformality in that scale is a function of direction.)

A properly drawn transfer grid, prepared on the basis of a macroscopic conformality, will place the point on the tangent to the great circle at the principal point. The angle between the chord and the

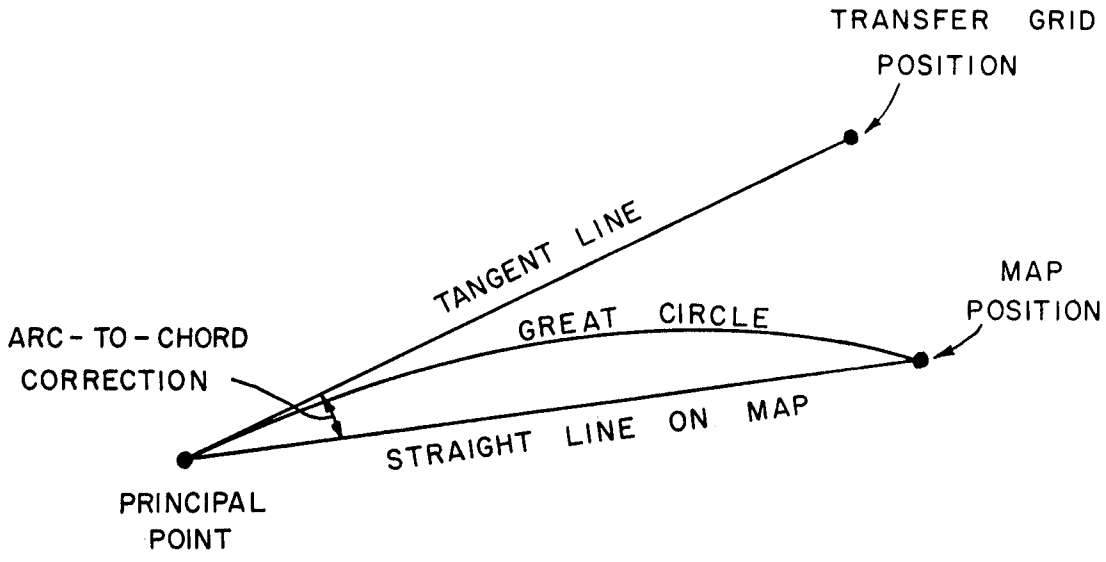

Fig. 1 Arc-to-Chord Correction

arc at the principal point is a measure of the acceptability of the projection.

A limit to the acceptable arc-to-chord correction is found in the acceptable error in location. A suitable criterion for the present purpose is an error of 50 miles at 1000-mile radius from the principal point, or 0.05 radian.

2.1 Mercator Map

The arc-to-chord correction for the Mercator map is approximately given by

$$C = \frac{\lambda_2 - \lambda_1}{2} \sin \frac{\phi_2 + \phi_1}{2} \tag{1}$$

where λ_1 and λ_2 are the longitudes of the principal point and arbitrary point, ϕ_1 and ϕ_2, their latitudes. The correction has its maximum

when the two points are at the same latitude. At a distance of 1000 miles,

$$\frac{\lambda_2 - \lambda_1}{2} = \frac{1000}{2 \times 4000 \cos\phi} \text{ radians,}$$

whence $C = 1/8 \tan\phi$ radians. The 0.05 radian limit is reached at $\phi = \text{arc tan } 0.4 = 22^\circ$. Thus the Mercator chart passes this test in the equatorial belt to about 20° latitude.

2.2 Lambert Conformal Projection

Here the arc-to-chord correction is

$$C = \frac{\lambda_2 - \lambda_1}{2} (\sin\phi_3 - \sin\phi_0) \tag{2}$$

where ϕ_0 is (approximately) the parallel midway between standard parallels, $\phi_3 = 2\phi_1 + \phi_2 / 3$, and λ_2, λ_1, ϕ_2, ϕ_1, are as before. Once again the maximum correction is achieved along a parallel, so $\phi_1 = \phi_2 = \phi_3 = \phi$. The formula becomes, for the conditions as before,

$$C = 1/8 \left(\tan\phi - \frac{\sin\phi_o}{\cos\phi}\right) \text{ radians} \tag{3}$$

Let us choose a midlatitude ϕ_0 so that $C = .05$ radian at $\phi = 18^\circ$, allowing a 4° overlap of validity between Mercator and Lambert maps. Then $\phi_o = 45^\circ$. The other extreme of validity is found at 63°. This coverage would be just adequate for a projected 47.7° orbit.

2.3 Transverse Mercator Map

Another possible projection is the transverse Mercator centered

on the orbital inclination. The conformal properties remain the same as those of the conventional equatorial Mercator, being acceptable within about 1400 miles of the great circle chosen as the "equator". A band of 2800 miles width, oriented along the satellite track, would be adequate for most circumstances.

3. Constancy of Scale

Another measure of the suitability of a map for our purposes is the constancy of scale over the part of the map to be used. For conformal maps symmetrical about the pole, the maximum rate of scale-change occurs along the meridians. Thus, the scale-change measure is in a sense orthogonal to the arc-to-tangent correction, which is at a maximum along parallels.

3.1 Mercator Map

The Mercator map, in the interests of preserving conformality and rumb-line straightness, shows extreme expansion of scale as the poles are approached. Only near the equator is there a reasonable constancy of scale. Figure 2 shows the rapid expansion of the Mercator scale above 20° latitude.

3.2 Lambert Conformal Projection

Here there are two standard latitudes, each true to scale. In between these latitudes the scale is somewhat shrunken; outside, it increases rapidly. Figure 2 shows the scale variation for a Lambert Conformal Map with standard parallels chosen to permit slight overlap with the Mercator map in its region of validity. Even though the overlap is slight, it will be seen that reasonable scale accuracy does not extend to latitudes greater than about $\pm 63^{\circ}$.

3.3 Transverse Mercator Map

Here the scale remains accurate near the great circle

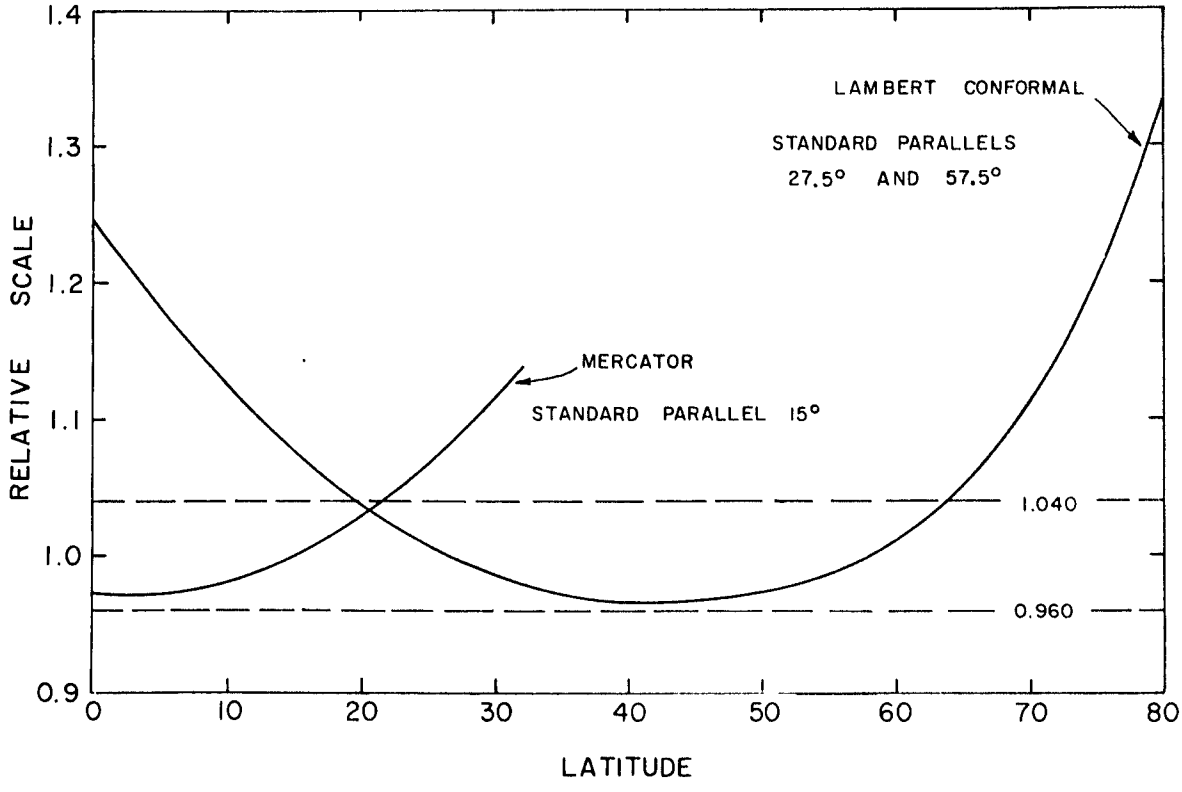

Fig. 2 Relative Scales of Selected Maps

chosen as the tangent circle, remaining within 4 per cent to a distance of about 1450 miles on either side of the circle. The benefits of the use of such a projection for satellite meteorological purposes is apparent. The problem becomes one of assuring that the satellite view will stay within the acceptable limits of the projection.

4. Map Selection

The transverse Mercator has been selected for use; very successful preliminary results with the Atlas 11C photographs using this map testify to its suitability for depicting satellite-obtained information. The map to be used was computed around a great circle inclined 51° to the equator; this compormise inclination distributes and diminishes slight orbital inclination of 49.4°.

The transverse Mercator maps are printed in three sections, at a scale of 1:7,500,000. They are arranged with dual marginal notations, so that one map can be used in the vicinity of either the southernmost or northermost portion of an orbit north of the equator, and merely needs be rotated 180° to be used south of the equator; the third chart is usable in either of two orientations for the southbound leg. Although there is a 20 per cent overlap endwide, the three maps may be arranged in an endless chain, if desired, though the satellite will progress further and further ahead of the great circle as the process continues. Parallel maps of the same variety cannot be joined, but pictures from two or possibly three orbits may be plotted with reasonable accuracy on the same map, provided that the camera axis remains along the spin axis.

5. Map Preparation

The computational formulae [21] which generate the transverse Mercator map (note: the Mercator is <u>not</u> a projection) were programmed for

$$y = \frac{a}{2} \log_e \frac{(1 + \sin\alpha \sin\phi + \cos\alpha \cos\phi \sin\lambda)}{(1 - \sin\alpha \sin\phi - \cos\alpha \cos\phi \sin\lambda)}$$

$$x = a \arctan\left(\frac{\sin\alpha \cos\phi \sin\lambda - \cos\alpha \sin\phi}{\cos\phi \cos\lambda}\right) \qquad (4)$$

x and y are coordinates along and perpendicular to the generating great circles, respectively. A is the radius of the earth, appropriately scaled to the map; α is the inclination of the great circle of tangency with respect to the equator; and ϕ and λ are latitude and longitude respectively.

Coordinates were computed for the intersection of 5° latitude and longitude lines. These were plotted to very large scale on graph paper.

Photographic reduction to the appropriate scale was performed and the maps were reproduced by offset printing on stock suitable for copying of the meteorological material written on it by Ozalid reproduction. The maps are printed in a dark yellow that does not interfere with black inscription, but which reproduces well by Ozalid and facsimile.

Blank page retained for pagination

APPENDIX D

INTERPRETIVE ABBREVIATED PLAIN LANGUAGE CODE

1. Preamble

$Y\ Y\ G\ G\ G_m\ G_m\ G_s\ G_s$:	Greenwich date and time of the first picture of the transmission, to the nearest second. For use at Central only, to be deleted in subsequent relays.
NN:	Orbit number for day described. (Central only)
XXXXX	Symbolic word identifier for coded message.
$Y\ Y\ G\ G\ G_T$:	Greenwich date, whole hour and tenths of the midpoint picture of a complete transmission.

2. Plain Language Code Form

SCAN: This designator, to be used only once in the message, indicates that the boundaries enclosing the entire area covered by the sequence of photographs will follow immediately. The form, describing the latitudes and longitudes (2 or 3 digits to the nearest whole degree) of all points necessary to adequately describe the area, is as follows:

37N63W 4398 32102 2568 etc.

Always list points so that area outlined remains to left of the line being generated.

Note: N, S, E, W designators are obmitted after the first group unless the bounding line crosses the equator, the Greenwich meridian, or the International Date Line in which case the new designator is stated in one group only.

CLOUD: This designator, to be used only once in the message, indicates that all which follows is cloud information; the form of each cloud area description group follows; one space will be transmitted between each character, and two spaces between each group.

$$N\ I\ f_I\ s\ w\ i\ f_i\ L$$

N--Cloud coverage of the particular type and within the particular area to be described: CLR - clear; SCTD - scattered; BRKN - broken; OVC - overcast.

Note: CLR will be used to describe a clear region within a cloud area; in general, any area within the "SCAN" region for which further data are not transmitted will be assumed "clear". See Note A.

I---Identification of an area of reflectivity:

a. Cloud genus (see "Contractions"), also species if identifiable (see Note B.); if could unknown, UNK will be entered.

b. Synoptic feature (see "Contractions"); to be described at this point only it its bounds coincide with those of cloud areas; otherwise, use a separate group, and code (N) as INTPRT. If cause of reflectivity is unidentifiable, code (I) as UNR.

f_I--Confidence factor; Whenever a subjective interpretation of the data is made, a factor expressing the confidence of the analyst in this interpretation is also indicated. Since all identifications including cloud genus and synoptic events are subjective interpretations, all such identifications must be followed by a confidence factor:

H--high confidence

M—medium confidence

L--low confidence

Note: When (a) and (b) of I are used in the same cloud group, each must be followed by f_I when appropriate.

s--Shape: Since all iregularly shaped areas are best described on a point-to-point basis, the only time this character will be used is to describe cloud areas which are roughly circular. In this case, CIR will be entered, followed by the latitude and longitude of its center, and the radius in nautical miles, that is, CIR 30N 72W 140. See Note A.

w--Width: Used only when "line" or "band" is described by I, in which case w is the average width of the band in nautical miles. See Note A.

i---Intensity: This character will have limited usefulness, probably confined to convective bands where an estimate of the intensity of the weather (not of the reflectivity, necessarily) can be made: WK - weak, MOD - moderate, STG - strong.

f_i-- Confidence factor: Used only in conjunction with "i" to express the confidence of the analyst in his intensity estimate.

L--Location: Latitude and longitude, to the nearest whole degree, of each point necessary to adequately describe the boundaries of the particular cloud area, if straight lines are drawn between all points so specified. Use

same method as that used to describe " SCAN" area. Not used for circular areas. When the latitude is $<10^{o}$, always precede single digit with a zero to avoid ambiguity.

Note: "X" used immediately (without an intervening space) after a location specification indicates that the boundary being described (or an extrapolation of it) intersects with (or begins at) and becomes coincident with "SCAN" or some other previously described boundary. See Note A.

Note A: A lone exception to the general descriptions for the "N", "s", "w" characters occurs when "I" is specified, "CLD STS". Clouds streets require the following descriptions:

- N - average cloud coverage within the bands only
- I - CLD STS
- s - Spacing: average space between center lines of adjacent streets, in nautical miles, measured normal to the lines.
- w - Width: average width of the bands in nautical miles.
- o - orientation: (additional character) average orientation of the lines as follows:

N	- north-south orientation
NNE	- north-northeast - south southwest
NE	- northeast - southwest
ENE	- east northeast - west-southwest
E	- east-west
ESE	- east-southeast - west-northwest
SE	- southeast - northwest
SSE	- south southeast - north northwest

L - location: limits of area enclosing streets, with two edges describing center lines of outermost bands in the area.

In the case where cloud streets are curved or where the outermost streets cannot be described adequately by L, insert an additional L group here which defines one typical street within the area.

Depending on the quality of the data, and its subsequent analysis, any or all of the f_I, s, w, i, and f_i characters may be omitted from any cloud group. A minimal group would thus consist of NIL (appropriately enough).

3 Contractions

Cloud Genera:

cirrus	CI
cirrocumulus	CC
cirrostratus	CS
altocumulus	AC
altostratus	AS
nimbostratus	NS
stratocumulus	SC
stratus	ST
cumulus	CU
cumulonimbus	CB

Cloud Forms:

cumuliform	CUFM
stratiform	STFM
mixed cumuliform stratiform	CUSTFM

Objective Synoptic Features (no confidence factor required):

cloud-genus unknown	UNK
reflective area - cause unknown	UNR
line	LN
band	BD
vortex	VTX
cloud streets	CLD STS

Subjective Synoptic Features (confidence factor required):

streets (use with cloud genus)	STS
front	FNT
squall line	SQL LN
frontal wave	FNTL WV
easterly wave	ELY WV
hurricane	HRCN
tropical storm	TROP STM
intertropical convergence	ITC
center	CTR
sector	SCTR
snow cover	SNW CVR

Descriptive Adjectives:

convective	CVTV
warm	WM
cold	CD
tropical	TROP
extra-tropical	XTROP
frontal	FNTL
convergence	CVGC

Note B: If cloud species are identifiable, and if there is time and/or necessity for their specification, their abbreviation, like those of the genera, will conform to those listed in the International Cloud Atlas, published by the World Meteorological Organization.

Blank page retained for pagination

APPENDIX E

A MANUAL OF EMERGENCY COMPUTATION PROCEDURES

1. Introduction

There is a possibility that, even with successful launch and telemetering contacts, it may be difficult to establish the attitude of a spin-stabilized satellite in inertial space, particularly in early orbits. If successful pictures are received from the satellite, it may be possible to reconstruct the attitude information necessary for picture location. The basic ingredients are reasonably good orbital information and pictures of sufficient quality to distinguish the horizon and/or landmarks. Under certain circumstances, successful operation of the sun-position sensors is also predicated. Methods are presented here for such auxiliary computations of attitude parameters. Methods are also presented for transformation of attitude parameters in case those provided are not directly suitable for the procedures of the program.

A secondary use of the methods covered in this appendix will be to verify attitude information provided from the central computation center. In particular they may serve to assist in resolving problems resulting from inaccuracy of the timing of picture taking.

Unfortunately the computational procedure involved in establishing actual orbital location from landmarks seen in the pictures is far too complicated mathematically to be embarked upon on a real time gasis with desk calculators. In a few cases it may be possible to establish the position along a known orbit if landmarks are available in appropriate parts of the picture. (On this regard, see also Chapter IV, Section 2.)

2.1 Situations Covered

The normal operating procedures of the satellite support

activities will provide, at each data-acquisition station, sufficient information on the position and attitude of the satellite to permit picture location. Ideally, the information provided will give, at equal increments of time, the geographical position of the satellite subpoint and the position of the "principal point", which is defined as the intersection of the camera axis with the surface of the earth. Also required are satellite height and nadir angle, defined as the angle between the optical axis of the camera and the vertical through the satellite. Additional information may be provided on the azimuth of the line connecting the satellite subpoint and the principal point on the earth's surface. This angle may be measured at either the subpoint or the principal point (In general the azimuth value' will be somewhat different depending on where it is measured due to the convergence of the meridians.)

A fiarly complex system is also provided to determine the rotary position of the satellite around the camera axis when no horizon is visible in the picture to establish the orientation. A series of sun-seeking photocells indicate the angle between a fiducial direction in the satellite image plane and the projection of the sun line on this plane. The "sun position" which is the orientation of the sun-line projection in this plane with respect to the line in the plane defined by the intersection with a vertical plane containing the camera axis (or in the case of a completely vertical satellite, a north-south oriented vertical plane) can then be provided from a central computing source.

Parts of this information may not be available either because of communication failures or because of component failures in the system. It is also possible that the data may not be provided in the most convenient form for subsequent computations because of what may have been a misunderstanding in the requirements for pre-computed data.

In the succeeding sections instructions are provided for coping with any of a number of contingencies. They can also serve as a check of the consistency of data provided.

The first three cases deal with the computations that will be required to relate solar position viewed from the satellite plane to solar position viewed from the earth's surface. At the time of this writing, it has not been made clear wehther solar data will be given at the principal point, at the subpoint, or transformed to "sun position" on the satellite image plane. Accordingly, Cases I and II deal with determining the sun position in the satellite plane from solar data at the principal point and the subpoint respectively. These computations will be useful in establishing the principal line on the photograph when no horizon is visible. Case III deals with determining the azimuth of the principal line from "sun position" data. This computation will be useful in establishing the position of the principal point.

The foregoing computations require a knowledge of the nadir angle. Should the nadir angle not be available, the method of Case IV may, may be used to compute it from the photographs if the height is known and a visible horizon is present. The method of Case V may also be used to establish the nadir angle if the height and the position of the principal point with respect to the subpoint are known. Case VI provides a method for computing the distance between the subpoint and the principal point when the nadir angle and satellite height are known.

In the absence of pre-computed solar data, it is necessary to use the information contained in the navigational almanacs to obtain solar position relative to the desired point on the earth's surface. Case VII describes the computations to be performed in this event.

For each of the cases, an abbreviated presentation is made of the formulae and procedures for the computation.

2.2 Special Instructions

2.2.1 Worksheet Headings

Worksheet headings are provided in Fig. 1 and 2 to simplify the preparation for emergency calculation. To set up a computation sheet for any given case, refer to the appropriate line (s) of Figs. 1 and 2 to obtain the column headings. These column headings are then written on a standard 11" x 17" computation form and constitute a step-by-step set of instructions for performing the calculations without reference to the formulae. Note that numbers appearing in these worksheet headings without a circle refer to the value that is in the column of that number. Circled numbers denote actual numberical values to be used in the computation. In general the circled numbers are merely to be inserted in the indicated column. When they are used in actual computation, they are generally referred to by their column number

2.2.2 Four Decimal Places

Carry out all computations to four places after the decimal point and round off to three places at the end for 1/10 degree accuracy.

2.2.3 Use of the Nautical Almanac or the Air Almanac

The day of the year and the time in z time are used as entries into the Nautical Almanac or the Air Almanac to obtain the Greenwich Hour Angle (GHA) and the declination of the sun(d).

The days of the year appear in order at the top of each page in the Almanacs. The days appear in groups of three in the Nautical Almanac and singly in the Air Almanac. Look up the data wanted. Then look down the left-hand column until the appropriate z time is reached which for present purposes is denoted as "GMT" in the Almanacs.

CASE I

DETERMINATION OF SUN POSITION (b) FROM PRINCIPAL POINT DATA $\tan b = \dfrac{\sin(\phi - A)}{\tan E \cos\psi - \cos(\phi - A)\sin\psi}$

COLUMN#	1	2	3	4	5	6	7	8	9	10	11	12	13	14	15	16	17	
OPERATION	ENTER E	ENTER ψ	ENTER ϕ	ENTER A	$(\phi - A)$ 3-4	SIN 5	COS 5	SIN 2	COS 2	TAN 1	9 x 10	7 x 8	11-12	$\frac{6}{13}$	$\frac{11}{8}$	(a) $0° < a < 90°$ $\cos^{-1}$ 15	(b) $\tan^{-1}$ 14	TEST LIMITS FOR (b)

CASE II

DETERMINATION OF SUN POSITION (b) FROM SUB-POINT DATA $\tan b = \dfrac{\sin(a - \theta)}{\cos(a - \theta)\cos n - \tan e \sin n}$

COLUMN#	1	2	3	4	5	6	7	8	9	10	11	12	13	14	15	16	17	
OPERATION	ENTER a	ENTER e	ENTER θ	ENTER n	1-3	SIN 5	COS 5	SIN 4	COS 4	TAN 2	7 x 9	10 x 8	11-12	$\frac{6}{13}$	$\frac{12}{9}$	(β) $0° < \beta < 90°$ $\cos^{-1}$ 15	(b) $\tan^{-1}$ 14	TEST LIMITS FOR (b)

CASE III PART 1 $(0° \le a \le 90°)$

DETERMINATION OF THE AZIMUTH OF THE PRINCIPAL LINE (θ) $\theta = a + 2\zeta$ WHERE $\zeta = \tan^{-1}\left(\dfrac{1}{\cos n \tan b}\right)$

COLUMN#	1	2	3	4	5	6	7	8	9	10	11	12	
OPERATION	ENTER n	ENTER b	ENTER a	ENTER e	ENTER 1	COS 1	TAN 2	6x7	$\frac{5}{8}$	(ζ) $\tan^{-1}$ 9 TEST LIMIT	10 + 10	(θ) 11+3	

CASE III PART 2 $(90° \le a \le n)$

DETERMINATION OF THE AZIMUTH OF THE PRINCIPAL LINE (θ) $\theta = a + \gamma + \zeta$ WHERE $\begin{cases} \gamma = \cos^{-1}(\tan e \tan n \cos\zeta) \\ \zeta = \tan^{-1}[1/(\cos n \tan b)] \end{cases}$

COLUMN#	1	2	3	4	5	6	7	8	9	10	11	12	13	14	15	16	17	18	19
OPERATION	ENTER n	ENTER b	ENTER a	ENTER e	ENTER 1	COS 1	TAN 1	TAN 2	6 x 8	$\frac{5}{9}$	(ζ) $\tan^{-1}$ 10 TEST LIMIT	TAN 4	COS 11	12x7	14 x 13	(β) $\cos^{-1}$ 14 $0° < \beta < 90°$	(γ) $\cos^{-1}$ 15 TEST LIMIT	3 + 11	(θ) 18 + 17

CASE IV

DETERMINATION OF NADIR ANGLE (n) FROM HORIZON POSITION $n = \sin^{-1}\dfrac{3437.9}{3437.9 + h} - \tan^{-1}\dfrac{H'}{254}$

COLUMN#	1	2	3	4	5	6	7	8	9	10	11	
OPERATION	ENTER 3437.9	ENTER 254	ENTER h	ENTER H	ENTER H' (FROM GRAPH)	1+3	$\frac{1}{6}$	$\sin^{-1}$ 7 BETWEEN -90° AND +90°	$\frac{5}{2}$	$\tan^{-1}$ 9 BETWEEN -90° AND +90°	(n) 8-10	

Fig. 1 Emergency Manual Worksheet Headings

CASE V — DETERMINATION OF NADIR ANGLE [n] FROM SUBPOINT AND PRINCIPAL POINT

$$\tan n = \frac{\sin(S/60)}{(h/3437.9)+1-\cos(S/60)}$$

COLUMN #	1	2	3	4	5	6	7	8	9	10	11	12	13
OPERATION	ENTER 3437.9	ENTER 60	ENTER 1	ENTER S	ENTER h	4/2	SIN 6	COS 6	5/1	3+9	10−8	7/11	(n) $\tan^{-1}$12 $0° \le n \le 180°$

CASE VI — DETERMINATION OF THE PRINCIPAL POINT TO SUBPOINT DISTANCE

$$\lambda = \sin^{-1}\{[1+(h/3437.9)\sin n]-h\} \qquad S = 60\lambda$$

COLUMN #	1	2	3	4	5	6	7	8	9	10	11
OPERATION	ENTER 3437.9	ENTER 1	ENTER h	ENTER n	3/1	5+2	SIN 4	7×6	$\sin^{-1}$8 ANGLE ≤ 90°	(λ) 9−4	(S) 60 × 10

CASE VII — DETERMINATION OF THE AZIMUTH AND ELEVATION OF THE SUN

$$\sin a \{[\cos d \sin(LHA)]/\cos e\}$$
$$\sin e \quad \sin \ell \sin d + \cos \ell \cos d \cos(LHA)$$

$$LHA = \begin{cases} GHA+L \\ \text{ie } GHA+Le \\ GHA-Lw \end{cases}$$

COLUMN #	1	2	3	4	5	6	7	8	9	10	11	12	13	14	15	16	17	18	19	20	21
OPERATION	ENTER GHA FROM ALAMANAC	ENTER d FROM ALAMANAC	ENTER L	ENTER ℓ	SIN 4	COS 4	SIN 2	COS 2	(LHA) IF Le: 1+3 Lw: 1−3	SIN 9	COS 9	5×7	8×11	6×13	SIN e 12×14	(e) $\sin^{-1}$15 $0° \le e \le 90°$	COS 16	8×10	18/17	SIN d / SIN ℓ 7/3	(a) $\sin^{-1}$19 (TEST LIMITS)

Fig. 2 Emergency Manual Worksheet Headings

Then go along horizontally to the column labeled "sun." Here is given the declination (d) and the Greenwich Hour Angle (GHA). These are entered into the computational formulae.

2.2.4 Correction for Lens Distortion

There must be a correction for the lens distortion where measurements from the picture are required. All measurements are made from the picture center. A typical graph is provided in Fig. 3 which directly converts measured distance from picture-center to the value to be used for computation.

2.2.5 Map Use

For some computations it is necessary to use a map to obtain distances, as between subpoint and principal point.

The principal point and the subpoint will be given with latitude and longtitude coordinates. Hence it is simply a matter of accurately plotting the principal point and the subpoint on a map and measuring the distance between them. Care must be taken to establish the scale of the map at the mean latitude of the line.

2.2.6 Definition of Angles

To minimize the possibility of confusion in the application of the formulae, consistent definitions of angles must be provided and adhered to rigidly. Accordingly, the positive direction of the principal line will be defined as running from the principal point to the satellite subpoint. The azimuth of the principal line is measured clockwise from (East of) North and will lie between 0° and 360°. The azimuth of the sun is also measured clockwise from North and will lie between 0° and 360°. The "sun position" will also lie between 0° and 360^{0}. The two elevation angles (satellite and sun) are measured from the plane tangent to the earth at the point of interest and lie between 0° and 90°. The

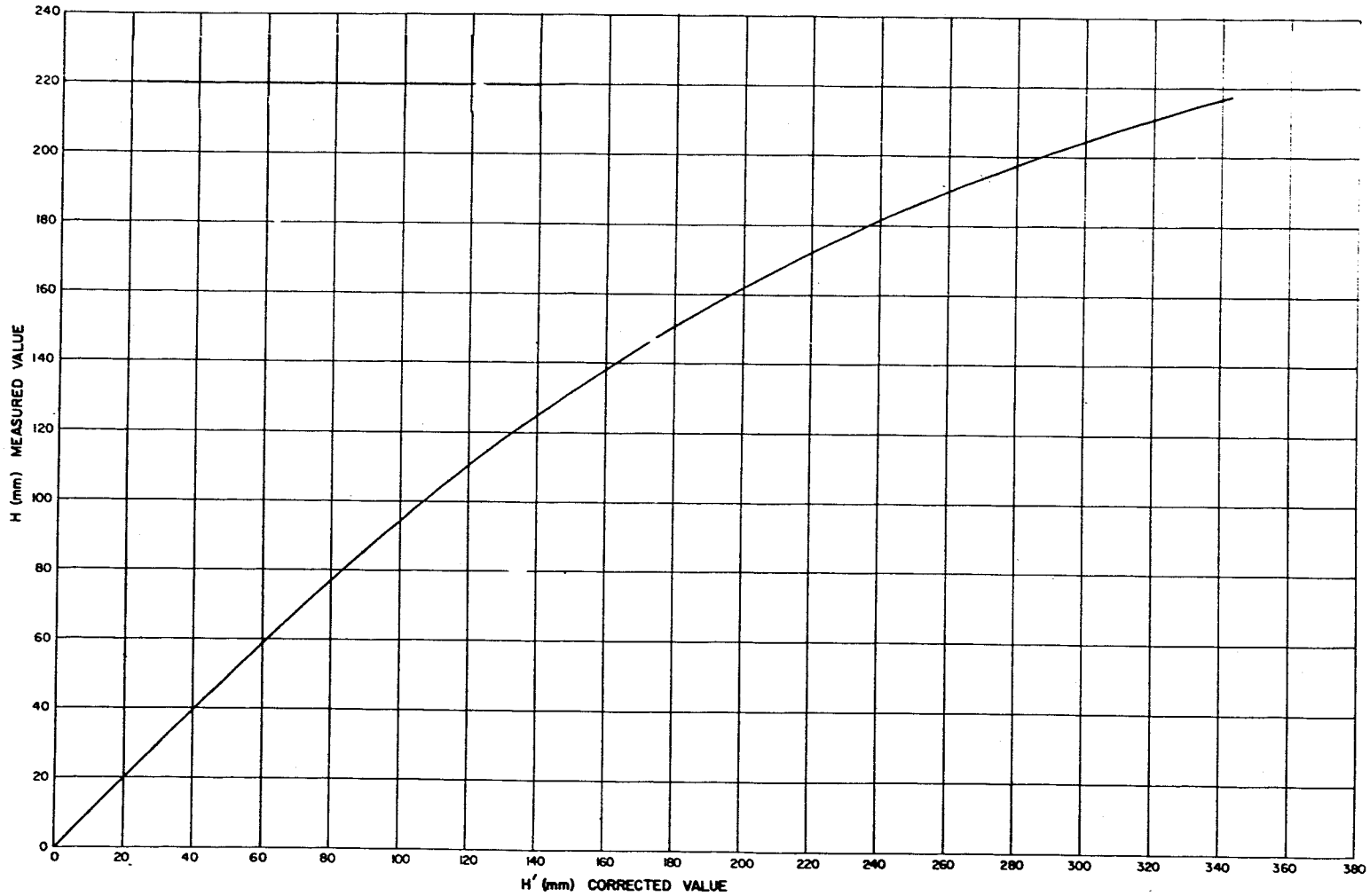

Fig. 3 Correction for Lens Distortion

tangent plane at the principal point will be referred to as the map plane, and the tangent plane at the subpoint will be referred to as the earth plane.

As noted above, all azimuth angles will lie between 0° and 360°. Any angles that are generated in the course of computing the azimuth angles should be converted into an angle between 0° and 360° by the addition or subtraction of the appropriate multiple of 360°.

The notation for the various pertinent angles are as follows:

- A Azimuth of the sun at the principal point on the map plane
- a Azimuth of the sun at the satellite subpoint on the earth plane
- E Elevation angle of the sun at the principal point from the map plane
- e Elevation angle of the sun at the satellite subpoint, from the earth plane
- ϕ Azimuth of the satellite at the principal point on the map plane
- Θ Azimuth of the satellite at the satellite subpoint on the earth plane
- ψ Elevation angle of the satellite from the principal point, from the map plane
- n Nadir angle of the satellite spin axis
- b "Sun position" or azimuth from the image of the principal line to the sun projection in the satellite plane.

3. Case I - To Obtain "Sun Position" from Solar Data at Principal Point

3.1 Given:

A, E, ϕ, and ψ

3.2 To Find

b

3.3 Computational Formula

$$\text{Tan } b = \frac{\sin(\phi - A)}{\tan E \cos\psi - \cos(\phi - A)\sin\psi} \tag{1}$$

Refer to Table 1 to determine the proper quadrant for b. In using Table 1 one must use the angle arc cos (Tan E cot ψ) when $\psi > E$. We denote this angle by α .

3.4 Procedure

Substitute in Eq. (1), using bounds as indicated, in Table 1.

4. Case II - To Obtain the "Sun Position" from the Solar Data at the Subpoint

4.1 Given

a, e, θ and n

4.2 To Find

b

4.3 Computational Formula

$$\text{Tan } b \quad \frac{\text{Sin}(a - \theta)}{\cos(a - \theta)\cos n - \tan e \sin n} \tag{2}$$

Refer to Table 2 to determine the proper quadrant for b. In using Table 2 one must use the angle arc cos (tan e tan n) when $90^{\circ} - n > e$. We denote this angle by β .

4.4 Procedure

Substitute in Eq. (2), using bounds as indicated in Table 2.

5. Case III - To Find the Azimuth of the Principal Line

5.1 Given

a, b, e, n

5.2 To Find

θ

5.3 Computational Formulae

$$\zeta = \arctan \frac{1}{\cos n \tan b} \tag{3}$$

Refer to Table 3 to determine the quadrant of ζ.

$$\gamma = \arccos (\tan e \tan n \cos \zeta) \tag{4}$$

$$\theta = a + \zeta + \gamma \tag{5}$$

If $e + n = 90^\circ$ (that is, $\tan e \tan n = 1$), Eq. (5) simplifies to:

$$\theta = a + 2\zeta$$

If $e + n > 90^\circ$ (that is, $\tan e \tan n > 1$), there is an ambiguity in the solution which cannot be resolved on the basis of the given data. However, this situation will be infrequently encountered in practice because a large enough n implies that the earth will probably not be in view of the camera. When such an event actually occurs, it is conceivable that landmarks on the photograph or adjacent nonambiguous photographs may resolve the ambiguity. As a general guide, if $90^\circ \leq b \leq 180^\circ$, $a \geq \theta \geq a - 180^\circ$ and if $180^\circ \leq b \leq 270^\circ$, $a - 180^\circ \geq \theta \geq a - 360^\circ$.

If $e + n < 90^\circ$, we again denote $\arccos (\tan e \tan n)$ by β, and refer to Table 4 to determine the quadrant of γ.

5.4 Procedure

If necessary, obtain the azimuth and elevation of the sun from the methods of Section 9. Measure b, the angle to the sunline in the picture (obtained with respect to a fiducial line on the picture from the sun-orientation sensor readout) from the principal line extension below the center of the picture (toward the subpoint). Clockwise is positive. Compute n separately from the methods of Section 6, if necessary. Substitute in the formulae above, noting the simplification if $e + n = 90^{\circ}$. Use Table 3 to determine the quadrant of γ.

6. Case IV - To Find the Nadir Angle of the Satellite from the Horizon Position

6.1 Given

h the height of the satellite (nautical miles)

H a measurement of the perpendicular distance from the center of the picture to the horizon, mm.

6.2 Computational Formula

$$n = \text{arc sin} \frac{3437.9}{3437.9 + h} - \text{arc tan} \frac{H^1}{254} \qquad (7)$$

Choose the arc sin and the arc tan to lie in the first quadrant (0° to 90°)

6.4 Procedure

Measure H in mm; it is positive when the horizon is above the center of the picture. Enter the chart (Fig. 3) to find H^1, the measurement corrected for lens distortion. Substitute in Eq. (7).

7. Case V - To Find the Nadir Angle of the Satellite from Known Subpoint and Principal Point Positions

7.1 Given

h the height of the satellite (nautical miles)

s distance between subpoint and principal point measured in nautical miles

7.2 To Find

n

7.3 The Computational Formula

$$\tan n = \frac{\sin \frac{s}{60}}{\frac{h}{3437.9} + 1 - \cos \frac{s}{60}} \qquad (8)$$

7.4 Procedure

Plot subpoint and principal point on a map; measure the distance. If it can be measured directly in degrees of latitude, omit the division by 60. Substitute in formula.

8. Case VI - To Determine the Subpoint to Principal Point Distance from the Nadir Angle

8.1 Given

h the height of the satellite (nautical miles)

n

8.2 To Find

λ the subpoint to principal point distance in degrees of latitude

8.3 The Computational Formula

$$\lambda = \text{arc sin} \left[\left(1 + \frac{h}{3437.9} \right) \sin n \right] - n \qquad (9)$$

Choose the arc sin to lie in the first quadrant (0° to 90°).

8.4 Procedure

Substitute in Eq. (9). Should the subpoint to principal point

distance be desired in nautical miles (s), multiply λ by 60.

9. Case VII - To Determine the Azimuth and Elevation of the Sun

9.1 Given

The latitude 1, and longitude L of the point on the earth's surface, the Greenwich Mean Time (z time), and the declination d and Greenwich hour angle (GHA) from the almanac

9.2 To Find

a (or A)

e (or E)

9.3 Computational Formulae

$$\sin e = \sin 1 \sin d + \cos 1 \cos d \cos (LHA) \tag{10}$$

$$\sin a = \frac{\cos d \sin (LHA)}{\cos e} \tag{11}$$

$$(LHA = L + GHA \tag{12}$$

(east longitude is positive, west longitude is negative -- that is, LHA = GHA + Le, LHA = GHA - Lw)

$0^{o} \leq e \leq 90^{o}$

$0^{o} \leq a \leq 180^{o}$ during local forenoon

$180^{o} \leq a \leq 360^{o}$ during local afternoon

Ambiguities may be resolved by reference to Table 5.

9.4 Procedure

Find the GHA and the declination in an Almanac, preferably the Air Almanac. Compute the LHA, first converting the longitude into degrees and minutes to facilitate addition $0.1^{o} = 6'$). Substitute in formulae and use Table 4 to resolve ambiguities. Note that these formulae may be used to obtain A (instead of a) and E(instead of e) if the latitude, longitude and z time refer to the principal point (instead

of the subpoint.) It would be necessary to substitute A for a and E for e on the worksheet headings, naturally.

TABLE 1

IF $\psi > E$

IF	THEN
$(\phi - A) = 0°$	$b = 360°$
$0° < (\phi - A) < \alpha$	$270° < b < 360°$
$(\phi - A) = \alpha$	$b = 270°$
$\alpha < (\phi - A) < 180°$	$180° < b < 270°$
$(\phi - A) = 180°$	$b = 180°$
$180° < (\phi - A) < 360° - \alpha$	$90° < b < 180°$
$(\phi - A) = 360° - \alpha$	$b = 90°$
$360° - \alpha < (\phi - A) < 360°$	$0 < b < 90°$
$(\phi - A) = 360°$	$b = 0°$

IF $\psi \leq E$

IF	AND $\psi < E$	AND $\psi = E$
	THEN	THEN
$(\phi - A) = 0°$	$b = 180°$	$b = 270°$
$0° < (\phi - A) < 180°$	$180° < b < 270°$	$180° < b < 270°$
$(\phi - A) = 180°$	$b = 180°$	$b = 180°$
$180° < (\phi - A) < 360°$	$90° < b < 180°$	$90° < b < 180°$
$(\phi - A) = 360°$	$b = 180°$	$b = 90°$

TABLE 2

IF(90°-n)> e

IF	THEN
$(a-\theta)=0°$	$b=0°$
$0°<(a-\theta)<\beta$	$0°<b<90°$
$(a-\theta)=\beta$	$b=90°$
$\beta<(a-\theta)<180°$	$90°<b<180°$
$(a-\theta)=180°$	$b=180°$
$180°<(a-\theta)<360°-\beta$	$180°<b<270°$
$(a-\theta)=360°-\beta$	$b=270°$
$360°-\beta<(a-\theta)<360°$	$270°<b<360°$
$(a-\theta)=360°$	$b=360°$

IF(90°-n)≤ e

IF	AND (90°-n)<e	AND(90°-n)=e
	THEN	THEN
$(a-\theta)=0$	$b=180°$	$b=90°$
$0°<(a-\theta)<180°$	$90°<b<180°$	$90°<b<180°$
$(a-\theta)=180°$	$b=180°$	$b=180°$
$180°<(a-\theta)<360°$	$180°<b<270°$	$180°<b<270°$
$(a-\theta)=360°$	$b=180°$	$b=270°$

TABLE 3

$n + e = 90°$

IF	THEN
$b = 0°$	$\zeta = 90°$
$0° < b < 90°$	$0° < \zeta < 90°$
$b = 90°$	$\zeta = 0°$
$90° < b < 180°$	$270° < \zeta < 360°$
$b = 180°$	$\zeta = 270°$
$180° < b < 270°$	$180° < \zeta < 270°$
$b = 270°$	$\zeta = 180°$
$270° < b < 360°$	$90° < \zeta < 180°$
$b = 360°$	$\zeta = 90°$

TABLE 4

$n+e < 90°$

FOR ζ

IF	THEN
$b = 0°$	$\zeta = 90°$
$0 < b < 90°$	$0° < \zeta < 90°$
$b = 90°$	$\zeta = 0°$
$90° < b < 180°$	$270° < \zeta < 360°$
$b = 180°$	$\zeta = 270°$
$180° < b < 270°$	$180° < \zeta < 270°$
$b = 270°$	$\zeta = 180°$
$270° < b < 360°$	$90° < \zeta < 180°$
$b = 360°$	$\zeta = 90°$

FOR γ

IF	THEN
$b = 0°$	$\gamma = -\zeta$
$0° < b < 90°$	$-\zeta > \gamma > -(\zeta + \beta)$
$b = 90°$	$\gamma = -(\zeta + \beta)$
$90° < b < 180°$	$-(\zeta + \beta) > \gamma > -(\zeta + 180°)$
$b = 180°$	$\gamma = -(\zeta + 180°)$
$180° < b < 270°$	$-(\zeta + 180°) > \gamma > \beta - (\zeta + 360°)$
$b = 270°$	$\gamma = \beta - (\zeta + 360°)$
$270° < b < 360°$	$\beta - (\zeta + 360°) > \gamma > -(\zeta + 360°)$
$b = 360°$	$\gamma = -(\zeta + 360°)$

TABLE 5

NORTHERN LATITUDES	LOCAL TIME: A.M.	NOON	P.M.	MIDNIGHT	SOUTHERN LATITUDES
$\sin e < \frac{\sin d}{\sin \ell}$	$0° < a < 90°$	$a = 0°$	$270° < a < 360°$	$360°$	$\sin e > \frac{\sin d}{\sin \ell}$
$\sin e = \frac{\sin d}{\sin \ell}$	$a = 90°$	UNDEFINED (DIRECTLY OVERHEAD)	$a = 270°$	UNDEFINED (DIRECTLY UNDERFOOT)	$\sin e = \frac{\sin d}{\sin \ell}$
$\sin e > \frac{\sin d}{\sin \ell}$	$90° < a < 180°$	$a = 180°$	$180° < a < 270°$	$a = 180°$	$\sin e < \frac{\sin d}{\sin \ell}$

References

1. Widger, William K., Jr., and C. N. Touart, 1957: "Utilization of Satellite Observations in Weather Analysis and Forecasting, "Bulletin of the American Meteorological Society, 38 (9), pp. 521-533.

2. Glaser, Arnold H., 1957: Meteorological Utilization of Images of the Earth's Surface Transmitted from a Satellite Vehicle, Final Report under Phase II, Contract No. AF19(604)-1589, Blue Hill Meteorological Observatory, Harvard University.

3. Dryden, W. A., 1958: Useful Satellite Orbits for Some High-Altitude Weather Observations, Scientific Report No. 1, Contract No. AF19(604)-1754, Florida State University.

4. Negley, Richard M., 1958: On the use of high-altitude cloud photographs as a basis for inferring the distribution of wind, temperature, pressure, and stability, Scientific Report No. 2, Contract No. AF19(604)-1754, Florida State University.

5. Dryden, Warren A., and Norman E. Prosser, 1959: Optimum utilization of satellite observations in weather analysis and forecasting, Final Report, Contract No. AF19(604)-1754, Florida State University

6. Ludlam, F. H., and L. I. Miller, 1959: Research on the Properties of Cloud Systems, Final Report, Contract No. AF61(514)-1292, Imperial College of Science and Technology, London, England.

7. Goody, R. M., 1954: The Physics of the Stratosphere. Cambridge University Press.

8. Godson, W. L., 1958: Meteorological Applications of Earth Satellites. Journal of The Royal Astronomical Society of Canada. Vol. 52, p. 49-56.

9. Danjon, A., 1954: The Earth as a Planet. University of Chicago Press. p. 727.

10. Goldshlak, L., Boucher, R. J., Glaser, A. H., 1959: A Summary of The State of the Art of Cloud-Weather Relationships. Allied Research Associates, Inc. Document No. ARA-594.

11. Singer, S. F., 1956: Meteorological Measurements from a Minimum Satellite Vehicle. University of Maryland.

12. Goldshlak, L., and Glaser, A. H., 1959: Development of Techniques for Meteorological Utilization of Satellite Pictures. Allied Research Associates, Inc., Document No. ARA-612.

13. Bjerknes, J., 1948: Detailed Analysis of Synoptic Weather As Observed from Photographs Taken on Two Rocket Flights over White Sands, N. M., Rand Corporation Report No. 887.

14. Singer S. F. and Wentworth, R. C., 1957: A Method for the Determination of the Vertical Ozone Distribution from a Satellite, Journal of Geophysical Research. Vol. 62, No. 2 p. 299.

15. Conover, J. H., 1959: Cloud Patterns and Related Air Motions Derived by Photography, Final Report, Contract No. AF19(604)-1589., Harvard University.

16. Kaplan, L. D., 1959: On the Inference of Atmospheric Structure from Remote Radiation Measurements, from a paper presented at the New York meeting of the Optical Society on 3 April.

17. Stakutis, V. J. and Brennan, J. X., 1956: Visibility from a Satellite at High Altitudes. "Scientific Uses of Earth Satellites". Edited by J. A. Van Allen. University of Michigan Press. p. 137.

18. Wexler H., 1954: Observing the Weather from a Satellite Vehicle. Journal of the British Interplanetary Society. Vol. 13, p. 269..

19. Franklin, William S., 1925: "An Elementary Treatise on Precision of Measurement", London: Constable & Co., Ltd., pages 7-8.

20. "Two Interim Codes for Teletype writer Transmission of Satellite Cloud Data," United States Weather Bureau Meteorological Satellite Section, 1959.

21. Deetz, Charles H. and Adams, Oscar S., 1945: "Elements of Map Projection", Coast and Geodetic Survey, Special Publication No. 68, 5th ed..

22. Möller, F., 1959: Measurements of atmospheric radiation by a black ball. J. Meteor., 16, pp. 87-90.

23. Houghton, H. G., 1954: On the annual heat balance of the Northern Hemisphere. J. Meteor., 11, pp. 1-9.

24. London, J., 1957: A study of the atmospheric heat balance. Final report, Contract AF19(122)-165, College of Engineering, New York University.

25. Murgatroyd, R. J., et. al., 1955: Some Recent Measurements of Humidity from Aircraft Up to Heights of About 50,000 ft. over Southern England. The Quarterly Journal of the Royal Meteorological Society. Vol. 81, No. 350. p.-533-37.

26. Kaplan, L. D., 1952: On the Pressure Dependence of Radiative Heat Transfer in the Atmosphere. Journal of Meteorology. Vol. 9, No. 1, p.--1-12.

27. Taylor, J. H. and Yates, H. W., 1957: Atmospheric Transmission in the Infrared. Journal of the Optical Society of America. Vol. 48, .

28. Kaplan, L. D. A Method for Calculation of Infrared Flux. Rossby Memorial Volume (to be published).

29. Kaplan, L. D., 1953: A Quasi-Statistical Approach to the Calculation of Atmospheric Transmission. Proc. Toronto Conf. 43-48.

30. Howard, J. N., Burch, D. L. and Williams, D., 1955: Near Infrared Transmission Through Synthetic Atmospheres. Geophys. Res. Papers No. 40. 244 pp.

31. Benedict, W. S., 1956: Theoretical Studies of Infrared Spectra of Atmospheric Gases. J. J. Hopkins University, Final Report Contract No. 19(604)-1001. 66 pp.

32. Palmer, C. H., Jr., 1957: Long Path Water Vapor Spectra, I and II. J. Opt. Soc. 47, 1024 and 1028.

33. Palmer, C. H., Jr., 1959: Program of 44th Annual Meeting of Opt. Soc. Am., Paper SB-39.

34. Callender, G. S., 1958: On the Amount of CO_2 in the Atmosphere. Tellus 10, 243-248.

35. Keeling, C. D., 1958: The Concentration and Isotopic Abundance of Atmospheric CO_2 in Rural Areas. Geochin. et. Cosmochim. A Cta 13, 322-334.

36. Paetzold, H. K., 1959: Vertical Atmosphere Ozone Distributions. Adv. Chem. Ser. No. 21, 209-220.

37. Walshaw, C. D., 1957: Integrated Absorption by the 9.6 Band of Ozone QJRMS, 83, 315-321.

38. Taylor, J. H. and H. W. Yates., 1956. Atmospheric Transmission in the Infrared. NRL Report 4759, 15 pp.

39. French, J. E. and K. R. Johannsen., 1953: Forecasting High Clouds from High-level Constant Pressure Charts. Proc. Toronto Conf. 160-171.

40. Handbook of Geophysics for Air Force Designers, Geophysics Research Directorate, AFCRC, 1957. Tables 1-7 and 1-15.

41. Hawksley, P. G. W., 1952: The Physics of Particle Size Measurement: Part II - Optical Methods and Light Scattering. Monthly Bulletin, British Coal Utilization Research Association. Vol. XVI, No. 4.

42. Smithsonian Meteorological Tables. Sixth Edition. Smithsonian Institution. 1951.

GRD RESEARCH NOTES

No. 1. Contributions to Stratospheric Meteorology, *edited by George Ohring, Aug 1958.*

No. 2. A Bibliography of the Electrically Exploded Wire Phenomenon, *W. G. Chace, Nov 1958.*

No. 3. Venting of Hot Gases Through Temperature Inversions, *M. A. Estoque, Dec 1958.*

No. 4. Some Characteristics of Turbulence at High Altitudes, *M. A. Estoque, Dec 1958.*

No. 5. The Temperature of an Object Above the Earth's Atmosphere, *Marden H. Seavey, Mar 1959.*

No. 6. The Rotor Flow in the Lee of Mountains, *Joachim Kuettner, Jan 1959.*

No. 7. The Effect of Sampler Spacing on Basic Analyses of Concentration Data, *Duane A. Haugen, Jan 1959.*

No. 8. Natural Aerosols and Nuclear Debris Studies, Progress Report I, *P. J. Drevinsky, C. E. Junge, I. H. Blifford, Jr., M. I. Kalkstein and E. A. Martell, Sep 1958.*

No. 9. Observations on Nickel-Bearing Cosmic Dust Collected in the Stratosphere, *Herman Yagoda, Mar 1959.*

No. 10. Radioactive Aggregates in the Stratosphere, *Herman Yagoda, Mar 1959.*

No. 11. Comments on the Ephemerides and Constants for a Total Eclipse of the Sun, *R. C. Cameron and E. R. Dyer, May 1959.*

No. 12. Numerical Experiments in Forecasting Air and Soil Temperature Profiles, *D. W. Stevens, Jun 1959.*

No. 13. Some Notes on the Correlation Coefficient, *S.M. Silverman, May 1959.*

No. 14. Proceedings of Military Geodesy Seminar, December 1958, Air Force Cambridge Research Center *(U), edited by O. W. Williams, Apr 1959. (SECRET Report)*

No. 15. Proceedings of the First Annual Arctic Planning Session, November 1958, *edited by Joseph H. Hartshorn, Apr 1959.*

No. 16. Processes for the Production and Removal of Electrons and Negative Ions in Gases, *S.M. Silverman, Jun 1959.*

No. 17. The Approximate Analysis of Zero Lift Trajectories, *Charles Hoult, Aug 1959.*

No. 18. Infrared Measuring Program 1958 (IRMP 58) – Activities, Achievements, and Appraisal *(U), M.R. Nagel, Jul 1959. (SECRET Report)*

No. 19. Artificial Radioactivity from Nuclear Tests up to November 1958, *E. A. Martell, Sep 1959*

No. 20. A Preliminary Report on a Boundary Layer Numerical Experiment, *M.A. Estoque, Oct 1959.*

No. 21. Recent Advances in Contrail Suppression, *(U), S. J. Birstein, Nov 1959. (CONFIDENTIAL Report)*

No. 22. A Note Comparing One Kilometer Vertical Wind Shears Derived from Simultaneous AN/GMD-1A and AN/GMD-2 Winds Aloft Observations, *H. A. Salmela and N. Sissenwine, Oct 1959.*

No. 23. Atmospheric Refraction of Infrared Radiation, *T. P. Condron, Oct 1959.*

No. 24. Natural Aerosols and Nuclear Debris Studies, Progress Report II, *M. I. Kalkstein, P. J. Drevinsky, E. A. Martell, C. W. Chagnon, J. E. Manson, and C. E. Junge, Nov 1959.*

No. 25. Observations of Jupiter Missile Re-Entry, *(U), R. G. Walker, R. E. Ellis and R. E. Hunter, Dec 1959. (SECRET Report)*

No. 26. Space Probes and Persistence of Strong Tropopause Level Winds, *H. Salmela and N. Sissenwine, Dec 1959.*

No. 27. A Relativistic Treatment of Strong Shock Waves in a Classical Gas, *A. W. Guess, Dec 1959.*

No. 28. Measurements of Flux of Small Extraterrestrial Particles, *H. A. Cohen, Jan 1960.*

No. 29. Proceedings of the Second Annual Arctic Planning Session, October 1959, *edited by Vivian C. Bushnell, Dec 1959.*

No. 30. Atmospheric Pressure Pulse Measurements, *(U), Elisabeth F. Iliff, Jan 1960. (SECRET Report -- Formerly Restricted Data)*

GRD RESEARCH NOTES (Continued)

No. 31. A Discussion of the Calder Equation for Diffusion from a Continuous Point Source, *W. P. Elliott, May 1960.*

No. 32. Lagrangian and Eulerian Relationships in the Absence of Both Homogeneity and Time Steadiness, *M. L. Barad and D. A. Haugen, May 1960.*

No. 33. Thermal Radiation from Rocket Exhausts at Extreme Altitudes, *(U) R. G. Walker, R. E. Hunter, and J. T. Neu, Jun 1960. (SECRET Report)*

No. 34. Thermal Radiation Measurement from an Aerobee Hi Research Rocket *(U), R. G. Walker, and R. E. Hunter, (SECRET Report) (to be published)*

No. 35. Additional Note -- Strong Vertical Wind Profiles and Upper-Level Maximum Wind Speeds Over Vandenberg Air Force Base, *H. A. Salmela and N. Sissenwine, May 1960.*

AD

Air Force Cambridge Research Center
Geophysics Research Directorate
Bedford, Mass.

CONTRIBUTIONS TO SATELLITE METEOROLOGY, edited by W.K. Widger, Jr., June 1960. 263 pp. incl. illus. tables, 42 refs. (GRD Research Notes No. 36; AFCRC-TN-60-427) Unclassified Report

This report discusses and/or analyzes and describes: a concept of a meteorological system; applications of meteorological satellites; studies of large-scale cloudiness in the Northern Hemisphere; cloud patterns as seen from altitudes of 250-850 mi; the possibility of measuring cloud velocities from a satellite; a system for the meteorological use of satellite television observations; a photogrammetric method of obtaining the camera axis and its application in determining the time of photos taken from a space vehicle; synoptic-scale radiation processes; studies of atmospheric radiation as observed from satellites; a preliminary investigation of the nature of the infrared view of the earth's atmosphere from

(over)

UNCLASSIFIED

1. Meteorological satellites
2. Meteorological data - Collecting methods
3. Meteorological data - Transmissions

UNCLASSIFIED

AD

Air Force Cambridge Research Center
Geophysics Research Directorate
Bedford, Mass.

CONTRIBUTIONS TO SATELLITE METEOROLOGY, edited by W.K. Widger, Jr., June 1960. 263 pp. incl. illus. tables, 42 refs. (GRD Research Notes No. 36; AFCRC-TN-60-427) Unclassified Report

This report discusses and/or analyzes and describes: a concept of a meteorological system; applications of meteorological satellites; studies of large-scale cloudiness in the Northern Hemisphere; cloud patterns as seen from altitudes of 250-850 mi; the possibility of measuring cloud velocities from a satellite; a system for the meteorological use of satellite television observations; a photogrammetric method of obtaining the camera axis and its application in determining the time of photos taken from a space vehicle; synoptic-scale radiation processes; studies of atmospheric radiation as observed from satellites; a preliminary investigation of the nature of the infrared view of the earth's atmosphere from

(over)

UNCLASSIFIED

1. Meteorological satellites
2. Meteorological data - Collecting methods
3. Meteorological data - Transmissions

UNCLASSIFIED

AD

Air Force Cambridge Research Center
Geophysics Research Directorate
Bedford, Mass.

CONTRIBUTIONS TO SATELLITE METEOROLOGY, edited by W.K. Widger, Jr., June 1960. 263 pp. incl. illus. tables, 42 refs. (GRD Research Notes No. 36; AFCRC-TN-60-427) Unclassified Report

This report discusses and/or analyzes and describes: a concept of a meteorological system; applications of meteorological satellites; studies of large-scale cloudiness in the Northern Hemisphere; cloud patterns as seen from altitudes of 250-850 mi; the possibility of measuring cloud velocities from a satellite; a system for the meteorological use of satellite television observations; a photogrammetric method of obtaining the camera axis and its application in determining the time of photos taken from a space vehicle; synoptic-scale radiation processes; studies of atmospheric radiation as observed from satellites; a preliminary investigation of the nature

(over)

UNCLASSIFIED

1. Meteorological satellites
2. Meteorological data - Collecting methods
3. Meteorological data - Transmissions

UNCLASSIFIED

AD

Air Force Cambridge Research Center
Geophysics Research Directorate
Bedford, Mass.

CONTRIBUTIONS TO SATELLITE METEOROLOGY, edited by W.K. Widger, Jr., June 1960. 263 pp. incl. illus. tables, 42 refs. (GRD Research Notes No. 36; AFCRC-TN-60-427) Unclassified Report

This report discusses and/or analyzes and describes: a concept of a meteorological system; applications of meteorological satellites; studies of large-scale cloudiness in the Northern Hemisphere; cloud patterns as seen from altitudes of 250-850 mi; the possibility of measuring cloud velocities from a satellite; a system for the meteorological use of satellite television observations; a photogrammetric method of obtaining the camera axis and its application in determining the time of photos taken from a space vehicle; synoptic-scale radiation processes; studies of atmospheric radiation as observed from satellites; a preliminary investigation of the nature

(over)

UNCLASSIFIED

1. Meteorological satellites
2. Meteorological data - Collecting methods
3. Meteorological data - Transmissions

UNCLASSIFIED

AD

a satellite; satellite observations of infrared radiation; detection of ozone amounts from satellite measurements; and a generalized, schematic flow chart for the reductinn and processing of satellite meteorological data.

UNCLASSIFIED

UNCLASSIFIED

AD

a satellite; satellite observations of infrared radiation; detection of ozone amounts from satellite measurements; and a generalized, schematic flow chart for the reduction and processing of satellite meteorological data.

UNCLASSIFIED

UNCLASSIFIED

AD

of the infrared view of the earth's atmosphere from a satellite; satellite observations of infrared radiation; detection of ozone amounts from satellite measurements; and a generalized, schematic flow chart for the reduction and processing of satellite meteorological data.

UNCLASSIFIED

AD

of the infrared view of the earth's atmosphere from a satellite; satellite observations of infrared radiation; detection of ozone amounts from satellite measurements; and a generalized, schematic flow chart for the reduction and processing of satellite meteorological data.

UNCLASSIFIED

AD

Air Force Cambridge Research Center
Geophysics Research Directorate
Bedford, Mass.

CONTRIBUTIONS TO SATELLITE METEOROLOGY, edited by W.K. Widger, Jr., June 1960. 263 pp. incl. illus. tables, 42 refs. (GRD Research Notes No. 36; AFCRC-TN-60-427) Unclassified Report

This report discusses and/or analyzes and describes: a concept of a meteorological system; applications of meteorological satellites; studies of large-scale cloudiness in the Northern Hemisphere; cloud patterns as seen from altitudes of 250-850 mi; the possibility of measuring cloud velocities from a satellite; a system for the meteorological use of satellite television observations; a photogrammetric method of obtaining the camera axis and its application in determining the time of photos taken from a space vehicle; synoptic-scale radiation processes; studies of atmospheric radiation as observed from satellites; a preliminary investigation of the nature of the infrared view of the earth's atmosphere from

(over)

UNCLASSIFIED

1. Meteorological satellites
2. Meteorological data - Collecting methods
3. Meteorological data - Transmissions

UNCLASSIFIED

AD

Air Force Cambridge Research Center
Geophysics Research Directorate
Bedford, Mass.

CONTRIBUTIONS TO SATELLITE METEOROLOGY, edited by W.K. Widger, Jr., June 1960. 263 pp. incl. illus. tables, 42 refs. (GRD Research Notes No. 36; AFCRC-TN-60-427) Unclassified Report

This report discusses and/or analyzes and describes: a concept of a meteorological system; applications of meteorological satellites; studies of large-scale cloudiness in the Northern Hemisphere; cloud patterns as seen from altitudes of 250-850 mi; the possibility of measuring cloud velocities from a satellite; a system for the meteorological use of satellite television observations; a photogrammetric method of obtaining the camera axis and its application in determining the time of photos taken from a space vehicle; synoptic-scale radiation processes; studies of atmospheric radiation as observed from satellites; a preliminary investigation of the nature of the infrared view of the earth's atmosphere from

(over)

UNCLASSIFIED

1. Meteorological satellites
2. Meteorological data - Collecting methods
3. Meteorological data - Transmissions

UNCLASSIFIED

AD

of the infrared view of the earth's atmosphere from a satellite; satellite observations of infrared radiation; detection of ozone amounts from satellite measurements; and a generalized, schematic flow chart for the reduction and processing of satellite meteorological data.

UNCLASSIFIED

AD

of the infrared view of the earth's atmosphere from a satellite; satellite observations of infrared radiation; detection of ozone amounts from satellite measurements; and a generalized, schematic flow chart for the reduction and processing of satellite meteorological data.

UNCLASSIFIED